

**UNIVERSITY OF AGRONOMIC SCIENCES  
AND VETERINARY MEDICINE OF BUCHAREST**

**FACULTY OF LAND RECLAMATION  
AND ENVIRONMENTAL ENGINEERING**

# **JOURNAL OF YOUNG SCIENTIST**

Land Reclamation, Earth Observation & Surveying,  
Environmental Engineering

**Volume III**

2015  
BUCHAREST

# *The IX-th National Student Symposium „IF – IM – CAD”*

**Organized by:**



University of Agronomic Sciences and Veterinary Medicine of Bucharest  
Faculty of Reclamation and Environmental Engineering

**Under the patronage of:**



Royal House of Romania

**In collaboration with:**



SC Iridex Group SRL



**esri Romania** Esri Romania



ASIF

## **EDITORIAL BOARD**

**General Editor:** Răzvan Ionuț TEODORESCU

**Executive Editor:** Andreea OLTEANU

**Members:** Mariana CĂLIN, Carmen CÎMPEANU, Elena CONSTANTIN, Sorin IONIȚESCU,  
Tatiana IVASUC, Raluca MANEA, Doru MIHAI, Alina ORȚAN, Mircea SEVASTEL, Ana  
VÎRSTA

## **PUBLISHER:**

**University of Agronomic Sciences and Veterinary Medicine of Bucharest, Romania**

**Faculty of Land Reclamation and Environmental Engineering**

Address: 59 Marasti Blvd., District 1, Zip code 011464, Bucharest, Romania

Phone: + 40 784 276 174

E-mail: [simpozionifimcad@gmail.com](mailto:simpozionifimcad@gmail.com)

Web: <http://simpozionifimcad.usamv.ro>

## **Copyright 2015**

*To be cited: Journal of Young Scientist, Vol. III, 2015*

*The publishers are not responsible for the content of the scientific papers and opinions published in the Volume.*

*They represent the authors' point of view.*

**ISSN 2344 - 1283; ISSN CD-ROM 2344 - 1291; ISSN Online 2344 - 1305; ISSN-L 2344 – 1283**

## SCIENTIFIC COMMITTEE:

- **Prof. Sorin CÎMPEANU** - University of Agronomic Sciences and Veterinary Medicine, Bucharest
- **Assoc. Prof. Răzvan TEODORESCU** - University of Agronomic Sciences and Veterinary Medicine, Bucharest
- **Prof. Raluca MANEA** - University of Agronomic Sciences and Veterinary Medicine, Bucharest
- **Prof. Philippe DONDON** - Ecole Nationale Supérieure d'Electronique, Informatique, Telecommunications, Mathematique et Mecanique de Bordeaux / Institut Polytechnique de Bordeaux (ENSEIRB-MATMECA / IPB), France
- **Prof. Carmen GRECEA** - University "Politehnica" of Timișoara
- **Prof. Paula IANCU** - University of Agronomic Sciences and Veterinary Medicine, Bucharest
- **Prof. Hakan KUTOGLU** - Head of Geomatic Engineering Department, Bülent Ecevit University, Turkey
- **Prof. Teodor Eugen MAN** - University "Politehnica" of Timișoara
- **Prof. Sevastel MIRCEA** - University of Agronomic Sciences and Veterinary Medicine, Bucharest
- **Prof. Mircea ORTELECAN** - University of Agronomic Sciences and Veterinary Medicine, Cluj-Napoca
- **Prof. Ioana SIMINEA** - University of Agronomic Sciences and Veterinary Medicine, Bucharest
- **Prof. Athanasios STYLIADIS** - The East Macedonia & Thrace Institute of Technology, Greece
- **Prof. Ana VÎRSTA** - University of Agronomic Sciences and Veterinary Medicine, Bucharest
- **Prof. Yılmaz YILDIRIM** - Bülent Ecevit University, Turkey
- **Prof. Alexandru BADEA** - University of Agronomic Sciences and Veterinary Medicine, Bucharest
- **Prof. Carmen CÎMPEANU** - University of Agronomic Sciences and Veterinary Medicine, Bucharest
- **Prof. Elena CONSTANTIN** - University of Agronomic Sciences and Veterinary Medicine, Bucharest
- **Assoc. Prof. Daniela BURGHILĂ** - University of Agronomic Sciences and Veterinary Medicine, Bucharest
- **Assoc. Prof. Levente DIMÉN** - University "1 Decembrie 1918", Alba Iulia
- **Assoc. Prof. Doru MIHAI** - University of Agronomic Sciences and Veterinary Medicine, Bucharest
- **Assoc. Prof. Elena NISTOR** - University of Agronomic Sciences and Veterinary Medicine, Bucharest
- **Assoc. Prof. Alina ORȚAN** - University of Agronomic Sciences and Veterinary Medicine, Bucharest
- **Assoc. Prof. Adrian ROȘCA** - University of Craiova
- **Assoc. Prof. Augustina TRONAC** - University of Agronomic Sciences and Veterinary Medicine, Bucharest
- **Assoc. Prof. Ioel VEREȘ** - University of Petroșani

- **Lecturer Mariana CĂLIN** - University of Agronomic Sciences and Veterinary Medicine, Bucharest
- **Lecturer Claudiu DRAGOMIR** - University of Agronomic Sciences and Veterinary Medicine, Bucharest
- **Lecturer Elena IONIȚESCU** - University of Agronomic Sciences and Veterinary Medicine, Bucharest
- **Lecturer Mădălina MARIAN** - University of Pitești
- **Lecturer Andreea OLTEANU** - University of Agronomic Sciences and Veterinary Medicine, Bucharest
- **Lecturer Tudor SĂLĂGEAN** - University of Agronomic Sciences and Veterinary Medicine, Cluj-Napoca

### **ORGANIZING COMMITTEE**

- Assoc. Prof. Răzvan TEODORESCU
- Prof. Raluca MANEA
- Prof. Ana VÎRSTA
- Lecturer Andreea OLTEANU
- Assoc. Prof. Daniela BURGHILĂ
- Lecturer Mariana CĂLIN
- Lecturer Nicoleta SÂRBU
- Assistant Tatiana IVASUC
- Assistant Veronica IVĂNESCU
- Assistant Mirela SANDU
- Assistant Raluca HÎRȚAN
- PhD stud Eng. Sorin IONIȚESCU
- Eng. Alexandru DUMITRU
- Mat. Anca DABIJA

### **VENUE**

**University of Agronomic Sciences and Veterinary Medicine of Bucharest**

**Faculty of Land Reclamation and Environmental Engineering**

**Address:** 59 Mărăști, Bvd, District 1, Zip code 011464

**E-mail:** [simpozionifimcad@gmail.com](mailto:simpozionifimcad@gmail.com)

**Web:** <http://simpozionifimcad.usamv.ro>

**Phone:** +40 784 276 174

## TABLE OF CONTENTS

### SECTION 01. ENVIRONMENTAL ENGINEERING

Paper ID	Authors	Affiliation	Paper Title	Page
01	Silviu BADEA, Andrei Liviu CHIRIȚĂ, Cristian ANDRONE, Bianca Georgiana OLARU	University of Agronomic Sciences and Veterinary Medicine of Bucharest	INDOOR AIR QUALITY ASSESSMENT THROUGH MICROBIOLOGICAL METHODS	12-17
02	Oana BANU, Diana GORGHIU	University of Agronomic Sciences and Veterinary Medicine of Bucharest	EVOLUTIONARY APPS IN AGRICULTURE	18-22
03	Claudiu Ovidiu BARBULESCU, Vlad Gabriel CODESCU	University of Agronomic Sciences and Veterinary Medicine of Bucharest	WATER QUALITY MONITORING FROM THE LAKES ON COLENTINA RIVER	23-30
04	Mihai FRÎNCU, Corina DUMITRACHE, Andrei Cristian DUMITRIU	University of Agronomic Sciences and Veterinary Medicine of Bucharest	PHYSICO-CHEMICAL AND MICROBIAL ANALYSIS OF POND WATER FROM USAMV DENDROLOGICAL PARK - BUCHAREST	31-36
05	Mihai FRÎNCU, Corina DUMITRACHE, Andrei Cristian DUMITRIU	University of Agronomic Sciences and Veterinary Medicine of Bucharest	SOIL FERTILITY ASSESSMENT THROUGH ENZYME ACTIVITY	37-40
06	Iulia Diana GLIGA, Madalina PRESECAN	University of Agronomic Sciences and Veterinary Medicine of Cluj-Napoca	CHOOSING THE OPTIMAL SOLUTION FOR REINTRODUCTION DEGRADED LAND SURFACE INTO THE FOREST CYCLE	41-44
07	Eren KARAKAVUZ	Bülent Ecevit University of Turkey, Environmental Engineering Department	PARTICULATE MATTER SIZE DISTRIBUTION AND COMPONENT ANALYSIS IN BULENT ECEVIT UNIVESITY FARABI CAMPUS, ZONGULDAK, TURKEY	45-48
08	Paul MĂRGINAS, Ervin SCHLESINGER	University of Agronomic Sciences and Veterinary Medicine of Cluj-Napoca	DESIGN OF A PRECAST REINFORCED CONCRETE BRIDGE ON THE „VALEA ROȘIE” MAIN FOREST ROAD, KM 1+110	49-54

09	Dorin TATARU, Andreea STANCI	University of Petrosani	ATMOSPHERIC POLLUTION CAUSED BY RADIOACTIVITY ISSUED BY THE ASH AND SLAG DEPOSITS FROM THE PAROSANI THERMAL POWER PLANT	55-58
10	Cristina- Iuliana TOMA	University of Pitesti, Faculty of Sciences	ENVIRONMENT QUALITY IMPROVEMENT AT THE UNIVERSITY OF PITESTI, A FORMER MILITARY SITE	59-62
11	Alikemal TOPALOĞLU	Bülent Ecevit University of Turkey, Environmental Engineering Department	THE USE OF ULTRAFILTRATION MEMBRANE SYSTEMS TO TREAT WASTE WATERS GENERATED FROM HARD COAL MINING	63-66

## SECTION 02. LAND RECLAMATION

Paper ID	Authors	Affiliation	Paper Title	Page
12	Adela Eleonora VISAN, Mihaela RADU, Emine ISMAIL	University of Agronomic Sciences and Veterinary Medicine of Bucharest	NEW DWELLING IN OLD- FASHION MANNER	69-72
13	Ştefan-Silvian CIOBANU	University of Agronomic Sciences and Veterinary Medicine of Bucharest	COLLAPSE SETTLEMENT SENSIBILITY ANALYSIS OF LOESSOID SOILS	73-76
14	Simona SBURATURA, Mihai-Cristian MUSCALU, Ancuta BODIRLAU	University of Agronomic Sciences and Veterinary Medicine of Bucharest	SAFETY STRUCTURAL ASSESSMENT OF REINFORCED CONCRETE BUILDINGS	77-82

## SECTION 03. WATER RESOURCES MANAGEMENT

Paper ID	Authors	Affiliation	Paper Title	Page
15	Adina CIOBANESCU, Georgiana DONE	University of Agronomic Sciences and Veterinary Medicine of Bucharest	ASPECTS OF ADVANCED WASTEWATER PURIFICATION	85-92

## SECTION 04. CADASTRE

Paper ID	Authors	Affiliation	Paper Title	Page
16	Iuliana Andreea APOSTU	University of Agronomic Sciences and Veterinary Medicine of Bucharest	3D MODELING OF A BUILDING FACADE	95-98
17	Andrei ARMAS, Ovidiu Stefan CUZIC	Polytechnic University of Timisoara, Faculty of Civil Engineering	CADASTRAL SURVEYS CONDUCTED WITHIN THE REPUBLIC OF MOLDOVA	99-105
18	Alina BĂLAN, Grigoraș-Mihnea GÎNGIOVEANU-LUPULESCU	University of Agronomic Sciences and Veterinary Medicine of Bucharest	USING GIS TO HELP US MAKE BETTER DECISIONS - MOUNTAIN DESTINATIONS -	106-108
19	Dorinuța BEȘA, Adina Mihaela MORAR, Nicoleta Alina MUREȘAN	University of Agricultural Sciences and Veterinary Medicine of Cluj-Napoca	ASPECTS CONCERNING TOPOGRAPHIC AND GEODETIC WORKS NECESSARY FOR DESIGNING AND DRAWING A CONSTRUCTION	109-114
20	Dumitru-Lucian BLĂGESCU, Ionuț-Alexandru BĂTRÎNACHE	University of Agronomic Sciences and Veterinary Medicine of Bucharest	MATLAB BASED APPROACH OF DECODING EGNOS MESSAGE	115-120
21	Alina BUZILĂ, Bogdan Ioan CIOBAN, Marcela Ionela HANDRO, Adrian Șerban PETRIC	University of Agricultural Sciences and Veterinary Medicine of Cluj-Napoca	ASPECTS OF SOLVING THE BASIC GEODETIC PROBLEM ON THE SPHERE	121-125
22	Ionut CAMPIAN, Tudor Alexandru FLOREA, Tania VRANCEANU, Mircea VUSCAN	University of Agricultural Sciences and Veterinary Medicine of Cluj-Napoca	SETTING THE REDUCE CORRECTIONS AT THE CHORD, FOR DIRECTIONS IN THE CASE OF THE 1970 STEREO PROJECTION	126-129
23	Răzvan Alex CIORBĂ, Radu Alexandru CREȚU, Mircea Emil NAP, Andreea Carmen ZAGOR	University of Agronomic Sciences and Veterinary Medicine of Cluj-Napoca	ESTABLISHING THE SPHERICAL EXCESS FOR THE GEODETIC NETWORKS OF THE THIRD ORDER	130-132
24	Alexandra-Maria DAMIAN,	University of Agronomic Sciences and Veterinary	CADASTRE IN EUROPE	133-137

	Andreea-Maria STANCU	Medicine of Bucharest		
25	Andrei Georgian DRAGHICI, Ioana VATRA	University of Agronomic Sciences and Veterinary Medicine of Bucharest	EVOLUTION OF HIGH SCHOOL EDUCATION IN IALOMITA COUNTY	138-141
26	Alina DUMITRU, Andra Maria DINOIU	University of Agronomic Sciences and Veterinary Medicine of Bucharest	ESTIMATING DEFORMATIONS OF GIURGIU-RUSSE BRIDGE SUPERSTRUCTURE USING ANALYTICAL PHOTOGRAMMETRY	142-146
27	Mihnea Mircea MITRACHE, Georgiana Maria MOTOI, Oana PIELEȘTEANU	University of Craiova, Faculty of Agriculture and Horticulture	TECTONIC PLATES: STUDY OF MOVEMENT AND DEFORMATION - AREA VRANCIOAIA	147-154
28	Teodora MOTOCESCU, Alexandru MIHALCEA, Dragos DRAGANESCU, Dan MOCANU	University of Agronomic Sciences and Veterinary Medicine of Bucharest	ROMANIA-THE LAND OF MYSTERY	155-158
29	Rares Catalin OROS, Diana-Ioana PLOSCARIU, Razvan Casian REBREAN, Vasile Beniamin TOLOMEIU	University of Agricultural Sciences and Veterinary Medicine of Cluj-Napoca	COMPARATIVE ANALYSIS REGARDING THE ACCURACY DETERMINATION OF A POINT, USING THE LINEAR INTERSECTION METHOD AND MULTIPLE COMBINED INTERSECTIONS METHOD	159-164
30	GrațIELA PASCAL, Ioana Georgiana TEPUȘ, Anamaria Cătălina SALE, Raluca Elena TĂUTU	University of Agricultural Sciences and Veterinary Medicine of Cluj-Napoca	ASPECTS REGARDING THE PROJECTION OF TOPOGRAPHIC ELEMENTS FROM THE TOPOGRAPHIC SURFACE ON THE REFERENCE SURFACE	165-169
31	Claudia PRĂJANU	Transilvania University of Brașov, Faculty of Silviculture and Forest Engineering	FACTORS THAT AFFECT THE PRECISION OF POINT COORDINATES TAKEN WITH GPS EQUIPMENT IN MOUNTAIN AREA OF	170-178

			BRAȘOV COUNTY	
32	Codruța-Rozica SILVĂȘAN- PAȘCA, Simona- Lenuța MLEȘNIȚE	University of Agricultural Sciences and Veterinary Medicine of Cluj-Napoca	STUDIES REGARDING THE DETERMINATION OF GEOMETRIC DIMENSIONS AND GEOMETRICAL DEVIATIONS COMPARING WITH THE PROJECTED ONES FOR FUEL TANKS	179- 184
33	Raluca Veronica ȘERBAN	Transilvania University of Brasov, Faculty of Silviculture and Forest Engineering	EXTENSION OF THE WATER NETWORK IN THE TOWN HOLBAV TECHNICAL AND LEGAL ASPECTS	185- 191
34	Daniela TRANA	“1 Decembrie 1918” University of Alba-Iulia	3D MODELLING	192- 196

#### SECTION 05. FUNDAMENTAL SCIENCES

Paper ID	Authors	Affiliation	Paper Title	Page
35	Ana ALEXANDRU	University of Agronomic Sciences and Veterinary Medicine of Bucharest	METHODS OF APPROXIMATING THE RIEMANN INTEGRALS AND APPLICATIONS	199- 206
36	Catalin BOTEĂ, Daniel Ionuț CARAMIDARU	University of Agronomic Sciences and Veterinary Medicine of Bucharest	ENERGETIC EFFICIENCY OF PUMPING STATION	207- 210



**SECTION 01**  
**ENVIRONMENTAL ENGINEERING**

## INDOOR AIR QUALITY ASSESSMENT THROUGH MICROBIOLOGICAL METHODS

Silviu BADEA, Andrei Liviu CHIRIȚĂ, Cristian ANDRONE, Bianca Georgiana OLARU

Scientific Coordinators: Professor PhD Carmen CÎMPEANU, Lecturer PhD Constanța MIHAI

University of Agronomic Sciences and Veterinary Medicine of Bucharest, 59 Mărăști Blvd, District 1, 011464, Bucharest, Romania, Phone : + 4021. 318.25.64, Fax: + 4021.318.25.67

Corresponding author email: olaru\_bianca1990@yahoo.com.au

### Abstract

*The aim of this study was to evaluate indoor-air microbiological contamination of the Land Reclamation and Environmental Engineering Faculty building from Bucharest. Samples were taken in May 2014, during both period of intense indoor activity (in the afternoon classes) and less indoor activity (during weekends). Total number of mesophilic aerobic bacteria, yeast and moulds from the air of selected rooms was determined using Koch sedimentation method. We used Petri plates filled with gelose medium to determine the total number of bacteria and Czapek-Dox Agar medium for the filamentous fungi identification. In many cases, a multiple growth bacteria and significant increase of filamentous fungi were observed, especially during intense indoor activity period. According to the standards of microbial air loading, the indoor air of the faculty is relatively clean.*

**Key words:** airborne bacteria, airborne fungi, indoor air, microbiological air quality.

### INTRODUCTION

The knowledge of microbial air contamination is an important criteria for assessment hygiene conditions. All around the world, the life style changes have resulted in a shift from open air environments to indoor environments at home and work places, where people spend a substantial time. (Chao et al, 2003, Molhave, 2011).

Healthy environment has a very strong connection with the human health (Botkin & Keller, 2007). Bacteria, fungi, pollen, viruses and mites can be sources of biological air contamination (Nevalainen and Seuri, 2005, Khan and Karuppayil, 2010). Clean air is what all living humans and animals needs for good health and well being. However, due to urban development, the air is continuously polluted. Urban ambient air is more polluted than overall atmosphere, due to high density of human population and their activities in urban areas. (Ling et al. 2012).

Human spend up to 80% of their lifetime either inside workplace or in their own homes. (Yang and al, 2007).

Some of the health effects of exposure to air

pollution, such as the impact on the respiratory and cardiovascular systems, have been extensively studied, thus it is well-known that exposure to air pollutants leads to an increase in mortality and morbidity rates of the population (Baccarelli et al, 2008; Kunzli et al, 2000, 2004).

Poor indoor environment quality could negatively affect the profits of any organisation as the costs of workers absence due to medical reasons and low productivity most often exceed the cost of energy use associated with maintaining acceptable standards. (Wong LT, Mui KW, Hui PS., 2007). The atmosphere is not a favourable environment for long-term survival of microbes. Indoor air quality can be defined as the air quality inside a building that will lead to occupant comfort and health. Indoor air quality is influenced by gas, microbial contaminants or particles that conduct to poor health conditions. Physical, chemical and biological factors can change indoor air quality. The physical factors include a range of issues from temperature, humidity and air movement to dust, lighting and noise, while chemical factors include pollutants arising

from paint, carpets, furniture, environmental tobacco smoke, cosmetics, drapes. For the biological factors, microorganisms play the main role, because the inhalation of bacterial, fungal and micro algal spores can cause an allergic reaction. A poor indoor air quality can cause a variety of short-term and long-term health problems including allergic reactions, respiratory problems, eye irritation, sinusitis, bronchitis and pneumonia. (Marmot et al., 2006).

Fungal flora can be hazardous for health, particularly in rooms with heating, ventilation and air conditioning systems in place. (La Serna I. et al, 2002).

Biological contamination of indoor air is mostly caused by bacteria, moulds and yeast. They can be dangerous as pathogenic living cells but they can also secrete some substances harmful for health. These are different kinds of toxic metabolism products, for example mycotoxins (Daisey J.M., et al, 2003).

The aim of this study was to assess the microbial contamination of indoor air from the Land Reclamation and Environmental Engineering Faculty building, located in Bucharest (FIFIM). The study embraced a measurement of the concentration of bacteria and fungi in the air of selected rooms and microbial composition of the air.

## MATERIALS AND METHODS

Total number of mesophilic aerobic bacteria, and filamentous fungi from the air of selected rooms was determined using Koch sedimentation method.

The Koch method do not require expensive instrumentation, it is fast and simple. Sedimentation method does not permit exact quantitative determination; some earlier observations reported that results of sedimentation method are usually higher than numbers obtained with the use of air samplers. (Fleischer M.,2006). However, data collected by sedimentation method allow the drawing of correct conclusions on types of microorganisms

present in the air and can give a good approximation of bacterial and fungal concentration.

Air microorganisms were settled gravitationally directly on the Petri plates filled with nutrient media and exposed in sampling points for a period of time. The number of microorganisms expressed as CFU/ m<sup>3</sup> was estimated according to Omeliansky's equation:

$$CFU/m^3 = \frac{n \cdot 100000}{S \cdot T}$$

n – number of colonies developed on the culture medium surface

S – surface of the Petri dish

T – exposure time of Petri dish in minutes

In order to assess the airborne bacteria and fungi from indoor FIFIM building, the samples were taken during two sampling periods, in May 2014. The first sampling period was on weekends and the second was during academic activity when the population density was found to be highest (academic staff, students and the public service requester), between 12-2 pm.



Figure 1. Thermostat for incubating samples (Microbiology lab CO3 – FIFIM)

The Petri dishes (108 plates) were exposed for 20 minutes on each sampling point. In each investigated room 2 Petri plates were placed, filled with nutrient medium as follow:

Gelose medium to determine the total number of bacteria, and

Czapek-Dox Agar for filamentous fungi identification.

Petri dishes were incubated for 24, 72, and 96 hours at 37°C to determine the total number of bacteria and for 3 days at 28°C to determine the fungal growths (figure 1).

Bacteria were identified by two arrays. The first one was the macroscopic estimation through description of colony and the second one was by microscopic estimation using

Gram dyeing. Diagnosis of filamentous fungi was based on estimation of morphological features of growth on Czapek medium.

The investigated places of the building encompass main halls, dean's office, lecture rooms, laboratories, library and toilets (table 1).

Table 1. Investigated rooms of the faculty (\* means the rooms with ventilation systems)

Rooms	Mark	Area (m <sup>2</sup> )	Cubature (m <sup>3</sup> )
<b>A - building</b>			
Ground floor hall	H <sub>0A</sub>	60	240
Laboratory*	A <sub>04</sub>	28	98
Toilets	T <sub>0</sub>	9	27
First floor hall	H <sub>IA</sub>	45	180
Dean office*	D	25	100
Board staff room*	BR	100	350
Second floor hall	H <sub>IIA</sub>	45	180
Lecture room*	A <sub>II1</sub>	120	400
Third floor hall	H <sub>IIIA</sub>	45	180
Lecture room*	A <sub>III4</sub>	36	108
Fourth floor hall	H <sub>IVA</sub>	45	180
Lecture room*	A <sub>IV2</sub>	36	108
<b>B- building</b>			
Library*	L	100	350
Hall	H <sub>B-C</sub>	30	120
Toilet	T <sub>II B</sub>		
Prof office*	O <sub>B</sub>	25	120
<b>C- building</b>			
Ground floor hall	H <sub>C0</sub>	40	160
Laboratory*	C <sub>03</sub>	40	140
First floor hall	H <sub>C1</sub>	30	120
Men Toilet	MT	4	12
Women Toilet	WT	4	12
Second floor hall	H <sub>CII</sub>	30	120
Men Toilet	MT	4	12
Women Toilet	WT	4	12

## RESULTS AND DISCUSSIONS

Quantitative variation of Microorganisms from indoor air of the Faculty

As expected, the air samples taken during afternoon academic activity have recorded in most cases higher values of germs total number in comparison with the samples taken on weekends. Strong relationship between Indoor air filamentous fungi contamination

The results concerning the average number of airborne filamentous fungi from different

occupant density, human activity and microorganisms concentration of the indoor air was reported in several other papers (Chao et al., 2003, Daisey et al., 2003, Khan and Karuppayil, 2011, Fleischer, 2006, Künzli et al., 2000).

### Indoor air bacterial contamination

The maximum level of mesophylic bacteria loading for clean air is less than 1500 CFU/m<sup>3</sup> and for infested air is greater than 2500 CFU/m<sup>3</sup> (SC 2009-16219/16.07.2009).

As can be observed in Figure 2, the bacterial growth of indoor air did not exceed the limit for fresh (clean) air quality (1500 CFU/m<sup>3</sup>) in any of the samples taken during weekends. In addition, the samples taken during the academic activity (in the afternoon classes) have not exceeded the bacterial load level in most cases.

However, there are some exceptions, especially in the central building (the A building). For instance, the lobby, the first, the second and the third floor halls (H<sub>0A</sub>, H<sub>IA</sub>, H<sub>IIA</sub>, H<sub>IIIA</sub>) and also the toilet from the ground floor (T<sub>0A</sub>) recording air bacterial loads that exceed the indoor air limit of infestation (> 2500 CFU/m<sup>3</sup>). The highest level of bacterial air infestation was recorded in the ground floor toilet (2 times higher than infestation limit), followed in descending order by the lobby (1.8 times), second floor hall (1.7 times), first floor hall (1.4 times) and the third floor hall (1.1 times). The reason for these exceeds is especially due to the poor natural ventilation of those rooms correlated with intensive traffic.

Five from the 24 selected rooms have had exceed of air bacterial load, which means that 24.2% from total cubature of indoor air investigated are infested with pathogenic mesophilic bacteria.

The remaining 75.8% is accounted for clean air. All the lecture rooms from the central building, the boardroom stuff, the library, and the whole investigated rooms from the B and C building of the Faculty did not counted bacterial growth values higher than 1500 CFU/m<sup>3</sup>, (the admissible value for clean air).

rooms of the building, sampling both on weekends and during academic activity are present in figure 3.

The admissible level for air fungi loading is 550 CFU/m<sup>3</sup> (SC 2009-16219/16.07.2009).

Sampling during afternoon academic activity reveals that only 36.1% from overall investigated rooms are proper regarding fungal air loading (e.g. the library, the boardroom stuff, the environmental sciences and microbiology laboratories, the first and the second floor halls of C building and the toilets from the second floor of the C building).

In all the other selected rooms the fungal growths exceed the air infested limit. From the total cubature 63.9% was infested with

filamentous fungi. The worst quality of indoor air was in the toilet from ground floor (T0A), where the level of air filamentous fungi exceeds over 14 times the admissible limit. Also, in the halls from A building (H0A and H1A) the fungal air contamination exceed the limit by 4 times, respectively by 6 times.

The fungal indoor air loading from the Dean office (D) and the amphitheatre (AII 1) exceeds twice time the admissible limit.

As can be observed the samples taken during weekend emphasize more clean indoor air than samples taken during student classis. However, the fungal air contamination of the Faculty buildings was higher than bacterial air contamination.

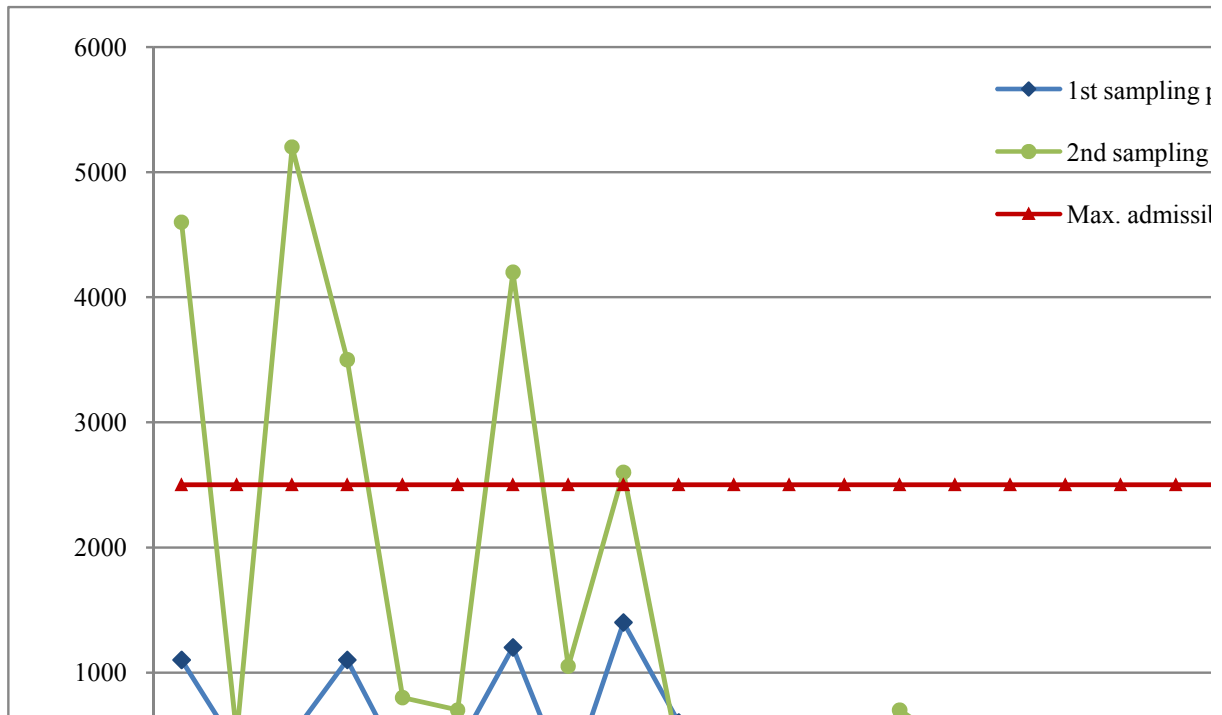


Figure 2. Bacterial load of indoor air from the Faculty building (CFU/m<sup>3</sup>)

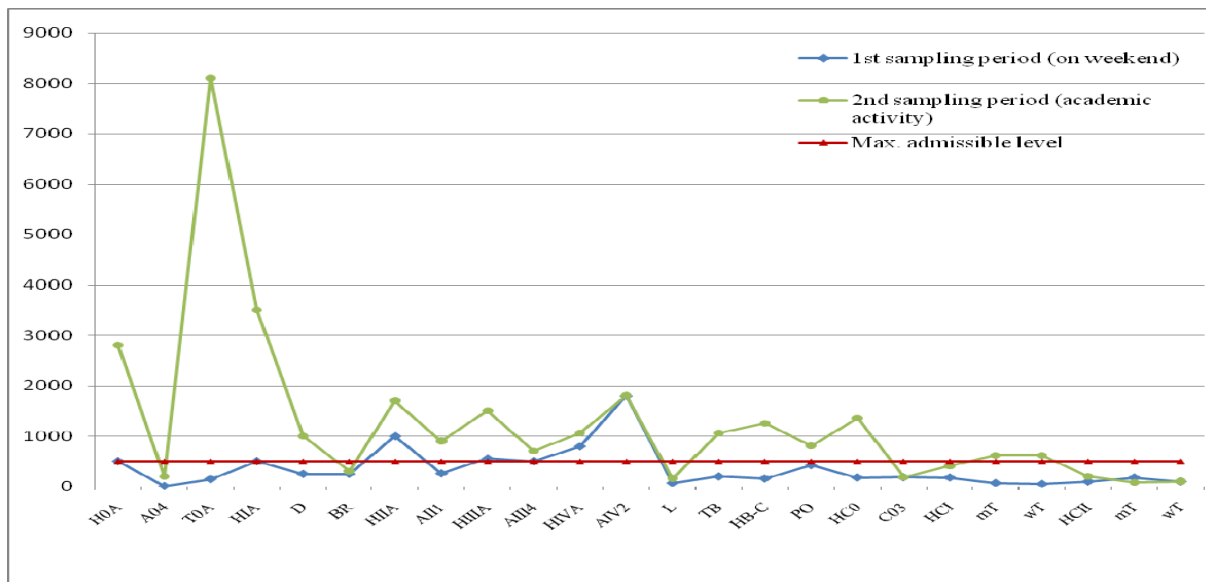


Figure 3. Fungal load of indoor air from the Faculty building (CFU/m3)

### Qualitative Analysis of Microorganisms from indoor air of the Faculty

Microbial indoor air quality was determined not only by quantitative variation of bacteria and fungi but by the presence of some particular microorganism species, which are very important for the people health occupying the Faculty rooms. Microscopic estimation with Gram dyeing showed that gram positive bacteria are dominated (e.g. *Bacillus* spp, *Streptococcus* spp, *Staphylococcus* spp.) (Figure 4).



Figure 4. Bacteria colonies from indoor air of Faculty

Quality characteristics of fungal flora isolated from the air of selected rooms showed domination of fungi genus like: *Penicillium*, *Aspergillus*, *Alternaria*, *Mucor*, and *Rhizopus* (Figure 5).

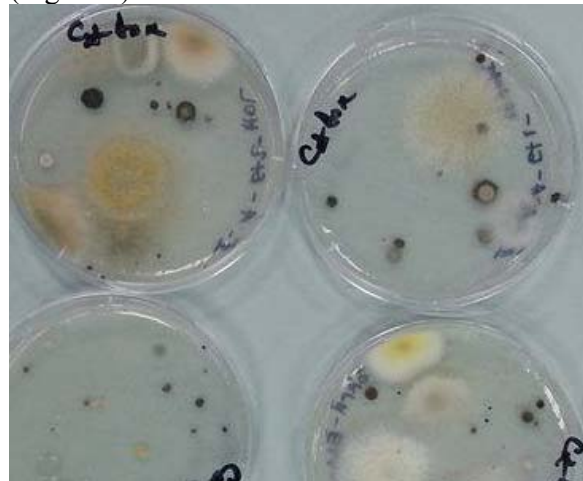


Figure 5. Fungi colonies from indoor air of Faculty

### CONCLUSIONS

The total number of germs growing from the air samples taken during afternoon academic activity have recorded in most cases higher values in comparison with the germs growing from the samples taken on weekends. Strong relationship between occupant density, human activity and microorganisms concentration of the indoor air was observed. In general, the fungal air contamination was higher than

bacterial air contamination. From the total investigated cubature of the Faculty buildings the statement of air quality is present as follow:

- for the A building

16,4 % represent clean air

14,9% relatively clean

59,7 % infested air

- for the B building

59% clean air

61% relatively clean air

0% infested air

- for the C building

68,7% clean air

31,3 % relatively clean air

0% infested air.

## ACKNOWLEDGEMENTS

This paper is part of the graduation projects presented in July 2014 by Badea Silviu, Chiriță Liviu Andrei and Androne Cristian. The work took place in Microbiology and Environmental Sciences laboratories from the Land Reclamation and Environmental Sciences Faculty (C03 and A04).

## REFERENCES

- Botkin and Keller, D.B. Botkin, E.A. Keller, 2007, Environmental science: Earth as a living planet.
- Chao et al., H.J. Chao, J. Schwartz, D.K. Milton, H.A. Burge, 2003, The work environment and workers health in four large office buildings, Environmental Health Perspectives, 111 (2003), pp. 1242–1248.
- Daisey J.M., Angel W.J., Apte M.G., 2003, Indoor air quality, ventilation and health symptoms in schools; an analysis of existing information Indoor Air 13,53.
- Khan and Karuppaiyl, A.A.H. Khan, S.M. Karuppaiyl, 2011, Practices contributing to biotic pollution in Airconditioned indoor environments, Aerobiologia, 27 (2011), pp. 85–89.
- Fleischer M, 2006, Microbiological control and airborne contamination in hospitals, indoor and built environment, 15 (1), 53.
- Künzli et al., 2000, N. Künzli, R. Kaiser, S. Medina, M. Studnicka, O. Chanel, P. Filliger, *et al.*, Public-health impact of outdoor and traffic-related air pollution: a European assessment, Lancet, 356 (9232) (2000), pp. 795–801.
- La Serna I., Dopazo A., Aira M.J. , Airborne fungal spores in the Campus of Anchieta (La Laguna, Tenerife/Canary Is.), Grana 41, 119, 2002
- Ling et al., 2011, Z. Ling, H. Guo, H. Cheng, Y. Yu, Sources of ambient volatile organic compounds and their contributions to photochemical ozone formation at a site in the Pearl River Delta, southern China, Environmental Pollution, 159 (2011), pp. 2310–2319.
- L.T. Wong, K.W. Mui, W.Y. Chan, 2007, An energy impact assessment of ventilation for indoor airborne bacteria exposure risk in air-conditioned offices, Original Research Article, Pages 1939-1944.
- Marmot et al., 2006, A.F. Marmot, J. Eley, S.A. Stafford, E. Warrick, M.G. Marmot, Building health: an epidemiological study of sick building syndrome in the Whitehall II study, Occupational and Environmental Medicine, 63 (2006), pp. 283–289.
- Nevalainen and Seuri, A. Nevalainen, M. Seuri, 2005, Of microbes and men, Indoor Air, 15 (2005), pp. 58–64.
- Yang et al., 2011, J. Yang, M. Xu, X. Zhang, Q. Hu, M. Sommerfeld, Y. Chen, Life-cycle analysis on biodiesel production from microalgae: Water footprint and nutrients balance, Bioresour. Technol., 102 (2011), pp. 159–165.
- \*\*\* SC 2009-16219/16.07.2009. "Determining of the pathogens species of indoor air from Timisoara's public and educational institutions". Elaborated by S.C. „SMART LAB DIAGNOSTICS” S.R.L Timișoara.

## EVOLUTIONARY APPS IN AGRICULTURE

Oana BANU, Diana GORGHIU

Scientific Coordinator: Lect. PhD. Eng. Alexandru CĂLIN

University of Agronomic Sciences and Veterinary Medicine of Bucharest, 59 Mărăști Blvd, District 1, 011464, Bucharest, Romania, Phone: +4021.318.25.64, Fax: +4021.318.25.67, Email: oana.banu95@hotmail.com , ddy\_dianna@yahoo.com

Corresponding author email: oana.banu95@hotmail.com

### Abstract

*The farming and ranching industries are undergoing a transformation, with innovative technologies being developed to improve the way agricultural enterprises are managed. Over the course of the last two years, a number of agriculture apps have been introduced with features like field mapping, planting calculations, spray logs and soil sampling tools. Precision Agriculture has evolved from a concept a half a decade ago into an emerging technology today. With an ever growing world population subject to famine, natural disasters, disease and conflict, changes must be made in agriculture to meet world concerns while remaining committed to sustaining the natural resources need for future production. Precision Agriculture is often described as the next great evolution in agriculture.*

**Key words:** agriculture apps, evolution, field mapping, technologies, transformation.

### INTRODUCTION

The purpose of this paper is to determine what precision agriculture is to offer ideas on expanding the concept to a more useful solution, to describe how Global Positioning System (GPS) and mobile mapping are integral components of decision-based precision agriculture and provide sources for additional information.

### MATERIALS AND METHODS

Most management strategies for precision agriculture match resource applications and agronomic practices with soil properties and crop requirements as they vary across a site. Sometimes referred to as site-specific or prescription application and generally includes:

Soil sampling - the ability to determine the physical characteristics and the variability of the soil in the field.

Variable rate application - the ability to precisely apply the required type and quantity

of nutrient of chemical needed to specific areas of the field.

Yield monitoring - the ability to accurately measure the yield and simultaneously record the location in the field.

Each of these components is necessary, but alone or together does not constitute precision agriculture.

### RESULTS AND DISCUSSIONS

Simplot Spray Guide from Plant Health Technologies, is designed to assist agricultural applicators, crop advisers and growers with the proper tank mixing sequence of crop protection products. Spray Guide also captures product use rates and application information and conveniently maintains comprehensive, accurate Spray Logs for easy record keeping. Following the proper mixing sequence helps users prevent product incompatibilities and can save applicators time and money by avoiding product loss and sprayer clean-out problems. Spray Guide provides the tank mixing sequence for over

1,300 common active ingredients and their tank mix partners. Included is a database of over 1,300 crop protection products from over 17 manufacturers. Mixing orders can contain up to 19 products from the following

categories: Herbicides (includes PGRs and Defoliant), Fungicides (includes Bactericides), Insecticides (includes Miticides and IGRs), Adjuvants, Foliar Nutrition.

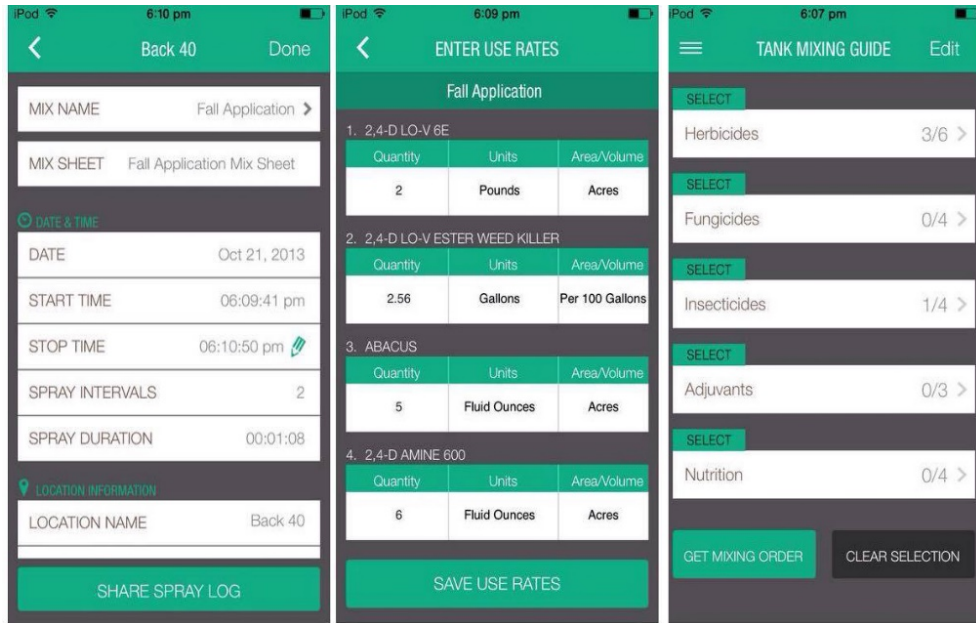


Figure 1. Simplot Spray Guide



Figure 2. Connected Farm

Connected Farmchange the way you use GPS for field mapping and scouting applications in agriculture. Trimble's Connected Farm scout app uses your smartphone or tablet for mapping field boundaries, locate irrigation pivots, marking flags and entering scouting information for points, lines and polygon areas. Scouting attributes include an extensive list of weeds, insects and diseases, and allows you to log the severity of a problem, crop conditions and more. Photos can be captured and integrated with your scouting attributes. The Connected Farm scout app is also compatible with Trimble's GreenSeeker handheld crop sensor. Start by entering NDVI (Normalized Difference Vegetation Index) readings from the handheld so that the app can automatically calculate the rate of Nitrogen. The geo-referenced location of the NDVI point is also saved in the app. The app is flexible to use with any crop such as corn, wheat, beans, cotton, vegetables and more. All data is sent via the cell of WI-FI connection to Connected Farm ([www.connectedfarm.com](http://www.connectedfarm.com)) where you can view, sort and print data online. The app is also compatible with Farm Works Software. Onsite is a cloud-based, mobile and desktop app for the agricultural industry that assists with file management and communications to and from the field by socially connecting people. Onsite is not intended to replace your current precision as software systems, but to complement and improve the efficiency of these solutions. In fact, we are already connecting into many of the agronomic and precision as software packages available today. When enabled, this app will utilize your GPS in the background. Continued use of GPS running in the background can dramatically decrease battery life. You can disable this option within the application.

AgFleet, developed by ZedX Inc., is a powerful decision-support system used to manage the productivity of more than 15 millions acres of agricultural land in North

America and continues to meet the ever-changing needs of growers, dealers and other professionals in the precision agriculture space.

AgFleet facilitates multiple processes for generating effective soil treatment plans. Each module within the framework is specifically designed to process information and data such as importing soil characteristics (Field Sampler), verifying irrigation needs (Irrigation Scheduler), managing costs associated to applying fertilizer and pesticide treatments (Record Keeper) and evaluating outcomes and recommendations for soil treatment (Field Sampler/Zone Maker).

JDLINK™ is John Deere's telematics system designed for customers and managers who desire to take their operation to the next level of productivity and efficiency without leaving the office! Using JDLINK™ information to optimize a machine is no different than pulling a soil sample to identify what nutrients are needed to produce a high yield. Using the power of JDLINK™ can optimize productivity, increase uptime, and boost profits with JDLINK™ information all from a laptop, desktop, or mobile device.

Keeping the overview over your fleet has never been easier and faster with this brand new app in your pocket! Monitoring and managing your machines outside the office within a couple of seconds is simple as never before!

Agrivi mobile application lets farmers get fast insight into their farming activities and register key activities right from the field. It is used as an extension and supporting feature to our fully featured web farm management solution. New mobile application users should setup their farms through our web application to get insight into their farming via mobile app. Agrivi farm management software helps farmers to take control over their plantations, improve productivity and increase profitability. Based on agricultural knowledge base of best-practice

production processes for over 60 crops, Agrivi guides farmers, improves their

productivity and increases productivity.

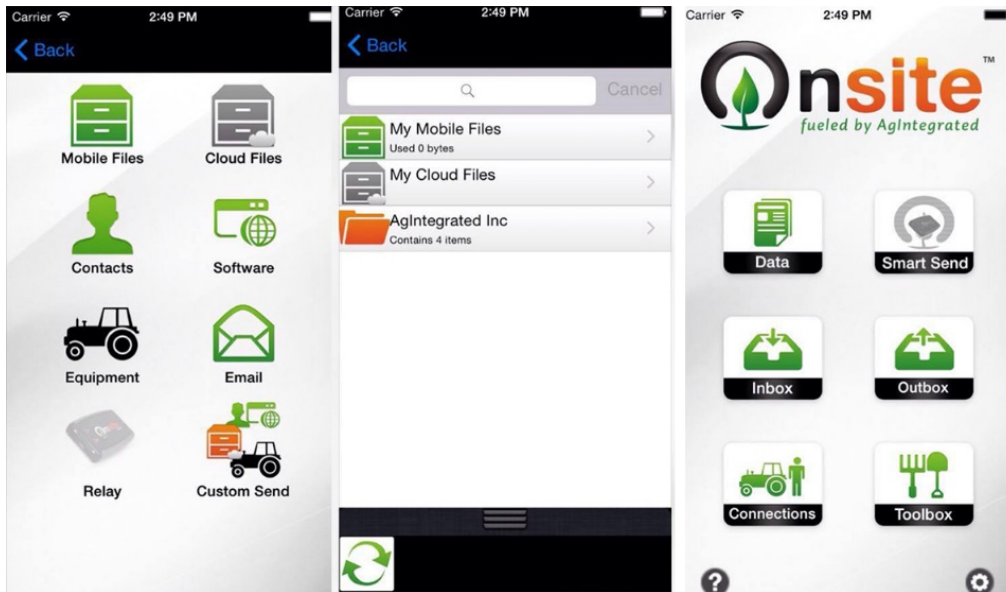


Figure 3. Onsite

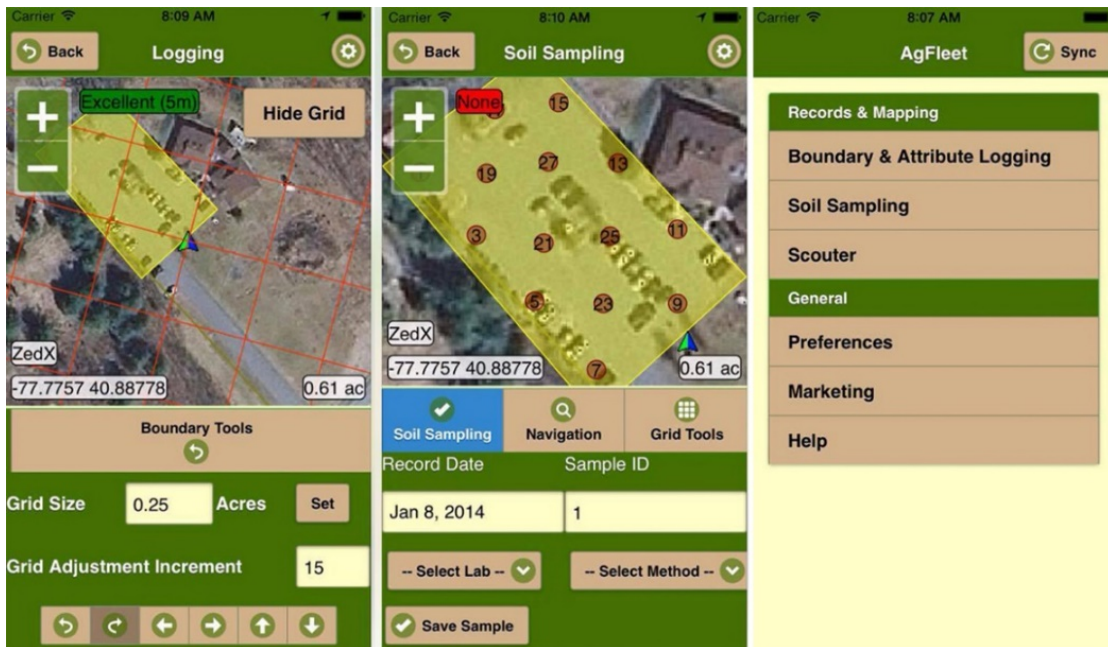


Figure 4. AgFleet

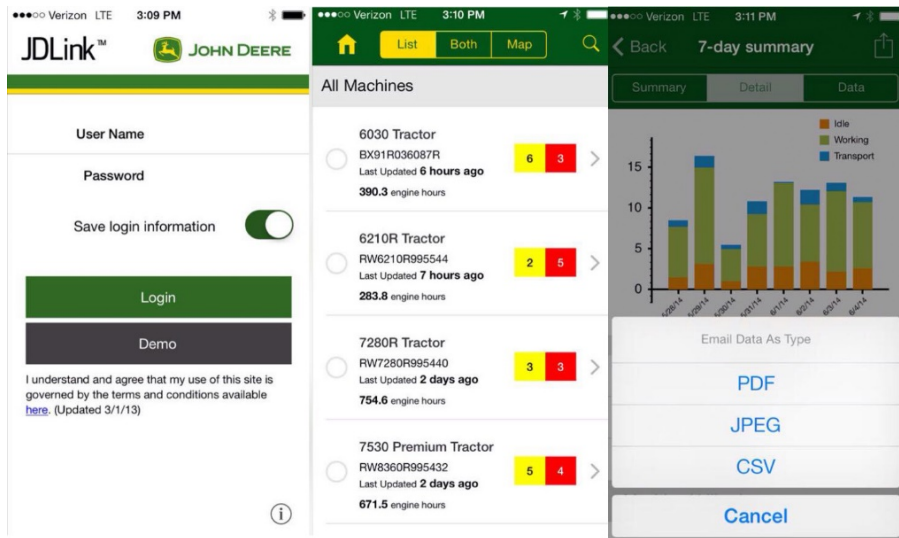


Figure 5. JDLink



Figure 6. Agrivi

## CONCLUSIONS

Precision agriculture is an agricultural system that has the potential of dramatically changing agriculture in this 21st century. Precision agriculture lends to most agricultural applications and can be implemented at whatever levels are required. Precision agriculture is based on information technology, which enables the producer to collect information and data for better decision making. Precision agriculture is a pro-active approach that reduces some of the risk and variables

common to agriculture. Precision agriculture is more environmentally sound and is an integral part in sustaining natural resources.

## REFERENCES

- Jon Boelts, Vice President of the Yuma County Farm Bureau, Yuma County, Arizona, USA
- John Deere's website: [www.deere.com](http://www.deere.com)
- Matt Hopkins, December 7, 2012, [Google+] New mobile Agriculture Apps
- Michael Rasher, Asian GPS Conference 2001, "The use of GPS and mobile mapping for decision-based precision agriculture"

## WATER QUALITY MONITORING FROM THE LAKES ON COLENTINA RIVER

**Claudiu Ovidiu BARBULESCU, Vlad Gabriel CODESCU**

**Scientific Coordinators: Prof. PhD Ana VIRSTA, Assist. Prof. PhD Mirela SANDU**

University of Agronomic Sciences and Veterinary Medicine of Bucharest, 59 Marasti Blvd, District 1, 011464, Bucharest, Romania, Phone: +4021.318.25.64, Fax: +4021.318.25.67

Corresponding authors emails: just.me\_claudiu@yahoo.com, codescu\_vlad@yahoo.com

### **Abstract**

*The aim of this study was to identify a number of physic-chemical parameters of water samples from the chain of Colentina River, to determine the degree of pollution of the lakes. Samples were taken directly from lakes Grivita, Baneasa, Herastrau, Floreasca, upstream and downstream, as required by law, kept at temperatures of 3-50C and analyzed in the same day. The chemical analyses were conducted in the Laboratory of Faculty of Land Reclamation and Environmental Engineering, University of Agronomic Sciences and Veterinary Medicine of Bucharest. Characterization of natural waters was based on the following analysis: pH, conductivity, turbidity, chloride, dissolved oxygen (DO), biochemical oxygen demand (BOD), ammonium, nitrites.*

**Key words:** Colentina River, water quality, surface water

### **INTRODUCTION**

It is well known that the majority of settlements, either villages or cities, were established in the vicinity of water streams, a characteristic which is generally valid along the history of humankind.

The Colentina River has its origins in the Sotanga-Doicesti area, near Targoviste and it flows through the Dambovita and Ilfov counties, "cutting" Bucharest from north-west to east. It finds its end, near Cernica, where meets the Dambovita River.

The river's stream measures 101 Km, with almost a third (37.4 Km) of its length passing through Bucharest.

In the last 60 years, important hydro-technical projects were implemented along the river's stream, projects that transformed the little mosquito infected river with poor neighborhoods along his sides (Figures 1,2,3) into a chain of lakes with multiple and popular recreations areas. (Giurescu, 1979).



Figure 1. Floreasca's pit before development (Caranfil,1963)



Figure 2. Herastrau Lake, 1935 (Caranfil,1963)



Figure 3. The effects of Colentina's drainage on Bucharest and the surrounding areas (Caranfil, 1963)

Colentina's water was used in Bucharest for fish breeding, agriculture irrigations and recreational events (Figure 4), (Giurescu, 1979; Caranfil, 1936)



Figure 4. Herastrau Lake, in present

From upstream to downstream, Bucharest is the home of the following lakes : Straulesti, Grivita, Baneasa, Herastrau, Floreasca, Tei, Plumbuita, Fundeni, Dobroesti, Pantelimon and all of them together totalize in a water surface of 1295 hectares.

In the paper we will focus upon 4 lakes, Grivita, Baneasa, Herastrau and Floreasca providing results and conclusions for different standard tests.

Based on the water analysis documents, carried on by the National Administration of Romanian Waters (N.A.R.A) together with the Administration of Lakes, Parks and Recreation Bucharest (A.L.P.R.B), it was concluded that all the lakes along the Colentina River's stream aren't affected by any serious contamination issues.

As the official results state, the pH and ammonium levels, taken during 2007-2010 in

the Grivita Lake were within the accepted limits, as well as the nitrates and nitrites. The only exception was registered in November 2007, when for the nitrates and nitrites, a spike value of 0.42 mg/l was reported (A.L.P.R.B.). In the Baneasa Lake, only the pH has slightly exceed the normal limits; others parameters remained within the accepted boundaries (A.L.P.R.B.). In the Herastrau Lake, the pH, ammonium and nitrates didn't exceed the maximum allowed limits. Isolated, the nitrites went over the norms with a 0.3 mg/l reported value (A.L.P.R.B.). The Floreasca Lake has all the parameters valid according to the standards with only a few isolated cases of an increase pH (8.5), (A.L.P.R.B.).

## MATERIALS AND METHODS

For our tests, we collected water samples from the 4 lakes (Grivita, Baneasa, Herastrau and Floreasca), from upstream to downstream, in March 2015 (Figure 5).



Figure 5. Collecting water samples

All the locations from which we gathered the water samples can be found on the Figure 6.

For each lake, all the references to "left bank" and "right bank" will address the direction of Colentina's stream, which is from north-west to south-east (in general).

All the data was registered and listed in Table 1. All the samples were carried in proper conditions that preserved their initial parameters and kept in brown, sterile bottles at 5°C until all the test began.



Figure 6. Distribution of collecting points along Colentina River

Table1. Details of sampling points

Lake	Coordinates	Altitude (m)	Point number	Location	Depth (m)
GRIVITA	44.50 <sup>0</sup> N 26.02 <sup>0</sup> E	84	1-1	Right bank	0.5
	44.49 <sup>0</sup> N 26.06 <sup>0</sup> E	80	1-2	Left bank	0.5
BANEASA	43.49 <sup>0</sup> N 26.08 <sup>0</sup> E	76	2-1	Right bank	0.5
	44.47 <sup>0</sup> N 25.0 <sup>0</sup> E	72	2-2	Left bank	0.5
HERASTRAU	44.47 <sup>0</sup> N 26.07 <sup>0</sup> E	83	3-1	Right bank	0.5
	44.47 <sup>0</sup> N 26.08 <sup>0</sup> N	81	3-2	Left bank	0.5
FLOREASCA	44.42 <sup>0</sup> N 26.11 <sup>0</sup> E	74	4-1	Right bank	0.5
	44.48 <sup>0</sup> N 26.10 <sup>0</sup> E	60	4-2	Left bank	0.5

All the measurements were done in the Environment Engineering Laboratory, part of the Land Reclamation and Environment

Engineering Faculty - U.A.S.V.M Bucharest. The parameters aimed during our tests were: pH, conductivity, turbidity,

dissolved oxygen (DO), biochemical consumption of oxygen (CBO<sub>5</sub>), chlorine, ammonium and nitrites.

### Measurement of pH, conductivity and dissolved oxygen

Using a multi-parameter device called HANNA HI 9828 equipped with a multi-sensor probe with a dedicated microprocessor we determined the pH, conductivity and the dissolved oxygen, important characteristics in assessing the water's quality.

At first, the probe is immersed in the sample, then easily moved in a circular pattern (2-3 times) until the value displayed by the device stabilizes, followed by the data recording (Figure 7).



Figure 7. Laboratory measurements of pH, conductivity and dissolved oxygen

### Measurement of the turbidity

The turbidity of the samples was determined using a stationary turbidity meter HI 88713. The device has a high precision, being able to provide accurate values in Nephelometric Turbidity Units (NTU). As steps, we first filled a 10 ml container with one of the water sample and placed it afterwards in the turbidity meter; closed the cover, pressed the "READ" button and after approximately 10 seconds we can record the data written on the display's device (Figure 8).



Figure 8. Determining the turbidity with a high precision stationary turbidity meter

### Measurement of the biochemical consumption of oxygen

The biochemical consumption of oxygen is determined with the help of incubation, in dark, at 20°C with the BDO5 Velp Scientifica device together with the proper accessories (Figure 9).



Figure 9. Determining the CBO of the water samples

### Measurement of the chlorine

The chlorine determination was possible by using the Mohr methodology.

The technique uses the titrimetric evaluation of the chlorine content within the water and it's a direct process for finding the chlorine concentrations between 5 mg/l – 400 mg/l. The method is based on the reaction between the chlorinate ions and the silver ions which leads to the appearance of an insoluble silver chlorine (Figures 10, 11).



Figure 10. Determining the chlorine using the titrimetric evaluation



Figure 11. Determining the chlorine using the titrimetric evaluation

### Measurement of ammonium and nitrites

In this case, we used the spectro-photo meter US-VIS PG T60 that can be found in the Environment Engineering Laboratory.

The spectrometric method of molecular absorption for determining the amount of nitrites in the water is standardized according to the SRISO 3048-2:1996 standard.

It's a process that uses the spectrometry in a visible spectrum together with  $\alpha$ -naphthylamine and sulfanilic acid.

Recipients with a 10 mm optical path are used and the absorbance is measured at a 520 nm wavelength (Figure 12).

The manual spectrometric method for finding the ammonium amount in the water is standardized according to the SRISO 7150-1:2001 standard.



Figure 12. Determining the nitrites from the collected samples

It is a performance procedure which uses the spectrometry in a visible spectrum in recipients with an optical path of 40 mm and a sample of 40 ml analyzed at a 650 nm wavelength (Figure 13).

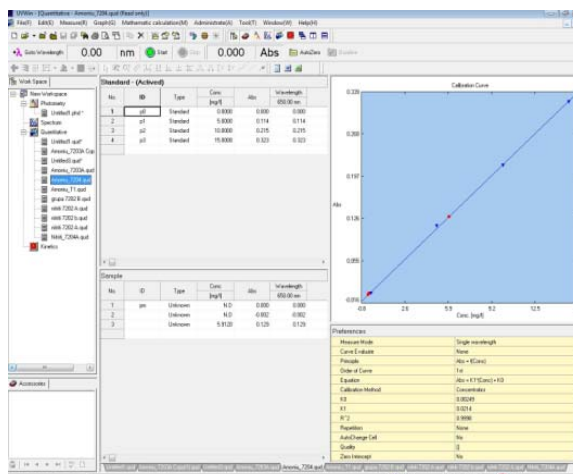


Figure 13. Determining the ammonium in the collected samples

## RESULTS AND DISCUSSIONS

For an accurate review of the water quality we selected 4 lakes to analyze: Grivita, Baneasa, Herastrau and Floreasca.

The relevant chemical parameters for our study and the values resulted after testing was pointed out in Table 2.

From a pH perspective, the water from Colentina River is weak alkaline, but the values are normal for surface water (Table

2). The pH values are ranging between 7.24 and 8.15.

The dissolved oxygen is the most important parameter of water quality from rivers and lakes, because oxygen has a vital importance for the aquatic ecosystems.

The oxygen level in natural water has to be at least 2 mg/l. A decreased level of oxygen leads to eutrophication in lakes.

For the oxygen quality indicator we observe the fitting of all the samples analyzed in the IIIrd class of quality according to OM 161/2006 with values between 5.21 and 5.93 with the exception of the samples collected from Grivita Lake where these values are between 4.59 and 4.73 which put it in the IVth class of quality.

The biochemical consumption of oxygen (CBO) represents the oxygen quantity in mg/l needed to oxidize the organic substances with the help of bacteria.

From lab testing we concluded that it's enough to determine the oxygen consumption after 5 days of preserving the samples (CBO5).

CBO5 values from the analyzed samples fit into the IIIrd class of quality pointing to a weak ecological state of water (Table 2).

Chlorine is found in nearly any type of natural water. The concentration can vary from few mg/l to higher concentration in residual water, in marine water and saline water. In the samples we collected from these lakes, chlorine was found in small amounts, normal for the first class of quality.

The values for ammonium ions, determined from the analysis are in range, except the sample from Baneasa Lake, with a value of 0.82 mg/l.

Ammonia occurs after water pollution by organic substances that undergo decomposition, the first step of degradation nitrogenous substances. Its presence indicates recent pollution.

From the perspective of the nitrites, the quality of water in the samples is in the limits of the first class of quality, presenting no sources of nutrients impurities. A slightly increased value is obtained in samples from Grivita Lake, with a value of 0.032 mg/l (Table 2).

Nitrites are found due to the pollution of water with organic matter, or by partial oxidation of the amino radical or by reducing nitrate.

The occurrence of nitrates in lakes is a bad sign, being observed in low concentration of oxygen. It's dangerous, especially for fishes and can cause eutrophication of lakes.

Turbidity is caused by solid particles that make the water less transparent. In our samples the turbidity had low values from 3.86 to 15 NTU.

Water conductivity is one of the most used indicators to determine the mineralization degree of the water.

In OM 161/2006 conductivity and turbidity aren't standardized.

Table 2. Physico-chemical parameters of water samples

Nr. crt.	Performed testing	M.U.	Sample name/ Determined values		M.O. 161/2006 Class of quality				
			Sample 1 (upstream)	Sample 2 (downstream)	I	II	III	IV	V
<b>Lake GRIVITA</b>									
1	pH	pH units	7.82	7.24	6.5 – 8.5				
2	Dissolved oxygen	mgO <sub>2</sub> /l	4.23	4.59	9	7	5	4	<4
3	BOD	mgO <sub>2</sub> /l	7.21	7.02	3	5	7	20	>20
4	Chlorine	mg/l	274.38	255.24	500	750	1000	1300	>1300
5	Ammonium	mg/l	0.47	0.35	0.4	0.8	1.2	3.2	>3.2
6	Nitrites	mg/l	0.019	0.032	0.01	0.03	0.06	0.3	>0.3
7	Turbidity	NTU	15.5	7.73	Are not standardized				
8	Conductivity	μS/cm	499	496	Are not standardized				
<b>Lake BANEASA</b>									
	pH	pH units	7.48	8.15	6.5 – 8.5				
	Dissolved oxygen	mgO <sub>2</sub> /l	5.21	5.63	9	7	5	4	<4
	BOD	mgO <sub>2</sub> /l	7.25	7.32	3	5	7	20	>20
	Chlorine	mg/l	273.67	770.87	500	750	1000	1300	>1300
	Ammonium	mg/l	0.26	0.82	0.4	0.8	1.2	3.2	>3.2
	Nitrites	mg/l	0.006	0.007	0.01	0.03	0.06	0.3	>0.3
	Turbidity	NTU	6.48	16.9	Are not standardized				
	Conductivity	μS/cm	512	587	Are not standardized				
<b>Lake HERASTRAU</b>									
	pH	pH units	7.33	7.68	6.5 – 8.5				
	Dissolved oxygen	mgO <sub>2</sub> /l	5.71	5.83	9	7	5	4	<4
	BOD	mgO <sub>2</sub> /l	7.23	7.78	3	5	7	20	>20
	Chlorine	mg/l	355.21	299.91	500	750	1000	1300	>1300
	Ammonium	mg/l	0.42	0.45	0.4	0.8	1.2	3.2	>3.2
	Nitrites	mg/l	0.009	0.021	0.01	0.03	0.06	0.3	>0.3
	Turbidity	NTU	6.99	3.86	Are not standardized				
	Conductivity	μS/cm	583	548	Are not standardized				
<b>Lake FLOREASCA</b>									
	pH	pH units	7.66	7.60	6.5 – 8.5				
	Dissolved oxygen	mgO <sub>2</sub> /l	5.87	5.93	9	7	5	4	<4
	BOD	mgO <sub>2</sub> /l	7.44	7.85	3	5	7	20	>20
	Chlorine	mg/l	265.87	443.12	500	750	1000	1300	>1300
	Ammonium	mg/l	0.33	0.29	0.4	0.8	1.2	3.2	>3.2
	Nitrites	mg/l	0.005	0.008	0.01	0.03	0.06	0.3	>0.3
	Turbidity	NTU	14.06	15	Are not standardized				
	Conductivity	μS/cm	500	503	Are not standardized				

Color legend		
	Quality calss I	Ecological state "very good"
	Quality calss II	Ecological state "good"
	Quality calss III	Ecological state "moderate"
	Quality calss IV	Ecological state "weak"
	Quality calss V	Ecological state "bad"

## CONCLUSIONS

Following the determination of water quality, we can mention the following conclusions for the 28 analyzed parameters. pH is within the limits for all the water samples;

The concentration of oxygen dissolved is reduced in the 4 lakes. An important problem was identified for the samples that came from the Grivita lake where the quality degree was 4;

Based on the CBO5 indicator, the water of lake Colentina fits in the IIIrd category of quality;

Chlorine was registered with values under the allowed limit in all 4 lakes;

Nitrites are present within the allowed limits except for the sample collected from the Grivita lake where we can observe an unwanted evolution of this indicator so the quality fits in the second class;

Ammonia indicator was registered with values under the limit, with one exception from Baneasa Lake.

CBO values present an increase from upstream to downstream which means the existence organic pollution. This is confirmed by the OD concentrations which one decrease from upstream to downstream. Further investigations have to be developed in order to ensure that there aren't illegal discharges along the lakes.

Lake's eutrophication can occur as a result of organic pollution so, obviously every

measure of stopping the pollution is welcome. In this sense a program that tracks the quality of Colentina River is very much needed correlated with a strong monitoring of all discharges – both intentional and unintentional.

Based on the water analysis done by the Administratia Nationala Apele Romane and Administratia Lacuri, Parcuri si Agreement Bucuresti between 2007 and 2010 it has been observed that lake indicators on the course of Colentina river were within the normal limits except for the nitrites which in 2007 and today in Grivita lake had a spike of 0.42 mg/l. Today the tendency is towards lightly degradation of the indicators especially the OD and CBO which have a moderately ecological stat

## REFERENCES

- Caranfil N. G., 1963. Efectele asanarii Colentinei asupra Bucurestiului și regiunilor invecinate. Buletinul Institutului Roman de Energie, 4(4), 5-42.
- Giurescu C.C., 1979. Istoria Bucurestilor. Editura Sport-Turism, București, 171.
- Stanescu S.V., 2011. Aspecte ale calitatii apei Raului Colentina pe traseul din Municipiul Bucuresti (Romania), Ecoterra, no. 27.
- \*\*\* Arhivele A.L.P.A.B
- \*\*\* Ordinul 161/2006 pentru aprobarea Normativului privind clasificarea calitatii apelor de suprafata in vederea stabilirii starii ecologice a corpurilor de apa.
- \*\*\* SRISO 3048-2:1996
- \*\*\* SRISO 7150-1:2001

## PHYSICO-CHEMICAL AND MICROBIAL ANALYSIS OF POND WATER FROM USAMV DENDROLOGICAL PARK - BUCHAREST

Mihai FRÎNCU, Corina DUMITRACHE, Andrei Cristian DUMITRIU

Scientific Coordinators: Prof. PhD Carmen CÎMPEANU Lect. PhD Constanța MIHAI

University of Agronomic Sciences and Veterinary Medicine of Bucharest, 59 Mărăști Blvd, District 1,  
011464, Bucharest, Romania, Phone: +4021.318.25.64, Fax: + 4021.318.25.67, Email:  
frincumihai18@yahoo.com

Corresponding author email: frincumihai18@yahoo.com

### Abstract

*The aim of this paper was to evaluate the water quality of the pond from Dendrological Park of our university. In this respect we used physical, chemical and microbiological analysis indicators, according to the Water Framework Directive (2000 /60 / EC). The physico-chemical parameters that we determined were: temperature, turbidity, electrical conductivity, pH and oxygen regime. Microbiological analyzes were performed to determine both the total counts of mesophilic bacteria ( which grow at 22 °C and 37 °C) and the presence of Enterobacteriaceae, especially E. coli (grow on specific medium at 37 °C). Monitoring of all parameters was carried out between July 2014 - March 2015. The results indicate low levels of alterations caused by human action and deviate only slightly from normal.*

**Key words:** pond water quality, physico-chemical parameters, mesophilic bacteria, E. coli.

### INTRODUCTION

The purpose of this study was to evaluate the water quality of the lake from University Dendrological Park.

The pond was created artificially two and a half years ago, by excavating a volume of soil, up to a maximum depth of 2m. The amount of soil removed was used to achieve an alpinarium located near the pond. The bottom of the pit was covered with impermeable PVC liner. The basin was filled with water from the distribution network. Until now, the water was not changed or refreshed. The biocenosis developed in this aquatic system is largely based on microorganism populations, so it's structure is unsaturated one. For this reason, the exchange of matter and energy between biocenosis and biotope are minimal and therefore the degree of self-regulation is very low. Trophic network is undeveloped, dominating the lower trophic cycles (organic matter - saprophytic bacteria or mineral matter - chemoautotrophic and chemolithotrophic

bacteria). On spring time, the lake is breeding habitat for frogs.

To assess water quality in order to inhabit the pond with new species of plants and fish were studied following physico-chemical parameters: temperature, turbidity, electrical conductivity, pH, oxygen and nutrient regime (nitrite, nitrate). Monitoring of all parameters was performed between July 2014 - March 2015, being able to observe their evolution in time.

### MATERIALS AND METHODS

Water quality monitoring involves making measurements that provide information necessary for an accurate assessment of water statement in relation to different effects and variable.

Water samples were collected in sterile containers with a capacity of 100ml, for all sampling stations during the four sessions, three in 2014 (July, September, November) and the other sampling session in March 2015. Samples were taken the morning after noon.

### *Determination of EC*

Electrical conductivity is a measure of the concentration of substances ionized water and is used as the indicator of the degree of mineralization of water. Electrical conductivity (EC) was measured using conductometric sensor (Figure 1). Conductivity calibration was performed with 1 M KCl solution.



Figure 1. Determination of the EC with conductometric sensor

### *Determination of pH*

The pH neutrality defines alkaline or acid water as having values from 0 to 14. Values between 0-6 characterize an acid pH, the 7 designates a neutral pH and alkalinity is between 8-14. Determination of pH was performed using pH sensor (Figure 2). Before taking readings, sensor calibration was performed in solutions of known pH (4, 7, and 9).

### *Determination of oxygen regime*

The oxygen regime shows interest in terms of water pollution. To determine the oxidizability were analyzed following indicators:

- Dissolved oxygen and oxygen saturation water (DO);
- Biochemical oxygen demand after 5 days at 20°C (BOD5);
- Chemical oxygen demand COD-Mn (using potassium permanganate).

### *Determination of Dissolved Oxygen (DO)*



Figure 2. Determination of pH with pH sensor

DO in the water is fixed to manganese hydroxide, manganic hydroxide to form. Manganic hydroxide is reacted with potassium iodide, iodine is released in an amount equivalent to the oxygen dissolved in the water. The iodine is then titrated with sodium thiosulfate in the presence of starch.

In a Winkler glass was added water sample without this bubble. Immediately, using micropipettes, was added to 1 ml of manganese chloride and 1 ml alkaline mixture (KI + NaOH). The vial contents were homogenized by rolling over several times; after complete settling of the precipitate and the supernatant was removed and continued with the addition of 3 ml of HCl up to complete dissolution of the precipitate. Quantitative content was passed in an Erlenmeyer flask and titrated with 0.01N thio-sulphate to obtain straw yellow coloration: after adding 1 ml of starch solution, titration was continued until complete bleaching solution.

### *Determination of BOD5*

Biochemical oxygen demand (BOD5) is the amount of oxygen consumed by the microorganisms over a period of time, biochemical decomposition of organic substances contained in water. The settling time is 5 days at a temperature of 20°C.

To determine the BOD5 we sampled water in two containers of known volume, under aseptic handling identical. The first sample is used to determine dissolved oxygen in water existing at the time of sampling, and the other was used to determine the biochemical oxygen present in the water after 5 days of storage in the dark at 20°C.

The calculation to determine the amount of BOD5 was performed using the following formula:

$$\text{mg BOD5 / l} = A - B$$

A = the amount of oxygen per litre of water existing in the sample at the time of harvest;

B = the amount of oxygen per litre of water existing in the sample after 5 days.

*Determination of COD<sub>Mn</sub>*

Chemical oxygen demand (COD<sub>Mn</sub>) is a global indicator of water pollution. COD determination method using K permanganate, is not recommended for water with high organic load.

In an Erlenmeyer beaker were added 100 ml of the water sample, 10 ml of H<sub>2</sub>SO<sub>4</sub> and 10 ml of KMnO<sub>4</sub>. The mixture is boiled for 10 minutes. After cooling, there were added 10 ml of H<sub>2</sub>C<sub>2</sub>O<sub>4</sub> to fading, followed by titration with KMnO<sub>4</sub> until the appearance of persistent pink colour. The amount of oxygen consumed was calculated using the following formula:

$$\frac{\text{mgO}_2}{\text{dm}^3} = \frac{v \cdot f \cdot 0,08}{v_1 - 2} \cdot 1000$$

V = ml of 0.01N sodium thio- sulphate used in the titration;

F = factor of the 0.01N sodium thio-sulphate solution;

0.08 = mg O<sub>2</sub> equivalent of a ml of 0.01N thio-sulphate;

v<sub>1</sub> = volume of glass, in ml;

2 = volume of reagents introduced for determining oxygen in millilitres.

*Determination of turbidity (T)*

Turbidity characterized water transparency due to the presence of fine particles in

suspension not submitted in time. Determination of turbidity was performed using WTW turbid-meter Turb 355 T / IR Turb 355 by measuring and comparing subjective suspension turbidity water samples analyzed transparency to that of a standard sample (Figure 3). Turbidity was expressed in nephelometric turbidity units (NTU).



Figure 3. Determination of turbidity using WTW Turb 355 T / Turb 355 IR turbidimeter

**RESULTS AND DISCUSSIONS**

Analyzed parameters that define the physical and chemical contamination of the water pond from the Dendrological Park are presented in Table 1.

Analyzed water pH ranges from slightly alkaline (7.96-8.3 for the investigated months of the year 2014) to moderately alkaline (9,1 in March 2015). In general, water surface is characterised by a pH between 6.5 and 8.5. Higher values of pH recorded in March 2015 is due to both lower CO<sub>2</sub> content and lower temperature (5.3 °C) compared with investigated months of 2014 year(Figure 4). The sampling in March was done in the afternoon when the CO<sub>2</sub> content is lower. In fresh water, decreasing temperature increases pH. Waters with high algal growth can show a diurnal change in pH. When algae grow and reproduce they use CO<sub>2</sub>. This reduction causes the pH to increase. This increase in pH may exceed 8.5,

especially during the spring when nutrients are readily available. Therefore, if conditions are favourable for algal growth, the water will be more alkaline. Maximum pH usually occurs in late afternoon, and pH will decline at night when cellular respiration adds CO<sub>2</sub> to water (Tucker and D'Abramo, 2008).

Water temperature vary with sampling seasons, and presented values between 5<sup>o</sup>C.-25<sup>o</sup>C, being correlated with air temperature (Figure 5).

Table 1. Physico-chemical parameter values of the investigate pond water

Parameter	Unit measurement	Admissible level for drinking water	Standards	Sample values			
				Jul	Sept	Nov	March
pH	pH units	≥ 6.5 ≤ 9.5	SR ISO 10523/2009	8.3	7.96	8.1	9.1
Temperatures	°C		-	25.0	21.5	18.4	5.3
DO	mg O <sub>2</sub> /l	6	STAS 6536-87	6.15	6.32	7.7	9.5
(CBO <sub>5</sub> )	mg O <sub>2</sub> /l	3	STAS 6536-87	1.05	1.7	1.92	1.52
(CCO-Mn)	mg/l	5	SR EN ISO 8467/2001	3.95	5.32	6.12	4.67
NO <sub>3</sub> <sup>-</sup>	mg NO <sub>3</sub> <sup>-</sup> /l	50	SR EN 7890-3/2000	73.92	71.6	71.12	59.5
EC	µS/cm	250	SR EN 27888/1997	528	515	508	425
TDS	mg/l	100	STAS 9187:1984	337.9	329.6	325.12	272
Turbidity	NTU	≤ 5	SR EN ISO 7027/2001	4.3	2.58	1.84	4.2

The electrical conductivity showed values between 425 and 528 µS/cm at 25°C (Figure 6), exceeding twice the value of 250 µS/cm indicated by the Water Framework Directive for unpolluted waters. The recorded values reflect load conditions with salt water. Based on EC can appreciate the nitrate content in mg NO<sub>3</sub>/l, if the CE in µS/cm is multiplied by 0.14 (Smith and Doran, 1996). Therefore, the calculations were considered estimates of nitrate concentrations (Table 1). As can be seen analyzed the nitrate content

of water varies between 59.5 and 73.9 mg/l, above 50 mg/l unpolluted water feature. Overtaking highlight an imbalance in the C:N ratio. This imbalance is quite natural if we consider that the aquatic ecosystem studied is undeveloped with lacking plants; only bacteria and cyanobacteria are the dominant species. Knowing the EC we can estimate the total content of dissolved solids (TDS) in mg/l, multiplying the CE in µS/cm with 0.64 (Rhoades, 1993).

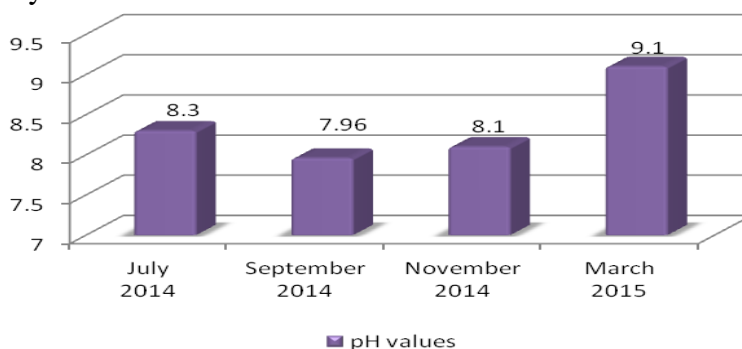


Figure 4. Seasonal pH variation of the pond water from the University Dendrological Park

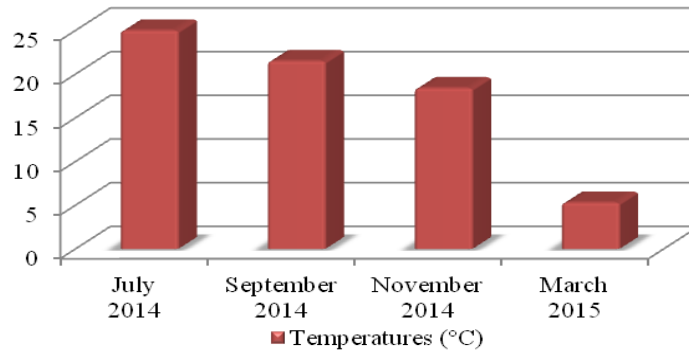


Figure 5. Seasonal temperature variation of the pond water from the University Dendrological Park

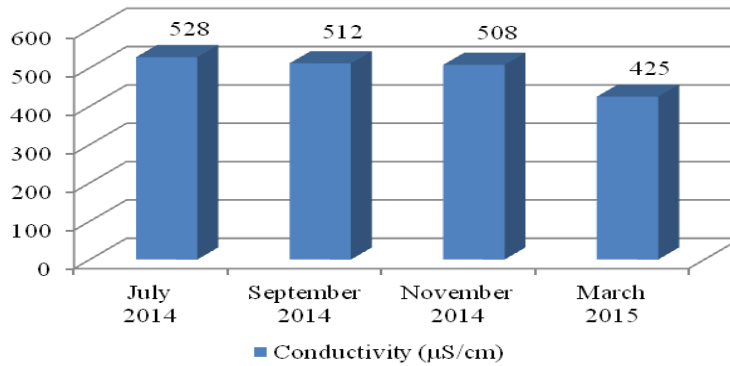


Figure 6. Seasonal Electrical conductivity variation of the pond water from the University Dendrological Park

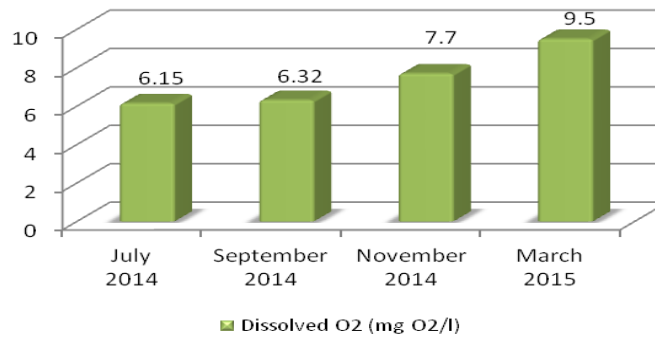


Figure 7. Seasonal dissolved oxygen variation of the pond water from the University Dendrological Park

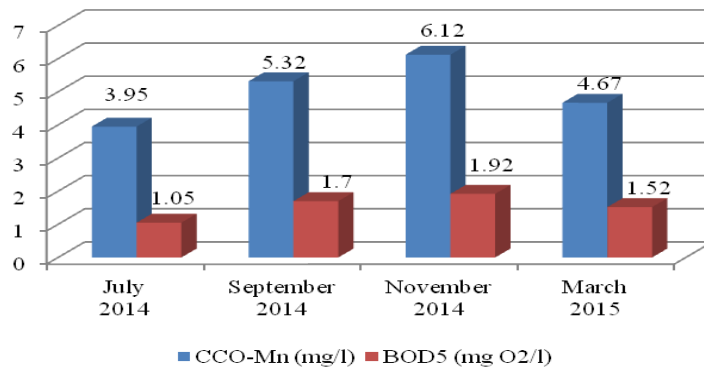


Figure 8. Seasonal COD and BOD variation of the pond water from the University Dendrological Park

Dissolved oxygen vary with the sampling season time. Recorded DO values range between 6.15 and 9.5 mgO<sub>2</sub> / l. The amount of dissolved oxygen varies indirectly proportional with temperature, with turbidity and organic matter values (Trufas, 1998). According to the standard values regarding to water surface quality (161/2006 Normative), the pond water analyzed during summer season fits to III-th quality class (DO range between 5-7 mg/l). DO determined during autumn belongs to II-nd quality class (> 7 mg/l), and the late autumn DO analysed belongs to I-st quality class (> 9 mg/l).

Organic load of the pond water was indirect determined by measure of COD<sub>Mn</sub> and BOD<sub>5</sub>. The COD<sub>Mn</sub> values range from 3.95 to 6.12 mgO<sub>2</sub> / l during the period of study and BOD<sub>5</sub> varied from 1.05 to 1.92 mgO<sub>2</sub> / l (Figure 8). Chemical and biochemical oxygen dements varies directly proportional to the amount of organic matter.

All the values obtained by determining oxygen consumption fit to domain that characterize drinking water (Table 1). Therefore organic matter content of the water is very small, and this fact it is perfectly correlate with lock of plant and animal populations of the investigated pond.

## CONCLUSIONS

In general, the physic -chemical parameter values fit the investigated pond water into II-nd quality water class.

The significant seasonal fluctuations which occurred in quality water of the pond is due to poor aquatic biodiversity and therefore due to reduce self-regulation capacity and low ecosystem integrity.

In summer time, the pond water has a tendency to overheat (25°C) due to increasing air temperatures and low depth of the pond (about

1.5 m). Therefore decreasing DO penalise water quality with a quality class (classifying the pond water into III-th class).

The water nitrate contents are correlated with EC. The sampling during all the seasons showed than nitrate values are higher enough to classification the pond water into III-th quality class.

Biochemical and chemical oxygen demands are low, therefore those parameters qualify the water body into I-st quality class.

These uneven qualities of the water body demonstrate the unstable equilibrium of the pond and certify his very young age (about 2 years from creation).

## REFERENCES

- Craig S.Tucker and Louis R. D'Abramo, 2008. Managing High pH in Freshwater Ponds. SRAC Publication No. 4604
- Clean Water Team (CWT) 2004. pH Fact Sheet, FS-3.1.4.0(pH). in: The Clean Water Team Guidance Compendium for Watershed Monitoring and Assessment, Version 2.0. Division of Water Quality, California State Water Resources Control Board (SWRCB), Sacramento, CA.
- Smith, J.L. si J.D. Doran. 1996. Measurement and use of pH and electrical conductivity for soil quality analysis. p. 169- 185. In: J.W. Doran and A.S. Jones (eds.) Methods for assessing soil quality. Soil Sci. Am. Spec. Publ. 49. SSSA, Madison, WI.
- Roades, J.D. 1993. Electrical conductivity methods for measuing and mapping soil salinity. p.201-251. In: D.L. Sparks (eds.) Advences in agronomy, Vol. 49. Academic Press, Inc, San Diego, CA.
- Trufas, C., 1998. Bazinul hidrografic al Prahovei. Calitatea apelor. Bucuresti, Societatea de Geografie din Romania
- Normativul 161/2006 privind calitatea apelor de suprafata.
- Lucrare de Licenta : " Evaluarea calității apei de suprafață din Parcul Dendrologic microbiologic si biochimic " - 2014. Absolvent Zamfir Radu ,Coordonatori Prof. Carmen Cimpeanu si SL Mihai Constanta

## SOIL FERTILITY ASSESSMENT THROUGH ENZYME ACTIVITY

Mihai FRÎNCU, Corina DUMITRACHE,  
Andrei Cristian DUMITRIU

Scientific Coordinators: Prof. PhD. Carmen CIMPEANU  
Lect. PhD. Constanta MIHAI

University of Agronomic Sciences and Veterinary Medicine of Bucharest, 59 Mărăști Blvd, District  
1, 011464, Bucharest, Romania, Phone: +4021.318.25.64, Fax: + 4021.318.25.67, Email:  
frincumihai18@yahoo.com

Corresponding author email: frincumihai18@yahoo.com

### Abstract

*Soil is an important component of all terrestrial ecosystems as well as fundamental resource in the agricultural production system that why monitoring of soil fertility is an important objective for the sustainable agro-ecosystems development. Changes in its physical, chemical and biological properties must be taken into account, in order to evaluate soil fertility. Biological indicators are suitable tools for predicting and assessing soil changes that are caused by both natural and anthropogenic factors. Among the biological features, soil enzymes are often used as indicator of soil fertility because they are very sensitive and respond to changes in soil management more quickly than other soil variables. In this respect, the objective of this paper was to determine enzyme activity of the soil from USAMV – Bucharest orchard in order to evaluate its fertility.*

**Key words:** soil enzyme activity, dehydrogenases, phosphatases, catalases, soil fertility

### INTRODUCTION

To understand the functioning of soils and to prevent soil damage due to both natural and anthropogenic factors, it is important to have suitable tools for predicting and assessing soil changes that are caused by environmental factors and management practices. Strategies based on biological indicators would be a suitable tool to evaluate the sustainability of the soil ecosystem. Studies of soil enzymes are important since they indicate the potential of the soil to support the biochemical processes that are essential for the maintenance of soil fertility. Soil enzymes regulate the functioning of the ecosystem and play key biochemical functions in the overall process of organic matter transformation and nutrient cycling in the soil system. They also take part in the detoxification of xenobiotics, such as pesticides, industrial wastes, etc. . Soil enzyme activities have been suggested as sensitive indicators of soil fertility since they catalyze the principal biochemical reaction that involves nutrient cycles in soil, are very

sensitive and respond to soil changes and can be easily analyzed within a few days using a small amount of soil

The total enzyme activity in soil consists of distinct intracellular and extracellular enzymes that originate from microorganisms (e.g., bacteria, fungi), from plants and animals (e.g., plant roots or residues, digestive tracts of small invertebrates). The same enzyme can originate from different sources and the exact origin as well as the temporal and spatial variability of their activity is difficult to identify. Intracellular enzymes exist in different parts of living cells, while extracellular enzymes are produced by living cells and secreted outside the cell as free enzymes in the soil solution. Some of these enzymes remain associated with the external surface of the root epidermal or microbial cell wall. The rest of the extracellular enzymes are either free in soil solution or adsorbed by argilo - humic complex. The amounts of free enzyme in soil are very low compared with enzymes adsorbed, due to their short life span [8]. Adsorbed enzymes are usually protected against

degradation but they reveal less activity than free enzymes.

Numerous factors can influence enzyme activity in soil. Natural parameters like seasonal changes, geographic location, in situ distribution, physical-chemical properties, content of clay and organic matter usually affect the enzyme activity level by influencing both the production of enzymes by organisms and their persistence under natural conditions.

The physical and chemical properties of a soil are involved in the immobilization and stabilization processes of most extracellular enzymes. A high content of clay or humus colloids is usually associated with stable but less active enzymes.

Enzyme activities often provide a unique integrative biological assessment of soil function, especially those that catalyze a wide range of soil biological processes, such as dehydrogenase, urease and phosphatase.

## MATERIALS AND METHODS

Enzyme assays were performed on soil samples collected in spring (March 2015) and consist of eight experimental variants: soil planted with fruit trees (apple, plum, apricot) and control (meadow) from a neighboring orchard area, the depths of the sampling were 0-20 cm, and 20-40 cm.

### *Phosphatase activity (PA)*

In order to determine PA was used Kramer and Erdei method (1995). Reaction mixture consisted of: 3 g soil, 2 ml of toluene, 10 ml of 0.5% disodium phenylphosphate solution, 0.3% ammonium alum solution, borax buffer and Gibbs solution. Incubation took place at 37 ° C for 24 hours. Measurements were performed using a spectrophotometer at a wavelength of 620 nm. PA is expressed in mg phenol / g dry weight soil.

### *Catalase activity (CA)*

The action of catalase refers to the decomposition of hydrogen peroxide (H<sub>2</sub>O<sub>2</sub>) with the production of molecular oxygen and water. Catalase activity and enzymatic cleavage of H<sub>2</sub>O<sub>2</sub> in the samples were determined by the method Kappen.

The reaction mixtures for the determination of CA containing: 3g soil, 10 mL of distilled water, 2 ml of 3% H<sub>2</sub>O<sub>2</sub> solution, 10 ml of 4M

H<sub>2</sub>SO<sub>4</sub>, distilled water were titrated with a solution of potassium permanganate (KMnO<sub>4</sub>) 0.05M. Incubation was done at room temperature for one hour. Expression of CA is in mg H<sub>2</sub>O<sub>2</sub> / g soil dry soil.

### *Dehydrogenase activity (DHA)*

DHA was determined with and without glucose added by the Casida method (Casida et al, 1964).

Reaction mixtures consisted of: 3 g soil, 3% TTC solution (chloro-triphenyl-tetrazolium), 1 ml of distilled water, 3% glucose solution, acetone. Incubation took place at 37 ° C for 24 hours. The color intensity directly correlating with DHA was spectrophotometrically determined at a wavelength of 440 nm. DHA is expressed in mg formazan / g soil dry soil.

## RESULTS AND DISCUSSIONS

Soil dehydrogenases are the major representatives of the oxidoreductase enzymes class. The activity of the DHA reflects the total range of the oxidative activity of soil microorganisms and may be considered a good indicator of the oxidative metabolism in soils, and therefore, of microbiological activity. Dehydrogenases oxidize soil organic matter by transferring protons and electrons from organic substrates to inorganic acceptors. Many specific dehydrogenases transfer hydrogen on either the nicotinamide adenine dinucleotide (NAD) or the nicotinamide adenine dinucleotide phosphate (NADP). Throughout mentioned co-enzymes hydrogen atoms are involved in the reductive processes of biosynthesis. These processes are part of the respiration pathways of soil microorganisms and are closely related to the type of soil and air-water conditions.

The DHA of investigated orchard and meadow soils are represent in the table 1. The values indicated a moderate activity of DHA for each soil cultures at each soil depths. This situation is correlate with the unexpected fluctuation of temperatures for this season of year (from 5.3 °C to 16 °C at the moment of samplings). These temperatures inhibit for certainly the normal microorganism developments.

Table 1. Enzyme activities (PA, CA, DHA) of orchard and meadow soils from University of Agronomic Sciences and Veterinary Medicine- Bucharest

Experimental variant	PA ( $\mu\text{g phenol / g soil}$ )	CA ( $\text{mg H}_2\text{O}_2 / \text{g soil}$ )	DHA ( $\mu\text{g formazan / g soil}$ )
<b>Soil Depth 0-20 cm</b>			
Meadow	245	3.2	4.3
Apple trees	210	0.42	4.5
Apricot trees	265	0.54	4.0
Plum trees	240	0.86	4.3
<b>Soil Depth 20-40 cm</b>			
Meadow	275	1.54	4.8
Apple trees	220	0.48	4.5
Apricot trees	225	1.84	4.5
Plum trees	250	1.28	4.3
Low activity values*	<b>&lt; 100</b>	<b>&lt; 0.5</b>	<b>&lt; 1</b>
Moderate activity values*	<b>100-150</b>	<b>0.5-1</b>	<b>1-5</b>
High activity values*	<b>&gt; 150</b>	<b>&gt; 1</b>	<b>&gt; 5</b>

*Phosphatases* are a group of enzymes that are of great agronomic value because they catalyze the hydrolysis of organic phosphorus compounds and transform them into an inorganic form of P, which is then assimilated by plants and microorganisms. Agricultural soils contain phosphatases in varying amount depending on the microbial count, the amount of organic materials, mineral and organic fertilizers, tillage and other agricultural practices. The relationship between the available P content and phosphatase activity in soil is complex. A positive, negative or no relationship can be observed between these properties.

Our study revealed a high PA (Table 1), and that could be correlated with the lack of fertilization in the period of sampling. Generally, a significant and positive relationship between phosphatase activity and P availability is obtained in soils that are not fertilized and/or those that have small amounts of nutrients in which a P deficiency occurs. An inverse relationship between these two parameters is usually observed in soils that are fertilized with P and/or those with a sufficient content of available P. There are

studies that show that phosphatase activity is inversely proportional to the plant available P content, which confirms the thesis that the production and activity of soil phosphatases is connected with the demand of microorganisms and plants for P. Phosphatases are typical adaptive enzymes and their activity increases when the plant available P content decreases. Kinetics studies indicate that orthophosphate ions, which are the product of the reaction that is conducted by the phosphatases, are competitive inhibitors of their activity in soil.

Catalase is an enzyme that catalyzes the decomposition of hydrogen peroxide to water and oxygen. It is a very important enzyme in protecting the cell from oxidative damage by reactive oxygen species (ROS). Likewise, catalase has one of the highest turnover numbers of all enzymes; one catalase molecule can convert approximately 5 million molecules of hydrogen peroxide to water and oxygen each second. Catalase is universal among plants, fungi, and almost all aerobic microorganisms.

Our results showed a low to moderate catalase activity (Table 1), that is correlated well with DHA, and therefore with moderate microbial activity in soils at the sampling times (at 5.3

°C air temperature). In an old article, Heinicke considered that the catalase activity would eventually prove as good an indicator of metabolism as do the temperature and pulse rate in the human body. The highest catalase activity was registered at the tree plantations that budding earlier (e.g. apricot and plum tress).

## CONCLUSIONS

The DHA values indicated a moderate activity for each soil cultures at each soil depths. This situation is correlate with the unexpected fluctuation of temperatures for this season of year (from 5.3 °C to 16 °C at the moment of samplings). These temperatures inhibit for certainly the normal microorganism developments.

The high PA could be correlated with the lock of fertilization in the period of sampling. Generally, a significant and positive relationship between phosphatase activity and phosphorus availability is obtained in soils that are not fertilized (like the University investigated soils).

The moderate catalase activity is correlated well with moderate DHA, and therefore with moderate microbial activity in soils at the sampling times.

## REFERENCES

- Baldrian P (2009) Microbial enzyme-catalyzed processes in soils and their analysis. *Plant Soil Environ* 55: 370-378.
- Baležentienė L (2012) Hydrolases related to C and N cycles and soil fertility amendment: responses to different management styles and agro-ecosystems. *Pol J Environ Stud* 21(5): 1153-1159.
- Skujins J (1978) History of abiotic soil enzymes research: Soil enzymes. (1stedn), Academic Press, New York, USA.
- Burns RG (1983) Extracellular enzyme-substrate interactions in soil. In: *Microbes in Their Natural Environment*. (1stedn), Cambridge University Press, London, UK.
- Burns RG (1983) Extracellular enzyme-substrate interactions in soil. In: *Microbes in Their Natural Environment*. (1stedn), Cambridge University Press, London, UK.

- Gianfreda L, Bollag JM (1996) Influence of natural and anthropogenic factors on enzyme activity in soil. In: *Soil Biochemistry*. (1stedn), Marcel Dekker Inc., New York, Basel, Hong Kong.
- Gianfreda L, Ruggiero P (2006) Enzyme Activities in Soil. In: *Nucleic Acids and Proteins in Soil*. (1stedn), Springer-Verlag, Berlin, Heidelberg, Germany.
- Nannipieri P, Gianfreda L (1998) Kinetics of enzyme reactions in soil environments. In: *Environmental particles – structure and surface reactions of soil particles*. John Wiley, Chichester.
- Nannipieri P, Sequi P, Fusi P (1996) Humus and enzyme activity. In: *Humic substances in terrestrial ecosystems* Elsevier Science, London.
- Nannipieri P, Kandeler E, Ruggiero P (2002) Enzyme activities and microbiological and biochemical processes in soil. In: *Enzymes in the environment. Activity, ecology and application*. (1stedn), Marcel Dekker, New York, USA.
- Kumar S, Chaudhuri S, Maiti SK (2013) Soil dehydrogenase activity in natural and mine soil – a review. *Middle-East J Sci Res* 13(7): 898-906
- Bandick AK, Dick RP (1999) Field management effects on soil enzyme activities. *Soil BiolBiochem* 31:1471-1479.
- Perucci P (1992) Enzyme activity and microbial biomass in a field soil amended with municipal refuse. *BiolFertil Soils* 14: 54-60.
- Amador JA, Glucksman AM, Lyons JB, Görres JH (1997) Spatial distribution of soil phosphatase activity within a riparian forest. *Soil Sci* 162: 808-825.
- Banerjee A, Sanyal S, Sen S (2012) Soil phosphatase activity of agricultural land: A possible index of soil fertility. *AgricSci Res J* 2(7): 412-419.
- Isobe K, Inoue N, Takamatsu Y, Kamada K, Wakao N (January 2006). "Production of catalase by fungi growing at low pH and high temperature". *J. Biosci. Bioeng.* **101** (1): 73–76. doi:10.1263/jbb.101.73
- Stefanic Gh., 1972, Third symposium of soil biology, Romania national society of soil science, 146-148
- Heinicke, A. J., 1922. Catalase activity as an indicator of the nutritive condition of fruit tissues. *Proc. Amer. Soc. Hort. Sci.* 19: 209-214.
- Băbeanu, C., Marinescu, G *On the use of enzymatic methods in the evaluation of fertility at the anthropically degraded soils*, Journal of Environmental Protection and Ecology 6, No 1, 14-18, 2005.
- Activitatea Enzimatică a Solurilor Degradate Comparativ cu a Entantrosolurilor Rezultate prin Nivelarea Haldelor de Steril de la Exploatarea Miniere de Suprafata Letca-Surduc Jud. Sălaj CĂȚINAȘ Ioana1\*, Gheorghe BLAGAI , Maria GHEORGHE2, Laura PAULETTE1, Ioan PĂCURARI, Mihai BUTA1, Mihaela MĂRGINEAN1, *ProEnvironment* 4 (2011) 151 – 153.

## CHOOSING THE OPTIMAL SOLUTION FOR REINTRODUCTION DEGRADED LAND SURFACE INTO THE FOREST CYCLE

Iulia Diana GLIGA, Madalina PRESECAN

Scientific Coordinators: Lect. PhD. Eng. Vasile CEUCA, Lect. PhD. Eng. Alexandru  
COLIȘAR

University of Agronomic Sciences and Veterinary Medicine of Cluj Napoca, No. 3-5, Mănăștur  
Street, 400372, Cluj-Napoca, România; Email: iuliagliga@yahoo.com

Corresponding author email: iuliagliga@yahoo.com

### Abstract

*The aim of this study is to determine the ecotop parameters used for restoration of degraded lands, which are not recommended to other uses. Afforestation reduces the extreme values of climatic factors (temperature, Evapotranspiration, wind speed); improves the air humidity and soil moisture; and favors site conditions for maintaining herbaceous and forestry vegetation development. The decreasing of land degradation and the gradually restoration of productive capacity under the direct effect of forest cultures could be analyzed by variation of precipitation retention by canopy. The results regarding canopy retentions were obtained by placing in situ several rain gauges with height of 25 cm and 100 cm. The precipitations retentions by canopy values were computed by the difference between the amount of rainfall recorded in open grounds and average values recorded at rain gauge installed in land cover with trees (in forest). Rains were grouped into classes, and the rainfall for each class being calculated as mean value of precipitation retained. The data obtained were highlighted with correlation between rainfall inside the forest and rainfall outside the forest. The curves of retention in the canopy layer were plot according to the height of rainfall and some characteristics of trees (species, age, consistency). The frequency of days with precipitation ranged from one month to another and from one season to another. The data set analyzed showed that rainfall triggered surface runoffs in seven day (5% of the total days computed). The slope of regression between monthly average rainfall index and the amount of rainfall previously recorded expresses an increase from a drought year to a rainy year. The average rainfalls per square meter inside the stand increased with the amount of rainfall quantity, the highest values were registered over 70 mm. Maximum discharge coefficients, determined by class of precipitation, highlighted the influence upon runoffs: the maximum value (0,219) being achieved by precipitation from 0 to 10 mm, although the maximum rainfall is obtained in the precipitation of more than 50 mm. Based on the computed data were determined regression equations between the runoffs amount and precipitation quantity, also, between rainfalls quantity and standard deviation of previous monthly.*

**Key words:** Degraded land, rainfall, surface drain, the canopy retention.

### INTRODUCTION

The situation of the degraded lands is a current issue, especially in the context of the decrease of surfaces covered with forest vegetation at national level. The re-introduction of these lands in the forest cycle is a priority in current and future actions of foresters, the importance of these actions resulting from: preventing soil erosion and its degradation; maintaining the category of use, the wood biomass production capacity, which is a very important element in the economy; the retention capacity of the carbon; the production of oxygen; creating the specific microclimate of the forest, which is a

particularly important factor from the socio-economic point of view.

In order to choose the optimum solution for the re-introduction in the forest cycle of the degraded land surfaces, one of the research methods is the study of water retention in the canopy, which represents the amount of water retained in stands' canopy, the latter depending on one hand on the structure and characteristics of the stand (species, age, consistency, quality of crown, surface of foliage) and, on the other hand, on the characteristics of rainfall (quantity of precipitation, duration and intensity of variation) and atmospheric conditions when rain occurs.

## MATERIAL AND METHOD

The present study was carried out within the improvement perimeter of Vaida Camaras, which covers a total area of 46 ha; a total number of 25 sample surfaces were set-up, covering an area of 2,000 square meters, the total area subject of the study being of 5 ha, which is about 11% of the surface of the Vaida Camaras improvement perimeter. The settlement of the sample plots was carried out using the grid method.

The types of stands taken into study were mixed stands, pine and acacia, their proportion of participation being in varying percentages in the content of the stand. Species were planted on bio-groups.

In order to quantify the amount of precipitation, a number of handcraft rain-gauges made of plastic bottles with a receiving surface 100 cm<sup>2</sup> were placed on the studied perimeter.

For the determination of the amount of precipitation retained by the canopy, one also placed rain-gauges in open field to be used as control.

Measurements were carried out during two growing seasons (2013 - 2014), between 15 March and 15 November, so as to quantify only the amount of liquid precipitation. The value of the retention in the canopy was obtained as difference between the amount of rain registered in the open field and the average of values recorded by the rain-gauges installed on the experimental plots within the forest.

In order to determine the variation of retention in the stands with different structural characteristics: composition, age, consistent, the experimental plots were installed as it follows:

- the first set of experimental surfaces, consisting of 7 sample surfaces, in the W of the improvement perimeter, where the stand has a composition of 7Pine 3Acacia, age 50, consistency 0.8.

- the second set of experimental surfaces, consisting of 6 sample surfaces, were placed in the N of the perimeter, being characterized by a composition of 8Pine 2Acacia, age 80, consistency 0.6.

-the third group of experimental surfaces,

consisting of 6 sample surfaces, were positioned in the E of the perimeter, having the following characteristics: 7Acacia 3Pine composition, age 70 and consistency 0.7.

- the fourth set of experimental surfaces, consisting of 6 sample surfaces, were located in the S of the perimeter, area characterized by a 6Pine 4Acacia composition 6, age 80, consistency 0.6.

The rainfalls were grouped into classes of precipitation, for each class of precipitation being calculated the average of precipitation retained in the canopy. The results obtained were used to draw graphs and to make correlations between the precipitation in open field and the ones inside the forest.

## RESULTS AND DISCUSSIONS

According to data, the frequency of days with precipitation is approximately equal for the two years taken into consideration, the lowest number of precipitation (88 mm) being registered in 2014, while the highest (90 mm) was registered in 2013. Concerning the distribution of precipitation on months, this varies from one year to another. As shown in Figure 1, in 2013 the months with the highest number of precipitation were March, June and September and the months with the fewest number precipitation registered were April and July. In 2014, the months with the highest number of precipitation were April, May and July and the fewest in June and November.

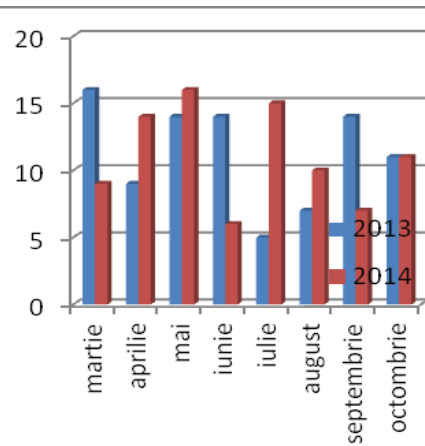


Figure 1. Number of days with precipitation

Analyzing the data regarding the amount of precipitation during the two years period,

when the research was carried out, one reached the following conclusions:

-for 2013, daily, the maximum amount of precipitation was registered on the 25th of June, when it reached 23 mm, while the rainiest month was June, the value of precipitation totalling 104 mm; the driest month was July, registering only 5 days with precipitation (28 mm)

-for 2014, the maximum daily level of precipitation was registered on the 23rd of July - 48 mm; from the month point of view, the rainiest month was July, with a value of approximately 118 mm, while the lowest amount of precipitation was registered in September and it was about 26 mm.

The retention of precipitation in the canopy was studied for the mixed stands, pine and acacia. Due to the fact that the duration of the observations was different (depending on the periods of setting the experimental surfaces), in order to compare and interpret the results, the rainfalls were grouped into classes of precipitation, establishing both average values (mm) of retention and the retention percentage for each class.

Table 1. Number of rainfalls registered and the retention in the stand consisting of:

Class of precipitation (mm)	Number of rainfalls registered and the retention in the stand consisting of:								
	Pine consistency/ age						3 Acacia and 7 pine consistency/ age		
	0,8/50			0,6/80			0,7/70		
	Nr. of events	Retention		Nr. of events	Retention		Nr. of events	Retention mm	%
mm		%	mm		%				
0-5	216	1.7	34	216	1.5	18	222	2.2	20
5-10	12	2.2	22	12	2.1	16	10	1.8	19
10-15	9	3.1	20.8	9	2.8	15	12	4.8	20
15-20	4	4.4	22	4	4.1	11	6	2	14
20-25	2	4.8	19.2	2	4.4	8.5	5	1.8	19
25-30	3	5.9	19.6	3	5.3	9.2	3	1	18
35-40	0	0	0	0	0	0	3	1.7	11
Total perioda	246	446	21	246		24	246		27

In pine stands, where the interception was characterized by the same number of events, differences were registered due to the age and consistency of the stand. Thus, the pine stand

of smaller age (50 years) and consistency (0.8) retained only 14% of precipitation, as compared with the 16% registered by the pine stand aged 80 years and with consistency 0.6. The lower values registered in the first case can be explained by the fact that in this stand no tending was carried out until now, the stands' canopy being unevenly developed and, in terms of the presence of foliar mass, it suffers due to its under-development. The mixed stand (acacia and pine) retained 19% of the precipitation. This high percentage is due to both a greater number of rainfall events registered and the presence of acacia that has characteristic foliage, determining a large area of retention.

The results obtained underline a fairly large variation of the percentage of retention in relation to the total amount of precipitation. Obviously, this variation (from 8.5% to 34%) is due not only to the amount of precipitation, but also to other characteristics of the stands (intensity, duration, composition of the canopy, age, consistent, etc.). However, the influence of the quantity is considered to be essential, especially since, after the increasing of the class interval from 0 to 5 mm, one could achieve the differentiation between the three types of compositions from the experimental surfaces in terms of water retention capacity in the canopy .

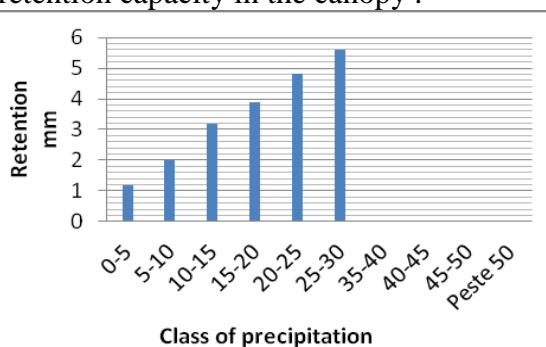


Figure 2. Distribution of retention in the canopy on classes of precipitation

It can be seen that the highest amount of precipitation retained by the canopy was registered in the class of precipitation 25-30 mm, followed by the class of precipitation 20-25 mm and the lowest value was registered in the class of precipitation 0-5 mm. It is to be noticed the fact that for the classes of precipitation over 30 mm the retention was 0, because during the period of time taken into

study, no values of precipitation over 30 mm were registered.

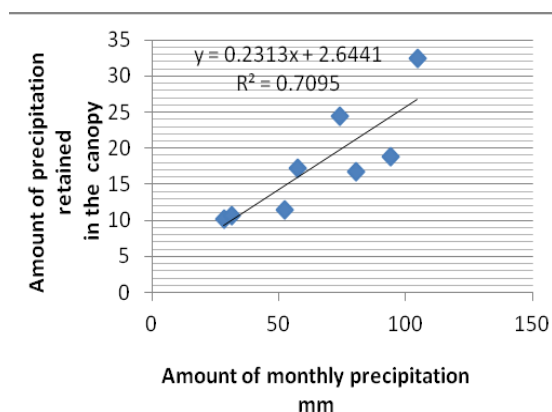


Figure 3. Correlations regarding the amount of monthly precipitation and the retention in the canopy

Analyzing figure 3, it can be concluded that between the amount of precipitation retained in the canopy and the amount of monthly precipitation in 2013, a direct and significantly distinct connection ( $r^2 = 0.7095$ ) can be established, according to the regression equation for each 10 mm of rainfall registered in 2013, the level of retention in the canopy was 2.4128 mm, respectively a rate of approximately 24% for the entire stand taken into study.

## CONCLUSIONS

For the two years during which the experiences were carried out, the precipitation registered variations both in terms of monthly quantities and intensity, as well as in terms of their frequency.

For the period between March 2013 and October 2013, the cumulative period of time with precipitation was of 90 days, when this event was reported, 84% of them being short term precipitation. In pine stands, the differences registered were induced by the age- and consistency of the stand.

The pine stand of smaller age (50 years) and consistency (0.8) retained only 14% of precipitation, as compared with the 16% registered by the pine stand aged 80 years and with consistency 0.6.

The lower values registered in the first case can be explained by the fact that, in this stand, no tending was carried out the work up to the present moment.

Within the portions of the stand where the composition was a fine mix of pine and acacia, the amount of precipitation was significantly higher in the studied interval, mainly due to the increased surface for the retention of the foliage in the acacia canopy, characteristic to deciduous species.

The installed stand is managed in the high-forest system, all trees fitting in the same class of age, the variables being represented by the composition and consistency. Within the perimeter studied and analyzed during the two experimental years, the exponential regression equations established a direct and significantly distinct connection between the amount of precipitation retained in the canopy and the amount of precipitation registered.

In the present study, the percentage of precipitation retained in the canopy registered an average of 20% for the portion of the pine stand aged 60 years and consistency 0.8; 23% on the portion of the pine stand aged 80 years old and consistency 0.6, and the highest value retention was recorded in the portion of mixed stands, where the composition was 7Pine 3Acacia, with values of 26%.

The optimal solution concerning the regeneration composition of the stand taken into study is the one which states the introduction of acacia; according to the carried out research, the amount of water that reaches the ground is able to generate erosion processes, which in the present situation is the lowest.

## REFERENCES

- Arghiriade, C., Abagiu, P., Ceucă, G., 1960: Contribuții la cunoașterea rolului hidrologic al pădurii. Studii și cercetări I.C.F. Editura Agrosilvică, București.
- Arghiriade, C., 1968: Cercetări privind capacitatea de retenție a apei în culturile tinere de protecție de pe terenurile degradate. Centrul de Documentare Tehnică pentru Economia Forestieră, București.
- Barbu, I., Popa, I., 2005: Variabilitatea spațio-temporală a coeficientului de variație al precipitațiilor în România. Analele ICAS, Vol. 48, pp. 3-20.
- Gaspar, R., 1988: Metoda de evaluare a scurgerii de suprafață generată de ploi în bazine hidrografice mici. In: Revista Pădurilor No. 3, pp.150-157.

## **PARTICULATE MATTER SIZE DISTRIBUTION AND COMPONENT ANALYSIS IN BULENT ECEVIT UNIVESITY FARABI CAMPUS, ZONGULDAK, TURKEY**

**Eren KARAKAVUZ**

**Scientific Coordinator: Prof. PhD. Yılmaz YILDIRIM**

Bülent Ecevit University, Environmental Engineering Department İncivez / ZONGULDAK – TURKEY, Phone: +903722574010, Fax: +903722572140 Email: karakavuz@gmail.com

Corresponding author email: karakavuz@gmail.com

### **Abstract**

*Air pollution by aerosol particles was evaluated in a site near BulentEcevitUniversityFarabi Campus in Zonguldak, TURKEY. The location was influenced by both road traffic emissions and domestic heating emissions. The experiment was done on January, 2015. Eight stage non-viable Andersen cascade impactor was used in the experiment. Collected particles were weighted and total particulate matter concentration was calculated  $143\mu\text{g}/\text{m}^3$  which is accepted as “critical” in air pollution control regulations in TURKEY. Eight stage values were converted to  $\text{PM}_{10}$ ,  $\text{PM}_{2.5}$  and  $\text{PM}_1$  values. Aim of the work was to estimate the effect of airborne particles on human health. Collected particles were analysed in Epsilon 5 X-Ray Fluorescence (XRF) spectrometer and content of particle matter were calculated.*

**Key words:** Particulate matter, Cascade impactor, XRF, Road traffic emissions, Domestic heating emissions.

### **INTRODUCTION**

Airborne particle associated problems, such as health problems (e.g. asthma problems; Anderson et al., 1992) and haze problems (e.g. visibility impairment; Pryor et al., 1997) are typical environmental issues in urban cities. The chemical composition, health impact, and rate of deposition of these particles vary significantly with the size of particles. Also different aerosol emission sources tend to have different aerosol mass size ranges (Y.C. Chan et al. 2005)

Concentrations of particulate matter in the ambient air are typically composed of complex mixtures of chemical species, originating from a wide range of natural sources and human activities. (Horikawa et al., 1991; Larsen and Larsen, 1998).

Several studies on the concentration of particulate matter have been reported in the literature (Lee et al., 1995; Sahu et al., 2001; Guo et al., 2003)

Zonguldak province has coal deposits. There are two thermal power plants, one iron and steel plant in Zonguldak region. Domestic heating and increasing number of vehicles features air pollution studies in Zonguldak

region. It is thought that particulate matter concentrations can be high in this region but only one study has been carried out at one point with an high volume air sampler. (Akyüz M, Çabuk H., 2008).

Particulate matter size and component analysis in this region has not been studied and this will show the effective pollution sources.

### **MATERIALS AND METHODS**

#### **General Sampling Method**

In this study The Andersen 1 ACFM Non-Viable Ambient Particle Sizing Sampler was used. The Andersen 1 ACFM Non-Viable Ambient Particle Sizing Sampler is a multi-stage, multi-orifice cascade impactor which normally is used in the environmental working areas to measure the size distribution and total concentration levels of all liquid and solid particulate matter.

A brief description of the operation of the sampling equipment follows;

1. Ambient gases enter the inlet cone and cascade through the succeeding orifice stages with higher orifice velocities form stage 0 to stage 7. Successively

- smaller particles are inertially impacted onto the collection plates.
- The clean gases are carried the vacuum tube and through the pump and exhausted.
  - A constant air sample flow of 1 ACFM is provided by a continuous duty, carbon-vane vacuum pump.
  - After sampling is completed, the sample time is recorded and tared collection plates and backup filter are removed for subsequent gravimetric and/or chemical determination.
  - Concentration levels are determined and the size distribution is plotted.

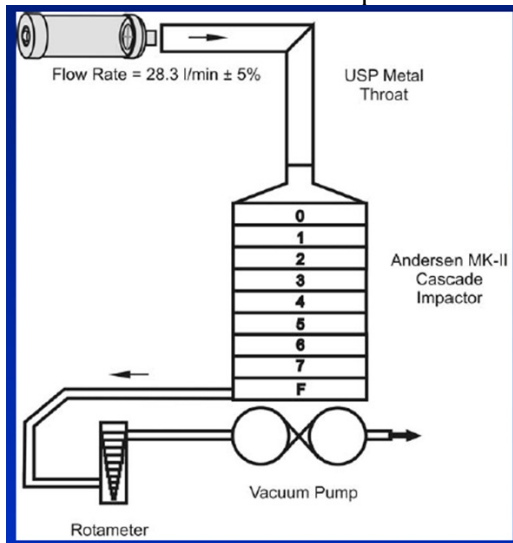


Figure 1. Working Principle of Cascade Impactor System

### Study Area and Sampling

To determine particulate matter amount, sampling point was selected at Bulent Ecevit University Farabi Campus.



Figure 2. Sampling point

Sampling period was between 05 January 2015-12 January 2015 and 24 hours each day. Flow rate of the pump was 28,3 l/min.

Before sampling filters were conditioned. Filters were heated at 103 °C at incubator for 1 hour and then filters were taken to a desiccator for 2 days at 20°C /%50±2 humidity and weighed. After

conditioning sampling was done. After sampling, filters were transferred to laboratory and taken to a desiccator for 2 days at 20°C /%50±2 humidity. Filters were weighed and amount of particulate matter was calculated.



Figure 3. Filter conditioning

## RESULTS AND DISCUSSIONS

Table 1 shows the results of the weighted filters and concentration of particulate matter. Concentration of total particulate matter was calculated 143 µg/m<sup>3</sup> which is accepted as “critical” in air pollution control regulations in Turkey.

Collected particles were analysed in Epsilon 5 X-Ray Fluorescence (XRF) spectrometer and content of particle matter were determined. XRF results were given at Table 2, Table 3 and Table 4 respectively.

## CONCLUSIONS

Calculated values show that particulate matter concentration in Bulent Ecevit University Farabi Campus is in critical levels. To determine the source of pollution studies will continue until summer. There are 3 factors that affect the results; domestic heating, traffic emissions and thermal power plant for Zonguldak. Samplings will continue at 3 different locations to determine sources.

## ACKNOWLEDGEMENTS

This research work is being carried out with the support of Bulent Ecevit University Scientific Research Projects Department with No 2014-770-473-30-05

Table 1. Concentration of particulate matters

Campus Area 1		Campus Area 1							
Filter Weigh Before Sampling		Filter Weigh After Sampling		a-b		dp (µm)	Stages	Weight %	Total %
	a		b						
K-1-1	0.2859	K-1-1	0.2868	0.0009	gr	> 9.0	Stage 0	14.75409836	14.75409836
K-1-2	0.285	K-1-2	0.2854	0.0004	gr	5.8-9.0	Stage 1	6.557377049	21.31147541
K-1-3	0.286	K-1-3	0.2864	0.0004	gr	4.7-5.8	Stage 2	6.557377049	27.86885246
K-1-4	0.2862	K-1-4	0.2868	0.0006	gr	3.3-4.7	Stage 3	9.836065574	37.70491803
K-1-5	0.2875	K-1-5	0.2878	0.0003	gr	2.1-3.3	Stage 4	4.918032787	42.62295082
K-1-6	0.2868	K-1-6	0.2878	0.001	gr	1.1-2.1	Stage 5	16.39344262	59.01639344
K-1-7	0.2858	K-1-7	0.2871	0.0013	gr	0.65-1.1	Stage 6	21.31147541	80.32786885
K-1-8	0.286	K-1-8	0.2869	0.0009	gr	0.43-0.65	Stage 7	14.75409836	95.08196721
K-1-9	0.2853	K-1-9	0.2856	0.0003	gr	< 0.43	F	4.918032787	100

Table 2. XR-F results for Sample Number 1 and 2

1 - 1					1 - 2				
Compound	Corr.(cps/mA)	Conc.	Unit	Status	Compound	Corr.(cps/mA)	Conc.	Unit	Status
Na	1.073	7.046	%	Calibrated	Na	1.080	7.068	%	Calibrated
Al	6.152	3.314	%	Calibrated	Al	5.985	3.215	%	Calibrated
SiO2	133.279	79.245	%	Calibrated	SiO2	134.088	79.324	%	Calibrated
S	0.204	227.510	ppm	Calibrated	S	0.247	275.081	ppm	Calibrated
Cl	2.270	1409.250	ppm	Calibrated	Cl	2.548	1576.302	ppm	Calibrated
K	245.187	4.955	%	Calibrated	K	246.106	4.957	%	Calibrated
Ca	140.933	2.512	%	Calibrated	Ca	140.575	2.497	%	Calibrated
Ti	340.640	0.308	%	Calibrated	Ti	33.239	0.300	%	Calibrated
Fe	12.909	637.118	ppm	Calibrated	Fe	12.562	617.590	ppm	Calibrated
Ni	0.610	14.978	ppm	Calibrated	Ni	0.565	13.813	ppm	Calibrated
Zn	934.781	1.784	%	Calibrated	Zn	936.476	1.780	%	Calibrated
Rb	0.846	4.563	ppm	Calibrated	Rb	0.688	3.695	ppm	Calibrated
Sr	2.343	102.552	ppm	Calibrated	Sr	2.376	103.567	ppm	Calibrated
Zr	1.815	61.027	ppm	Calibrated	Zr	1.896	63.522	ppm	Calibrated
Pd	0.151	2.879	ppm	Calibrated	Pd	0.150	2.848	ppm	Calibrated
Ag	0.341	6.545	ppm	Calibrated	Ag	0.403	7.701	ppm	Calibrated
Ba	245.926	0.590	%	Calibrated	Ba	248.294	0.594	%	Calibrated
Sum		100.000	%		Sum		100.000	%	

Table 3. XR-F results Sample Number 4 and 6

1 - 4					1 - 6				
Compound	Corr.(cps/mA)	Conc.	Unit	Status	Compound	Corr.(cps/mA)	Conc.	Unit	Status
Na	1.064	6.882	%	Calibrated	Na	1.038	6.837	%	Calibrated
Al	6.238	3.363	%	Calibrated	Al	6.165	3.324	%	Calibrated
SiO2	132.984	79.250	%	Calibrated	SiO2	133.229	79.358	%	Calibrated
S	0.149	166.431	ppm	Calibrated	S	0.417	467.921	ppm	Calibrated
Cl	3.732	0.232	%	Calibrated	Cl	2.461	1534.336	ppm	Calibrated
K	246.369	5.002	%	Calibrated	K	248.170	5.040	%	Calibrated
Ca	137.965	2.472	%	Calibrated	Ca	137.902	2.473	%	Calibrated
Ti	34.822	0.316	%	Calibrated	Ti	34.324	0.312	%	Calibrated
Fe	11.938	591.985	ppm	Calibrated	Fe	11.977	594.294	ppm	Calibrated
Ni	0.453	11.171	ppm	Calibrated	Zn	930.307	1.784	%	Calibrated
Zn	933.261	1.789	%	Calibrated	Rb	0.741	4.015	ppm	Calibrated
Rb	0.875	4.780	ppm	Calibrated	Sr	2.355	103.518	ppm	Calibrated
Sr	2.392	105.065	ppm	Calibrated	Zr	1.904	64.295	ppm	Calibrated
Zr	1.937	65.374	ppm	Calibrated	Pd	0.158	3.020	ppm	Calibrated
Pd	0.044	0.826	ppm	Calibrated	Ag	0.371	7.133	ppm	Calibrated
Ba	248.726	0.598	%	Calibrated	Ba	246.894	0.594	%	Calibrated
Sum		100.000	%		Sum		100.000	%	

Table 4. XR-F results Sample Number 8

1 - 8				
Compound	Corr.(cps/mA)	Conc.	Unit	Status
Na	1.069	7.044	%	Calibrated
Al	5.770	3.120	%	Calibrated
SiO2	133.606	79.416	%	Calibrated
S	0.326	364.463	ppm	Calibrated
Cl	2.537	1579.355	ppm	Calibrated
K	246.221	4.992	%	Calibrated
Ca	137.734	2.464	%	Calibrated
Ti	32.618	0.296	%	Calibrated
Fe	12.039	595.603	ppm	Calibrated
Zn	939.048	1.796	%	Calibrated
Rb	0.748	4.020	ppm	Calibrated
Sr	2.493	109.429	ppm	Calibrated
Zr	1.836	61.934	ppm	Calibrated
Pd	0.197	3.748	ppm	Calibrated
Ag	0.452	8.693	ppm	Calibrated
Ba	249.385	0.600	%	Calibrated
Sum		100.000	%	

## REFERENCES

- AyşeBozlaker, AysenMuezzinoglu, Mustafa Odabasi (2007). Atmospheric concentrations, dry deposition and air–soil exchange of polycyclic aromatic hydrocarbons (PAHs) in an industrial region in Turkey. *Journal of Hazardous Materials* 153 (2008) 1093–1102
- Cindoruk, S.S., Tasdemir, Y., 2007. The determination of gas phase dry deposition fluxes and mass transfer coefficients (MTCs) of polychlorinated biphenyls (PCBs) using a modified water surface sampler (WSS). *Science of the Total Environment* 381, 212e221.
- Esen, F., Cindoruk, S.S., Tasdemir, Y., 2006. Ambient concentrations and gas/particle partitioning of PAHs in an urban site in Turkey. *Environ. Foren.* 7, 303–312.
- EylemDemircioglu, AysunSofuoglu, MustafaOdabasi (2010). Particle-phase dry deposition and air–soil gas exchange of polycyclic aromatic hydrocarbons (PAHs) in Izmir, Turkey. *Journal of HazardousMaterials* (Article in Pres).
- Garban, B., Blanchoud, H., Motelay-Massei, A., Chevreuil, M., Ollivon, D., 2002. Atmospheric bulk deposition of PAH's onto France: Trends from urban to remote sites. *Atmospheric Environment* 36, 5395e5403.
- Golomb, D., Barry, G., Fisher, G., Varanusupakul, P., Koleda, M., Rooney, T., 2001. Atmospheric deposition of polycyclic aromatic hydrocarbons near New England coastal waters. *Atmospheric Environment* 35, 6245e6258.
- Mehmet Akyüz, Hasan Çabuk.(2008). Particle-associated polycyclic aromatic hydrocarbons atmospheric environment of Zonguldak, Turkey. *Science of the Total Environment* 405, 62–70
- Park, J.S., Wade, T.L., Sweet, S.T., 2002b. Atmospheric deposition of PAHs, PCBs, and organochlorine pesticides to Corpus Christi Bay, Texas. *Atmospheric Environment* 36, 1707–1720.
- Tsapakis, M., Apostolaki, M., Eisenreich, S., Stephanou, E.G., 2006. Atmospheric deposition and marine sedimentation fluxes of polycyclic aromatic hydrocarbons in the Eastern Mediterranean Basin. *Environmental Science and Technology* 40, 4922–4927
- ÜlküAlverŞahin, BurcuOnat, BaktygulStakeeva, Tuba Ceran, Pınar Karim 2012 PM 10 concentrations and the size distribution of Cu and Fe-containing particles in Istanbul's subway system *Transportation Research Part D* 17 (2012) 48–53
- Y.C. Chan, P.D. Vowles, G.H. McTainsh, R.W. Simpson, D.D. Cohen, G.M. Bailey, G.D. McOrist 2005 Characterisation and source identification of PM10 aerosol samples collected with a high volume cascade impactor in Brisbane Australia *The Science of the Total Environment* 262 2000 5 ] 19

## DESIGN OF A PRECAST REINFORCED CONCRETE BRIDGE ON THE „VALEA ROȘIE” MAIN FOREST ROAD, KM 1+110

Paul MĂRGINAS, Ervin SCHLESINGER

Scientific Coordinator: Lect. PhD. Eng. Vasile CEUCA

University of Agronomic Sciences and Veterinary Medicine of Cluj Napoca, 3-5 Mănătur St.,  
400372, Cluj-Napoca, Romania

Corresponding author e-mail: paulicim@gmail.com

### Abstract

*This project contains the designing of a precast reinforced concrete bridge on main forest road “Valea Roșie”, km 1+110. The bridge will be sized for 2<sup>nd</sup> category of loading (according to STAS 3221-74) and it will be designed with one lane. The hydraulic capacity was determined after the flow hazard and river geomorphology. It is necessary to size the main beams of the bridge to support the load, the bending moments and the oblique section of them. The deck size must be calculated to resist its own weight and the layers above it. There are differences between beam and deck design; the load being the common factor design for both. The final phase consists of predimensioning, designing and verification of abutment. The design process ends with determining optimal size in correlation with service the bridge is expected to provide. This project contains the designing of a precast reinforced concrete bridge on the “Valea Roșie” main forest road, km 1+110. The bridge will be sized for 2<sup>nd</sup> category of loading (according to STAS 3221-74) and it will be designed with one lane. The hydraulic capacity was determined based on the flow hazard and river geomorphology. It is necessary to size the main beams of the bridge so as to support the load, the bending moments and their oblique section. The deck size must be calculated to resist its own weight and the layers above it. There are differences between beam and deck design, the load being the common factor design for both. The final phase consists of predimensioning, designing and verification of abutment. The design process ends with determining the optimal size in correlation with service the bridge is expected to provide.*

**Key words:** flow hazard, river geomorphology, lateral erosion

### INTRODUCTION

The space for water flow under the bridges is sized at maximum flows, with higher or lower probabilities of occurrence depending on the class of importance they are assigned to. The bridges and culverts located on forest roads are dimensioned in terms of hydraulic for the same degree of protection (insurance) as the roads they serve.

It is considered that a bridge operates under normal conditions when the water leakage occurs by ensuring adequate space for floating debris moving. In these conditions, a long time operation does not endanger traffic on the bridge.

The flow calculation  $Q_c$  is the water flow at which the dimensional elements of the bridge (opening, deck bench-mark, depth of foundation, etc.) are calculated and has a theoretical probability of exceeding equal to

the degree of protection required for normal operating conditions.

As compared to the flow calculation  $Q_c$ , the verification flow  $Q_v$  is a higher water flow which enables the verification of the applied solution. It has the probability of exceeding equal to the degree of protection required for special operating conditions. At this level, the operation of the bridge is limited to short periods of time. When the verification flow  $Q_v$  is determined using indirect methods, its value is increased by 20%.

### MATERIALS AND METHODS

For the execution of the bridge's design and its use in safety conditions, it was necessary to determine several parameters, as it follows: hydraulic calculation of the bridge, to determine the maximum water flows, depending on the class of importance the bridge is enclosed to; calculation of the main

beams of the bridge, which is done according to the loads they are subjected to, requests and resistance to bending moments; calculation of the component slabs; predimensioning, calculation and verification of abutment.

## RESULTS AND DISCUSSIONS

Building a bridge over a stream changes its natural flow regime. The reduction of section through partial occlusion of the riverbed by bridge piers and abutments determines an increasing speed under the bridge and its level upstream the bridge. Increased water velocity subject to a modified regime as compared to the natural one, should be moderate so as not to brutally affect the natural balance of the riverbed, not to cause dangerous scouring for the bridge foundations or other downstream arrangements.

Water flow and velocity at a given level are determined using the relations:

$$Q = A \cdot V$$

$$V = C \cdot \sqrt{R \cdot J}$$

Where:

A – area of the cross section of the watercourse;

R – hydraulic radius,  $R = A/P$ ;

P – wetted perimeter of the cross section;

J – hydraulic slope;

C – Chezy coefficient,  $C = R^y/\eta$ ;

$\eta$  – riverbed roughness;

y – coefficient, 1/6 for water courses in lowland areas and 1/4 for water courses in hilly areas.

When determining the opening, the following assumptions are allowed:

- The level of water under the bridge subject to a modified regime is the same as under natural conditions;
- The speed water under the bridge  $V_p$  is higher as compared to its natural regime  $V$ ;  $V_p = E V$ , where E is the scouring coefficient of the riverbed,  $E = 1,1 \dots 1,5$ ;  $V_p = 2,518 \text{ m/s}$ ;
- The riverbed is not subject to scouring;
- Increased water velocity under the bridge is based on its increasing level upstream of the bridge.

The area required for water flow under the bridge  $A_p$ , measured between abutments, the

natural water level in natural conditions and the riverbed not affected by scouring, are determined following the relation:

$$A_p = \frac{Q_c}{\mu \cdot V_p}$$

Where:

$Q_c$  – flow calculation;

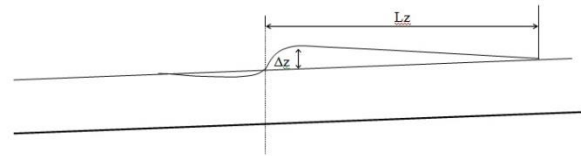
$\mu$  – coefficient of riverbed occlusion by bridge piers and abutments ( $\mu = \varepsilon e$ );

$\varepsilon$  – hydraulic contraction coefficient;

e – coefficient that takes into account the area occupied by bridge piers.

The deck bench-mark is established so that the water level at the flow calculation, respectively the verification flow and the lowest part of beams, ensure the normal height for free passage of the floating.

Reducing the drainage section, through partial occlusion of riverbed by bridge piers and abutments, increases the level of water upstream the bridge, which is called backwater ( $\Delta z$ ). It is necessary to know the value of the backwater in order to prevent the overflow of water over the sides.



The cant level value can be calculated approximately using the relation:

$$\Delta z = \frac{V_p^2 - V^2}{2 \cdot g}$$

where:

$V_p$  – average speed in the bridge section;

V – speed in natural conditions;

g – gravitational acceleration.

The cant level extends on a length ( $L_z$ ) which is determined base on the relation:

$$L_z = \frac{2 \cdot \Delta z}{J}$$

where:

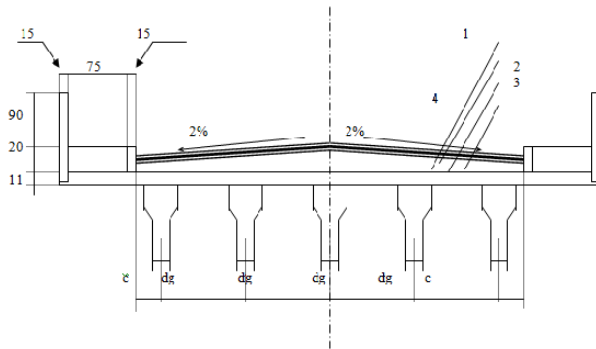
J – free surface water slope which can be approximated with the riverbed slope.

If the average velocity under the bridge ( $V_p$ ) is higher than the average drive speed of the material within the riverbed ( $V_a$ ), in flood conditions, the riverbed is deepening by scouring. General scouring (afg) occur throughout the section of the riverbed and are proportional to water depth (h).

$$afg = ha-h = h(E-1) = 0,422 \text{ m}$$

Because of local currents, around bridge piers and abutment, supplementary scouring can appear, also called as local scouring. The evaluation of local scouring by calculation is often accompanied by large errors due to their dependence on many factors with random appearance, difficult to master via formulas.

### Cross section scheme of the bridge



1. road 2\*2,5cm-----ashpalt concrete;
2. protection blanket 2cm--- cement concrete;
3. waterproofing 1cm-----3 mill board layers cemented with bitumen;
4. slope concrete and levelling blanket, min. 2 cm----- cement concrete.

Over the slab, a slope concrete is poured, having a 2% inclination and a border height of at least 2 cm. On top of all comes the road which consists of 2 layers of ashpalt concrete (2x2,5 cm), the waterproofing (1 cm) and some layers of waterproofing protection (3 cm).

The payloads are given by loading of people, convoys of vehicles A10 and tracked vehicles S40. Loading of people is calculated by formula:

$$p_o = 1,4 \cdot p_n \cdot 2 \cdot T$$

where  $p_n = 3 \text{ kN/m}^2$ , and  $T = 0,75 \text{ m}$ .

Therefore,  $p_o = 6,3 \text{ kN m}$ .

The transverse distribution calculus requires the calculation of the stiffness coefficient of the network of beams, that represents the base on which the lines of influence of the reaction are removed from the tables for the network with three simply supported beams.

The distribution coefficient  $Z$  is established using the formula:

$$Z = \frac{I_a}{I_g} \cdot \left( \frac{L_c}{2 \cdot d_g} \right)^3$$

where:

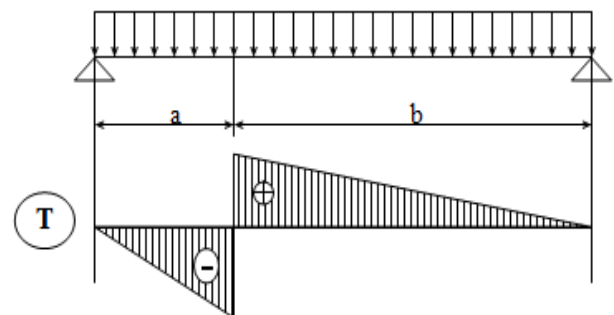
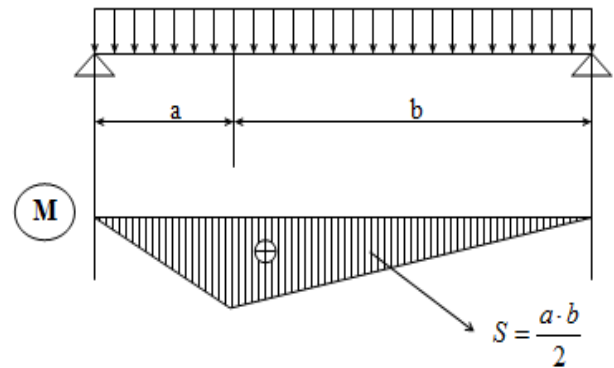
- $I_a$  – moment of inertia of the crosspiece,

$$I_a = \frac{(2 \cdot d_g + b_2) \cdot h^3}{12};$$

- $I_g$  – moment of inertia of the main beam;
- $L_c$  – calculating opening;
- $d_g$  – distance between beams.

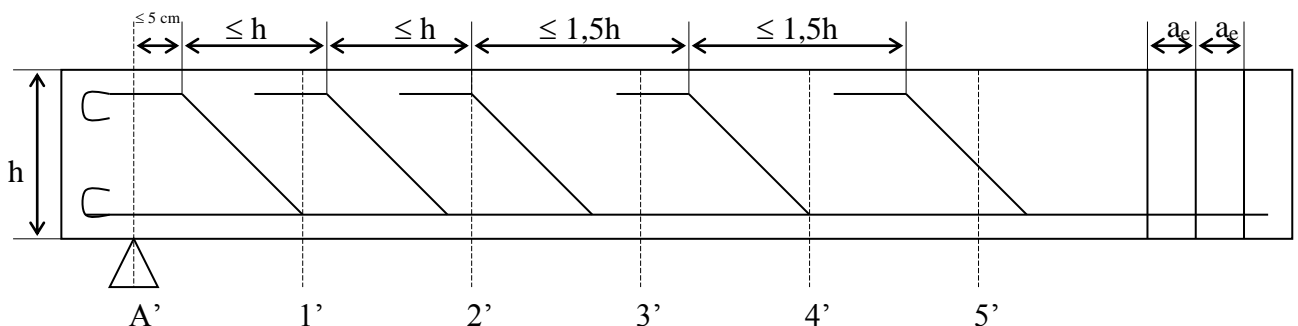
In order to capture as accurately as possible the way that the beams are loaded, they will be divided into 10 sections. Due to the fact that the values are symmetrical, the calculus will be made only for 5 sections of the beam.

The drawing of the calculus hypothesis is presented as it follows.

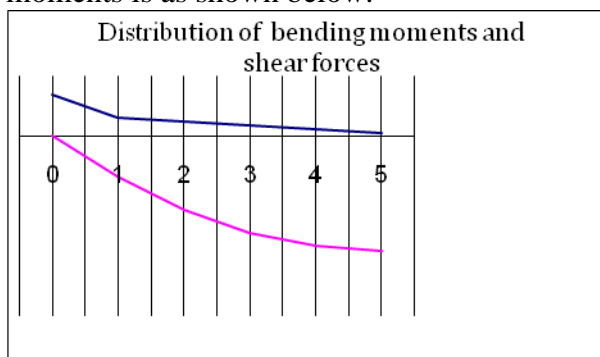


For the calculation at bending moments, it is used the B300 concrete brand with the tensile strength  $R_c = 140 \text{ daN/cm}^2$ . It is also used the reinforcement PC52 that has a torsion resistance  $R_a = 29 \text{ kN/cm}^2$ . The beam is treated as a section in the form of "T". For this, from the maximum available width of a beam ( $b_k$ ), only a beam portion is taken ( $b_p$ ), which is calculated as it follows:  $b_p = m_c \cdot b_k$ , where  $m_c$  is a coefficient that depends on the ratio between  $b_k$  and calculating opening. The values of  $m_c$  are given in tables according to this ratio.

In order to increase the resistance of the beam to the effect of shear forces, used stirrups and inclined reinforcement will be used. The inclined reinforcement is made by raising a maximum of 70% of the longitudinal reinforcement resistance, as it is no longer necessary for taking the bending moments. The remaining 30% and at least 2 bars remain straight up beyond the abutment. The reinforcement scheme is shown below:



The distribution of shear forces and bending moments is as shown below:



For calculations readiness, the following considerations are taken into account:

- The stirrups will be adopted from OB37 with  $R_{tr} = 2100 \text{ daN/cm}^2$ ;
- The distance between stirrups,  $a_e = 20 \text{ cm}$ , in compliance with the conditions imposed;
- The diameter of stirrups,  $d = 10 \text{ mm}$ ;

- The concrete brand B300 with  $R_t = 10 \text{ daN/cm}^2$

The bridge slab is loaded by its own weight and the layers above the slab (road, waterproofing, slope concrete), as well as the weight of payloads (vehicles, people). The calculation of slab in console is different from the calculation of central slab, having in common only the loadings.

Loading of parapet is a concentrated action. Loading of slab and the protective layers can be distributed evenly or unevenly, but in order to simplify calculations, one uses a uniform loading of pavement and another loading of road.

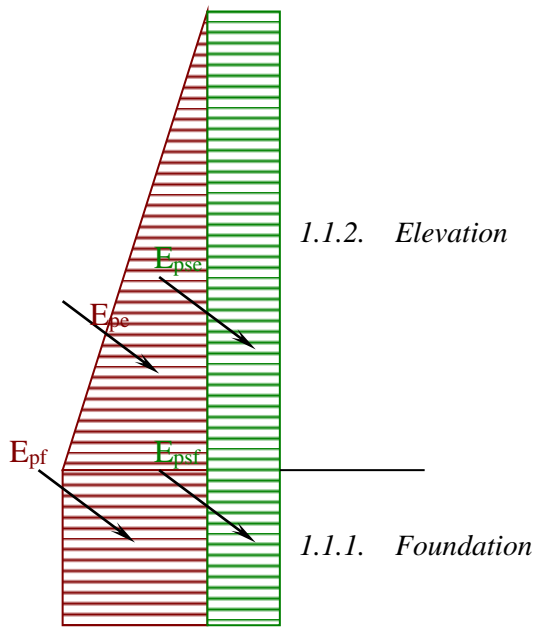
Experimentally it has been found that the loading determined by the concentrated force is distributed within the slab by angles of about  $45^\circ$ , so that only a part of the slab is subject to loadings. Based on this finding, one can calculate also the slabs in console from the bridges made of beams.

The surface on which the loading of the wheel is transmitted to the slab, is obtained from the distribution of loading at  $45^\circ$  and is considered to be a rectangle with sides  $a$  and  $b$ , where  $a = a_0 + 2s$  and  $b = b_0 + 2s$ , "s" being the thickness of the layers of the road.

The central slab is charged by the direct loading of vehicles and the permanent one, as well as the compound effect of the main beams. The dominant loading results from the direct charge. Since the ratio of the length and width of the panel is higher than 2, the slab is calculated and it is reinforced only on the short side direction.

The abutment is calculated using the method of limit states, mainly on the strength and stability. This calculus standardized by STAS 10111/1-1997.

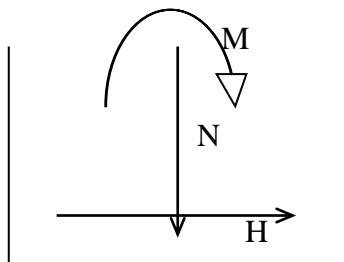
The diagram of ground pushing is shown below:



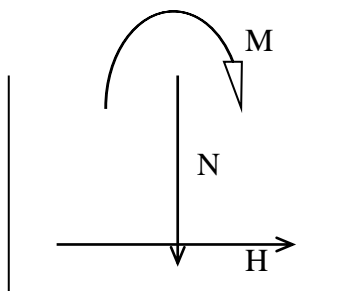
Usually, it is checked the base of the elevation and the base of the. The checks that are made are the following:

- sliding check;
- tilting check;
- resistance of the foundation soil check;
- concrete sections check.

*Sliding check*



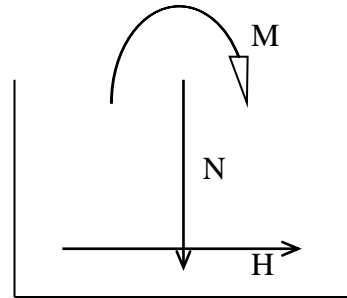
*Tilting check*



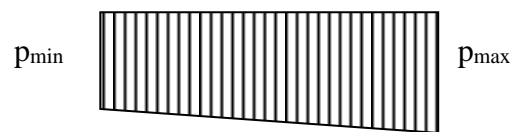
In practice, one of the terms of the equilibrium expression is much lower than the other. Usually, the bridges with one or two

lanes,  $a_x$  is much lower than  $a_y$  and as a result the relation becomes:  $\frac{e_y}{a_y} \leq \sqrt{m}$ .

*Resistance of the foundation soil check*



$$p_{\min, \max} = \frac{N}{A} + \frac{M}{W} \leq p_c$$

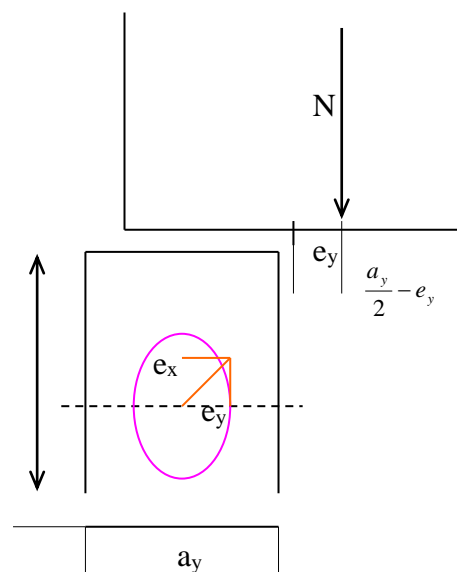


$A$  – surface of the base;  $A = a_y \cdot a_x$

$$W = \frac{a_x \cdot a_y^2}{6}$$

$p_c$  – conventional pressure

*Concrete sections check*



$$\frac{\sum H_i}{\sum N_i \cdot \mu} \leq 0.8$$

$$H \leq 0.8 \cdot T$$

$$T = \mu \cdot N$$

$$N \leq 0.9R_b A_a$$

$R_b$  – concrete resistance to compression;

$A_a$  – active area.

$$A_a = 2 \cdot a_x \cdot \left( \frac{a_y}{2} - e_y \right)$$

These checks are made in the following calculation assumptions:

- $C_1$  – abutment without drainage and embankment, acts only its own weight. Abutment can only be tilt back to the wall. Tilting check is carried out;
- $C_2$  – abutment with drainage and embankment set-up, acts its own weight and ground pushing. Tilting and sliding checks are carried out;
- $E_1$  – abutment deck loaded of convoy  $A_{10}$ ;
- $E_2$  – abutment deck loaded with special vehicles  $S_{40}$ .

## CONCLUSIONS

In conclusion, if all these steps will be respected and followed accordingly when designing a bridge, a durable and resistant construction work will be achieved.

## ACKNOWLEDGEMENTS

The present design plan was drawn with the support of Mr. Lecturer Vasile Ceuca, PhD, for all problems and difficulties encountered.

## REFERENCES

- Corlăţeanu S., 1964. Forestry transport, Didactic and pedagogic publisher.
- Dretz P., Knigge W., Lopfler H., 1984. Walderschliesung. Verlag Paul – Parey Hamburg – Berlin.
- Mătăşaru T., 1996. Roads, Technic publisher, Bucharest.

## **ATMOSPHERIC POLLUTION CAUSED BY RADIOACTIVITY ISSUED BY THE ASH AND SLAG DEPOSITS FROM THE PAROSANI THERMAL POWER PLANT**

**Dorin TATARU, Andreea STANCI**

**Scientific Coordinator: Prof. PhD. Aurora STANCI**

University of Petrosani, 20 Universitatii street, 011464, Petrosani, Romania,  
Phone: +40721044767

Corresponding author email: dorin.tataru@yahoo.com

### **Abstract**

*Through exploitation the coal are brought to the surface some of the radioactive elements in the earth's crust. Coal used in the process of Thermo-electric power station (CET) Paroşeni produce from burning slag and ash, which is deposited in the Valley Căprişoara. It is known that, radioactive elements in the coal not burn and not oxidize, so that radioactive waste of ash is more concentrated. In this paper we propose to determine the distribution of radionuclides in ash and slag in deposits and surrounding areas. These measurements are necessary because the nature and energy of radiation emitted are conditional of ways the irradiation of organisms.*

**Key words:** *pollution, radioactivity, ash and slog.*

### **INTRODUCTION**

Assessment of environmental factors in an area at a time is given by air quality, water, soil, the health of the population, the scarcity of plant and animal species recorded. The man contributes to the environmental changes through its various activities, household or technological. The mining and energy industries are the most powerful factors of environmental pollution they are responsible for air, water and soil pollution. The mining operations of coal, by technological activities, bring to the surface natural radioactive isotopes found in the depths of the Earth. Natural radioactive isotopes can enter into the chemical elements of the biosphere or stand as material deposits, raising the level of radioactivity in the area above the normal.

### **THEORETICAL CONSIDERED**

Thermo-electric power station Paroseni is one of the sources of pollution in the Jiu Valley by emissions on the chimney and ash stored in the deposits of ash and slag that results from technological process.

Thermo-electric power station Paroseni is situated on a lower terrace on the right bank

of the river Jiu, near the town of Vulcan, at 8-10 m from the railway Vulcan – Paroseni – Lupeni. This location was determined by the existence of numerous coal mining in the area. It is bordered to the north with the railway Livezeni – Lupeni, south with Route DN 66 Livezeni - Uricani, east access road to Paroseni Mining Exploitation and west of the river Jiu of West.

Thermo-electric power station Paroseni is a electrical plant of heating with cogeneration that provides electricity and heat. Works with coal as a base fuel and provides heat for the residents of the four mining towns in the area, namely: Petrosani, Vulcan, Lupeni, Aninoasa. For producing electricity the power plants use as a source of primary fuel, fossil fuels. The chemical elements that by reaction with oxygen develop heat (exothermic reactions) are coal, hydrogen and sulphur. The final product resulting from the burning of coal is carbon dioxide, water and sulphur dioxide. Solid fuels, towards others fuel, contain and much sterile, which is to be found in the process of combustion in the form of slag and ashes.

All products resulting from the combustion of solid fuel are pollutants, in the sense that they are changing the balance in the external

environment, or acting directly on the animal and plant kingdom.

Solid fuels contain natural radioactive isotopes in natural concentrations which by burning lead to concentration in the combustion products. Radioactive isotopes in the products of combustion, which escapes into the atmosphere (gas, smoke and fly ash), broadcasts under the action of air currents and they are lodged gradually on soil, water and vegetation, causing the radioactive contamination of them.

By burning coal, results slag that settle on the furnace bottom the ash that escapes from filters of the chimney and get into the atmosphere, from where they are deposited on the soil, and hot gases and volatile.

Radioactivity of the coal and ash is mainly given by the content of uranium, thorium, potassium, and radium (over 80%) (Maunat and Mauna, 2008). The average concentration of  $^{238}\text{U}$  and  $^{232}\text{Th}$  in charcoal is 20 Bq/kg and that of  $^{40}\text{K}$  is 50 Bq/kg, but can vary by orders of size (UNSCEAR, 2000). So, the accumulation of uranium in coal can vary from place to place depending on the deposit and the geological period in the region. In the coal of Romania were found value to six times more and for  $^{40}\text{K}$  and for  $^{238}\text{U}$  the values are twice as large. (Botezatu et al., 2002). In addition one can find radionuclides by  $^{235}\text{U}$ ,  $^{214}\text{Pb}$ , and trace amounts of bismuth, polonium etc. After the data provided and published by Bradley (1993) it shows that these radionuclides are mainly responsible for the emission of radiation.

The filters installed at the chimneys of power stations do not fully retain fly ash and radon which are released entirely into the atmosphere, which leads to an increasing atmospheric radioactivity. To this increased radioactivity it is added the contribution of its

descendants  $^{210}\text{Pb}$ ,  $^{214}\text{B}$ , which are fixed on aerosols. This power plant that uses solid fuels to produce electricity burn huge amounts of fuel, which leads to emanations of fly ash and radioactive isotopes in atmosphere that can not be neglected because they are causing radioactive pollution of the environment. The produced radioactive pollution should not be neglected because it is continuous pollution. Population living in areas affected by radioactive pollution produced by power plants based on burning fossil fuels annually receives an additional dose of 300-500  $\mu\text{Sv}/\text{year}$ .

## RESULTS AND DISCUSSIONS

Radioactive isotopes of potassium  $^{40}\text{K}$  and radioactive elements by uranium and thorium series are the main elements that give natural radioactivity to rocks. The energies of gamma radiation emitted by the radioactive elements are distinct for each item. Potassium emits gamma radiation with energy of 1.46 MeV while uranium and thorium series emits gamma radiation of different values.

Fly ash released through the chimneys, the fine dust of ash driven by the wind from the dumps of slag-ash and the coal dust derived from deposits of coal or from the transportation and its preparation together constitute a solid contaminant, that is found in the form of aerosol, are the pollution factors from Thermo-electric power station Paroseni area.

Monitoring reports to environmental factors prepared by Environmental Protection Agency Western Region shows that the dumps produce, especially in summer, a important pollution of air with powders (because ash is dry and the wind is taken).

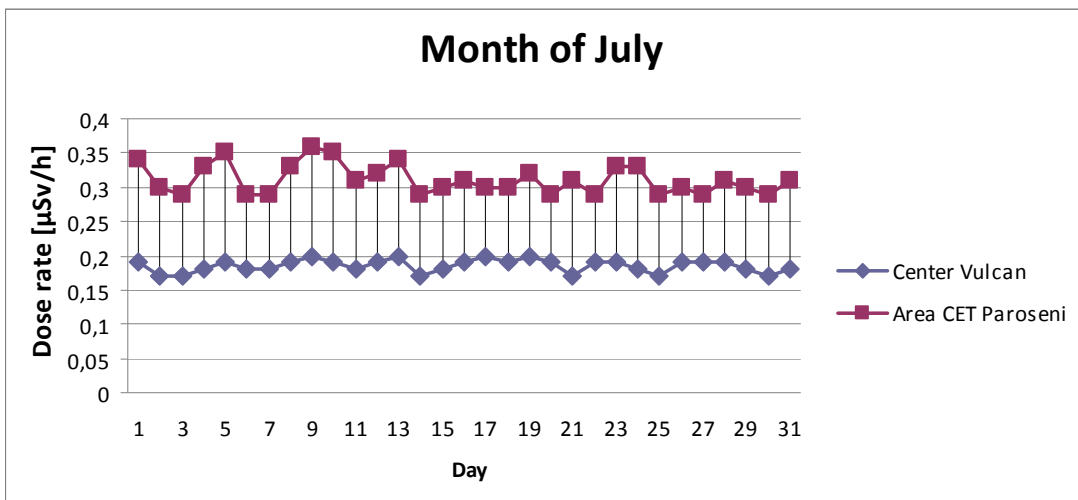


Figure 1: The radioactive pollution of the atmosphere in the month of July

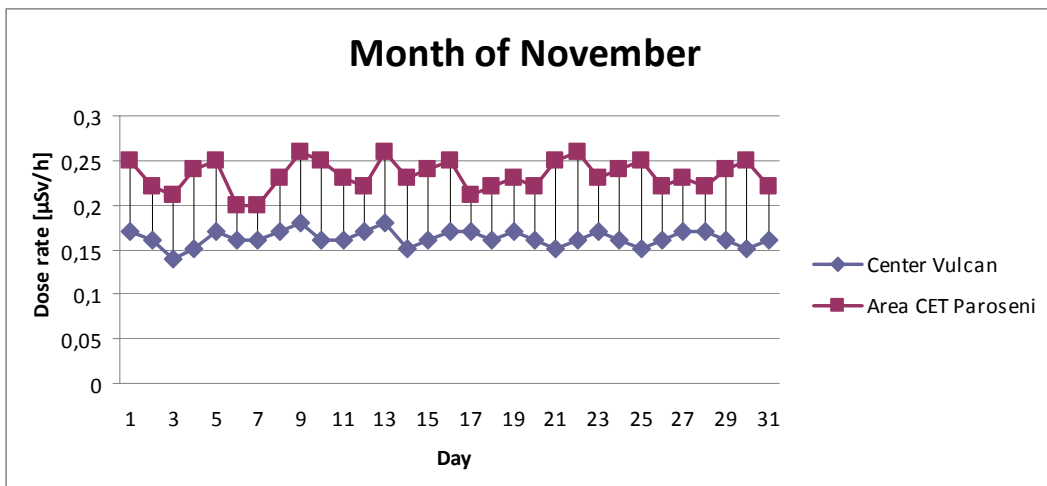


Figure 2: The radioactive pollution of the atmosphere in the month of November

To determine the radioactive pollution of the atmosphere in the Thermo-electric power station Paroseni area, measurements were performed gamma absorbed dose rate in air during the months of July and November 2014, with Gamarad-DL7 radiations detector. Measurements were performed in the Thermo-electric power station Paroseni area and in downtown Vulcan and the results are presented in the graphs in figures 1 and 2. From experimental measurements is observed the flow rates dose are high in the Thermo-

electric power station Paroseni area, exceeding permissible limit value  $0.250 \mu\text{Sv} / \text{h}$ , while the town of Vulcan measured values are below the limits set for the European Union.

Flow rates of the dose are high in the ash and slag deposit due to the presence in it of radioactive elements exceeding permissible limit value  $0.250 \mu\text{Sv} / \text{h}$ , even in neighbouring areas (Figure 3).

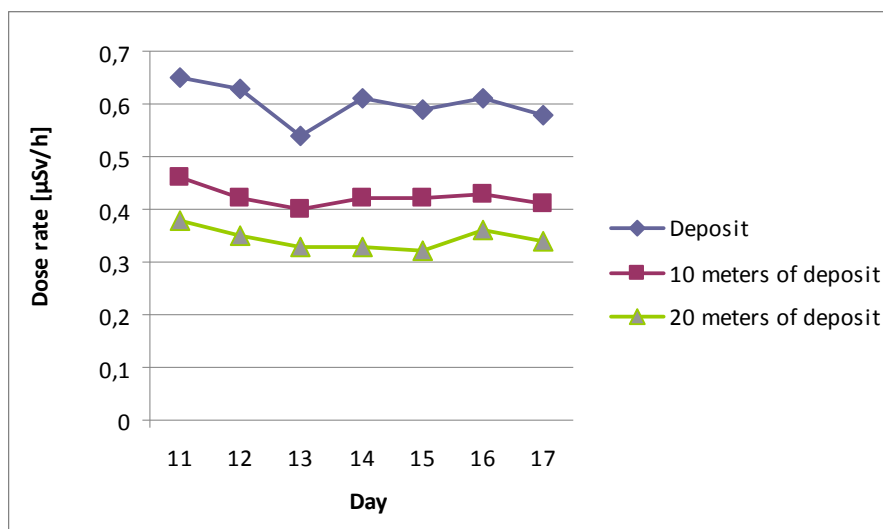


Figure 3: The radioactive pollution of the atmosphere in the ash and slag deposit, and the surrounding areas

## CONCLUSIONS

Following the technological process of Thermo-electric power station Paroseni radioactive elements are released into the atmosphere with fly ash and radon, which can not be retained by the filters in the chimneys. Of measurements made during two months it observed a higher dose rate in the Thermo-electric power station Paroseni towards centre of Vulcan, faster growth in the month of July, when we add the dust pollution high from slag and ash deposits

The slag and ash from furnace falling into a water bath, is off, removed and inserted into a crusher for shredding. From crushing the slag is mixed with water and transported in ash and slag deposit from Caprisoara Valley. Dose rate measurements in this area indicate a high content of radioactive elements, both on the surface of the deposit and the surrounding areas.

Even if the dose rate values are not very large, radioactive pollution is an important factor of pollution by the large amount of ash and slag discharged (about 130,000 m<sup>3</sup>).

Radionuclides existing in the environment can be transferred to humans through water or food, great importance has 40K by fact it is primarily responsible for radiation dose received by humans. Radon is stored in the atmosphere air, in the particles of dust and water droplets, and by inhalation, reaches the lungs being a high risk of disease.

## REFERENCES

- Claudiu Margin, Mircea Moldovan, AndraRadaLurian, Dan ConstantinNiță Gabriel Dobrei, ConstantinCosma, Radioactivity Sărmășag lignite, Salaj county, Ecoterra, no. 29, 2011.
- Ildiko Melinda Varga, Robert Begy, Dan Constantin Niță ConstantinCosma, Preliminary results regarding the radioactivity level in the Zăghid mining area environmental, LES PRESSES AGRONOMIQUES DE GEMBLOUX & BIOFLUX PUBLISHING HOUSE, ISBN 978-606-8191-14-0, 2011, p.196-210A.
- Marcu Gh., Marcu Teodora, Radioactive elements - environmental pollution and radiation risks, Technical Publishing House, București, 1995
- Maunat T., Mauna A. A., 2008 - The coal burning product radioactivity, WEC regional Energy Forum FORENT Reference no S5-14-en, 7 pp.

## ENVIRONMENT QUALITY IMPROVEMENT AT THE UNIVERSITY OF PITESTI, A FORMER MILITARY SITE

Cristina- Iuliana TOMA

Scientific Coordinator: Lect. PhD. Eng. Mădălina- Cristina MARIAN

University of Pitesti, Faculty of Sciences, Targu din Vale street, no. 1, 110040, Pitesti, Romania,  
Phone: +4034.845.31.00, Fax: + 4034.845.31.23

Corresponding author email: yulyana0108@yahoo.com

### Abstract

*The present article is meant as a detailed presentation of the problems which can occur in the conversion of military sites into other centres, through entrepreneurship. The area looked into is located in Rimnicu Vilcea, where the University of Pitesti, after taking over a part of the original area, carries out some of its activities. This study is meant to be a criterion for sustainable development, namely environmental, landscape restoration proposed by contributing to environmental quality improvement and pollution sources reduction by removing the aspect of "vacant land", degraded and untidy. The studied area has a surface area of 72820 square metres and there are 23 buildings on it. The land measurements have been made with specific topographic equipment: GPS SOUTH S86-T and Pentax total station W-822NX, using RTK-kinematic method. The planimetric coordinate values have been registered for each point in the 70's Stereo System. In order to identify the species of trees and shrubs resistant to environment and microclimate conditions, a small dendrologic study has been made. The plants have been planted as naturally as possible in order to fix the soil and to create a show of vegetation through foliage, colour and fragrance. Thanks to the chromatic change of the foliage, the thickness and transparency of the crown, the varied forms and volumes, the vegetation will ensure the variety of the landscape, making the area more alive.*

**Key words:** dendrologic study, environmental quality, improvement, landscape restoration, vacant land.

### INTRODUCTION

There are many vacant lands in the country. These lands must be cleaned and the tree branches must be cut. No waste should exist there. These lands must be rearranged by finding the most efficient solutions.

Taking poor care of these lands has become a matter of public interest. In addition to bringing a negative impact on urban landscaping, they can also turn into real outbreaks of infection, endangering, in some cases, the health, life and safety of the citizens.

Municipalities can fine the owners, both natural and legal persons, who do not provide a minimum hygienisation of the lands by maintenance, disinfection and cleaning. Regular trimming of vegetation and disposal of wastes, by cleaning the storage places with the materials which are to be used, must also be provided. (<http://www.agerpres.ro>). The access routes should be cleaned too, by fencing the vacant lands and disposing of the wastes. The competent authorities must be notified

regarding the taking away of the stray dogs which could endanger the life and physical integrity of the people.

The area that was studied is located at the outskirts of Vilcea, being adjacent to the industrial area, where the University of Pitesti has a land as place of work (including buildings) which is used for teaching purposes. This area belonged to a former military unit in Vilcea. The land and the buildings related to the military base belonged to the Ministry of Interior and Defence. Our aim is to achieve one of the criteria of the sustainable development, those regarding the environment, by restoring the landscape that we propose.

The importance of this topic contributes, by its solution, to the improvement of the environmental quality and reduction of the sources of pollution.

### MATERIALS AND METHODS

For completing the technical part of the work, following the recognition of the land and its

surroundings, for identifying the points within the geodetic network with known coordinates that allows the connection to the Stereo System 79 and provides the necessary precision, the following topographic equipment has been used: GPS SOUTH S86-T and Total Station Pentax W-822NX, using the RTK method - kinematic measurements. The work was done from four stations (Figure 1), due to visibility.

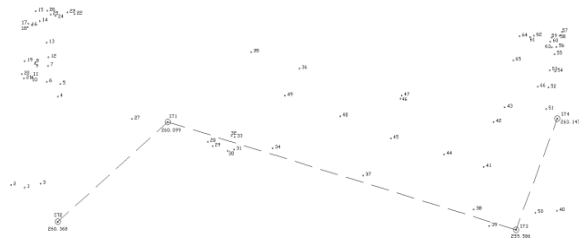


Figure 1. Sketch of the location of stations (sights) and offshoot points

The planimetric survey of the topographic details was done by radiation, the position of the characteristic points being determined. The results were verified through their integration into the tolerances required by the Office of Cadastre and Real Estate Publicity. The writing of the plan with X, Y coordinates was done at 1:1000, with specialized program ACAD, ensuring a high precision of calculations and graphical accuracy. For the classification of the area the ortophotoplan was used. One of the most important criteria for the implementation of the work was choosing the species of plants and landscaping style for the area that has been studied. In order to determine the species of trees and shrubs resistant to environmental conditions and microclimate of the area, a dendrological study was done, in which each species was briefly described with details regarding the ornamental importance, ecological requirements, scientific name, elements about origin and habitat.

## RESULTS AND DISCUSSIONS

The area which has been studied has a surface of 72820 sq (Figure 2) and it encloses 23 buildings (Table 1). This area is part of a total surface of 11.8 hectares, cadastral number 14419.

Table 1. Data on existing buildings

No. construction	Built area (sq)	Name Construction
C1	222	PAV M6 Munition Storehouse
C2	228	PAV H Storehouse
C3	16	PAV Y2 Bodei
C4	138	PAV Y1 Bodei
C5	235	PAV H1 Storehouse
C6	218	PAV T Bodyguard
C7	322 (161 footprint area)	PAV C Sickroom
C8	212	PAV F1 Storehouse
C9	53	PAV L CL Station
C10	51	PAV O Post Trafo
C11	68	PAV U1 Control point
C12	3617 (1329 footprint area)	PAV B Headquarter In the current use of the University
C13	4	PAV L1 CL Station
C14	153	PAV Y9 Metal shack
C15	51	PAV G1 Pump Station
C16	52	PAV P1 Technical Point
C17	162	PAV R1 Storehouse
C18	93	PAV R7 Fire Protection Building
C19	43	PAV R2 Storehouse
C20	7	PAV R3 Storehouse
C21	367	PAV Y6 Enclosure
C22	565	PAV D Central Heating
C23	848	PAV N1 Workshop

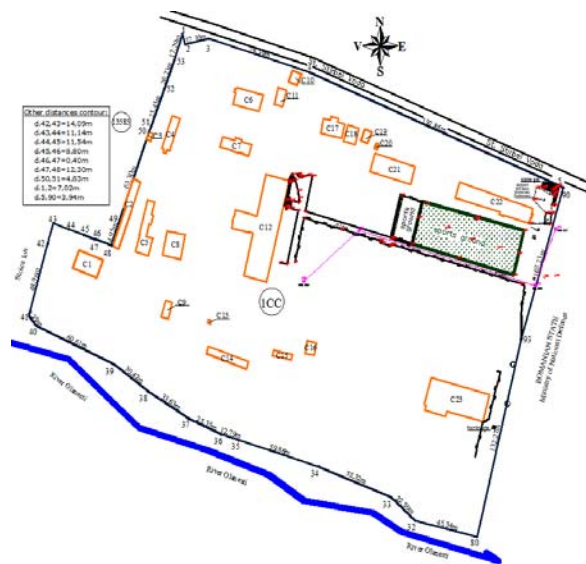


Figure 2. Reporting of the measured points and presentation of the studied site

Framing in the area through ortophotoplan (Figure 3) highlights the southern vacant land.



Figure 3. Framing in the area

The topographic survey revealed the following existing landscaping: pedestrian alley = 662sq (0.91%), parking = 377sq (0.52%), green spaces = 2136sq (2.93%), sports area = 2591sq (3.56%).

The vacant land area covers a surface of 17122sq (23.51%), with the proposal of getting rid of the metal shack C14. The dendrological study (Table 2) includes the surfaces in the corners of the C12 construction and the surface related to the pedestrian alley, taking into account that for marking the vertical rigid and monotonous lines of the building, groups of trees with columnar crown are planted in the corners. The main aim for the pedestrian alley is the decorative-recreative one. (Sofletea and Curtu, 2008)

Table 2. Description of the proposed species

Name	Characteristics
 Weeping willow <i>Salix babylonica</i>	A medium-sized tree (up to 15m tall), with long, flexible, glabrous shoots of yellowish-green colour. They must be planted in wet places, away of constructions, because their roots grow very fast and they are long and thick.
 Black locust <i>Robinia pseudacacia</i>	It is a tree up to 25-30 m tall with a dense system of root, a strain with early, thick rhytidome, deep and wide stitched, rare, bright crown. It has imparipinnate compound leaves and white, sweet-scented flowers.
Name	Characteristics

 Silver birch <i>Betula Pendula Lacinata</i>	A medium-sized deciduous tree with leaves that turn yellow in autumn. Resistant to frost, modest to soil fertility, it avoids the excessively wet and calcareous soils. It is not resistant to excessive drought.
 <i>Euonymus fortunei 'Emerald Gaiety'</i>	It has a slow growth, a height of 0,5-1 m. Requirements: well-drained soils, partial or partially shaded light, alkaline, acidic or neutral soils.
 <i>Abies alba</i>	Resin tree with a slow growth, a height of 50 m, the leaves are needle-like, flattened, green with white stripes. Requirements: fertile, wet soil, semi-shade, resistant to frost.
 Blue spruce <i>Picea pungens</i>	This resin tree has a slow growth and it is up to 40 m tall, needle-like leaves, that are dark green on top and have two long white stomata in strips below.
 Pine spruce <i>Picea abies</i>	Conifer tree that can be up to 50 m tall. It has a pyramidal-conical shape crown which is always green and dark green needle-like leaves.
 Magnolia <i>Magnolia x soulangiana</i>	It is also called sauce magnolia. It is a shrub of 7-8 m with obovate leaves, white, pink and purple flowers.
 Wistaria <i>Wistaria</i>	Strongly twisted roots, green stems, big, blue-violet, sweet-scented flowers grouped in pendent racemes of 15-20 cm, they blossom in May-June; large, soft pods, persistent on branches in winter.
 Lilac <i>Syringa vulgaris</i>	Part of the family oleaceelor and is a species that blooms in spring. It is a shrub whose height can be up to seven meters with straight branches and stems little edge. Odorous flowers from violet to purple and white.

From a functional perspective, by the proposal that was made (Figure 4), the anti-erosion part was ensured by the characteristic of the green

spaces to prevent erosion and degradation of rocks, to retain alluvial materials and to build up the shores of the water courses. From a decorative point of view, the green plantations improved one of the essential principles, namely the harmony, by linking the natural green spaces to the built spaces. In terms of health, the proposed arrangement contributes to the shaping the diurnal temperatures variations, increase of relative humidity of air, oxygen enrichment of the atmosphere, decrease of wind speed. All these features lead to the reduction of fatigue.



Figure 4. The layout of arrangement

Redevelopment project included alongside landscape restoration and resolution of access roads the malfunctioning by restoring auto route, resizing car park and the introduction of bicycle lanes and a corresponding parking (Figure 5).

## CONCLUSIONS

The project proposed an arrangement of plants in a natural way so that it fixes the soil and also creates a spectacle of vegetation through foliage, colour and scent. The recommended species of trees and shrubs are resistant to

environmental conditions and microclimate in the area.

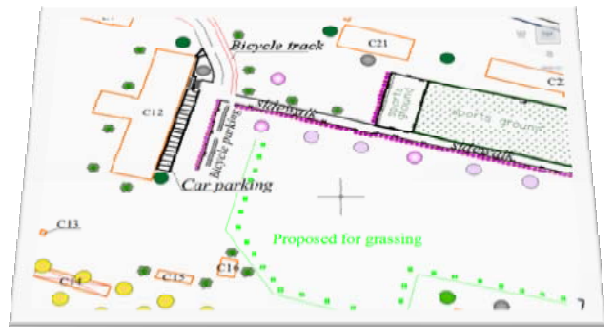


Figure 5. Detail of the arrangement

The chosen species have a great impact from an artistic point of view. The proposed arrangement leads to the harmonization of the built environment with the natural one, for the integration into the landscape and enhance of visual positive effects.

It shows up the buildings by directing the viewer, filtering the images and making of an interplay of light and shade, colour and texture. The work, through the solution it brings, contributes to the improvement of the environmental quality and reduction of sources of pollution.

We estimate of expenditure after achieving a necessary investment, the estimate must include the costs of maintenance. It will take into consideration the alternative fleet maintenance by students during practice. These are students of horticulture and those specializing in environmental engineering.

## REFERENCES

- Sofletea N., Curtu L., 2008. Dendrology. Publisher "For Life", Brasov.  
<http://www.agerpres.ro/comunicate/2013/10/29/comunicat-de-presa-deputatul-pc-ovidiu-raetchi>, accessed on 25.03.2015, at 16.

## THE USE OF ULTRAFILTRATION MEMBRANE SYSTEMS TO TREAT WASTE WATERS GENERATED FROM HARD COAL MINING

Alikemal TOPALOĞLU

Scientific Coordinator: Prof. PhD. Yılmaz YILDIRIM

Bulent Ecevit University, Environmental Engineering Department İncivez / ZONGULDAK – TURKEY, Phone: +903722574010, Fax: +903722572140, Email<sup>1</sup>: akemal\_topal@hotmail.com

Corresponding author email: akemal\_topal@hotmail.com

### Abstract

*The recent studies regarding the membrane technologies indicate that the membrane process applications involve for providing the high quality drinking water and increasing the use of industrial water consumption. The membrane process has been used in applications such as wastewater treatment, industrial water production, water softening, and in the separation of compounds having different molecular weights. Of using in many membrane process Microfiltration (MF) and Ultra filtration (UF) are low pressure filtration processes that are used for pathogen and suspended solids removal as seen in many studies (Guo et al., 2010; Yang et al., 2014). In this study, we investigated the possibility of using microfiltration (MF) and ultrafiltration (UF) membrane systems for treatment of wastewater generated from underground hard coal mining of Kozlu Basin. In first stage of this study, the wastewater was treated using MF membrane filtration system. The MF membrane filtration system was composed of the flat sheet MF membrane module equipped with Polivinilflorid (PVDF) membranes purchased from MICRODYN-NADIR membranes, Germany. The MF membrane has a filter area of 140 cm<sup>2</sup> and average pore diameter of 0.2 µm as given by supplier. In second stage of study, the effluents of MF were treated using UF membrane filtration. The UF membrane filtration system was composed of the flat sheet UF membrane module equipped with Polyethersulfone (PESH) membranes purchased from MICRODYN-NADIR membranes, Germany. The UF membrane has a filter area of 140 cm<sup>2</sup> and molecular weight cut-offs (MWCOs) of 50 KDa as given by supplier. In the experimental study, the raw water was provided from discharge point of underground hard coal mining of Kozlu Basin. In order to determine the total treatment performance of the MF/UF system, water samples were taken from inlets and outlets of the MF and UF membrane systems, respectively. The pressures were fixed at 1 and 2.5 bars for MF and UF, respectively during the experimental study. In test of wastewater, total coliform, turbidity, conductivity, pH, nitrite, nitrate, phosphate, sulphate, sodium, potassium, chemical oxygen demand (COD), total suspended solids (TSS), calcium, magnesium and total hardness as parameters were analysed in raw and treated water. The results were compared with Turkish Standards (TS 266) and European Union (EC).*

**Key words:** membrane, wastewater treatment, hard coal mining, water reuse

### INTRODUCTION

Membrane filtration is basically based on placing a selective barrier between two phases. As a result of exerting a driving force to one side of the membrane, components are transported towards the membrane surface. Therefore, some components pass through the membrane (permeate) and others are retained according to their size (retentate). In industrial application, different membrane systems and configurations might be arranged, including pretreatments and other treatment stages based upon different technologies, in order to meet

those target water quality standards (Ordonez et al., 2014).

The membrane is the key of the membrane separation technology, and it directly affects process efficiency and practical application value. At present, almost all membranes for industrial processes are made from inorganic materials or organic polymers. The organic polymers include organic polymer membranes are made of organic polymers such as polysulfone (PSF), poly(ethersulfone) (PES), poly-acrylonitrile (PAN), polyamide, polyimide, poly(vinylidene fluoride) (PVDF) and polytetrafluoroethylene (PTFE). Therein, PVDF is one of the most used membrane materials and has been paid much attention by

researchers and manufacturers in recent years (Liu et al., 2011; Kang and Cao., 2014). It exhibits high mechanical strength, good chemical resistance and thermal stability as well as excellent aging resistance, which are very important for the actual application of separation membranes. Moreover, PVDF shows good process ability to prepare flat sheet, hollow fiber or tubular membranes (Liu et al., 2011). Owing to the features, in first stage of this study, we assume it would appropriate to use PVDF membrane for MF so as to treat raw wastewater. Besides, of another membrane material, PES is one of the most important polymeric materials and is widely used in separation fields. PES and PES-based membranes show outstanding oxidative, thermal and hydrolytic stability as well as good mechanical property. The membranes has always asymmetric structure (Barth et al., 2000; Zhao et al., 2013). Though PES and PES-based membranes have been widely used, they have disadvantages. The main disadvantage of the membrane is related to its relatively hydrophobic character (Zhao et al., 2013). Therefore, in second stage of this study, PESH membrane having hydrophilic character was employed for wastewater treatment.

In the present study, the raw water was provided from underground hard coal mining and the total treatment performance of the MF/UF system was determined. In the total treatment performance of wastewater, total coliform, turbidity, conductivity, pH, nitrite, nitrate, phosphate, sulphate, sodium, potassium, chemical oxygen demand (COD), total suspended solids (TSS), calcium, magnesium and total hardness as parameters were analysed in raw and treated water and permeate water quality of UF membrane system was compared with Turkish Standards (TS 266) and European Union (EC) in order to assess its usability as a drinking water service or the other processes.

## MATERIALS AND METHODS

Before MF/UF experiments, raw wastewater were analysed. MF and UF experiments were performed by using a cross-flow flat-sheet membrane for the filtration of the wastewater generated from underground hard coal mining. The flow sheet of the membrane filtration

system was shown in figure 1 and cross flow flat sheet test unit in lab scale was shown in figure 2.

The membranes used in this work were:

- 1) Polivinilflorid (PVDF), hydrophobic, average pore diameter of 0.2  $\mu\text{m}$
- 2) Polyethersulfone (PESH), hydrophilic, MWCO 50 kDa

In the first stage of experimental studies, the wastewater generated from the underground coal mining works was treated using MF membrane filtration system. During the membrane filtration process, MF membrane system was constantly run at trans-membrane pressure (TMP) of 1 bar. In the second stage of experimental studies, the effluents of MF were treated using UF membrane filtration system. During the membrane filtration process, UF membrane system was constantly run at TMP of 2.5 bars.

In following, according to the procedure outlined in standard methods, quality parameters, which are total coliform, turbidity, conductivity, pH, nitrite, nitrate, phosphate, sulphate, sodium, potassium, COD, TSS, calcium, magnesium and total hardness, were analysed in permeates of MF and UF.

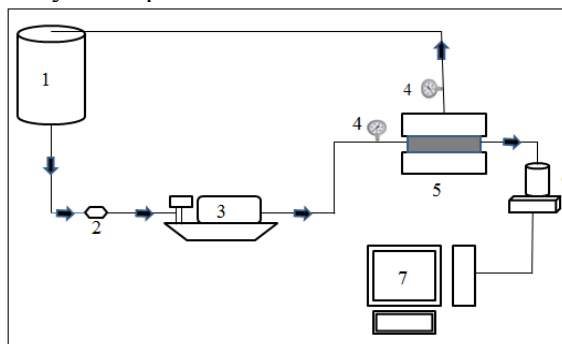


Figure 1. Laboratory scale membrane flow diagram (1. Waste water tank 2. Flow meter 3. High pressure pump 4. Manometer 6. Electric balance 7. Computer)



Figure 2. Cross flow flat sheet test unit in the lab scale

In the study, the wastewater from underground mining was operated in cross-flow batch mode. In this manner, the feed crosses the cell adjacent to the membrane surface and the permeate passes through the cell vertical to the membrane surface. In other words, the feed was pumped to the cross-flow cell from the tank and the permeate was taken out of the loop and collected in an Erlenmeyer flask and measured using an electric balance, and the retentate was completely returned to the tank. This cycle was repeated continuously. By the time the pump heated, it was needed to cool, so the feed tank was equipped with cooling water coil and heat exchanger. The cell consisted of two rectangle parts and was made of stainless steel. During the experiments, flow rate, trans membrane pressure (TMP), and temperature were carefully controlled.

seen in Table I, total the removal efficiency of turbidity, TSS, phosphate, sulphate and COD were found as 99%, 65%, 80% 98% and 72%, respectively. In other words removal efficiencies of turbidity, TSS, phosphate, sulphate and COD for MF/UF system were relatively high. In the meantime, total coliform as a bacteriological parameter were not detected at the all water samples. In conclusion; according to Table I, the effluent of UF is roughly suitable for the TS 266 and (EC). However, for drinking water suitability, the other parameters such as cadmium, lead, iron, chromium, cobalt, nickel and copper must also be examined. As conclusion, this study shows that polluted water from underground hard coal mining were treated by MF/UF membrane system and may be used as drinking water.

## RESULTS AND DISCUSSIONS

Table I shows the test results and removal efficiencies of raw and the treated water. As

Table 1. The test results and removal efficiencies of raw and the treated water.

Water quality parameters	Waste water from underground mining	Permeate of MF membrane system	Permeate of UF membrane system	Total removal Efficiency (%)	Turkish Standards Institute (TS 266)	European Union (EC)
T. coliform (number/100 ml)	0	0	0	0	0	0
Turbidity (NTU)	100,5	3,6	0,82	99	5	4
Conductivity ( $\mu\text{s}/\text{cm}$ )	1257	907	886	30	2500	2500
pH	8,06	8,54	8,68	-	6,5-9,5	6,5-9,5
Nitrite (NO <sub>2</sub> -) mg/L	0,008	0,005	0,0044	45	0,5	0,5
Nitrate (NO <sub>3</sub> -) mg/L	0,99	0,684	0,644	35	50	50
Phosphate (PO <sub>4</sub> <sup>2-</sup> ) mg/L	0,0038	0,0022	0,00076	80	-	-
Sulphate (SO <sub>4</sub> <sup>2-</sup> ) mg/L	51	1,03	0,94	98	250	250
Sodium (Na <sup>+</sup> ) mg/L	173,43	176,8	184,6	-	200	200
Potassium (K <sup>+</sup> ) mg/L	2,6	2,3	2,3	12	-	-
COD mg/L	56	16	16	72	-	-
TSS mg/L	17	12	6	65	-	-
TDS mg/L	624	567	511	18	-	-
Calcium (Ca <sup>2+</sup> ) mg/L CaCO <sub>3</sub>	60	50	45	25	-	-
Magnesium (Mg <sup>+</sup> ) mg/L CaCO <sub>3</sub>	68	62	64	6	-	-
Hardness mg/L CaCO <sub>3</sub>	128	112	109	15	500	500

## CONCLUSIONS

In conclusion, the effluent of UF is suitable for the TS 266 as well as (EC). However, for drinking water suitability, the other parameters such as cadmium, lead, iron, chromium, cobalt, nickel and copper must also be examined. As conclusion, this study shows that polluted water from underground hard coal mining were treated and may be to serve as drinking water. Also, this study shows that the wastewater can be recyclable and reusable.

## REFERENCES

- Guo H., Wyart Y., Perot J., Nauleau F., Moulin P., 2010. Low pressure membrane integrity tests for drinking water treatment: a review. *Water Res*, 44 (1), 41-57.
- Yang Y., Lohwacharin J., Takizawa S., 2014. Hybrid ferrihydrite-MF/UF membrane filtration for the simultaneous removal of dissolved organic matter and phosphate. *Water Res*, 65 177-185
- Ordonez R., Hermosilla D., Merayo N., Gascó N., Blanco C. & A., 2014. Application of Multi-Barrier Membrane Filtration Technologies to Reclaim Municipal Wastewater for Industrial Use. *Separation & Purification Reviews*, 43:263–310.
- Liu F., Hashim N.A., Liu Y.T., Abed M. R. M., Li K., 2011. Progress in the production and modification of PVDF membranes. *J. Membr. Sci*, 375:1–27.
- Barth C., Goncalves MC., Pires ATN., Roeder J., Wolf B.A symmetric polysulfone and polyethersulfone membranes: effects of thermodynamic conditions during formation on their performance. *J Membrane Sci*, 169:287–99.
- Zhao C., Xue J., SUN S. (2013). Modification of polyethersulfone membranes – A review of methods, *Progress in Materials Science*, 58, 76–15.

**SECTION 02**  
**LAND RECLAMATION**



## NEW DWELLING IN OLD-FASHION MANNER

Adela Eleonora VISAN, Mihaela RADU, Emine ISMAIL

Scientific Coordinator: PhD. Arch. Ioana TUDORA

University of Agronomic Sciences and Veterinary Medicine of Bucharest, 59 Mărăști Blvd, District 1, 011464, Bucharest, Romania, Phone: +4021.318.25.64, Fax: + 4021.318.25.67

Corresponding author email: adela.eleonora@gmail.com

### Abstract

*As known, nowadays we are facing new ecological pressures, when land, water and clean air are not anymore regarded as infinite resources. As an example, in Bucharest, the current urban sprawl has begun to destroy the most valuable land and open-space resources. All along the Colentina river there is an impressive potential of creating green areas, but also new dwellings combined with peri-urban agriculture, not forgetting about heritage. All the 13 lakes have their own identities, but which are not fully taken care of. It can easily be noticed the lack of management of these lakes- the shores are in a bad condition, inaccessible, the water is far from being clean and, what is more, water pollution happens without any refrain. What we suggest is to design cycle tracks, walking paths, beach areas, sportive areas, decks, restaurants, greenways, community gardens, agricultural areas, all intelligently integrated in a eco-neighbourhood along Grivita lake. Also, reinforcing the shores and reassuring the continuity of the existing ecosystems are important aspects of our project. All in all, our aim is to tackle the social, economical and ecological issues all together. This would mean to rise the quality of living in the peripheral areas of Bucharest, create social mixity and also encourage the small commerce which is an extremely important aspect for the community*

**Key words:** evolution, green areas, Colentina river, quality of living.

### INTRODUCTION

The landscape, in all its shapes and functions is everything that we can look at. Of course, the esthetical role is extremely important. However, it is even more important to correctly understand and be aware of all its aspects.

The lakes along the Colentina river have been created in the '30s (Figure 1).

However, instead of being one of the most attractive areas in Bucharest, the lack of maintenance of these lakes has minimized the potential and beauties of this chain of lakes.

Grivita Lake encounters an impressive variety

of areas with high potential, therefore multiple possibilities of improvement and development.

There are four directions that we have focused on, which can be treated all together in order to create a unity and complexity in the area. These directions are: urban sprawling, tourism and leisure, sustainable agriculture, but also heritage and identity. As our purpose is to increase the quality of living and also an identity for the place, it is highly necessary to combine these four elements.

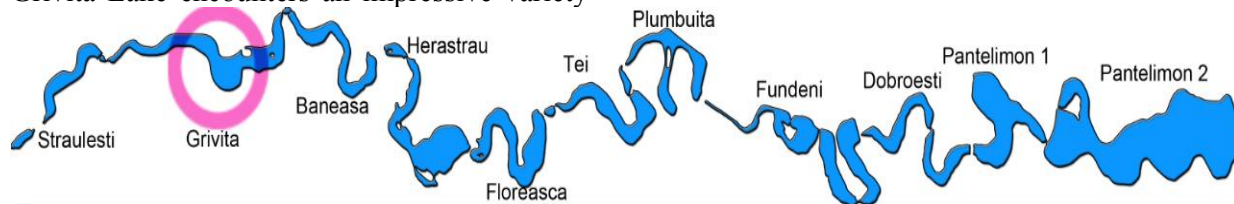


Figure 1. Colentina's Chain of Lakes

## MATERIALS AND METHODS

Our aim is to design a neighbourhood according to both ecological principles and sustainable aspects (Ruano, 1998). Therefore, we propose that the areas affected by urban sprawling to be inserted into a high-density neighborhood, which will also include community gardens and small local commerce areas in order to develop a sustainable economy. Large scale agriculture can not be ignored, the rich fields offering not only good quality cultures, but also new working possibilities, especially for people with low or no income.

In order to limitate the tendency of urban tissue to spread towards the lake, where the risk of flooding is increased, we find suitable the design of different open green areas. In the northern part we suggest the expansion of Baneasa forest which would become a natural limit and will also have an extremely important role in reducing air pollution.

Also, we encourage people to use non-pollutive means of transport by creating bicycle tracks and walking paths. Also, a better connection between the northern and the southern parts of the lake is assured by pietonnal bridges. A cycling track is proposed to connect Damaroia neighborhood- proposed as a historical area- and the military forts along the ring road of Bucharest. Moreover, besides the designed corridors and public green areas, our wish is to explore the wetland which already has an important ecological function.

## RESULTS AND DISCUSSIONS

The General Urbanistic Plan of the Capital (see The General Urbanistic Plan of Bucharest, 1996-2000) requires the new constructions to depart between 30 and 50 meters from the waterfront, but this legal provision has not been respected, each owner building as pleased, with no streets nor Figure 2. Urban tissue and floodplain owner building as pleased, with no streets nor utilities.

Approximately 60% of the new houses are build on the floodplain area. (Figure 2) Moreover, most of them are extremely close to the lake, even though it is banned in the Water Law (see The Water Law, no. 107/1996).

However, the main issue is the lack of coherence and identity of the area. Because of this, what we propose is to create a living high-density neighborhood, which will have collective housing instead of the spread single-houses (Freilich et al., 2010). Also, this will allow to have mixed community-oriented instead of private-focused, while small-scale commerce, community gardens and public spaces would improve the neighbourhood's unity (Tozzi and D'Andrea, 2014).

In order to sustain the idea of an active and healthy community we suggest outdoor activities such as cycling, sailing, exploring nature, sun bathing, reading, etc.

As known, green corridors have an important ecological role. It is highly recommended to have trees in the built areas for multiple reasons. On the other side, we suggest to extend this corridors on the agricultural area also, not only because of the ecological purpose, but also for the benefits they bring to cultures.



Figure 2. Urban issue and flood-plain

In what the Grivita pond (the wetland in the northern part) is concerned, we can easily remark the need to control the amount of reed which has taken over in the past few years. Although it provides shelter to insects and animals, enriching the ecosystem, it is important to decide where to keep them and where to clear them, in order to attract the visitors and not to block the view.

So, in this wall of vegetation we propose open areas, decks and observatories.

The main material in making these elements is specially-treated wood. It is mandatory to use a wood core with high durability, as it has to

cope with the conditions faced by the field (alternating wet - dry).

Also, regarding the extension of Baneasa forest, this may become a natural barrier in order to prevent the well-known and common urban sprawling.

As we wish to involve the community in our project, the plantations will be done with the help of everyone interested. The planting will be done in vegetative rest (fall, after leaf falling/ spring before burgeoning). A mixture species will be chosen, in order to create diversity.

This operation can be performed in a voluntary event, by involving children, students, residents in the neighborhood, environmental NGOs etc.

In parallel, water samples will be taken and its quality will be analyzed. In case of existing pollution sources, ecological measures will be applied.

What is more, it is highly needed a shore rehabilitation and slopes, which can be achieved using synthetic sheet piling (PVC and composite material). This is a fast method, and also has a lifespan of over 50 years and it is a convenient alternative to traditional materials (iron, concrete, gabions or rockfill).

The presented changes are suggested in the strategy plan (Figure 3).

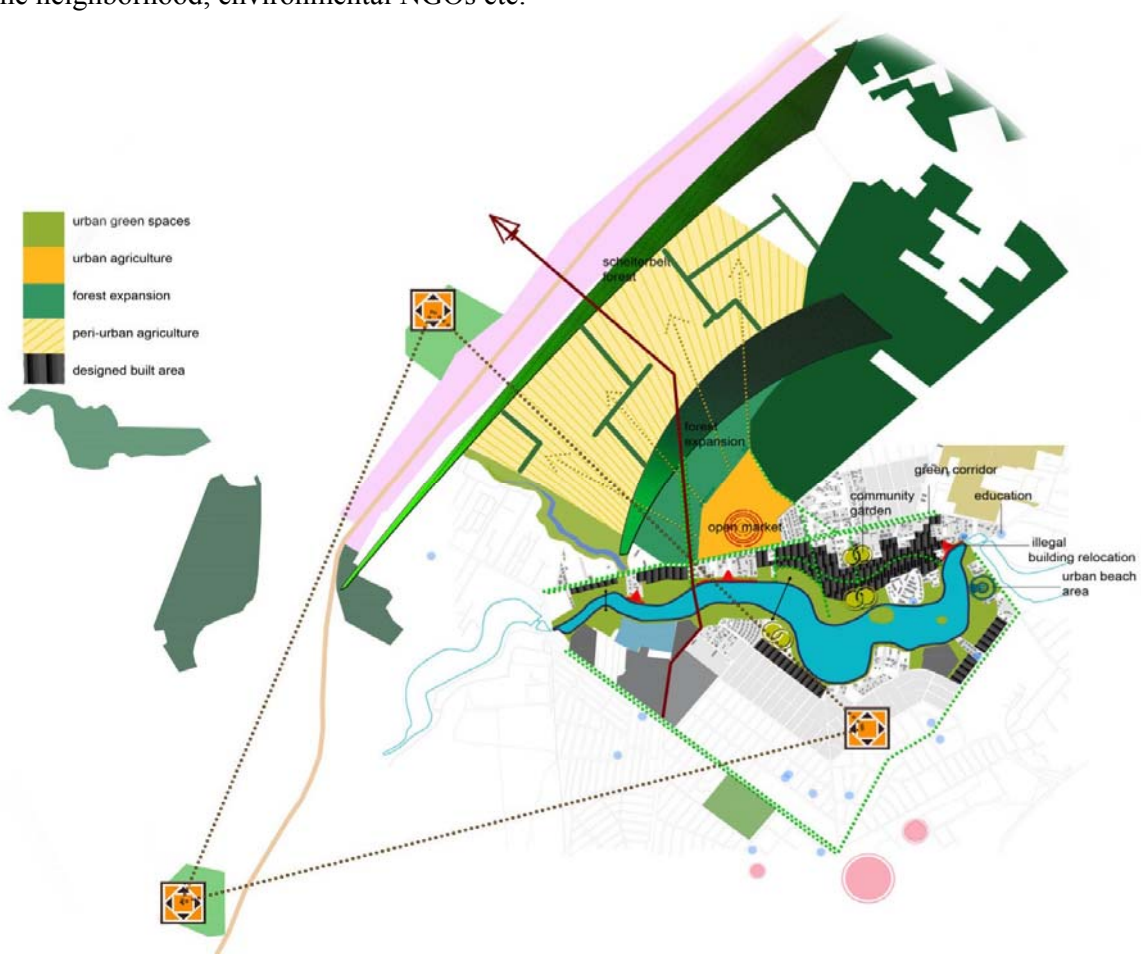


Figure 3. Strategy for the detailed area

## CONCLUSIONS

All in all, we are aware of the necessity of creating a balance among social, economical and ecological aspects all gathered in friendly neighbourhood. Our aim was to give life to an

area which had no logical built tissue. The main idea of this project is to transform the site near Grivita Lake into new sustainable neighbourhood, while recreating a relationship between human and nature.

Moreover, it is extremely important to awaken population's awareness regarding the ecological

aspects, as we are facing new challenges with nowadays problems with deforestations, pollution and climat changes

## **REFERENCES**

- Ruano M., 1998, Eco Urbanism. Introduction, p. 7- 25  
The General Urbanistic Plan of Bucharest, 1996-2000  
The Water Law, no. 107/1996
- Freilich R.H., Sitkowski R.J., Mennillo S.D., 2010, From Sprawl to Sustainability. Smart Growth, New Urbanism, Green Development and Renewable Energy, Second Edition, p. 15- 20
- Tozzi N., D'Andrea N., 2014, "French eco-neighbourhoods and community gardens", Vertigo-la revue électronique en sciences de l'environnement (online), 14th volume, no. 2, <http://vertigo.revues.org/15031>. Vauban Neighbourhood, Fribourg-en-Brisgau, Germany

## COLLAPSE SETTLEMENT SENSIBILITY ANALYSIS OF LOESSOID SOILS

Ștefan-Silvian CIOBANU

Scientific Coordinators: Prof. PhD. Eng. Ioana SIMINEA, Assist. PhD. Eng. Tatiana IVASUC

University of Agronomic Sciences and Veterinary Medicine of Bucharest, 59 Mărăști Blvd, District 1, 011464, Bucharest, Romania, Phone: +4021.318.25.64, Fax: + 4021.318.25.67

Corresponding author email: ciobanustefans@gmail.com

### Abstract:

*Collapsibility of the loess is strongly governed by water content and the magnitude of applied stress. Under an increasing load, the critical pressure at which collapse started to occur was greater for the loess with lower water content. At natural water content the critical pressure was greater than the overburden pressure. The greatest problem with collapsible soils arises when the existence and extent of the collapse potential are not recognized prior to construction. Settlements associated with development on untreated collapsible soils usually lead to expensive repairs. A comparative study between natural undisturbed and compacted samples of collapsible soils was performed. An attempt was made to relate the collapse potential to the initial moisture content.*

**Key words:** loessoid soils; collapse behaviour; settlement analysis

### INTRODUCTION

Loessoid soils are also known in the scientific literature as collapsible soils. The expression “soil collapse” is used to describe a wetting-induced deformation in collapsible soils (Figure 1). These soils have an open structure as the particles are held together by a temporary bonding. If the loess becomes saturated, the material structure collapses and records large supplementary settlements. (Ciobanu, 2014)

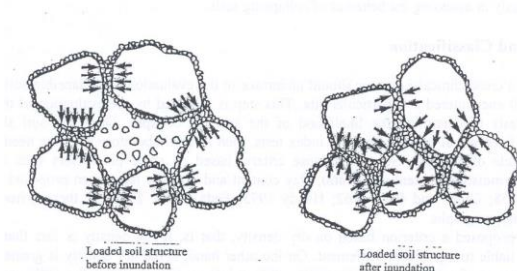


Figure 1. The collapse occurred after inundation of the soil (Al-Rawas, 2000)

Supplementary settlement to wetting ( $I_m$ ) is defined by vertical deformations occurred with the growth of humidity, loessoid soils reports much higher values compared to soils based on clay or sand in natural form under the same values of stress. Supplementary settlement to wetting is influenced by the weight of the sheet

( $I_{mg}$ ) and under the compressive load transmitted by foundations ( $I_{mp}$ ). (Siminea, 2006).

### MATERIALS AND METHODS

In order to calculate the settlement we have to take in consideration the type of the soil. For normal soils the settlement is calculated according to STAS 3300-77, using the method of summing the elementary sheets. In this algorithm the soil is separated into elementary sheets until the required depth, where  $\sigma_z < 0,2\sigma_g$  (in this case it is necessary to find the depth of active area and the value for  $\sigma_{gz}$  - geological load for specific sheet - Figure 2). On vertical axis, at the limit of sheets we determine the vertical pressure exercised by the net pressure from the base of the foundation calculated with the following relation:

$$\sigma_z = \alpha_0 \times P_n \quad (1)$$

Where:

- $\alpha_0$  index for distribution of vertical efforts toked from table based on L/B and z/B reports
- L the length of the foundation (m)
- B the width of the foundation (m)
- z the depth of the layer from the separation limit to the base of the foundation
- $P_n$  the pressure on the base of the

foundation calculated with the relation:

$$P_n = -\frac{P + G_f}{A_f} - \gamma D_f \quad (2)$$

In our case:

$P$  = the pressure exercised by the foundation kN

$G_f$  = the weight of the foundation (kN)

$A_f$  = LB = the area of the foundation (m<sup>2</sup>)

$\gamma$  = the specific weight of the soil (kN/m<sup>3</sup>)

$D_f$  = the depth of the foundation (m)

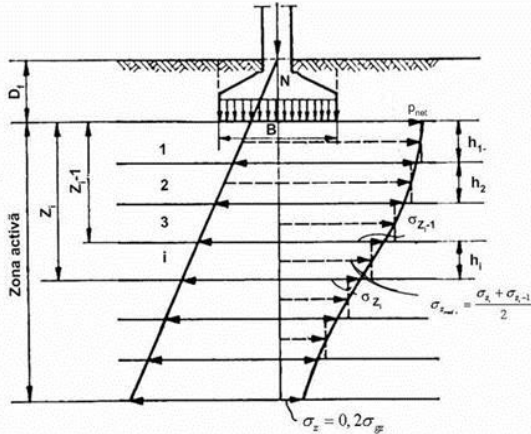


Figure 2. The calculation of the settlement

The settlement is calculated with the following

$$s = 100\beta \sum_1^n \frac{\sigma_{zi}^{med} \cdot h_i}{E_i} \quad (3)$$

formula

where

$\beta$  = correction index = 0.8

$\sigma_{zi}^{med}$  medium vertical stress in the elementary sheet calculated with the next formula:

$$\sigma_{zi}^{med} = \frac{\sigma_{zi}^{sup} + \sigma_{zi}^{inf}}{2} \quad (kPa) \quad (4)$$

$h_i$  = the thickness of the elementary sheet

$E_i$  = the linear deformation module (kPa) (Atanasiu, 1983)

From 2014, the method for the determination of settlement, for leosoid soils, is made using a different algorithm.

The hypothesis for determination of settlement is built on the assumption of direct foundation on saturated loessoid soil.

The calculations were made according to Romanian normative in force (NP 124/2014).

This normative calculate the settlement according to European legislation in Civil Engineering (EUROCOD 7).

In order to calculate the settlement, the following characteristics were taken into

consideration.

$I_{mg}$  – Supplementary settlement to wetting under own weight (geological action)

$I_{mp}$  – Supplementary settlement to wetting under the action of loads transmitted by foundation (for compression loads)

$s$  = The total of supplementary settlement from wetting  $s = I_{mg} + I_{mp}$  (5)

Calculations uses the results of compressibility test in laboratory and on field (if is possible)

The supplementary settlement to wetting, under geological load is calculated on entire thickness sensible to wetting ( $i_{m3} \geq 2\%$ ) with the relation:

$$I_{mg} = \sum_1^N i_{mg} \cdot h_i \quad (6)$$

where:

$N$  = the number of elementary sheets

$h_i$  = the thickness of the elementary sheets

$i_{mg}$  = the index of supplementary settlement from wetting of the elementary sheet under his own weight and it can be obtain with the duple edometer test with the following relation :

$$i_{mg} = \varepsilon_{gi} - \varepsilon_{gn} \quad (7)$$

where:

$\varepsilon_{gi}$  = the specific deformation of wetted soil (calculated with volumetric weight of saturated soil)

$\varepsilon_{gn}$  = the specific deformation of natural soil (geological pressure accorded to the middle of the sheet calculated with the volumetric weight of natural soil)

The supplementary settlement to wetting from geological load  $I_{mg}$  represent a criteria for a classification to group A ( $I_{mg} < 5cm$ ) or group B ( $I_{mg} > 5cm$ ) and it has to be calculated into the first phase, no matter what situation that will occur after.

The supplementary settlement from wetting under the load transmitted by foundation ( $I_{mp}$ ) is calculated from the depth of foundation ( $D_f$ ) for all deformable areas with the following relation

$$I_{mp} = \sum_{1(D_f)}^N i_{mp} \cdot h_i \quad (8)$$

Where:

$N'$  = the number of elementary sheets in the deformable area from the soil

$h_i$  = the thickness of the sheet

$D_f$  = the depth of foundation

$i_{mp}$  = the index of specific settlement from wetting under the load transmitted by foundation, it can be obtain from the double edometric test with the following relation:

$$i_{mp} = \varepsilon_{pi} - \varepsilon_{gi} \quad (9)$$

Where

$\varepsilon_{pi}$  = specific deformation for wetted soil using the relation:

$$p_i = \sigma_{gi} + \sigma_z \quad (10)$$

$\sigma_{gi}$  = specific deformation of wetted soil for  $\varepsilon_{gi}$ ,  
 $\varepsilon_{gi}$  = the specific deformation of wetted soil (calculated with volumetric weight of saturated soil)

$\sigma_z$  = the vertical stress from the foundation load in the middle of the sheet according to NP 112/2004.

The supplementary settlement from wetting is calculated with

$$s = I_{mg} + I_{mp} \quad (11)$$

The settlement is realized for deformable areas from the soil. (NP 124/2014)

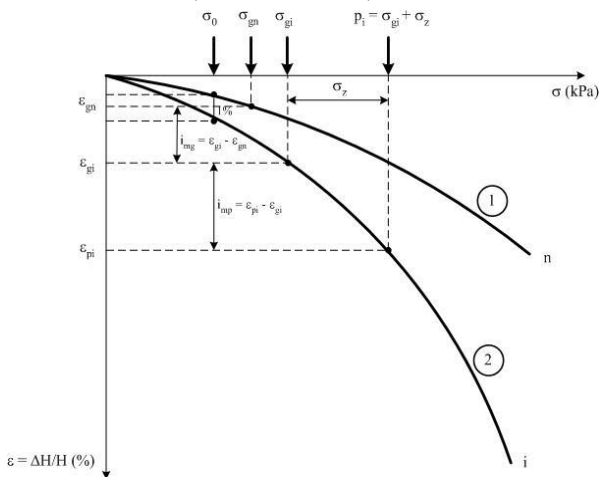


Figure 3. Curves of compression for unmodified sample: with natural humidity (curve 1) and initially saturated (curve 2)

## RESULTS AND DISCUSSIONS

In order to calculate the settlement for a non collapsible soil and for a leossoid soil the dimension of foundation are considered:  $L = 2.5 \text{ m}$   $B = 2.5 \text{ m}$  and  $D_f = 1.5 \text{ m}$ .

For a non-collapsible soil, we used the following values: specific weight  $\gamma = 20 \text{ kN/m}^3$ , the pressure exercised by the foundation  $P = 1500 \text{ kN}$ , the linear deformation module  $E_i = 20000$  and the pressure exercised by the foundation was calculated and resulted  $p_{med} = 239.32 \text{ kN/m}^2$ .

To realize the settlement calculation, the specific deformation for every sheet,  $\sigma_z$  and  $\sigma_{gz}$ , was extracted from the Figure 4 (first one realised for a natural sample of soil wetted at 300kPa vertical load and the second curve was made for a initially saturated sample of loessoid soil).

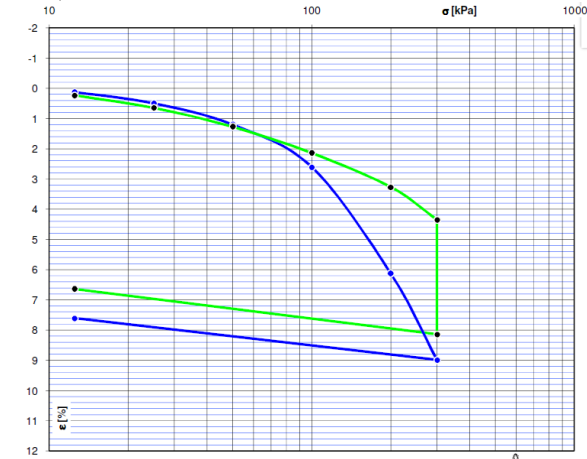


Figure 4. Curves of compression on a loessoid soil (green curve – for a sample with natural humidity and blue curve – for a sample initially saturated) (NP 124/2004)

The difference between settlements, depending on the type of the soil, can be seen in the Figure 5.

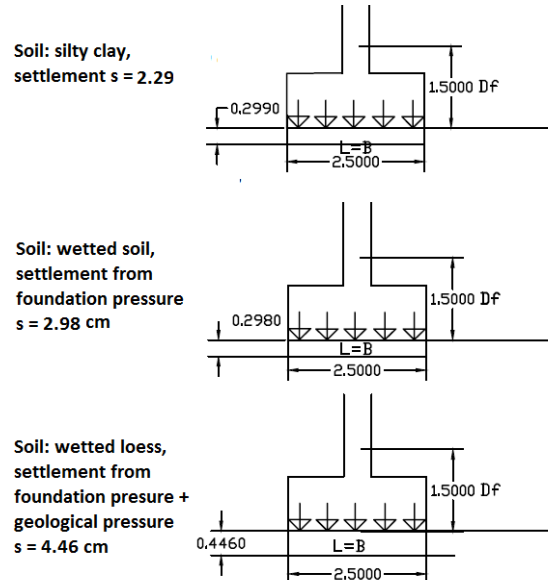


Figure 5. The difference of settlement for differet soil types

The calculations conducted to determine the settlement are shown in Table and Table 2.

Table 1. settlement determination for normal soil

H	n=L/B	z/B	$\alpha_0$	pn	$\sigma_z$	$\sigma_{gz}$	$0.2\sigma_{gz}$	$\sigma_{zi}$ med	E	s
m				kN/m <sup>2</sup>	kPa	kPa	kPa	kPa	kPa	mm <sup>2</sup>
1.5	1	0	1.00	239.32	239.32	30.00	6.00	215.39	20000	8.62
2.5	1	0.4	0.80	239.32	191.46	50.00	10.00	149.58	20000	5.98
3.5	1	0.8	0.45	239.32	107.70	70.00	14.00	84.96	20000	3.40
4.5	1	1.2	0.26	239.32	62.22	90.00	18.00	50.26	20000	2.01
5.5	1	1.6	0.16	239.32	38.29	110.00	22.00	32.31	20000	1.29
6.5	1	2	0.11	239.32	26.33	130.00	26.00	22.74	20000	0.91
7.5	1	2.4	0.08	239.32	19.15	150.00	30.00	16.75	20000	0.67
Total									22.88	

Table 2. settlement determination for leossoid soil

sample with natural humidity						sample initially saturated						
$\gamma$ kN/m <sup>3</sup>	pn kN/m <sup>2</sup>	$\sigma_z$ kPa	$\sigma_{gz}$ kPa	$0.2^*$ $\sigma_{gz}$	$\gamma_{sat}$ kN/m <sup>3</sup>	pn sat kN/m <sup>2</sup>	$\sigma_z$ kPa	$\sigma_{gz}$ kPa	$0.2^*$ $\sigma_{gz}$	$I_{mg}$	$I_{mp}$	s
16.80	243.8 0	243.8	25.2	5.04	20.00	240.9 2	240.9 2	30.00	6.00	0.46	5.40	5.86
16.80	243.8 0	195.0	42.0	8.40	20.00	240.9 2	192.7 4	50.00	10.00	0.84	5.00	5.84
16.80	243.8 0	109.7	58.8	11.76	20.00	240.9 2	108.4 1	70.00	14.00	1.40	4.20	5.60
16.80	243.8 0	63.4	75.6	15.12	20.00	240.9 2	62.64	90.00	18.00	1.90	3.80	5.70
16.80	243.8 0	39.0	92.4	18.48	20.00	240.9 2	38.55	110.0 0	22.00	3.00	3.80	6.80
16.80	243.8 0	26.8	109.2	21.84	20.00	240.9 2	26.50	130.0 0	26.00	3.00	3.80	6.80
16.80	243.8 0	19.5	126.0	25.20	20.00	240.9 2	19.27	150.0 0	30.00	4.20	3.80	8.00
Total										14.80	29.80	44.60

## CONCLUSIONS

The determination of settlement for leossoid soil is according to the normative NP 124/2014.

The algorithm for calculation of the settlement for leossoid soils compared to the algorithm for calculation of settlement for normal soils is more complicated and it's include more information, using the hypothesis of supplementary settlement from geological weight and foundation weight.

The settlement of a leossoid soil is almost double compared to a normal soil which is not sensible to wetting, the phenomenon being caused by the collapse of the leossoid soils.

For minimization or elimination of the collapse phenomenon caused by the wetting

of the soil we must stabilize the soil using improving methods.

## REFERENCES

- Al-Rawas A.A. – 2000 State-of-the-Art Review of Collapsible Soils Science and Technology, Special Review (2000) 115-135 ©2000 Sultan Qaboos University.
- Atanasiu C., et al., 1983. Geotehnica si Fundatii – Exemple de calcul. Editura Didactica si Pedagogica Bucuresti.
- NP 124/2014 Normativ privind fundarea pe pamanturi sensibile la umezire.
- Siminea I., 2006 Bucuresti Geotehnica si Fundatii Editura Bren.
- Stefan C., 2014 .Geotechnical characterization of loessoid soils and improvement methods. International Student Symposium "IF IM CAD".

## SAFETY STRUCTURAL ASSESSMENT OF REINFORCED CONCRETE BUILDINGS

Simona SBURATURA, Mihai-Cristian MUSCALU, Ancuta BODIRLAU

Scientific Coordinator: Lect. PhD. Eng. Claudiu-Sorin DRAGOMIR

University of Agronomic Sciences and Veterinary Medicine of Bucharest, 59 Mărăști Blvd, District 1, 011464, Bucharest, Romania, Phone: +4021.318.25.64, Fax: + 4021.318.25.67

Corresponding author email: sburatura.simona93@gmail.com

### Abstract

*In all seismic areas, local and state officials and prudent property owner, establish procedures to assess the safety of buildings and other important structures following a main seismic event. Such decisions, in most cases, are based on visual inspections of possible damage to the structure. If the structure appears damaged, it is necessary to further examine and assess as to whether the damage condition of the structure presents an unsafe environment for the occupants of that structure. If available, instrumental measurements of shaking of a building or a nearby ground site are very useful to decision makers. In this sense the paper present a method to assess the building safety of Reinforced Concrete structures using seismic records made by seismic station. Both dynamic analysis and processing/recording of seismic events are made using modern techniques and equipment existent in Reinforced Concrete Laboratory. Mention that seismic equipment for strong motion records belongs National Seismic Network for Construction of National Institute for Research and Development in Construction, Urban Planning and Sustainable Spatial Development., „URBAN-INCERC”, and equipment was installed here on the base of cooperation protocol signed by the two institutions. The paper results are conclusive and are discussed both on the charts and analytical results obtained. The activities of this research were conducted under the supervision of PhD. Claudiu-Sorin DRAGOMIR, Lecturer in the Department of Environment and Land Reclamation at the Faculty of Land Reclamation and Environment Engineering Faculty in Bucharest in Bucharest.*

**Keywords:** seismic action, digital accelerographs, building response, building safety.

### INTRODUCTION

An earthquake is a sudden and powerful, vertical, horizontal or torsion movement of the Earth's crust caused by underground dislocations, volcanic eruptions, tidal forces, meteors colliding the Earth and so on. In case of converging movements of two tectonic plates and especially in the subduction process, the tension created is enormous. When the detension happens earthquakes take place. Earthquakes can intervene in steady state of surface structures of areas, by producing cracks in the bark, followed by collapses, landslides, land subsidence etc.

Earthquakes and landslides may cause negative effects on buildings and construction assemblies which can manifest disastrous by:

- totally or partial destruction (collapse) of vulnerable buildings;
- destruction or damage of parts (structural or

non-structural) of buildings;

- destruction/damage of equipment and facilities, of public networks with vital utility (water, gas, electricity, heat, transport, communications);
- fires and explosions in buildings or districts / municipalities;

According to seismic risk assessments, the most vulnerable buildings in this regard are tall buildings of reinforced concrete frame and closing walls or partition walls (masonry) made before 1941 and the old buildings with masonry walls and wooden floors.

### MATERIALS AND METHODS

#### Seismic monitoring of the territory of Romania

Seismic hazard in Romania is due to Vrancea seismic source and several sub-layered surface seismic sources (Banat, Fagaras,

Dobrogea, etc.). Vrancea source is decisive for the seismic hazard for about two thirds of Romania, while surface source contributes more to local seismic hazard.

In Europe, Romania's seismicity can be characterized as medium, but with the particularity that earthquakes with the focus in Vrancea subcrustal source can cause damage over large areas including neighboring countries.

Vrancea earthquakes were noticeable in Europe on surfaces that have reached 2 million square kilometers.



Figure 1. 1977 earthquake

Compared to Vrancea seismic source, other zones of Romania show a reduced activity, more active lately proved to be the Banat zone. In this area it occurred in the last decade relatively strong surface earthquakes (depth outbreaks  $h \leq 10$  km):

- on July 12, 1991 (magnitude  $M_s = 5.7$  Surface Waves),
- July 18, 1991 ( $M_s = 5.6$ ) on December 2, 1991 ( $M_s = 5.6$ , 5 injured, ~ 1000 buildings collapsed or severely damaged, 4,000 homeless people).

The peak acceleration of ground motion recorded was about 13% of gravitational acceleration.

Other active crustal seismic zones are Fagaras and Dobrogea areas.

### Equipment

There are different devices for measuring the characteristics of earthquakes. The most important of these, are the accelerographs and the seismographs. The most popular scales of measuring are Richter Scale and the Mercalli Scale.

A seismograph is a device that measures and records ground movements, in order to analyze seismic movements caused by earthquakes, explosions and other sources. Sometimes earthquakes are caused artificially,

for geophysical prospecting. A seismometer is a similar device which is restricted to the measurement of seismographs; recording function being taken over by other devices. Seismographs record a zigzag wave which shows the variable amplitude of the land oscillations under the device.

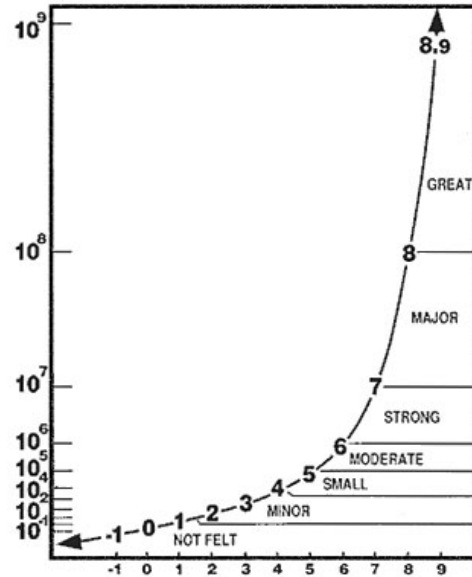


Figure 2. Richter Scale

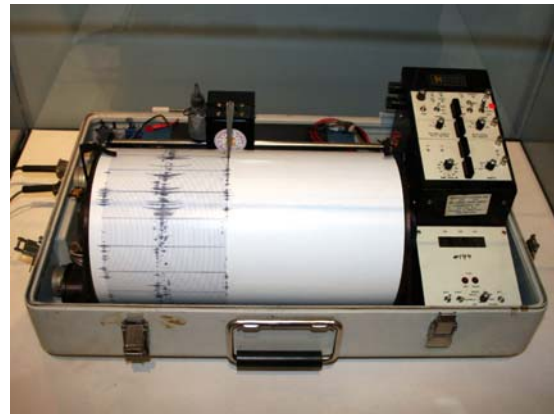


Figure 3. Seismograph

There are also seismographs with an even higher accuracy, which increases recording telluric movements and they can record earthquakes anywhere in the world. The exact timing, location and magnitude can be determined from the data recorded by seismographs.

The equipment presented in Figure 4 is installed in the laboratory of concrete from the Faculty of Land Improvement and Environmental Engineering and it is an integral part of the National Seismic Network

for Construction of the National Institute of Research-Development for Construction, Urban Planning and Sustainable Territorial Development (URBAN-INCERC).



Figure 4. Digital Accelerograph GMS-18 GeoSIG.

Seismic resistance depends on the characteristics conferred by applying some traditional methods of construction or engineering that was improved over time. Equivalent seismic forces method Structures vibrations generated by the random movement of the bearing base during an earthquake generates inertial forces. In the current design, modal maximum seismic forces of inertia can be represented by equivalent conventional forces static applied. Linear static calculation process is known as "equivalent lateral forces method" and underpins all regulations for earthquake resistant design of buildings. Conventional seismic forces (computing) depend on the structural and dynamic characteristics of seismic action, represented by the absolute acceleration response spectrums. Equivalent seismic forces are obtained by the independent treatment of each proper mode of vibration  $k$ , characterized by its own vibration period  $T_k$ , the eigenvector  $s_k$  and the equivalent modal mass  $m_k$ . For each proper mode of vibration of the structure with a finite

number of dynamic degrees of freedom (DOF) is considered a dynamic system equivalent to a DOF, with the same vibration period and the same base shear force. Maximum modal level seismic forces distribution obtained by modal base shear force distribution according to the vector of vibration acts as lateral static force at structure levels.

## RESULTS AND DISCUSSIONS

### Seismic analysis of the spatial structure of reinforced concrete using Autodesk Robot

According to the design code, to the indicative P100-1: 2013 and to the method of calculation - the equivalent static forces, shear force corresponding base its fundamental mode for each main horizontal direction considered in the calculation of the building is determined as follows

$$F_b = \gamma_1 \xi_d(T_1) m \lambda$$

$S_d(T_1)$  the ordinate of the spectrum design response corresponding to the fundamental period;

$T_1$  = fundamental proper period of vibration of the building from the plane containing the horizontal direction considered;

$m$  = total mass of the building calculated as the sum of the masses of level;

$\lambda$  = correction factor that takes into account the contribution of its fundamental mode

Effective modal mass associated with it, whose values are:

- $\lambda = 0.85$  if  $T_1 \leq T_C$  and the building has more than two levels;
- $\lambda = 1.0$  in other cases.

Fundamental proper periods  $T_1$  and  $T_2$  are determined on the basis of some structural dynamic calculation methods.



Figure 5. Reinforced concrete structures analyzed ( $S_I$  and  $S_{II}$ )

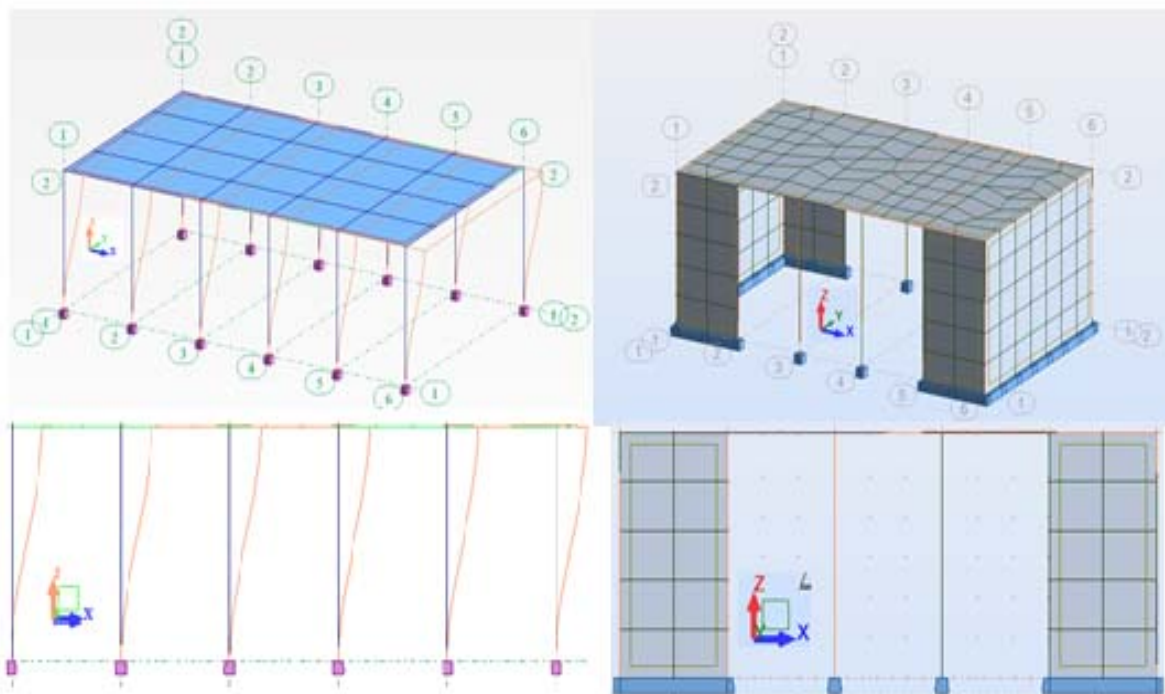


Figure 6. Spatial deformed structures ( $S_I$  and  $S_{II}$ )

The maximum value of displacement at the top of the structure was found in node 51 and has the value:

- For structure  $S_I$  :  $d= 5,82$  mm;
- For structure  $S_{II}$  :  $d= 0,00089$  mm;

Table 1. Oscillation periods corresponding to the values of the 3 fundamental mode

Mode	Period $S_I$ (s)	Period $S_{II}$ (s)
Mode 1	0,27	0,09
Mode 2	0,23	0,08
Mode 3	0,21	0,07

Checking the maximum displacement under seismic design code, indicative P100-1: 2013 Annex E

$q$  = behavior factor specific to the type of structure

$$q = 3,5 \times 1,15 = 4,02$$

Checking the ultimate limit state (ULS) for S I

Checking the status of the ultimate limit is aimed at avoiding loss of human life from the attack of a major earthquake, very rare, that can occur in the life of a building, by preventing the total collapse of the non-structural elements. It seeks both to achieve sufficient safety margin compared to the stage of transfer structural elements.

The verification of movement is based on the relation:

$$d_r^{ULS} = eq d \leq d_{r,a}^{ULS}$$

$d_r^{ULS}$  = relative displacement level under seismic action associated to ULS;

$c$  = factor of amplification movements, which take into account that for T:

$$c = 3 - 2,5 \frac{T_1}{T_c} = 3 - 2,5 \frac{0,27}{1,00} = 2,325$$

$d_{r,a}^{ULS}$  = allowable value of drift movement level, is equal to 0,025h (where h is the height of level).

$$d_{r,a}^{ULS} = 0,025h = 0,025 \times 6100 = 152,5 \text{ mm}$$

Checking the ultimate limit state (ULS) for SII

The verification of movement is based on the relation:

$$d_r^{ULS} = eq d \leq d_{r,a}^{ULS}$$

$d_r^{ULS}$  = relative displacement level under seismic action associated to ULS;

$c$  = factor of the amplification movements, which take into account that for T:

$$c = 3 - 2,5 \frac{T_2}{T_c} = 3 - 2,5 \frac{0,07}{1,00} = 2,775$$

$d_{r,a}^{ULS}$  = allowable value of drift movement level, is equal to 0,025h (where h is the height of level).

$$d_{r,a}^{ULS} = 0,025h = 0,025 \times 6100 = 152,5 \text{ mm}$$

## CONCLUSIONS

The article presents a modern method of structural analysis and validation of the

method of structural rehabilitation works using a mix of structural reinforced concrete walls. A global assessment method takes into account the structural use of structural features as well as the period of oscillation of the structure. Investigation of seismic equipment used for the existing structure in reinforced concrete laboratory within the FIFIM. Records obtained are processed with specialized software GeoDAS from GeoSIG, Switzerland. Own periods of the structure is input data in structural analysis carried out with the ROBOT. Finally, by using the process of verification of lateral displacement of structures, the annex E of the code of seismic design of indication P100-1: 2013 is done at the State checking the last ultimate limit (ULS).

The bottom line is that the maximum displacement at the top of the structure does not exceed the permissible value and, at the same time, the proposed solution is validated through the proposed structural.

## REFERENCES

- A. Aldea, T. Kashima, D. Lungu, R. Vacareanu, S. Koyama, C. Arion, "Modern Urban Seismic Network in Bucharest, Romania", First International Conference on Urban Earthquake Engineering, Tokyo Institute of Technology, Japan, March 8-9, 2004.
- C.S. Dragomir, M.C. Calin, "Dynamic response parameters and damage assessment of educational building located in earthquake prone area", Proc. of 15th World Conference Earthquake Engineering in Lisbon, Portugal, Paper ID 1940, 10 pag., September 2012.
- C.S. Dragomir, A. Virsta, "Assessment of buildings vulnerability using non-destructive testing", Proc. of International Multidisciplinary Scientific GeoConference Conference SGEM, Albena, Bulgaria, 2013.
- I.S. Borcia, "Processing of strong motion records specific for the territory of Romania", PhD Thesis, Technical University of Civil Engineering, Bucharest, Romania, 2006.
- M. Celebi, "Current Practice and Guidelines for USGS Instrumentation of Buildings Including Federal Buildings", in Proc. COSMOS Workshop on Structural Instrumentation, USA, 2001.
- \*\*\*Ministry of Regional Development and Public Administration: Romanian Earthquake Design Code – Part I – Design Provisions for Buildings, P100-1/2013, 2013, Romania.



**SECTION 03**  
**WATER RESOURCES MANAGEMENT**



## ASPECTS OF ADVANCED WASTEWATER PURIFICATION

Adina CIOBANESCU, Georgiana DONE

Scientific Coordinator: Prof. PhD. Eng. Paulina IANCU

University of Agronomic Sciences and Veterinary Medicine of Bucharest, 59 Mărăști Blvd, District 1, 011464, Bucharest, Romania, Phone: +4021.318.25.64, Fax: + 4021.318.25.67, Email: adee.adina05@yahoo.com , georgina.done@yahoo.com

Corresponding author email: georgiana.done@yahoo.com

### Abstract

*The problem of wastewater treatment is an important issue for environmental protection. Businesses with different specific according to the law are required to carry wastewater treatment products. In the meat preparation units appear special problems . The case study shows solutions for removing nitrogen and phosphorus from meat preparation units and cold storage- Mogosoaia.*

**Key words:** advanced treatment, denitrification, wastewater treatment plant

### INTRODUCTION

The human actions modifying substances penetrate water quality features, leading to an imbalance in the environment. The problem must be related to water quality and use. Conditions quality varies from one use to another, and the range considered acceptable varies in a wide range.

Water quality is most affected by the discharge of human waste water. Therefore, the main practical measure to protect surface water quality is to wastewater treatment.

Water purification is a complex process of retention and neutralization harmful substances dissolved or colloidal suspensions, present in municipal and industrial wastewater, which are not supported in the aquatic environment where the wastewater is treated and allows restoring the physicochemical properties of water before use.

### MATERIALS AND METHODS

#### Processes for removing pollutants from wastewater

Waste water purification can be achieved by methods that are based on the physical, chemical and biological properties which differ according to the type of pollutants and their concentrations in the waste water.

Primary stage (mechanical treatment) consists of retention systems bodies and large suspension (barbecues, site), separation of oils and fats by flotation (grease separators, settling solids in suspension, made in sand-clearing basins and decanters). Secondary stage (biological treatment) is carried out based on biochemical processes that remove colloidal solids and biodegradable organic compounds. It is made in activated sludge basins in biological filters or lagoons.

Advanced treatment of wastewater or tertiary stage, is a new technological solution from wastewater retention especially nitrogen and phosphorus compounds and other contaminants whose chemical and biological structure do not allow be retaining and disposing of in a conventional treatment plant.

#### Nitrogen and Phosphorus removal from wastewater

The chemical elements nitrogen and phosphorus are known as nutrients, the substances necessary for life. In situations where these quantities exceed the allowable limit in wastewater pose a negative impact on the environment, becoming aggressive pollutants to groundwater, surface water, soil and air. In the case of surface water eutrophication occurs frequently.

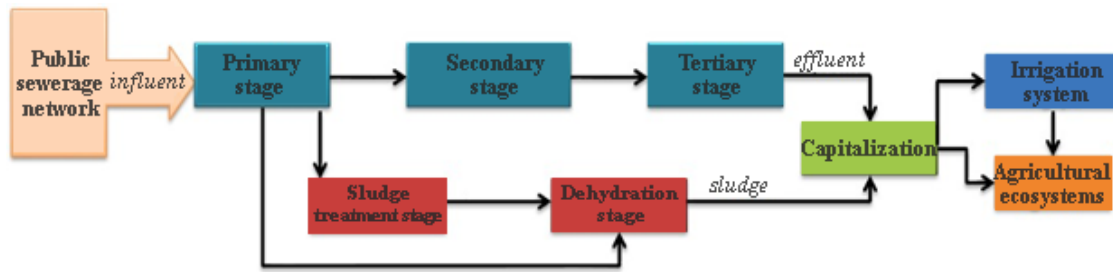


Figure 1. General scheme of water and sludge circuits in treatment plant



Figure 2. General scheme of all wastewater treatment plants

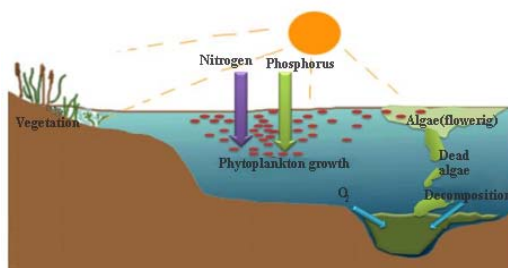


Figure 3. Eutrophication scheme

**Biological nitrogen removal methods from wastewater:**

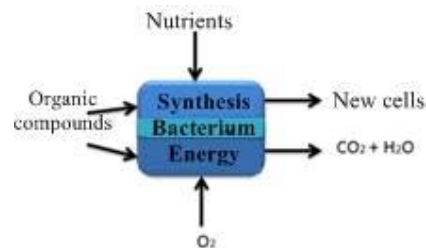
Domestic wastewater containing organic nitrogen, 60%, and inorganic ammonium about 40%. Biological nitrogen removal from wastewater is done sequentially by nitrification and denitrification.

Nitrification stage:

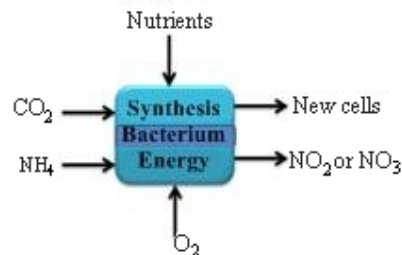
Nitrification is the oxidation of ammonium to nitrite and then of oxidation of nitrite to nitrate, by autotrophic microorganisms. The process can take place in pools suspension or biofilm. The most common method is to achieve nitrification in the same pool that carry and remove carbon compounds (single-sludge system), the process is similar to the activated sludge process, requiring an aeration basin, a decanter and a recirculation system.

Nitrification consists of two important processes: reduction of organic matter,

which is carried out by aerobic heterotrophic bacteria (figure 4.a.) and ammonia reduction of nitrogen (nitrification itself) is performed using autotrophic aerobic bacteria populations (figure 4.b.), which oxidize ammonium to nitrate with intermediate formation of nitrite.



a) aerobic heterotrophic



b) aerobic autotrophic

Figure 4. Schematic representation of the metabolism of the bacteria involved in the nitrification

Biochemically speaking, nitrification process involves more than successively oxidation of ammonia to nitrite by bacteria

Nitrosomonas and of nitrite to nitrate by Nitrobacter. It involves many intermediate reactions and enzymes.

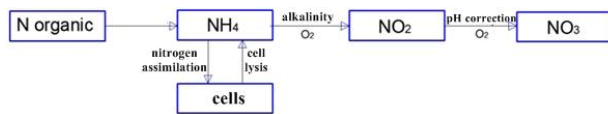


Figure 5. Nitrification scheme

Factors influencing the nitrification are: temperature, dissolved oxygen concentration, pH and alkalinity, organic carbon ratio influent / nitrogen system.

**Denitrification stage:**

Nitrification process is continued with biological denitrification and consists in the progressive reduction of nitrate to nitrite and nitrite to molecular nitrogen finally, using an oxygen-free environment under the action of denitrifying bacteria. The prerequisite of this reaction is the lack of molecular oxygen instead, to ensure bacterial respiration, nitrate is taken.

The transformation of nitrate in a more easily removed form is achieved by bacteria like Achromobacter, Aerobacter, Alcaligenes, Bacillus, Brevibacterium, flavobacteriu, Lactobacillus, Micrococcus, Proteus, Pseudomonas and spirillum.

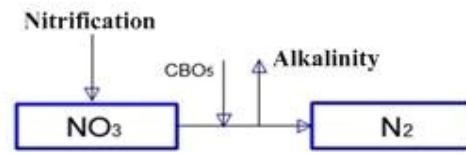


Figure 7. Denitrification process scheme

In the process of denitrification, nitrate and nitrite acts as the electron acceptor in the electron transport chain in the same way as the oxygen.

The process involves the transfer of electrons from a donor electron (eg. The organic substrate) to an acceptor electron oxidized (eg. Oxygen, nitrate, nitrite). Theoretical stoichiometric equations reveal donor electron mass (eg carbon substrate) and acceptor (eg oxygen, nitrate and nitrite) consume, mass of cells produced during any biological process.

Factors influencing the denitrification are: temperature, dissolved oxygen concentration, pH and the presence of the organic layer.

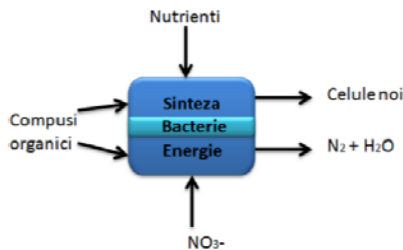


Figure 6. Schematic representation of anoxic heterotrophic bacterial metabolism

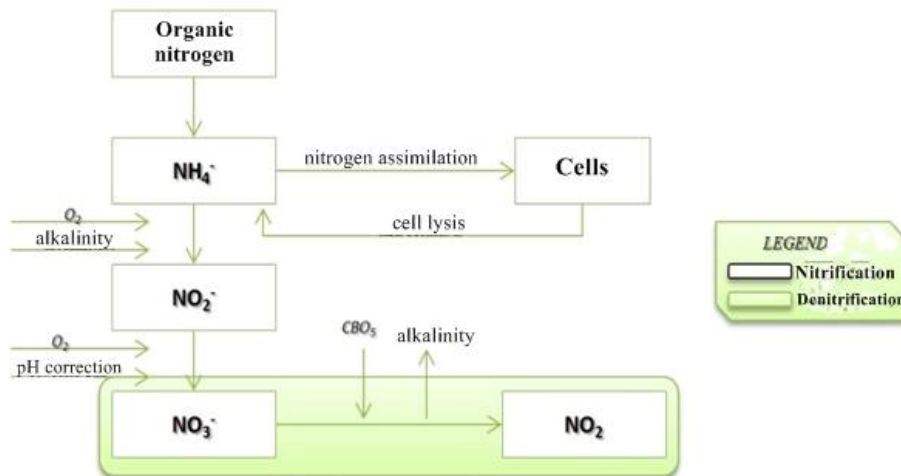


Figure 8. Nitrification – denitrification chart

**Methods of removing phosphorus from wastewater:**

Removing phosphorus as advanced treatment process can be achieved either by physico-chemical, or on biological pathway.

Chemically removing phosphorus from wastewater, especially loaded with manure, are made based on precipitation and adsorption processes under the influence of coagulants, which connect the form of sparingly soluble salts of iron, aluminum and cadmium, which then decanted. Transformation of phosphorus compounds using these reagents precipitation in achieving a suitable pH conditions leads to the formation of phosphate ( $PO_4^-$ ) sparingly soluble and easily sediment flocculants. These compounds have good adsorption capacity of organic phosphates and polyphosphates. To ensure the formation of agglomerates is recommended that the reagents introduced into the pool to be constantly moving.

Biological method is based on the exposure of microorganisms to alternative aerobic or anaerobic conditions. For removal of phosphorus, it is done in two

steps, the effect of aerobic and anaerobic bacteria. To remove phosphorus by biological, it is necessary in the waste water subjected to the treatment process to be a satisfactory quantity of organic substances easily degradable in order to form organic acids and enrichment reserve substances for bacteria.

Phosphorus is retained by incorporating orthophosphates, polyphosphates and organically bound phosphorus in the cellular tissue, total phosphorus is removed from the system depending on the amount of biological floaters actually produced.

- Anaerobic Process / Onix (A / O):

This procedure involves removing phosphorus in biological stage while the oxidation of organic substances based on carbon. The concentration of phosphorus in the effluent depends largely on the ratio of BOD5: P wastewater influent.

- The PHOSTRIP process:

This process involves removing phosphorus sludge line. Thus, part of the return activated sludge is directed into the anaerobic tank for stripping phosphorus

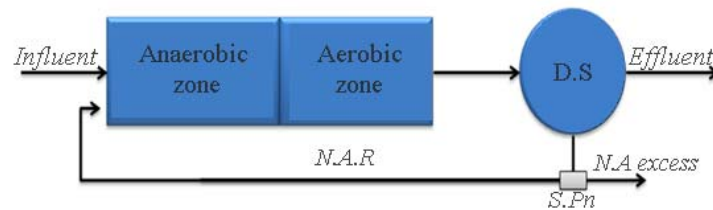


Figure 9. The flowchart of removing phosphorus, A / O

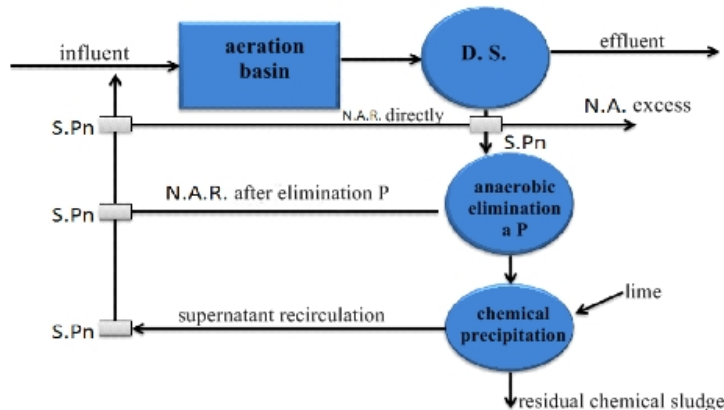


Figure 10. The flowchart of phosphorus removal, PHOSTRIP

- Basins with running sequential process:  
It involves removal of phosphorus in 4 phases: filling, mixing or aeration, sedimentation and draining.

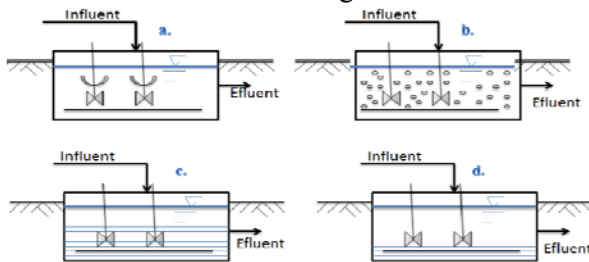


Figure 11. Flowsheet of phosphorus removal in the basin with running sequence (a. fill the basin; b. ongoing biological process - mixing or aeration; c. sedimentation process; d. drain the tank)

## RESULTS AND DISCUSSIONS

Case studies – Wastewater treatment plants for meat preparation unit and warehouse frigorific Mogosoia

Characterization of industrial unit

The warehouse is certified for cold storage, meat processing and trade under intra-Community rules, including sanitary veterinary authorization for intra-Community trade in food of animal origin. Meat processing plant has a processing capacity of 10 tons of meat per shift (8 hours) and can process meat and meat products of pork, beef, mutton, chicken, turkey, except fish.

Processed products:

The unit will provide processing and processing of meat and delicatessen products, including products ready for selective distribution, ex. grilled minced meat rolls and sausage, automatic packaging from 500 grams to 25 kg per casserole. Minced meat production will have a capacity of 2 tons per hour, free pregnancy 3.5 tons per hour, reaching up to 40 tons of minced meat daily.

- Average daily flow  $Q_{zi}$  med: 12.28 m<sup>3</sup> / day
- Maximum daily flow  $Q_{zi}$  max: 16 m<sup>3</sup> / day
- The average hourly rate  $Q_o$  avg: 1.53 m<sup>3</sup> / day

- The maximum hourly rate  $Q_o$  max: 4 m<sup>3</sup> / day

- Working time: 8 hours / day

Treatment plant

The treatment plant consists of mechano-chemical and biological treatment stage. Mechano-chemical treatment step consists of: grinded rare, grill often, mixing tank, flotation unit adios chemicals. From homogenization tank, wastewater is pumped into the grill (filtration plant) and then the dissolved air flotation unit (DAF) with automatic system of recruitment, timer and addition of chemicals. The operating principle of this dissolved air flotation units is based on the formation of fine air bubbles with sizes ranging from 30-50 micrometres in suwspensie adhering particles, grease, oil, grease, etc.

It utilizes dosing of chemicals (coagulant and flocculant) before placing in water concentration unit. They coagulation-flocculation processes take place after which it can hold about 80-90% of the total suspended solids in wastewater and existing fat and 50-60% of BOD5 and COD loads.

Before arriving in flotation unit, the water goes through a chemical mixing system where chemical injection occurs from precipitation and flocculation system. The precipitation and flocculation system is the precipitating agent dosing unit and the flocculant preparation and dosing unit. Particles float to the surface are removed mechanically and are downloaded to the upper phase separation compartment using a scraper, while the treated water will be discharged by gravity and go biotreater. The particles settled out of the concentration unit are removed by pneumatic valve for sediment extraction and collected sludge storage tank.

The whole process is fully controlled through a control panel. Biological treatment step consists of: tank selection, denitrification tank, nitrification tank and sedimentation tank.

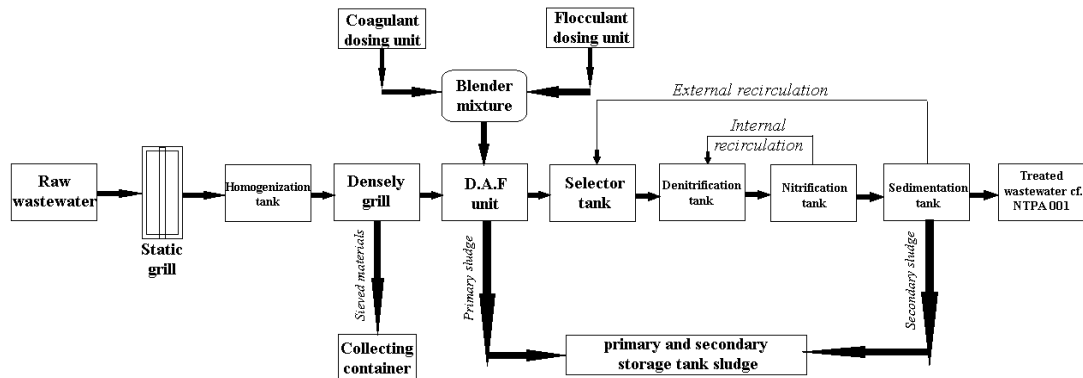


Figure 12. Operating Chart station

### Pool of denitrification

From selector mixture wastewater-biological sludge reaches the denitrification tank. Denitrification is the biological process of transformation of nitrates into nitrogen gas under the influence of biochemical catalysts

Part of nitrate is formed in the next stage of nitrification. This part of nitrates will be reintroduced in the denitrification tank as external recirculation flow rate of sedimentation in the selector. In this way, the necessary quantities of nitrates are placed in the denitrification tank for nitrogen removal.

Specific binding of bacteria anoxic activated optional in this basin, metabolize organic substrate in the presence of adequate amounts of nitrates as "oxidants" in place of molecular oxygen. Part of organic pollution is eliminated while simultaneously reducing nitrates. This process is accompanied by release of nitrogen in the atmosphere. Furthermore, by removing a portion of the nitrogen in this stage will be significantly reduced tendency flotation (by removing gaseous nitrogen) which would lead to flotation sludge is downloaded, thus adversely affecting the operation of sedimentation.

### Pool of nitrification

From the denitrification tank, wastewater and biomass mixture passes in nitrification tank, where aerobic treatment and cultivation of activated sludge is. Here are kept optimal aeration conditions necessary for the growth of microorganisms groups,

### Treated water quality and yields

aerobic conditions under which biomass is able to use and break down of wastewater organic substrate (organic pollutants).

To maintain a high concentration of dissolved oxygen in wastewater-sludge mixture and maintain turbulent conditions in the aeration tank (to prevent unwanted sedimentation sludge) tank is aerated and homogenized content.

Pressurized air from a blower is injected through porous membranes with high efficiency specially designed for fine bubble diffusers are installed in the bottom of the basin, to obtain a better homogeneity and a maximum amount of oxygen dissolved in wastewater

### Water quality

#### Wastewater influent parameters

- COD concentration: 1200-1400 mg / l
  - BOD5 concentration: 500-600 mg / l
  - SS concentration: 500-600 mg / l
  - total nitrogen concentration: 50-100 mg / l
  - total phosphorus concentration: 50-70 mg / l
  - The concentration of fat: 66-180 mg/l
- pH: 6.5 to 8.5

#### Total daily loads

- Charging COD: 19,2- 22.4 kg / day
- BOD5 load: 8 to 9.6 kg / day
- Charging SS: 8 to 9.6 kg / day
- Charging total N: 0.8 to 1.6 kg / day
- total P load: 0.8 to 1.12 kg / day
- Charging fat: 1.06 to 2.88 kg / day
- pH: 6.5 to 8.5

Daily flow of wastewater		Q = 16 m <sup>3</sup> /day
The quality of treated water and wastewater treatment plant efficiency		
-CBO <sub>5</sub>	< 25 mg/l	> 91%
-CCO <sub>Cr</sub>	< 125 mg/l	> 95,83%
-MTS	< 60 mg/l	> 90%
-Fats	< 20 mg/l	> 85%
-total N	< 15 mg/l	> 97,14%
-total P	<2 mg/l	> 88,89%
-pH	6,5-8,5	

## CONCLUSIONS

By analyzing the characteristics of the influent wastewater treatment station and influent characteristics, result in a reduction of 97% nitrogen and 89% phosphorus.

## REFERENCES

- Iancu P., 1999. Canalizari si epurarea apelor uzate. GLOBUS Publisher. Bucharest
- Ianculescu O., 2001. Epurarea apelor uzate. MATRIXROM Publisher. Bucharest
- Stancu M., 2013. Statie de epurare ape uzate pentru < Unitatea de Preparare a Carnii si Depozit Frigorific, Comuna Mogosoaia, Sat Mogosoaia, Judetul Ilfov >” – Dissertation Thesis
- <http://www.creeaza.com/legislatie/administratie/ecologie-mediu/Epurarea-avansata-tertiara-a-a987.php>
- <https://www.wikipedia.org/>



**SECTION 04**  
**CADASTRE**



## 3D MODELING OF A BUILDING FACADE

Iuliana Andreea APOSTU

Scientific Coordinator: Assoc. Prof. PhD Gabriel POPESCU

University of Agronomic Science and Veterinary Medicine of Bucharest, 59 Marasti Blvd,  
District 1, 011464, Bucharest, Romania, Phone: +4021.318.25.64, Fax: +4021.318.25.67

Corresponding author email: iulianaapostu@yahoo.com

### Abstract

*This paper aims to present how 3D modeling technique based on digital images demonstrates usefulness of photogrammetry and accurate 3D visualization of real object that presents regular shapes (buildings, monuments, artifacts). The 3D model of a building facade has been obtained using Agisoft Photoscan software using two photos and the accuracy of this model is less than one pixel. We can also made a 3D analysing on the model. Totally automated workflow provides the ability to process images without advanced knowledge of modeling or processing thousands of aerial or terrestrial images. The importance of this application reflects the accessibility of this software that can process photos captured with a resonable camera using in fact a „low-cost” photogrametric technology, the photogrammetry becoming the best alternative of standard measuring techniques.*

**Key words:** 3D modeling, „low-cost” photogrametric technology, stereomodel

### INTRODUCTION

Photogrammetry is a measurement technologies of obtaining reliable information about physical objects and the environment through the process of recording, measuring and interpreting photographic radiant energy and other phenomena , in order to determine the three-dimensional coordinates of points on an object. This informations are achieved using stereoscopy, which is measurements made in two or more photographic images taken from different positions (different views). In principal, the 3D coordinates define the locations of object points in the 3D space. The image (photography) coordinates define the locations of the object points' images on the film or an electronic imaging device. The exterior orientation of a camera defines its location in space (translation) and its view direction (orientation). The inner orientation defines the geometric parameters of the imaging process. This is primarily the focal length of the lens, but can also include the description of lens distortions. Further additional observations play an important role in extracting this relations for 'solving' the images, such as: scale bars, basically a known

distance of two points in space, and known fix points (anchor points), the connection to the basic measuring units is created (Neffra A. Matthews, 2008). In the beginning of photogrammetry and space records, normal photographic cameras (nonmetrics) had a particularly role for land registration (Popescu, 2013).

### MATERIALS AND METHODS

To create the 3D model of the Chemistry building faade I used the digital photogrammetry, a science that consist in using computers to create spatial-relation between photos/photograms and reality. This technique has become an effective alternative to classical facade surveying buildings, but achieving those applications specific to any project stages terrestrial measurements exactly necessary planning, recognition of land for measurement campaign organization, performance measurement and data processing itself to obtain results with technical and scientific value. To obvious the „low-cost” phtogrammetric techniques used in recreating the 3D model, I used Agisoft Photoscan program. The principle of data

acquisition using photogrammetric method seeks to information about physical objects and the environment from a distance without physical contact them through recording, measuring and interpreting photographic images metric called frames. Before taking the photos we have to plan a shooting session (Figure 1.) which consists in a sketch that contains the locations of the object is photographed, so to respect both the transverse and longitudinal coverage (between 60-70 % for longitudinal coverage and 25-30 % for trasverse coverage). In order we have taken two photos in front of the building(VILCEANU B., 2013). For the georeferencing we have measured two distances (putting two levelling staffs on both corners of the building).

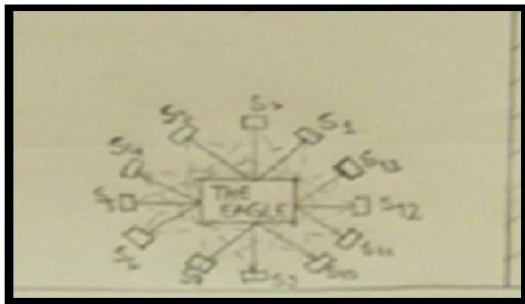


Figure 1. Shooting session (Vilceanu, 2013)

## RESULTS AND DISCUSSIONS

The first step is the phase field in which we have take this photos (Figure 2, Figure 3) with a Sony camera that has a focal length of 4.7 mm, 12 pixels. The size of each photos is 2048x1152. The only condition to use this program is that you can use a camera up to 5 pixels. Also if we have a smartphone that respect this condition and it have an internet connection we can make photos with the geographic coordinates (latitude, longitude). Also the photos have both longitudinal coverage.

For the georeferecing and to define the model scale I have measure two distances (in fact we have put two levelling of four meters staffs on both corners of the building and I have applied in the model this model).



Figure 2. First (left) picture



Figure 3. Second (right) picture

The second step consist in digital processing using the Agisoft Photoscan program. To succed in this operation I folow the workflow: -first of all I have imported the photos using the sugestive comand:”Add photos” -for better processing I have selected the interest area using the instruments on the toolbar (“Intelligent scissors”—select the interest area’s points-“Invert selection”-“Add selection”); -then I have alinged the photos using the comand: “Align photos” (Figure 4.). Practical I have overlapp the photos to create the dens cloud using a the high accuracy setting;

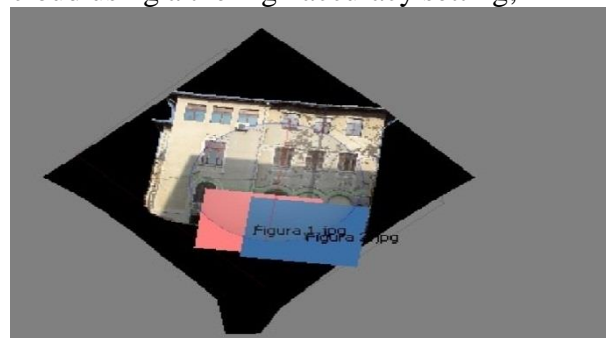


Figure 4. Perspective view (Agisoft program)

- the next step is building the geometry of the dense cloud using the comand: "Build geometry". In this moment we have a structure of the model but without a texture;
- the folow step is building texture using the comand: "Build texture". In this moment we have a model similar with the photos but in a good perspective using the mirror effect. (Figure 5, Figure 6).

To georeference the model I have applied the measured distance on the model.



Figure 5. The building model(sharp texture)



Figure 6. The building model (smooth texture)

## CONCLUSIONS

The traditional photogrammetry is based on stereo or multi-image restitution of a block of overlapping images and collinearity equations allow us to determine the 3D model of the overlapped area. A sequence of overlapping images is acquired with calibrated digital cameras. Geo-referencing and block control is obtained, depending on hardware and processing facilities:

- measuring a set of ground control points by Total station or GPS;
- determining the camera position by a GPS tied to the camera and synchronized with the image acquisition.

Homologous image point coordinates are measured (manually or automatically by image correlation software) in every image. Bundle block adjustment provides image orientation. Object point coordinates are determined by triangulation or multiple intersections. (Curtaz M., 2012).

In conclusion, the low-cost photogrammetric technology have a lot of possibilities to process the images no matter how they are taken (with nonmetric cameras, with metric cameras or with a multi-spectral camera) if we account the conditions.

Agisoft program is capable to generate a quick raport of our work that contains the accuracy (in pixels) of model, the number of photos , how many points have been resulted from the model(the dense cloud).

From the survey data results that I have overlapped two images with an error of 0.46 x pixel size (Figure 7).

### Survey Data

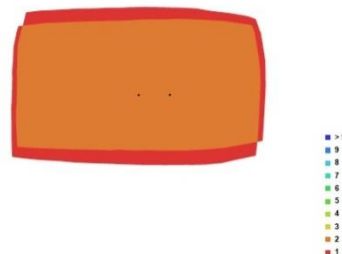


Fig. 1. Camera locations and image overlap.

Number of Images:	2	Camera stations:	2
Flying altitude:	35.3118 m	Tie-points:	563
Ground resolution:	0.0123953 m/pix	Projections:	1126
Coverage area:	0.000336471 sq km	Error:	0.45711 pix

Figure 7. Survey data from Agisoft report

### Digital Elevation Model

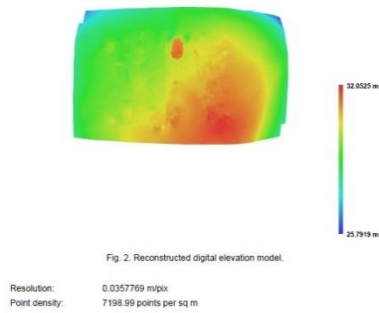


Figure 8. Digital elevation model from Agisoft raport

In this picture we can see how many points have been resulted from the model (in the dense cloud).

Nevertheless we can process images with a good precision using a low-cost equipment.

### REFERENCES

- CURTAZ M., 2012, Terrestrial photogrammetry (TP), P6 Permafrost and Natural Hazards.
- KRAUS K., 1997. Photogrammetry. Vol.1: Fundamentals and Standard Processes; Vol.2: Advanced Methods and Applications. Dümmler, Bonn.
- NEFFRA A. Matthews, 2008, ,Aerial and Close-Range Photogrammetric Technology: Providing Resource Documentation, Interpretation and Preservation, Technical Note 428.
- POPESCU G., 2013, Lectures of Stereo-Photogrammetry & Photointerpretation
- VILCEANU B., 2013 , Aplicatii practice in fotogrametria digitala

## CADASTRAL SURVEYS CONDUCTED WITHIN THE REPUBLIC OF MOLDOVA

**Andrei ARMAS, Ovidiu Stefan CUZIC**

**Scientific Coordinator: Prof. PhD. Eng Eugen Teodor MAN**

Polytechnic University of Timisoara, Faculty of Civil Engineering, Department of Hydrotechnical Engineering, George Enescu 1/A Timisoara 300022, Romania,  
Phone: +40765702919 e-mail: ing.armasandrei@gmail.com; cuzic\_ovidiu@yahoo.com;  
eugen.man@upt.ro

Corresponding author email: ing.armasandrei@gmail.com

### **Abstract**

*The paper aimed to present the organization of immovable property registering process encompassed in cadastral works made in Republic of Moldova. It is based on the 828-XII / 25.12.1991 law from Moldova's land code especially on the 12th and 13th articles. The four main registering categories are divided into primary, selective, massive and current recording of immovable property followed up by the principles and objectives of the registering process. An illustration of a primary massive registration of a field acquired under the law reveals a chain of certain particularities concerning content of immovable property, manner of acquiring the property and method of organization of registering process. Acquiring the property rights under the law has its own particularities as well. Further on, the 12th article provides that a committee is gathered in order to establish the various social categories of people that are entitled to receive land as owners whereas actual ascription of property is regulated by the 13th article, both of them assuring the legal foundation on which the right of property is formed. As a conclusion, the forming of immovable property implies the materialization of the right acquired under the 12th article of the land code. Moreover, the 12th article provides a rights authentication title for the land owner issued by central and local authorities.*

**Key words:** *cadastre, immovable property, land code, property rights, registration.*

### **INTRODUCTION**

The recording or registration, in the Immovable goods Book, of basic information and details concerning it and its rightful owner represents a "state registration" due to its content. The four main registering categories are divided into primary, selective, massive and current recording of immovable property. The selective recording represents an action taken by the state that has the purpose of registering an immovable property separately both primarily as current. The current registration represents an action taken by the state that has the purpose of modifying the content of previously written information in the immovable property book. The massive registration represents an action taken by the state that has the purpose of recording in an

organized form more immovable goods found in a specific territory.

### **MATERIALS AND METHODS**

One particularity of the primary massive registration is the fact that it is made without the demand (acceptance) of immovable property owner.

The primary massive registration is made under a state order using centralized financial resources after an unique method. The regulation that initiated the primary massive registration was approved through Government Decision nr. 1030 / 12.10.1998.

The power invested by the Cadastral immovable goods law and Regulation regarding the means of primary massive registration making helped in elaborating instructions (in October 1998) concerning registration of immovable goods and rights to them.

A decisive role in the process of primary massive registration of immovable goods is the correct selection of locality. It is obvious that the success of massive registration depends a great deal on co-operation (support) of public local authorities. Through this local authorities bear some obligations concerning the process of massive registration.

The first cadastral Project in Moldova had the purpose to: elaborate proper legislation, norms and instructions; to coordinate and control massive recording cadastral works. In the process of primary massive registration most private property lands, designated to agriculture were recorded.

The selective registration is made under owner's decision because it is obvious that the potential of such a recording does not satisfy solicitations of all owners in current status.

In such conditions the primary selective registration is applied, which will always be on the map. Therefore primary selective registration is not a periodic activity concerning the implementation step of cadastre but a permanent one that will last throughout the existence of cadastral system.

The primary selective recording has its particularities: in the process of recording, supplementary cadastral works is mandatory: of identification, of determination of immovable goods, etc.

It is important that the applicant of a primary selective recording to correctly formulate its will. However, field reality proves that one will meet a variety of instances that need to be dealt with.

The content of cadastral works will depend a great deal on the structure (content) of immovable good that is to be recorded, such as: a land free of constructions, installations, plannings; a land which has constructions, installations, plannings; a house (multiple constructions) placed on a foreign land; an isolated room (an apartment) belonging to a construction placed on a foreign land; a basement.

Contents of cadastral works, necessary for registering the immovable good will be different in every instance. To all of this cadastral informational system requirements

are added. Nowadays cadastral works necessary for recording immovable goods are made by local cadastral offices; the executor must know all requirements of the unique coordination system used in the informational system, etc.

Learning from other countries' methods, all cadastral works that are connected to immovable goods registration are made by licensed companies in this field, including private ones.

The current registration is made under selective and massive form. Up to now it is concluded that massive registration both primary and current is made mostly out of public interest. However, the private interest in registration of immovable goods is not less important. The right of property on goods can be achieved only if it is registered in the immovable property Book. Only in such a condition a transaction will be legal, possible, protected. This is the main reason of current selective registration of immovable goods.

The primary recording is an inevitable activity in the conditions of cadastral informational System implementation. Moreover, the social-economic development anticipates the creation or disparition of some immovable goods.

The current massive registration is made on purpose of realizing the state economic policy and under various Government programs, for example the one oriented towards realizing the fiscal policy.

Taxation of immovable goods, appointing fiscal payments according to their market value requires a massive market evaluation. For this, gathering supplementary information about immovable goods that are already registered in the Book is required.

The principles of registration: the legal status of immovable goods Book is settled in the cadastral Law of immovable goods no.1543 – XIII issued in 25.02.1998. According to this, the immovable goods Book is the basic document in the practice of immovable goods cadastre (Buzu, 2002).

The information in the above Book will be considered truthful as long as it is not confirmed otherwise. The first actions of

immovable goods registering in the Book were made starting with the year 1998.

The recording of immovable goods is made by respecting some basic principles such as: obligation of registration, public interests of registration, private interests of registration, transparency of registration.

Registering the immovable goods is a compulsory activity and it is dictated by the cadastral Law of immovable goods no. 1543 – XIII / 25.02.1998 (art.5). The compulsory principle comes from the state’s obligation to protect owners rights, and is imposed by the public and private necessity.

Regarding the public interests, the state is concerned that all immovable goods to be registered in the Book, this benefits the fiscal policy of the state as well as ownership protection.

Regarding the private interests, it is in every owner’s interest to have the immovable good registered and rights regarding it. Otherwise an unregistered good or rights concerning it is not recognized by other persons. This can create great difficulties in goods exploitation and having rights about it.

Transparency represents another registering principle, which imposes an open trait of immovable goods registration. The body that makes the recording (cadastral territorial office) is required to issue to any physical or legal entity information about the registered immovable good.

Correct determination of registration object in the Book of immovable goods is of great interest for the informational system of cadastre and it includes: immovable goods, ownership rights on the immovable goods. Immovable good as object of registration can have various forms: a land free of any construction or arrangement, a land that has constructions and arrangements, an open space that has constructions and arrangements, a basement under which there is a mine or another underground construction

In practice, the social-economic necessities impose to register not only the immovable good but also a portion of it. Therefore one can have: the immovable good as a whole, a land

free of any construction, a land together with all the constructions and arrangements, a separate construction, an isolated room, a irrigation system, a vineyard or fruit trees.

No matter the elements of immovable good that are to be registered, all these will be joined to the land (land sector) as a primary unit in the cadastral structure. The Law of immovable goods cadastre no. 1543 –XIII / 25.02.1998 expresses the consecutivity of registration (Book entries).

In cases when constructions, isolated rooms, arrangements, are object of recording, they can be registered only in the conditions in which the land will be registered. The isolated place (apartment) will be registered in the same conditions in which the whole construction will, on the registered land it sits.

Therefore the procedure can be simple or composed. In cases where a land where a construction exists belongs to a person, the construction belongs to another one, and the isolated place belongs to a third person, registration of the whole ensemble of legal connections dictated by the situation given will be applied.

Property right as object of recording arise out from the principle that the good and right over it represents an integral unit. Even though the law in force recognizes the concept of goods “without ownership”, this situation has a short, provisory nature. Despite recognizing that some goods are without ownership it is well known that such goods, during this lack of ownership period, become public property (Figure 1).

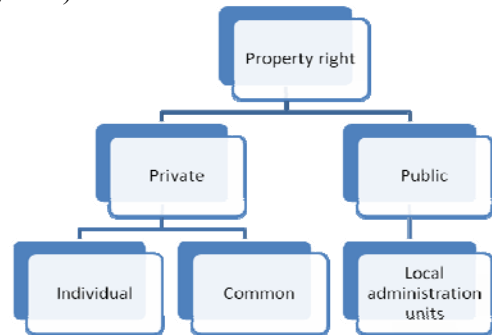


Figure 1. Property rights

For a better understanding of ownership rights as object of registration it is necessary for the

structure of ownership rights to be known. The ownership right is made of: possession right, right to use, disposal right, and a variety of types of property right.

Subjects of ownership rights are owners of immovable goods and other bearers of patrimonial rights: citizens of Republic of Moldova, foreign citizens, stateless persons, legal entities domestic and foreign, international organizations, the Government of the republic (in the name of Republic of Moldova), district and regional councils in the name of local public authorities.

Other real rights given by the Civil Code: usufruct, the right to use and occupancy, easement, the right to use the land, to use it as a deposit.

In a generalized manner usufruct, the usage, occupancy, easement, and the right to use the land, are usage rights that will be recorded according to the law, in the Book of immovable goods. The deposit, being a debt, it is also registered in the Book, accordingly to the law (Gutu, 2003).

Therefore, registration of a usage right can be made only with the condition when the good and property right on it are already registered. In all cases, registering other real rights will be made on demand.

Register entries of immovable goods and rights concerning them in the immovable goods Book are made as recordings by a designated person –a registering clerk. Entries are divided in three categories as follows: registration, provisional entry and the action of taking notice.

Any entry in the Book is identified, i.e. oriented towards a actual immovable good. The cadastral code/number acts as an identifier formulated according to cadastral-territorial structure of the republic. Each entry has a number and the date attached, the clerk being responsible for the accuracy of all entries.

The registration pins ownership and other real rights over immovable rights in the Book, it is not only about making recordings but also about making modifications in the immovable goods Book's file. This is a valid process for all four registration types. Introduction of modifications in the content of the Book is

made through updating the files and Book and rectifying errors.

The update is made on the public authorities' or land owners' initiative, the first being made mostly for fiscal purposes while the latter is made for obtaining a loan (mortgage).

Economic reasoning can bring other reasons for information updating both for public or private interest. Rectifications are in order in cases of technical or juristic errors. According to their content errors can also be divided into the ones that provoked material wrongs and the ones that did not.

Provisional entries are materializing in the acquirement, modification or cancelation of ownership or other real rights.

Acquiring a right through applying a provisional entry can take place in the conditions in which the subject does not hold all rightful documents concerning the good. For gathering all necessary paperwork the clerk establishes terms and can apply a provisional entry.

The provisional entry has only one condition: that the owner, through supplementary papers to justify its right over the good. Such an entry does not translate into an absolute, final right, i.e. its holder will not be recognized as owner until the entry is replaced by registration. However, this entry does not exclude other subject's right to present convincing documents regarding the immovable good and obtaining property rights.

Modifying ownership through applying provisional entries can take place due to some conditions –like passing property rights from one person to another- which are included in the entry. Such a condition can be the mortgage.

When the land owner did not respected the mortgage contract terms, the property right can be modified in the benefit of another person. Cancelation of such a right due to provisional entry can occur if the immovable good is to be terminated; it can also take place due to court orders or mortgage contracts.

It is important to be clarified when the provisional entry will apply in the context of mortgage. It shall be applied only when the

immovable good being on mortgage is sold by owner and when the assets are dealt with.

The action of taking notice refers to registering the debt claim –obligations, assets- and the property right appears consecutively to the recordings made in the Book. The date when the application is forwarded remains as registration date.

This process is made according to the law or by request of the interested parties.

## RESULTS AND DISCUSSIONS

In practice, in the recording of immovable goods a chain of certain particularities are found out. Analyzing them proves that they are motivated by: content of immovable good, the way of obtaining rights on the immovable good, method of registration process organization.

Obtaining property rights under the law has its particularities. In such cases the law establishes in detail both subject as well as object of property rights (Ganju, 2000).

The following example of primary massive registration of a land designated for agriculture acquired under the law is relevant for analyzing ownership. Article 12 from the Land Code (law 828 / 25.12.1991) can shed some light regarding ownership under the law.

In the case of the example given, “conditions of the law” formulated by the 12th article are: land councils establish lands that remain in public property, within the territorial-administration unit (sets aside up to 5% from land with agricultural destination for social development needs of the district and sets aside proper places to be used as public grazing fields).

The difference between total surface of the territorial-administration unit and land surfaces assigned to public property makes up the privatization fund. Land councils establish the equivalent share that is attributed to private property.

The content of cadastral works will depend a great deal on the structure (content) of immovable good that is to be recorded, such as: a land free of constructions, installations, plannings; a land which has constructions,

installations, plannings; a house (multiple constructions) placed on a foreign land; an isolated room (an apartment) belonging to a construction placed on a foreign land; a basement.

The authentication of ownership on the equivalent share is achieved through to local public administration resolution, by issuing a ownership paper confirming this right.

The actual assigning of land shares is made in accordance with the 13th article of the Land Code which states the following: location of the land which will be assigned as equivalent shares will be determined by the village (district) or city without the share bearer’s demand, on the basis of territory organization. The project of territory organization, is approved by the village /district /city’s hall, on proposal from land council. When elaborating this project the list of group owners of shared land will be taken into account, as well as the sequence of land assigning (Botnarenco, 2012).

On share’s owner demand, during project development, the village /city hall can decide to actual assign on the spot the share of land and garden from land outside the settlement in one single area.

The share of land that is given on the spot according to the organizational project can be divided depending on the situation in maximum 3 lands (arable land, vineyard, fruit trees).

The above mentioned regulations, extracted from the 12th and 13th article made the legal ground for ownership of arable lands. They precisely establish the object (arable land) and the subject (its owner) of land property.

The 12th article actually transformed itself in a 10 year activity project for the local public authorities. On its basis, central and local public authorities took many important actions: created the lists of persons who obtained ownership over the arable land; determined total surface of lands that were supposed to be assigned in property and their deployment (privatization fund for each town); they calculated the medium surface of arable lands that is supposed to be assigned to someone that had the certain rights; developed

the territory organization project; actually assigned lands to each owner according to the approved list and project; developed the ownership bearer act.

In order for the land surface assigned to each citizen to be determined, firstly, the surfaces for privatization funds for each location were determined. In the process, the following scenario was adopted: arable lands supposed to be kept for social development of the community were determined; from the total surface of arable lands, the ones for social development were excluded; identification of large areas for privatization and an analysis of characteristics was made.

It is important to be mentioned that not all communities were under privatization. The funds designated for privatization in the manner described above were approved through Government resolution.

For determining the surface supposed to be assigned to a citizen was based on the social equity, which applied in the privatization process in Moldova implies that each citizen who will have the right to own arable land will obtain equal share.

In order to find a solution to this issue, the "equivalent land share" formula was applied. Each citizen acquired in property a land that includes an equal grad-hectare number. During that stage it was discovered that an equal number of grad-hectare will respect the social equity principle.

Unfortunately, recent discoveries revealed that this purpose was not achieved, the main reasons being: each community in the republic owned a different privatization fund; equality of grad-hectares number of assigned lands cannot be considered equal from an economic point of view.

Actual locating the land for privatization was made on the basis of a land organization project. The purpose of the project was to minimize the surface factors in privatization process. The projects were developed by specialists in the field of territory organization. The formation of immovable good (land) implies the materialization of the right acquired due to the 12th article of the Land Code. This article offers the required

information but the land itself is determined by some concrete measurements. The land surface calculated according to the 12th article was named "equivalent land share".

The equivalent share of land is connected to the quality of soil this is what differentiate it from a regular surface of land. Therefore, the smaller the share surface is, the higher fertility rate has the soil.

The equivalent share of land represents a product (resulted from multiplication) between the physical surface and fertility rate. Each citizen of a community that according to the 12th article that disposes of right to have a share, obtained a share (a product) equal to everyone's. one of the most important and expensive actions that were ever undertaken in the process of privatization (obtaining ownership on behalf of the 12th article) was developing and establishing actual acquired land.

Assigning actual land was made by applying the "ticket drawing" principle. It is obvious that concerning quality and quantity, lands are different.

In the process of concrete land allocation the degree of kinship was also taken into consideration for assigning them closer one to another. In reality most of citizen's lands were not assigned in nature. Their spatial location was determined in the cadastral plan. Assigning in nature of lands was another step of the allotment process.

It is necessary to establish that the 12th article ascertain the application of ownership authentication title only on condition that the right is acquired without payment in the privatization process.

The ownership authentication title for equivalent share of land is made on grounds of local public administration resolution by issuing a title that confirms this right. Application of the respective title for authentication of other rights will not be valid. Furthermore, in the conditions of the law and by effect of the administrative document public property lands are transmitted in the management of public company or to territorial-administration units.

It is important that this document (ownership authentication title) to coincide with the content of the local council's decision. This decision also includes information about persons, sizes of equivalent land shares that is owned; the document includes information concerning the absolute surface (but not equivalent) and its spatial location on which the ownership spreads.

It is obvious that these two surfaces (from the local council's decision and ownership authentication title) will not coincide in the process of arable land privatization.

Concerning the actual measurement procedure was made in respect to the 13th article of the Land Code, law no.828. For each land an ownership authentication title was issued. In most of the cases, for surfaces of land owned the citizens received multiple titles.

The spatial arrangement is established through the cadastral plan. In the content of ownership authentication title an excerpt from the cadastral plan is also included which establishes the spatial arrangement.

In order to respect the indications given in the local council's decision in the process of releasing the ownership authentication titles, the latter are authenticated by signature of the local council's designated person.

The scenario concerning the registration of a property right on a arable land acquired under the conditions of the law is the following: the local public administration authorities identified through respective titles ownership of land owners, presented the ownership authentication titles to the territorial cadastral offices for primary massive registration; the territorial cadastral offices control the truthfulness of presented documents (in this case the ownership authentication title) writes down in the immovable property Book files, apply the registration stamp on every document, opens cadastral files for each land, gives a copy of the registered document to the owner.

## CONCLUSIONS

This paper aimed at proving that at the moment it is hard to imagine economic

relations isolated from cadastre. Being an information system it influences the economy on three important levels: real estate market relations, fiscal policy and property rights protection.

The major economic influence can be both positive and negative, but the cadastral mechanism by its content does not allow economic relations with a strong negative social or environmental impact. Clearly, the constant development of the cadastral informational system will make it be more operative in finding negative economic influences and provide ways for protection.

In general terms the importance of cadastral works is of great importance in drawing up the informational system of a given territory (here Republic of Moldova) being able to rapidly supply with data accurate data to all institutions from various sectors of the national economy.

Because it is conceived as a informational system of all lands and immovable property no matter their destination or owner it can be said that cadastre is for the market economy an important instrument that supplies the documents that give security to all transactions that concern real estate goods. A informational system of modern cadastre can only be created on the grounds of an adequate science and practice.

## REFERENCES

- Botnarenco I., 2012. Cadastre of immovable goods in Moldova. Pontos publishing house, Chisinau, 107-117; 123-130.
- Buzu O., 2002. Organization of evaluation activity. Central Printing house Publishing, Chişinău, -426.
- Gînju V., Guţu V., 2000. Cadastre of immovable goods, Vol. IV. Central Printing house Publishing, Chişinău, -672.
- Gutu D., 2003. Role of cadastre in the development of the real estate market. Didactic-scientific Magazine, Poligrafic ASEM Publishing house, Year II.
- \*\*\*Government Resolution no. 1030 / 12.10.1998
- \*\*\* - Land Code (Law no. 828 – XII / 25.12.1991)
- \*\*\* - LAW of REPUBLIC of MOLDOVA Cadastre of immovable goods No.1543-XIII / 25.02.98 published in The Official Monitor of R. Moldova no.44-46/318 appeared on 21.05.1998.

## USING GIS TO HELP US MAKE BETTER DECISIONS - MOUNTAIN DESTINATIONS -

Alina BĂLAN, Grigoraș-Mihnea GÎNGIOVEANU-LUPULESCU

Scientific Coordinator: Assoc. Prof. PhD. Eng. Doru MIHAI

University of Agronomic Sciences and Veterinary Medicine of Bucharest, 59 Mărăști Blvd, District 1, 011464, Bucharest, Romania, Phone: +4021.318.25.64, Fax: + 4021.318.25.67

Corresponding author email: gingio\_mihnea@yahoo.com

### Abstract:

*In this paper we aim to show the benefits of presenting and analyzing a certain topic using GIS, presentation which provides a good help for the people in charge of deciding something important. In our case, a company wants to offer the employees a small trip somewhere in a mountain resort where they can improve their skills of working as a team and create a closer connection between them. The company has a few options but it's hard to make a choice for a certain destination, so someone decides to make a StoryMap which can be shown to the employees and to the people responsible for deciding the destination in order for them to choose the best option. The same method can be used for choosing an adequate location when a company wants to expand or someone wants to open a new store. GIS can be used for any study or observation related to the location of something, having a large field of application. In our paper we will analyze a few possible mountain destinations in terms of which one has the most ski slopes, which one offers the best possibilities for accommodation and which one has the best location from a geographical point of view. There will also be a short presentation of each mountain resort containing some pictures from the resort and possibly even some live images from the ski slopes, so the people in charge of making the decision will be very well informed about each possible destination. In parallel with this StoryMap we will also locate the respective places in a 3D scene, which will increase the understanding of the geographical location for that area. As a conclusion, this paper aims to show the benefits of using GIS in order to make the best decisions.*

**Key words:** analysis, application, GIS, resort, StoryMap.

## INTRODUCTION

Deciding the location of an event or the location for building something has always been a major problem for the people in charge of making that call. There is a lot of pressure because for example if someone decides to send some people in a certain resort (in our case) and when they get there they find out that is not what they needed, it will be very hard to repair the mistake and also more money will be spent. So, for any problem that relates to the location of something it is recommended to make a GIS analysis first. In this paper we show a simple example of how to use an ArcGis Online application to help us make better decisions and we also highlight some of the latest technology in the field of spatial analysis.

## MATERIALS AND METHODS

In order to make this application we used ArcGis Online platform. At first we needed a

basemap to start with and the easiest place to do that is by going to [www.arcgis.com](http://www.arcgis.com) and selecting Map from the top part of the screen.

After doing that we were able to choose from a variety of basemaps, as seen below (Figure 1):

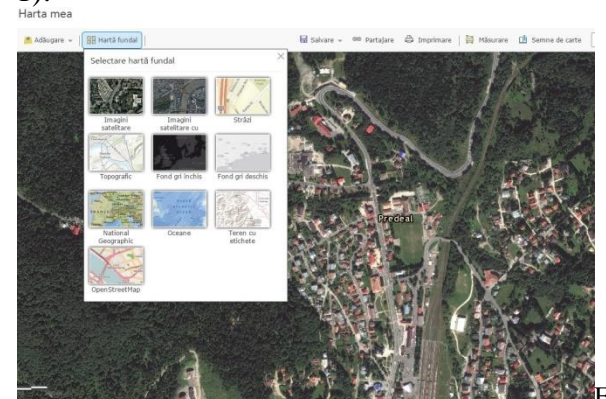


Figure 1. Choosing a basemap in ArcGis Online

After we decided what basemap we want to use, we can go and edit the map, add different locations that we want to see on the map and also for each location we can add details, information or just something that we want to appear when we will click that point

on the map. After adding all the points that we wanted on the map, we need to save the map. The map can now be seen from any device (Figure 2):



Figure 2. ArcGIS Online. Map seen from IOS mobile device

We can also use the mobile devices to collect points from a certain area, for example if we want to have a map with the places where a certain flower grows in the park nearby we can go there with any mobile device and use Collector for ArcGIS application to put them on a map.

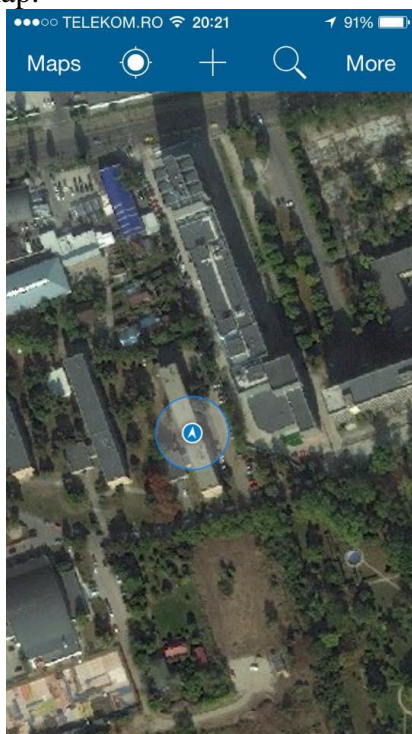


Figure 3. Collector for ArcGIS application on IOS device

The map can be shared with everyone, so it's also very useful as a way of transmitting information. After we added all the points and informations on the map and also saved it, we need to find a way to present it. A simple way is to create a StoryMap. We can do this by going to [www.storymaps.arcgis.com](http://www.storymaps.arcgis.com) and follow some simple steps. A StoryMap combines maps created using ArcGIS Online with any multimedia content like videos, photos, text etc. So a StoryMap lets us present all kind of informations about places while seeing those places on an interactive map. There are many StoryMap templates and we can even create a custom template which suits our needs. A basic template consists of a side panel and a main scene. In the side panel we can put any kind of information like text, videos, photos, links to different sites. The side panel has a few sections, each one providing informations about a certain place on the map. In the main scene we can import the map that we created using ArcGIS Online or a map created by anyone with an ArcGIS account so this is very helpful if you want to use different maps for different locations.

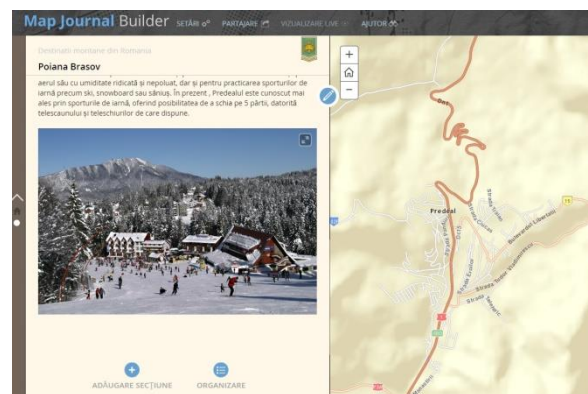


Figure 4. StoryMap

After creating all the sections for each location in our map, we saved and shared the StoryMap. It can be accessed from any device connected to the internet, and that is a very useful feature in case we need to present it to someone and we were not prepared for that.

## RESULTS AND DISCUSSIONS

Although we would initially think that sending some people in a small trip it is not

that difficult , there are some things to consider before making a decision. We need to think about the cost , about the accommodation , about the distance between where they live and where they need to go and about what activities they can do once they get there. The cost of the trip is obviously one of the most important things to consider , so in the analysis of each possibility that will be the main criterion. After we collect all the informations that we need and take into consideration what we want to obtain , we will have a StoryMap that can be easily understood by anyone , that can be presented in just a few seconds anywhere and from any device.

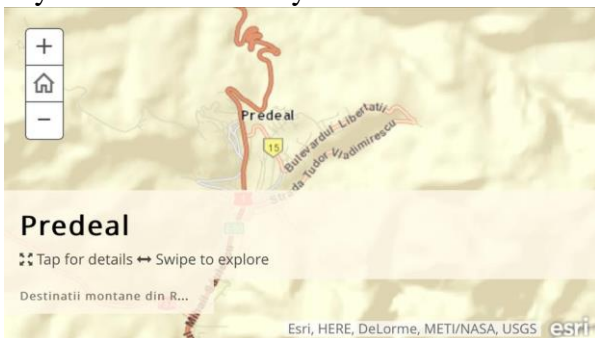


Figure 5. StoryMap seen from IOS device

Also the technology is rapidly evolving , so very soon the map used to identify our interest points will not be just a 2D map , it will be a 3D map containing possibly even a rough representation of the buildings in the area. That will make a huge difference in the perception of the space around our interest point and will definitely improve the understanding of the geographical location for a certain place.

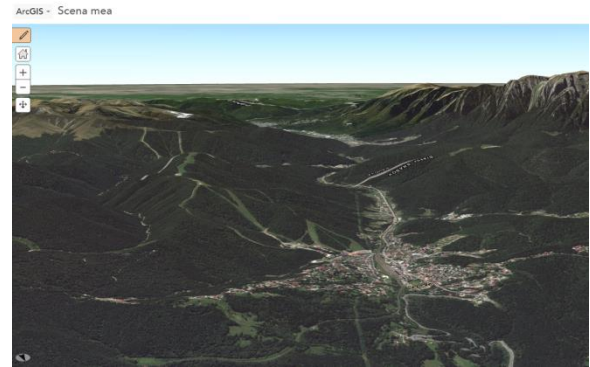


Figure 6. 3D scene in ArcGis Online

## CONCLUSIONS

The paper aims to reveal how any person, without any training in GIS can use [www.arcgis.com](http://www.arcgis.com) website in order to create and share spatial information with anyone in the world and how GIS is used to help us make better and more efficient decisions in our daily activities.

Also , GIS technology will be more and more present in our daily life as the cities evolve and the need for efficiency will rise.

## ACKNOWLEDGEMENTS

Esri is continuously developing advanced features encouraging experts from all fields of work to share information and to connect Esri is developing new features in the field of cartography, cloud GIS, enterprise GIS, GIS and CAD, GIS and science, mobile GIS, open sources, and the interoperability offers multiple ways for the users to use GIS tools.

## REFERENCES

- Mihai Doru, 2014, Geomatica in reabilitarea lucrarilor de imbunatatiri funciare - ISBN 978-973-0-18036-7.
- Mihai Doru, 2014 , Curs Sisteme Informationale Geografice  
[www.arcgis.com](http://www.arcgis.com)  
[www.esri.ro](http://www.esri.ro)

## ASPECTS CONCERNING TOPOGRAPHIC AND GEODETIC WORKS NECESSARY FOR DESIGNING AND DRAWING A CONSTRUCTION

**Dorinuța BEȘA, Adina Mihaela MORAR, Nicoleta Alina MUREȘAN**

**Scientific Coordinators: Prof. PhD Eng. Mircea ORTELECAN, Lect. PhD Eng. Tudor  
SĂLĂGEAN**

University of Agricultural Sciences and Veterinary Medicine of Cluj-Napoca, Calea Mănăștur 3-5,  
400372, Cluj-Napoca, Romania | Tel: +40-264-596.384 | Fax: +40-264-593.792 E-mail:  
contact@usamvcluj.ro

Corresponding author email: besa\_dorinutza@yahoo.com

### **Abstract**

*The following paper regards the creation of the digital plan necessary for the design and trace of a construction situated in the town of Colibita, in the Bistrita-Nasaud county. Further, the paper presents the methods of tracing and the study of accuracy in regards to the transposition on terrain of the projected objective. The methods used for drawing in a plan of the projected points of a construction results combining topographic mapping elements (angles and horizontal distances) and deploys according of well defined procedures. Before starting a construction, first you should realize the preparing of terrain by topographical point of view. This fact consists of an ensemble of operations made at office for making the construction at that terrain. For drawing of the projected elements, polar coordinates method has been chosen. This is the most used method of drawing, it is used for drawing on the terrain of project points in case if exists a drawing base or a drawing network, a poligonometric network, a topographic construction network.*

**Key words:** angles, digital plan, poligonometric network, topographic, terrain.

### **INTRODUCTION**

This paper is part of the diploma project, which aims to draw and design a construction relating to a property in the area Colibita.

In order to design the objective mentioned it is necessary to create digital terrain model.

On the digital support has passed the location of the building and calculate the coordinates of points of construction.

Topo-geodetic operations have targeted achieving digital support and implementation in the field of building design.

In order to achieve the topographical plan has gone from a network of triangulation in the area of interest, then a passing to the geodetic networks and the lifting realization network.

From the lift network have been determined the coordinates of terrain detail.

After placing the lens designed on digital plan was passed in the calculation of the required elements themselves.

### **MATERIALS AND METHODS**

Triangulation network taken into study is presented in the form of three rectangles with two diagonal (Figure 1).

In order to follow the stabilization of the axis from a planimetric and altimetric perspective, the following operations were carried out: the compensation and verification of angles, the calculation of the orientations, the calculation of the sides, and the calculation of the coordinates with respect of these supporting axis points (Ghițău, 1975; Ortelecan et al., 1998).

The higher order geodetic axis was offset by the conditional measurement method (the variation of the coordinate points) and indirect measurement method (the variation of angles and directions) (Rădulescu, 2003; Rusu, 1978).

In order to remedy the system equations of corrections contains six equations of figure and three equations of pol.

The error equations:

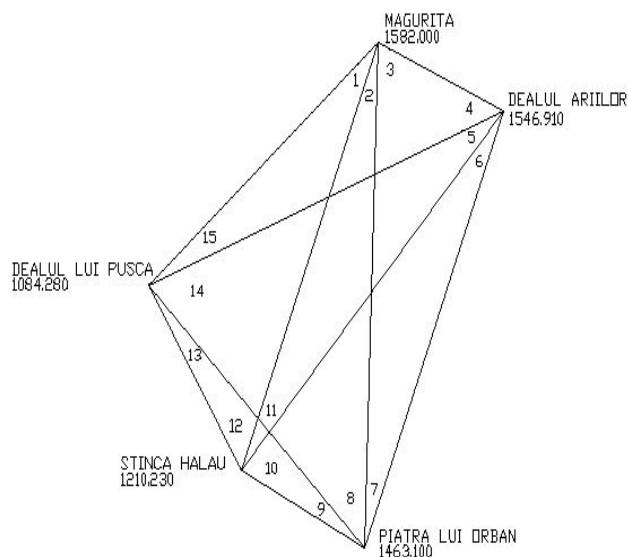


Figure 1. Sketch triangulation network

$$\left\{ \begin{array}{l}
 v_2 + v_4 + v_5 + v_7 + w_1 = 0 \\
 v_5 + v_7 + v_8 + v_9 + v_{10} + w_2 = 0 \\
 v_2 + v_3 + v_8 + v_{10} + v_{11} + w_3 = 0 \\
 v_8 + v_{10} + v_{11} + v_{12} + v_{13} + w_4 = 0 \\
 v_1 + v_2 + v_3 + v_4 + v_{13} + w_5 = 0 \\
 v_1 + v_{12} + v_{13} + v_{14} + v_{15} + w_6 = 0 \\
 d_1 v_1 - d_{13} v_{13} + d_4 v_4 - d_{22} v_2 - d_{23} v_3 + d_{11} v_{11} - d_3 v_3 + d_{12,14} v_{12} + d_{12,14} v_{14} - d_{12} v_{12} + w_7 = 0 \\
 d_{4,5} v_4 + d_{4,5} v_5 - d_7 v_7 - d_9 v_9 - d_{10} v_{10} - d_{3,8} v_8 - d_{3,8} v_8 + d_2 v_2 - d_{11} v_{11} + w_8 = 0 \\
 d_4 v_4 - d_5 v_5 + d_7 v_7 - d_{3,8} v_3 - d_{3,8} v_3 + d_{14} v_{14} - d_6 v_6 + d_{1,2} v_1 + d_{1,2} v_2 - d_{13} v_{13} + w_9 = 0
 \end{array} \right.$$

$$B = \begin{pmatrix} a_1 & b_1 & \dots & i_1 \\ \vdots & \vdots & & \vdots \\ a_{15} & b_{15} & \dots & i_{15} \end{pmatrix}; B^T = \begin{pmatrix} a_1 & a_2 & \dots & a_{15} \\ \vdots & \vdots & & \vdots \\ i_1 & i_2 & \dots & i_{15} \end{pmatrix}; w = - \begin{pmatrix} w_1 \\ w_2 \\ \dots \\ w_9 \end{pmatrix}; v = \begin{pmatrix} v_1 \\ v_2 \\ \dots \\ v_{15} \end{pmatrix}$$

$$A = \begin{pmatrix} a_1 & b_1 \\ a_2 & b_2 \\ \dots & \dots \\ a_{16} & b_{16} \end{pmatrix}; A^T = \begin{pmatrix} a_1 & \dots & a_{16} \\ b_1 & \dots & b_{16} \end{pmatrix}; l = - \begin{pmatrix} l_1 \\ l_2 \\ \dots \\ l_{16} \end{pmatrix}; v = \begin{pmatrix} v_1 \\ v_2 \\ \dots \\ v_{16} \end{pmatrix}; P = \begin{pmatrix} 1 & 0 & \dots & 0 \\ 0 & -1 & \ddots & \vdots \\ \dots & \dots & \dots & \dots \\ 0 & \dots & 0 & -1 \end{pmatrix}; X = \begin{pmatrix} dx_P \\ dy_P \end{pmatrix}$$

The error equations system can be written as a matrix, as follows:

$$B^T v = w$$

Where, B – the coefficients matrix

v - the corrections matrix

w – the unclosing matrix

Putting the minimum condition, result:

$$v^T v - 2k^T (Bv - w) \rightarrow \min$$

Is calculated:

$$k = (B^T B)^{-1} w$$

$$v = B (B^T B)^{-1} w$$

Corrections are calculated using the most probable value of the angles.

$$(\hat{1}) = \hat{1} + v_1$$

$$(\hat{2}) = \hat{2} + v_2$$

.....

$$(15) = 15 + v_{15}$$

The standard deviation or mean square error of measurements in the case of a single conditioned measurement is calculated and is given by :

$$S_0 = \pm \sqrt{\frac{[vv]}{r}}$$

Where, r is the number of geometric condition.

To develop the network of support was switched to thickening of network.

Writing equations of correction system.

Initially supposed to write a system of twenty equations with seven strangers:  $\Delta x_p, \Delta y_p, \Delta z_A, \Delta z_B, \Delta z_C, \Delta z_D, \Delta z_E$ .

In order to simplify the equations apply rules 1 and 3 of equivalence of Scheiber, becoming the system in the form of:

$$a_2 \Delta x_p + b_2 \Delta y_p + l_2 = v_2$$

$$\frac{a_2}{\sqrt{3}} \Delta x_p + \frac{b_2}{\sqrt{3}} \Delta y_p = v_2'$$

$$a_5 \Delta x_p + b_5 \Delta y_p + l_5 = v_5$$

$$\frac{a_5}{\sqrt{3}} \Delta x_p + \frac{b_5}{\sqrt{3}} \Delta y_p = v_5'$$

$$a_8 \Delta x_p + b_8 \Delta y_p + l_8 = v_8$$

$$\frac{a_8}{\sqrt{3}} \Delta x_p + \frac{b_8}{\sqrt{3}} \Delta y_p = v_8'$$

$$a_{11} \Delta x_p + b_{11} \Delta y_p + l_{11} = v_{11}$$

$$\frac{a_{11}}{\sqrt{3}} \Delta x_p + \frac{b_{11}}{\sqrt{3}} \Delta y_p = v_{11}'$$

$$a_{14} \Delta x_p + b_{14} \Delta y_p + l_{14} = v_{14}$$

$$\frac{a_{14}}{\sqrt{3}} \Delta x_p + \frac{b_{14}}{\sqrt{3}} \Delta y_p = v_{14}'$$

$$-a_{16} \Delta x_p - b_{16} \Delta y_p + l_{16} = v_{16}$$

$$-a_{17} \Delta x_p - b_{17} \Delta y_p + l_{17} = v_{17}$$

$$-a_{18} \Delta x_p - b_{18} \Delta y_p + l_{18} = v_{18}$$

$$-a_{19} \Delta x_p - b_{19} \Delta y_p + l_{19} = v_{19}$$

$$-a_{20} \Delta x_p - b_{20} \Delta y_p + l_{20} = v_{20}$$

$$\frac{-[a]}{\sqrt{5}} \Delta x_p + \frac{-[b]}{\sqrt{5}} \Delta y_p = v'$$

We get a system of sixteen equations with two unknowns.

The system of equations can be written in the form of matrix, as follows:

$$AX + l = V$$

Where, A – the coefficients matrix

X – the unknowns matrix

l – the free terms matrix

V – the corrections of measured matrix

Putting the minimum condition  $V^T pV \rightarrow \min$ , we get the unknowns matrix which takes the form:

$$X = (A^T pA)^{-1} A^T pl$$

The standard deviation or mean square error of measurements in the case of a single conditioned measurement is calculated and is given by :

$$S_0 = \pm \sqrt{\frac{V^T pV}{n - k}}$$

Where, n – the number of initial equations

r – the number of initial unknowns

To realize the lift network has created a traverse in closed circuit and were determined the coordinates of station with the following formulas:

$$X_i' = X_{i-1} + d_{i-1,i} * \cos \theta_{i-1,i}$$

$$Y_i' = Y_{i-1} + d_{i-1,i} * \sin \theta_{i-1,i}$$

Where, i=P,1,2,...7

Coordinates are the errors:

$$W_X = X_i - X_i'$$

$$W_Y = Y_i - Y_i'$$

$$W_{X,Y} = \sqrt{W_X^2 + W_Y^2}$$

Tolerance:

$$T = 0.003\sqrt{[D]} + \frac{[D]}{5000}$$

Orientations are errors:

$$W_\theta = \theta_{P1} - \theta_{P1}'$$

$$T_\theta = 20^{cc} \sqrt{n}$$

$$C_{\theta^\circ} = \frac{W_\theta}{n}$$

## RESULTS AND DISCUSSIONS

As mentioned at the beginning, in order to design the building was realize the topographical plan which contain the level curves of the land (Figure 2 and 3).

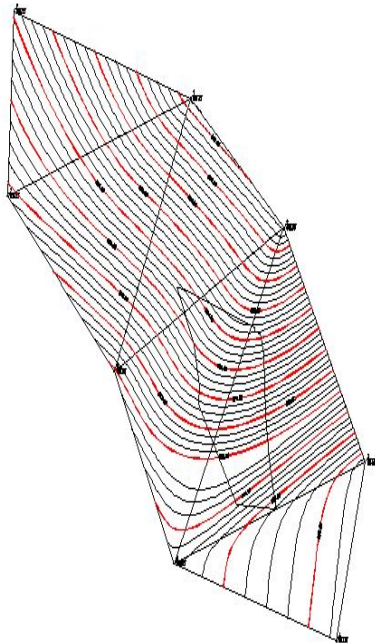


Figure 2. Polar coordinates method

Taking into consideration that all the details of the construction are determined by their axes, the tracing of the construction will consist of the following: drawing axes from the network and trace in detail towards the axes

materialized on the ground (Coșarcă, 2011; Cristescu, 1978).

The design and implementation will take into account the basic axes and intermediate axes (Pop and Ortelecan, 2005). The basic axes are the axes that form the external contour of the construction (Figure 4).

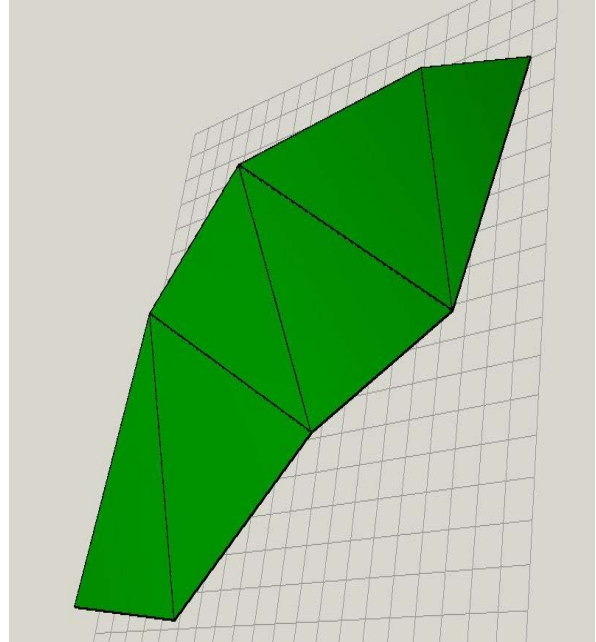


Figure 3. 3D model of the terrain

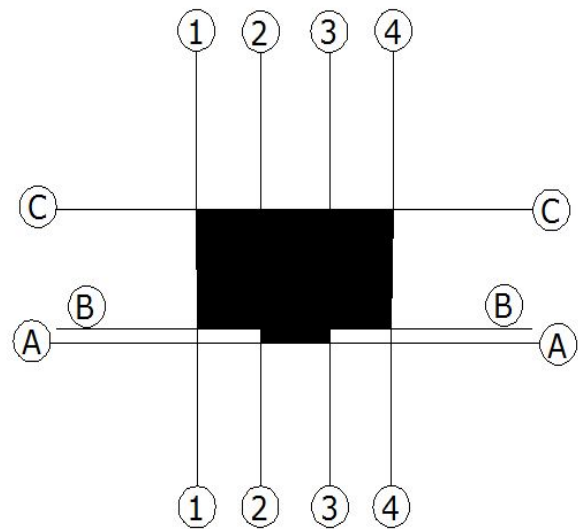


Figure 4. The basic axes of a construction

Trace the plan of the building is done by the method of polar coordinates (Figure 5).

For the trace of characteristic points of construction, during the preparation of topographical, are calculate the polar tracking items ( $\beta$  and  $d_{6-1c}$ ).

Coordinates of 6 and orientation  $\theta_{6-1c}$  are known from the composition of trace, and 1c, the coordinates are taken from the topographical plan.

$$\beta = 400 - (\theta_{6-7} - \theta_{6-1c})$$

$$d_{6-1c} = \frac{X_{1c} - X_6}{\cos \theta_{6-1c}} = \frac{Y_{1c} - Y_6}{\sin \theta_{6-1c}} = \sqrt{\Delta x^2 + \Delta y^2}$$

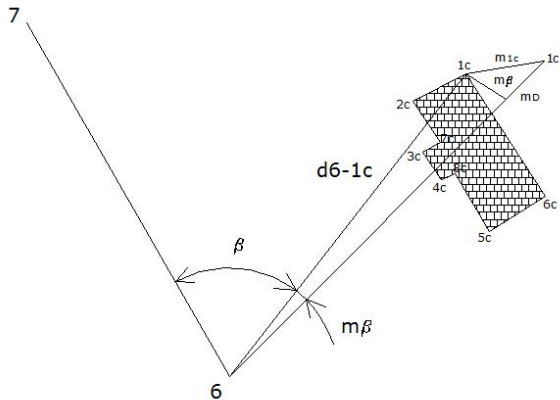


Figure 5. Polar coordinates method

Polar method is reduced to trace on the ground the steering angles  $\beta$  and the polar distances. The average position error of the point drawn is calculated using the relationship:

$$m_{1c} = \pm \sqrt{m_D^2 + D^2 \frac{(m_\beta)^2}{(\varphi^{cc})^2} + m_f^2}$$

Where,

$m_D$  – the error trace distance

$m_\beta$  – the error trace angle

$m_f$  – the fixing error of the point 1c on the ground

The precision of the tracing of the horizontal angles: The precision of the tracing of angle  $\beta$  from the project depends on the centering error of the stationary point ( $m_e$ ), the centering error of the covered mark or the error of reduction ( $m_r$ ), the actual errors of measurement ( $m_m$ ), the instrumental errors ( $m_i$ ), and of the influence of

external conditions (mCE). The average tracing error of quadratic field directions on the ground, with the help of theodolite is given by:

$$m_d = \pm \sqrt{m_e^2 + m_r^2 + m_i^2 + m_m^2 + m_{CE}^2}$$

Applying the principle of the equal influence of error components, as such:

$$\pm m_e = \pm m_r = \pm m_i = \pm m_m = \pm m_{CE} = \pm m$$

The comparison from above becomes:

$$m_d = \pm m\sqrt{5}$$

Conforming to the error theory and the method of least squares, the error mean square trace angle  $\alpha$  is given by:

$$m_\beta = m_d\sqrt{2}$$

However,

$$m_d = \pm m\sqrt{5}$$

From which, the result is:

$$m_\beta = \pm m\sqrt{10}$$

The above relationship is determined, in a roughly the value of each factor first component which will allow choosing or checking the measuring process and the characteristics of the theodolite that will be used to trace:

$$m = \pm \frac{m_\beta}{\sqrt{10}}$$

Calculation of the necessary accuracy of tracking, on the ground, angles from project, start from allowed tolerance to trace a direction.

It is necessary through the project 1cm tolerance.

$$T = 1cm$$

$$T = (2 \div 3)m_\beta \rightarrow m_\beta = \frac{T}{2} \div \frac{T}{3}$$

Table 1. Calculation of the trace elements

	$\beta$	d
$\beta_1$	142,8622	90,574
$\beta_2$	146,9495	76,393
$\beta_3$	154,3198	78,589
$\beta_7$	153,5978	80,247
$\beta_4$	61,0042	81,640
$\beta_5$	67,6282	78,218
$\beta_6$	73,2738	91,358
$\beta_8$	61,8845	83,148

## CONCLUSIONS

The precision offered by total station Leica TCR 705 with which we executed all the operations of land within this work fully satisfy the need for accuracy by the beneficiary of the work required both in terms of the accuracy and precision of the angles as well as trace precision from project.

## ACKNOWLEDGEMENTS

This research work was carried out with the support of University of Agricultural Sciences and Veterinary Medicine of Cluj-Napoca,

## REFERENCES

- Cosarca, C., Engineering surveying, 2011;  
Cristescu, N., Engineering surveying, Didactic and pedagogic Publishing House, Bucharest, 1978.  
Ghitau, D., Geodesy and gravimetry, Didactic and pedagogic Publishing House, Bucharest, 1975.  
Ortelecan, M., Palamariu, M., Bendea, H., Problems in plotting the mining works, University of Petrosani Lithography, 1998.  
Pop, N., Ortelecan, M., Engineering surveying, AcademicPres Publishing House, Cluj-Napoca, 2005.  
Radulescu, Gh., Engineering surveying, Risoprint Publishing House, Cluj-Napoca, 2003.  
Rusu, A., Surveying with elements of Geodesy and photogrammetry, didactic and pedagogic Publishing House, Bucharest, 1978.

## MATLAB BASED APPROACH OF DECODING EGNOS MESSAGE

Dumitru-Lucian BLĂGESCU, Ionuț-Alexandru BĂTRÎNACHE

Scientific Coordinator: PhD. Eng. Vlad Gabriel OLTEANU

University of Agronomic Sciences and Veterinary Medicine of Bucharest, Faculty of Land Reclamation and Environmental Engineering, 59 Mărăști Blvd, District 1, 011464, Bucharest, Romania

Corresponding author email: blagesculucian@gmail.com

### Abstract

As the European GNSS Agency (GSA) is emphasizing its efforts in implementing EGNOS based operations in various domains, such as maritime navigation or precision farming, and as the European Commission (EC) is considering extending the EGNOS coverage to Eastern Europe, it becomes demanding to start using EGNOS at national level. A first step in such direction is decoding the transmitted messages. This paper presents a MATLAB approach of decoding different EGNOS messages types and extracting the necessary information for computing the protection levels. In order to test the decoded messages, the European Space Agency's SBAS Teacher tool will be used for comparison.

**Key words:** EGNOS, MATLAB,

### INTRODUCTION

The European Geostationary Navigation Overlay Service (EGNOS) is a satellite based augmentation system (SBAS) developed by the European Space Agency, the European Commission and EUROCONTROL. As the current Global Navigation Satellite System (GNSS) alone cannot meet all the requirements for a reliable navigation system, it needs to be augmented by The European Geostationary Navigation Overlay Service. As currently defined, these requirements are as follows: accuracy (difference between the measured position at any given time to the actual or true position), integrity (ability of a system to provide timely warnings to users when it should not be used for navigation), continuity (ability of a system to perform its function without (unpredicted) interruptions during the intended operation), availability (ability of a system to perform its function at initiation of intended operation).

EGNOS is part of a developing multi-modal inter-regional SBAS service, which is able to support a wide spectrum of users in many different areas of applications, such as aviation, maritime, rail, road, agriculture. Similar SBAS systems have already been implemented by the US (Wide Area

Augmentation System – WAAS) and Japan (MTSAT Satellite based Augmentation System - MSAS). Development of other augmentation systems is being investigated in other regions of the world as well (e.g. GPS Aided GEO Augmented Navigation – GAGAN in India and System of Differential Correction and Monitoring – SDCM in Russia). All of these systems and their foreseen coverage is shown in Figure 1.

The EGNOS system differs from conventional GPS system in three key aspects: the provision of integrity positioning with a safety-of-life quality, a better accuracy than GPS (downs to about 1 to 2 m) and the possibility of establishing a geographical position with legal guarantees.

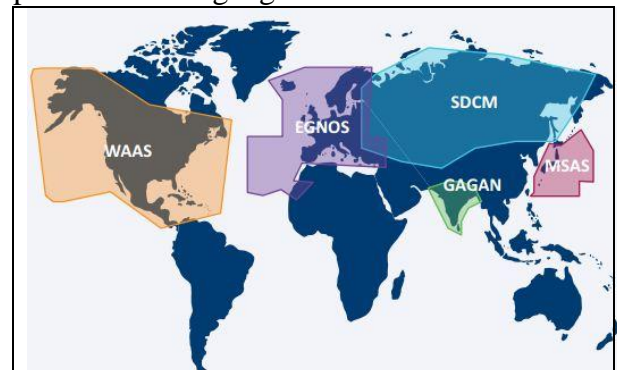


Figure 1: Worldwide SBAS systems [http://egnos-portal.gsa.europa.eu/]

In order to allow the analysis of previous EGNOS messages for different reasons, ESA has launched a service called EGNOS Message Server (EMS). Which is accessible free-of-charge, using File Transfer Protocol. EMS stores the augmentation messages broadcast by EGNOS in hourly text files, which are organized over a pre-defined hierarchy of directories (Figure 2).

Nume	Dimensiune	Data modificării
[directorul părinte]		
PRN120/		05.01.2015, 00:00:00
PRN122/		05.01.2015, 00:00:00
PRN124/		05.01.2015, 00:00:00
PRN126/		05.01.2015, 00:00:00
PRN131/		05.01.2015, 00:00:00
PRN136/		19.12.2014, 00:00:00
xferstat.dat	647 kB	01.04.2008, 00:00:00

Figure 2: EGNOS Message Server directories

Furthermore, in order to enhance SBAS understanding at user level, ESA in association with Iguassu developed SBAS Teacher, a tool which permits users to encode or decode different EGNOS message types. A snapshot of the Tool is shown in Figure 3.

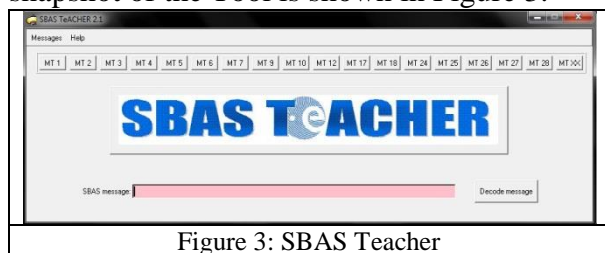


Figure 3: SBAS Teacher

This paper describes a MATLAB approach of decoding different EGNOS messages types and extracting the necessary information as a first step in computing the protection levels and using the benefits brought by EGNOS.

## MATERIALS AND METHODS

As stated before, our aim is to implement MATLAB algorithms which decode all the EGNOS message types. To accomplish this we used EGNOS Message Server (EMS) as primary data source, the European Space Agency's SBAS Teacher tool to encode different messages, and MATLAB as development platform.

MATLAB is a numerical computing environment which allows matrix manipulations, implementation of algorithms, creating of different graphical user interfaces while providing many other engineering

solutions. MATLAB users come from various backgrounds of engineering, science, and economics. And is widely used in academic and research institutions. Our goal is to develop a simple MATLAB application which decodes EGNOS messages and afterwards extract the information needed to compute the protection levels which is the main goal of EGNOS users. In this paper, attention will be focused on messages types MT6, MT9, MT25 and MT26. Figure 4 represents a diagram that contains the necessary steps to decode the messages in MATLAB.

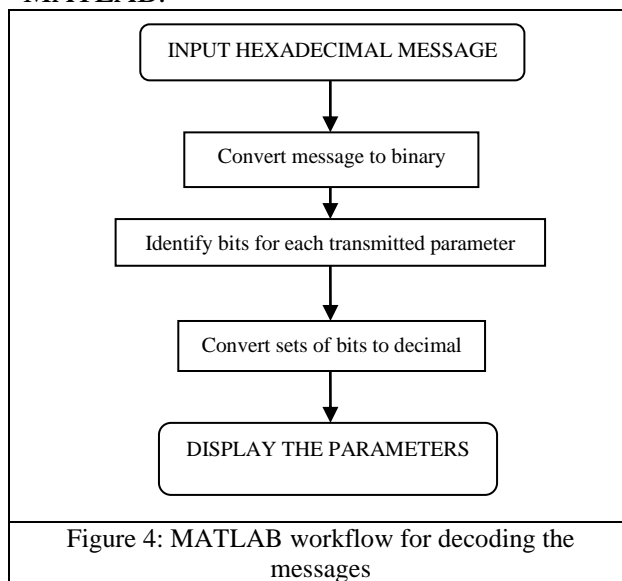


Figure 4: MATLAB workflow for decoding the messages

The first step in decoding the message is to transform it from hexadecimal (as it is given in the EMS archived files) to binary, thus breaking it down into bits which can be easily handled in MATLAB. The resulting binary message is a 250 bits string (Figure 5), in which we know the first 8 bit is the preamble, the next 6 bit indicating the messages types, and the last 24 bit are assigned to the Cyclic Redundancy Check (CRC).

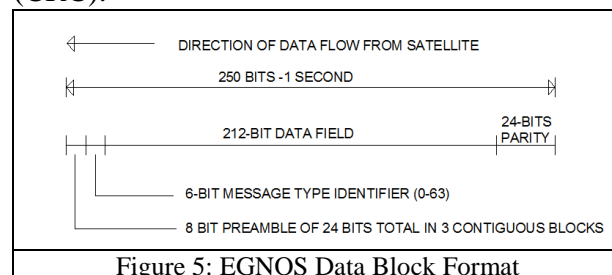


Figure 5: EGNOS Data Block Format

In this step the major difficulty consisted in identification of bit groups that needs to be decoded into the transmitted parameters as

not many information is given in the literature. The identification of these groups of bits contained in the 212 bits data field was accomplished by changing the parameters and encoding multiple messages in SBAS Teacher. Afterwards the messages were decoded in MATLAB to observe in the binary string which group of bits is altered. Through several attempts, and based on available information we accomplished to decode the MT's mentioned above.

The decoding was performed by repeated attempts because there is no free of charge documentation available on the decoding algorithm. The only resource that we relied on was a presentation about EGNOS done by Research group of Astronomy and Geomatics (gAGE/UPC) from Polytechnic University of Catalonia)

MT6 (Figure 6) contains integrity information for 51 satellites, which is the maximum number of satellites that can be present in the PRN mask. This message also includes IssueOf Data Fast Corrections (IODFj) (j=2...5) to relate the User Differential Range Estimate Indicator (UDREI) to the fast corrections included in messages of type 2 to 5 or 24.

MT6 can be used in two different ways: on one hand, it allows the fast corrections to be updated infrequently while on the other hand, it may be also used in case of satellite alert conditions. It has to be remarked that this message does not include an Issue Of Data PRN Mask (IODP) and hence the link to the PRN mask is not provided within the message. The UDRE indicators included in MT6 do apply to the satellites defined in the last received PRN mask.

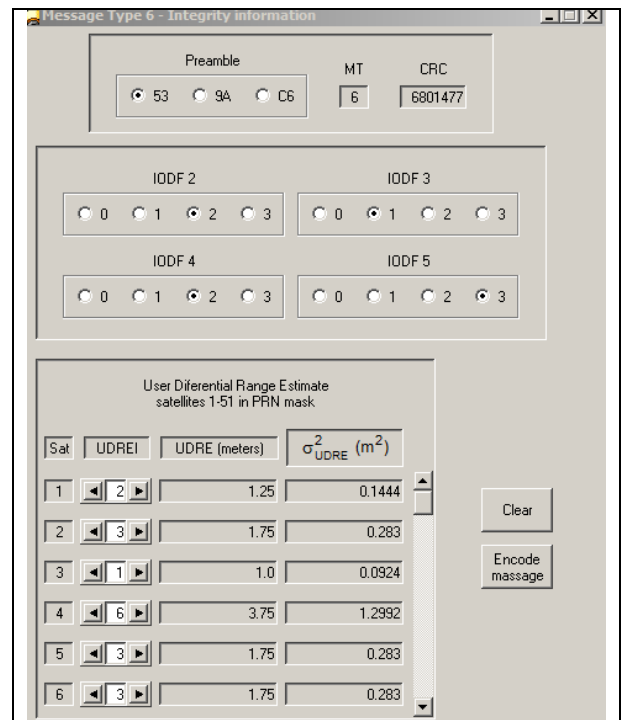


Figure 6: Message type 6-Integrity information

Message type 9 contains the information about the GEO navigation (Figure 7). As GEO satellites do not belong to any global or regional satellite positioning system, ephemeris for those satellites are not available to the users. Therefore, it is the SBAS that is in charge of providing the user with the GEO ephemeris (“The EGNOS SBAS Message Format Explained”, Daniel Porras Sánchez & César PisoneroBerges, GMV S.A).

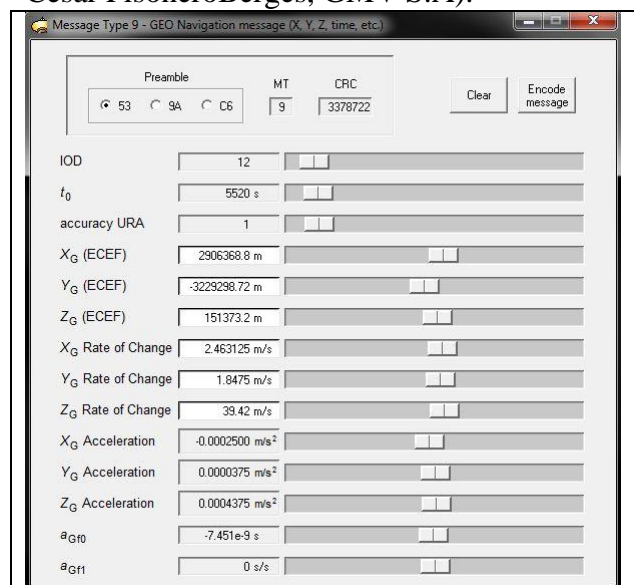


Figure 7: SBAS TeACHER Message Type 9 - GEO Navigation parameters

Message 25 provides corrections for satellite ephemeris and clock errors (Figure 8). The

data block is divided into two parts. The first bit of each part is the velocity code, which if it's set to 1 indicates that in that part of the message clock drift and velocity corrections are included, otherwise only the clock offset and position corrections are provided, but for two satellites instead of 1. Therefore the message can consist of corrections for 1, 2, 3 or 4 satellites, depending on the values of the velocity bits and how many satellites are being corrected ("The EGNOS SBAS Message Format Explained", Daniel Porrás Sánchez & César PisoneroBerges, GMV S.A).



Figure 8: SBAS TeACHER Message Type 25 – Long term satellite error corrections

Message type 26 provides the vertical ionospheric delays and their accuracies for the IGP's identified by the band number and the IGP number (Daniel Porrás & Cesar Pisonero, 2006).

## RESULTS AND DISCUSSIONS

For decoding the MT6 we encoded with SBAS Teacher a simple message multiple times, changing each time the same parameter until we could identify the bits which define that specific parameter. In this example we will choose to find the IODF 2 parameter and try to isolate the group of bits that define it.

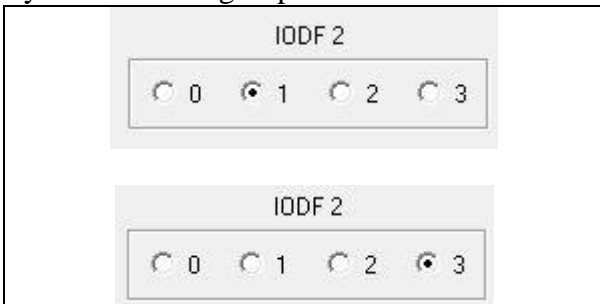


Figure 9: IODF 2 for MT6

In Figure 9 MT6 was encoded once with the IODF 2 value set to "1" and once with the IODF 2 value set to "3". After the hexadecimal string generated by SBAS Teacher was decoded using our MATLAB application we searched in the binary strings for "01" (the binary equivalent of decimal "1") and "11" (the binary equivalent of decimal "3") (Figure 10)

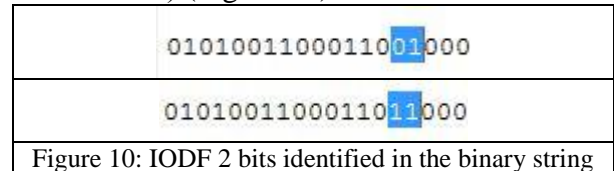


Figure 10: IODF 2 bits identified in the binary string

The same algorithm was used to decode the rest of the message, as well as for the other message types.

For the MT9 the message was converted into binary in MATLAB and obtained a 250 bits string, a user friendly form to work with. A small part of it may be seen in Figure 11. In Figure 12 one can observe a side by side comparison between the parameters decoded with the MATLAB program and the same parameters encoded with SBAS Teacher.

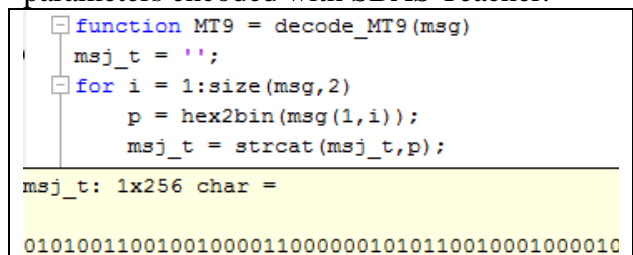


Figure 11: Message Type 9 decoded in a sequence of ones and zeros

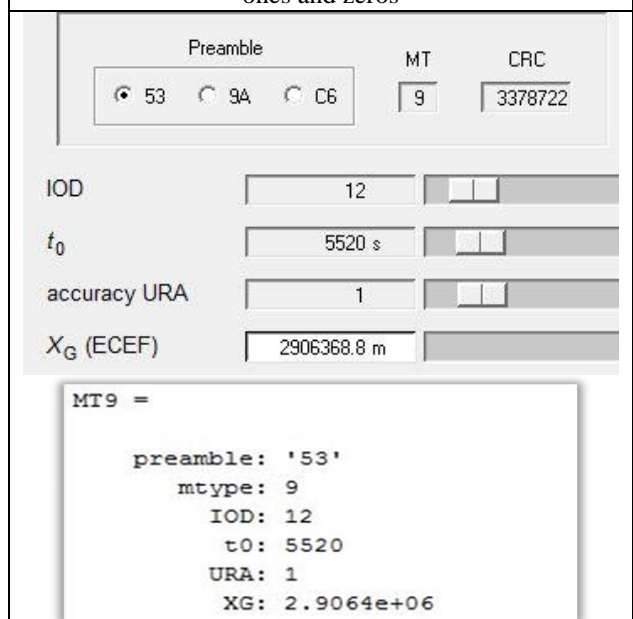


Figure 12: Comparison between MATLAB and SBAS

Figure 13 and Figure 14 present the results of the EGNOS messages decoding application for MT25. Comparing these results with the parameters from the Figure 7 it can be seen that the numbers are similar, so the decoding algorithm is working properly.

```

MT25 =

  preamble: '53'
  mtype: 25
  velocity: 0
    prn1: 17
    iode1: 27
  delta: [1x1 struct]
    prn2: 1
    iode2: 11
  IODP: [1x1 struct]
  velocity1: 0
    prn3: 1
    iode3: 6
    prn4: 0
    iode4: 0
  Parity: '1000101111110000111110011'

```

Figure 13: The results of the MATLAB decoding program for message 25

```

delta.x1=-2.75
delta.y1=7.875
delta.z1=3.75
delta.af01=-6.98492e-08

```

Figure 14: The results of the MATLAB decoding program for message 25

To test the reliability of the decoding program, a series of different messages were generated using SBAS Teacher and decoded using the following MATLAB decoding program.

```

function MT26 = decode_MT26(msg)
msj_t = '';
for i = 1:size(msg,2)
    p = hex2bin(msg(1,i));
    msj_t = strcat(msj_t,p);
end
%Preambul
MT26.preamble =
strcat(num2str(bin2dec(msj_t(1:4))),n
um2str(bin2dec(msj_t(5:8))));
%Tip mesaj
MT26.mtype = bin2dec(msj_t(9:14));
% Band Number
MT26.band = bin2dec(msj_t(15:18));
% Block ID
MT26.block = bin2dec(msj_t(19:22));
% IGP Vestical Delay Estimate
MT26.deley=zeros(15,1);
for i=1:15
    MT26.deley(i,1) =

```

```

bin2dec(msj_t(23+13*(i-1):23+13*(i-
1)+8))*0.125;
end
% Grid Ionopheric Vertical Error
Indicator (GIVEI)
MT26.GIVEI= zeros(15,1);
MT26.GIVE= zeros(15,1);
MT26.sigmaGIVE = zeros(15,1);
for i = 1:15
    MT26.GIVEI(i,1) =
bin2dec(msj_t(32+13*(i-1):32+13*(i-
1)+3));
    [MT26.GIVE(i,1),
MT26.sigmaGIVE(i,1)] =
chooseGIVEI(MT26.GIVEI(i,1));
end
% Issue of Data
MT26.issue = bin2dec(msj_t(218:219));
end

```

IGP	GIVEI	GIVE (meters)	$\sigma_{GIVE}^2$ (m <sup>2</sup> )	
1	1	0.6	0.0333	0.250 m
2	2	0.9	0.0749	1.250 m
3	3	1.2	0.1331	5.000 m
4	4	1.5	0.2079	8.875 m
5	5	1.8	0.2994	9.875 m

Preamble:  53  9A  C6    MT: 26    CRC: 5678742  
 Band number:  0  1  2  3  4  5  
 Block ID:  0  1  2  3  4  5

GIVEI=1	GIVE=0.6	sigmaGIVE=0.0333
GIVEI=2	GIVE=0.9	sigmaGIVE=0.0749
GIVEI=3	GIVE=1.2	sigmaGIVE=0.1331
GIVEI=4	GIVE=1.5	sigmaGIVE=0.2079
GIVEI=5	GIVE=1.8	sigmaGIVE=0.2994

Figure 15: Comparison between SBAS and MATLAB decoding



## ASPECTS OF SOLVING THE BASIC GEODETIC PROBLEM ON THE SPHERE

Alina BUZILĂ, Bogdan Ioan CIOBAN, Marcela Ionela HANDRO , Adrian Șerban PETRIC

Scientific Coordinators: Prof. PhD. Eng. Mircea ORTELECAN, Lect. PhD. Eng. Tudor SALĂGEAN

University of Agricultural Sciences and Veterinary Medicine, 3-5 Mănăștur street, 400372, Cluj-Napoca, România Tel: +40-264-596.384 | Fax: +40-264-593.792

Corresponding author email: handro.marcela@yahoo.com

### Abstract

*The purpose of this paper is to present the methods of solving the basic geodetic problems. Taking advantage of numerical integration, we solve the direct and inverse geodetic problems on the ellipsoid. In general, the solutions are composed of a strict solution for the sphere plus a correction to the ellipsoid determined by numerical integration. The problems in geodesy are usually reduced to two main cases: the direct problem, given a starting point and an initial heading, find the position after traveling a certain distance along the geodesic; and the inverse problem, given two points on the ellipsoid find the connecting geodesic and hence the shortest distance between them. Much of the early work on these problems was carried out by mathematicians—for example, Legendre, Bessel, and Gauss—who were also heavily involved in the practical aspects of surveying. If the Earth is treated as a sphere, the geodesics are great circles (all of which are closed) and the problems reduce to ones in spherical trigonometry. For a sphere the solutions to these problems are simple exercises in spherical trigonometry, whose solution is given by formulas for solving a spherical triangle.*

**Key words:** Geodetic problems, ellipsoid, sphere

### INTRODUCTION

Based on observations made on the terrestrial surface, projected on the reference ellipsoid, we are going to establish by calculation the positions of the first order geodetic points in a particular coordinate system used on the ellipsoid. The ultimate goal of the calculations performed on the reference ellipsoid is the determination of geodetic coordinates, latitude  $B$  and longitude  $L$  of the points from geodetic networks support which are obtained through a series of rigorous processing operations of astronomic-geodesic determinations following several phases: calculation of coordinates in the preliminary stage necessary interim processing and calculation of final coordinates after finishing proper compensation. Therefore, it can be appreciated that this sort of calculation occupy a very important volume, which is why they are known in the literature as well as the solving of basic geodetic problems. The basic first geodesic problem, called direct geodetic

problem, consists of determining the geodetic coordinates  $B_2$ ,  $L_2$  of point  $S_2$  (Figure 1) and  $A_2$  geodetic azimuth (also called inverse geodetic azimuth) depending on the coordinates  $B_1$ ,  $L_1$  of the  $S_1$  point, geodetic azimuth  $A_1$  (also called direct geodetic azimuth) and the length of the geodetic line  $s$ , between points  $S_1$  and  $S_2$  (Moldoveanu, 2002).

The successive use of direct geodetic problem is also known as coordinated transportation (Ortelecan, 2006).

The second basic geodetic problem, also called inverse geodetic problem consists in determining the length of the geodetic line  $s$  and direct geodetic azimuth  $A_1$  and inverse geodetic azimuth  $A_2$ , when the geodetic coordinates of points  $S_1$  and  $S_2$  are known. Geodetic inverse problem is used to deduct the original elements (geodetic azimuth and distance) necessary to determine the coordinates of all points of a geodetic network, as well as a method to check the calculations

made at direct geodetic problem (Ortelean and Sălăgean, 2014).

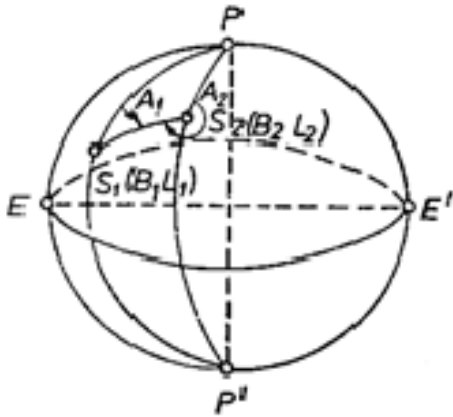


Figure 1. Sphere

## MATERIALS AND METHODS

There are several criteria for the classification of methods and procedures for calculating geodetic coordinates on the reference ellipsoid, depending on the element considered mainly to be determined.

One of the current classification criteria used, considers as the geodetic main element the length of the geodesic line, denoted by  $s$ . From this point of view, can be distinguished the Taylor series method, Legendre method, in the case of small distances, below 60 km; average method arguments Gauss for medium lengths ( $60 < s < 600\text{km}$ ) and in case of great distances ( $600 < s < 20000\text{ km}$ ) using Bessel's method. Another aspect to be considered in effective solutions relates to the accuracy of the calculations of geodetic coordinates, where we can distinguish between exact methods and approximate methods. As the geodesic distances increase, accuracy in calculations has special significance. As in other geodetic calculations, but also in the geodetic based problems, it is desired that errors in the calculation to be about 10 times smaller than the average errors that characterize the operation in the field. Thus, it can be shown that in the first-order geodetic triangulation, in which intervened geodetic distances, averaging 30-40 km, it was necessary that the approximation calculation for geodetic coordinates  $B$  and  $L$  to be  $\pm 0''$ , 0001, for geodetic azimuths, denoted by  $A$  to be  $\pm 0''$ , 001, and for geodetic distances (geodesic lines), denoted by  $s$ , to be  $\pm 0$ , 001 m.

## RESULTS AND DISCUSSIONS

### The method for replacing the surface of the ellipsoid with Gauss sphere

In approximation limit allowable, for short distances ( $s < 60\text{ km}$ ), can assimilate the ellipsoid surface with the surface of a sphere of Gauss average radius.

#### Solving the inverse problem

It is known :

Dl. Hoia:  $B=46^{\circ}46'06.45315''$  N

$L=23^{\circ}32'13.25030''$  E

Dl. Steluta:  $B=46^{\circ}48'17.54003''$  N

$L=23^{\circ}34'56.24439''$  E

We will refer to figures 2 a and 2 b, on which we , as a first step , write formulas for the half the sum and half the difference for sinus and cosines in spherical triangles:

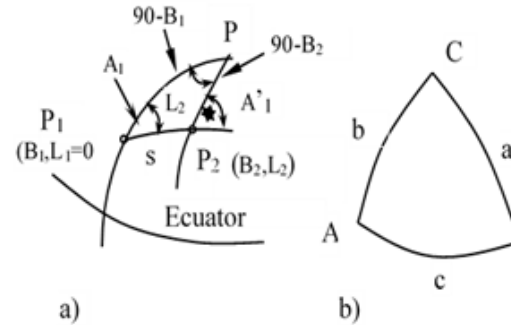


Figure 2.a. The triangle on the sphere;

2b. Corresponding spherical triangle

$$\begin{aligned} \sin \frac{a}{2} \cos \frac{B-C}{2} &= \sin \frac{b+c}{2} \sin \frac{A}{2} \\ \sin \frac{a}{2} \sin \frac{B-C}{2} &= \sin \frac{b-c}{2} \cos \frac{A}{2} \end{aligned} \quad (1.1)$$

$$\cos \frac{a}{2} \cos \frac{B+C}{2} = \cos \frac{b+c}{2} \sin \frac{A}{2}$$

$$\cos \frac{a}{2} \sin \frac{B+C}{2} = \cos \frac{b-c}{2} \cos \frac{A}{2}$$

By identifying P1PP2 and CAB triangles, result:

$$\begin{aligned} A &= L2 & a &= s \\ B &= 180 - A_1' & b &= 90 - B1 \quad (1.2) \\ C &= A1 & c &= 90 - B2 \end{aligned}$$

and with their help is calculated:

$$\frac{B-C}{2} = \frac{180^\circ - A_1' - A_1}{2} = 90^\circ - \frac{A_1' + A_1}{2};$$

$$\frac{b-c}{2} = \frac{90^\circ - B_1 - (90^\circ - B_2)}{2} = \frac{B_2 - B_1}{2} \quad (1.3)$$

$$\frac{B+C}{2} = \frac{180^\circ - A_1' + A_1}{2} = 90^\circ - \frac{A_1' - A_1}{2};$$

$$\frac{b+c}{2} = \frac{180^\circ - B_1 - B_2}{2} = 90^\circ - \frac{B_1 + B_2}{2}$$

$$\frac{A}{2} = \frac{L_2}{2}; \quad \frac{a}{2} = \frac{s}{2}$$

By replacing the equality ( 1.3 . ) to ( 1.1. ) there is obtained:

$$\text{I} \quad \sin \frac{s}{2} \sin \frac{A_1' + A_1}{2} = \cos \frac{B_2 + B_1}{2} \sin \frac{L_2}{2}$$

$$\text{II} \quad \sin \frac{s}{2} \cos \frac{A_1' + A_1}{2} = \sin \frac{B_2 - B_1}{2} \cos \frac{L_2}{2} \quad (1.4)$$

$$\text{III} \quad \cos \frac{s}{2} \sin \frac{A_1' - A_1}{2} = \sin \frac{B_2 + B_1}{2} \sin \frac{L_2}{2}$$

$$\text{IV} \quad \cos \frac{s}{2} \cos \frac{A_1' - A_1}{2} = \cos \frac{B_2 - B_1}{2} \cos \frac{L_2}{2}$$

Dividing equalities I to II and III to IV we obtain:

$$\text{tg} \frac{A_1' + A_1}{2} = \frac{\cos \frac{B_2 + B_1}{2}}{\sin \frac{B_2 - B_1}{2}} \text{tg} \frac{L_2}{2} = 0,851380316$$

$$\text{tg} \frac{A_1' - A_1}{2} = \frac{\sin \frac{B_2 + B_1}{2}}{\cos \frac{B_2 - B_1}{2}} \text{tg} \frac{L_2}{2} = 0,000287959$$

In the relations ( 1.5 ), the coordinates of " P1 " and " P2 " being known, result that "B1", "B2" and "L2" are known; so by solving the system of equations can be determined azimuths "A1" and "A1'".

$$A_1' + A1 = 2 \arctg 0,851380316 = 80,82083795$$

$$A_1' - A1 = 2 \arctg 0,000287959 = 0,032997671 \quad (1.6)$$

By solving the system we get:

$$* A_1' = (80,82083795 + 0,032997671) / 2 = 40^\circ,42691781 = 40^\circ 25' 36'',90411564$$

$$* A1 = (80,82083795 - 0,032997671) / 2 = 40^\circ,39392014 = 40^\circ 23' 38'',11249892$$

To calculate the value of the geodetic line, equalities I are divided to equalities III, and for verification, equalities II are divided to equalities IV:

$$\text{tg} \frac{s}{2} = \frac{\sin \frac{A_1' - A_1}{2}}{\sin \frac{A_1' + A_1}{2}} \text{ctg} \frac{B_2 + B_1}{2} = 0,00041733$$

$$s' = 2 \arctg 0,00041733 = 0,047822488$$

$$s = s'R = 5317,716276$$

$$\text{tg} \frac{s}{2} = \frac{\cos \frac{A_1' - A_1}{2}}{\cos \frac{A_1' + A_1}{2}} \text{tg} \frac{B_2 - B_1}{2} = 0,00041733$$

$$s' = 2 \arctg 0,00041733 = 0,047822488$$

$$s = s'R = 5317,716276 \text{ m}$$

Solving the direct problem

We consider the points P1 and P2 ( Fig .3 ) located on a sphere of average radius, calculated based on the center of gravity of the spherical triangle P1PP2 .

Geodetic coordinates of the point P1 (DI Hoia) are known,

$$B = 46^\circ 46' 06'',45315 \text{ N} \quad L = 23^\circ 34' 56'',24439 \text{ E}$$

Azimuth direction of P1P2:

$$A1 = 40,25,36,90411564$$

length of the geodesic line

$$s = 5317,716276 \text{ m.}$$

We will determine the coordinates of the point P2 ( B2 , L2 ) and inverse azimuth denoted by A2.

To facilitate relations writing we choose a certain spherical triangle whose elements are represented in Fig .3b .

To solve the problem, we write formulas of three adjacent elements in this triangle and we get:

$$\begin{aligned} \sin \frac{a}{2} \cdot \cos \frac{B-C}{2} &= \sin \frac{b+c}{2} \cdot \sin \frac{A}{2}; \\ \sin \frac{a}{2} \cdot \sin \frac{B-C}{2} &= \sin \frac{b-c}{2} \cdot \cos \frac{A}{2}; \\ \cos \frac{a}{2} \cdot \cos \frac{B+C}{2} &= \cos \frac{b+c}{2} \cdot \sin \frac{A}{2}; \\ \sin \frac{a}{2} \cdot \sin \frac{B+C}{2} &= \cos \frac{b-c}{2} \cdot \cos \frac{A}{2}; \end{aligned} \quad (2.1)$$

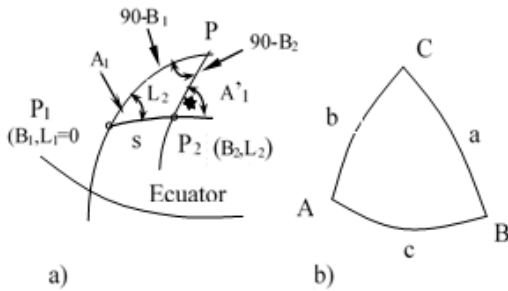


Figure 3.a. The triangle on the sphere;  
3b. Corresponding spherical triangle

Spherical triangle ABC identified with spherical triangle P1P2P leads to the equalities:

$$\begin{aligned} A &= A'1 & a &= 900 - B2 \\ B &= 1800 - A'1 & b &= 900 - B1 \\ C &= L2 & c &= s' \end{aligned} \quad (2.2)$$

and with their help:

$$\begin{aligned} \frac{B-C}{2} &= \frac{1800 - A'1 - L2}{2} = 900 - \frac{A'1 + L2}{2}; & \frac{b+c}{2} &= \frac{900 - B1 + 8826}{2} \quad (2.6) \\ \frac{B+C}{2} &= \frac{1800 - A'1 + L2}{2} = 900 - \frac{A'1 - L2}{2}; & \frac{b-c}{2} &= \frac{900 - B1 - s}{2} \\ \frac{A}{2} &= \frac{A'1}{2}; & \frac{a}{2} &= \frac{900 - B2}{2} \end{aligned} \quad (2.3)$$

Introducing the equalities ( 2.3. ) in ( 2.1. ) is obtained :

$$\begin{aligned} \text{I} \quad \sin \frac{900 - B2}{2} \sin \frac{A'1 + L2}{2} &= \sin \frac{900 - B1 + s}{2} \sin \frac{A'1}{2} \quad \text{II} \\ \sin \frac{900 - B2}{2} \cos \frac{A'1 + L2}{2} &= \sin \frac{900 - B1 - s}{2} \cos \frac{A'1}{2} \quad \text{III} \\ \cos \frac{900 - B2}{2} \sin \frac{A'1 - L2}{2} &= \cos \frac{900 - B1 + s}{2} \sin \frac{A'1}{2} \quad \text{IV} \\ \cos \frac{900 - B2}{2} \cos \frac{A'1 - L2}{2} &= \cos \frac{900 - B1 - s}{2} \cos \frac{A'1}{2} \end{aligned} \quad (2.4)$$

By dividing the relationships I and II ; III and IV is obtained :

$$\begin{aligned} \text{tg} \frac{A'1 + L2}{2} &= \frac{\sin \frac{900 - B1 + s}{2}}{\sin \frac{900 - B1 - s}{2}} \text{tg} \frac{A'1}{2} \\ &= 0,368643823 \\ \text{tg} \frac{A'1 - L2}{2} &= \frac{\cos \frac{900 - B1 + s}{2}}{\cos \frac{900 - B1 - s}{2}} \text{tg} \frac{A'1}{2} \\ &= 0,367746477 \end{aligned} \quad (2.5)$$

Solving the system of equations ( 2.5 ) are obtained unknowns " A'1 " and " L2 " according to geodetic coordinates of the point " P1 " and geodesic length "s".

Inverse azimuth: A2=A'1+200g.

$$A'1 + L2 = 2 \arctg 0,368643823 = 40,4721939$$

$$A'1 - L2 = 2 \arctg 0,367746477 = 40,3816417$$

$$A'1 = (40,4721939 + 40,3816417) / 2 = 40,4269178$$

$$81 = 40^\circ 25' 36'', 90411564$$

$$L2 = (40,4721939 -$$

$$40,3816417) / 2 = 23,58229011 = 23^\circ 34' 56.24439$$

To find the geodetic latitude of the point " P2 " ( B2 ) relations I and III; II and IV are divided:

$$\text{tg} \frac{90 - B2}{2} = \frac{\sin \frac{A'1 - L2}{2}}{\sin \frac{A'1 + L2}{2}} \text{tg} \frac{90 - B1 + s}{2} = 0,39587$$

$$\text{tg} \frac{90 - B2}{2} = \frac{\cos \frac{A'1 - L2}{2}}{\cos \frac{A'1 + L2}{2}} \text{tg} \frac{90 - B1 - s}{2} = 0,39587$$

$$8826$$

$$90 - B2 = 2 \arctg 0,395878826 = 43,19512777$$

$$B2 = 90 - 43,19512777 = 46,80487223$$

$$= 46^\circ 48' 17.54003''$$

The two relations (2.6 ). Determine exactly the same size, the latitude " B2 " of point " P2 " .

Geodetic coordinates	Degrees [ ° ]	Minutes [ ' ]	Seconds[ " ]	Decimal Degrees
B1	46	46	6,45315	46,76845921
L1	23	32	13,2503	23,53701397
B2	46	48	17,54003	46,80487223
L2	23	34	56,24439	23,58229011
L=L2-L1	0	2	42,99409	0,045276136

Coordonate geodezice	Grade [ ° ]	Minute [ ' ]	Secunde[ " ]	Grade Decimale
B1	46	46	6,45315	46,76845921
L1	23	32	13,2503	23,53701397
A1	40	23	38,11249892	40,39392014
s[m]	s[rad]=s/R	s'[decimal]	s[".'." ]	
5317,716276	0,0008347	0,04782249	0°2'52".16095726	

## CONCLUSIONS

As a result of the performed calculations it is observed that the geodetic coordinates of the second point of the direct geodetic problem are the same with the coordinates of the point of the inverse geodetic problem.

For small areas using the calculation method of average radius sphere offers acceptable accuracy for practical work.

Calculation of geodetic coordinates on the average radius sphere can also be used for large areas reported on a small scale.

In the case of large areas, when calculating geodetic coordinates on the sphere, deformations that occur when projecting the linear elements off the ellipsoid on the sphere should be taken into account.

## REFERENCES

- Moldoveanu C, 2002. Geodezie. Noțiuni de geodezie fizică și elipsoidală. Poziționare – Editura Militară, București
- Ortelecan M., 2006. GEODEZIE, Editura AcademicPres, Cluj-Napoca
- Ortelecan M., Salagean T., 2014. Geodezie - Lucrări practice, Editura Risoprint, Cluj-Napoca

## SETTING THE REDUCE CORRECTIONS AT THE CHORD, FOR DIRECTIONS IN THE CASE OF THE 1970 STEREO PROJECTION

Ionut CAMPIAN, Tudor Alexandru FLOREA, Tania VRANCEANU, Mircea VUSCAN

Scientific Coordinators: Prof. PhD Eng. Mircea ORTELECAN, Lecturer PhD Eng. Tudor SĂLĂGEAN

University of Agricultural Sciences and Veterinary Medicine of Cluj-Napoca, Calea Mănăştur 3-5,  
400372, Cluj-Napoca, Romania | Tel: +40-264-596.384 | Fax: +40-264-593.792  
Email: tudor.aflorea@gmail.com

Corresponding author email: tudor.aflorea@gmail.com

### Abstract

The first step to be run as part of the compensation is to determine preliminary coordinates. They are determined with a precision low accuracy generally depends on the purpose and length of the sides of the network considered. Because the projection system used officially in Romania is 1970 stereographic system for processing observations is usually a two-dimensional system still will consider that this plan is the reference surface which will reduce geodetic observations. If the geodesic network of the distance measurements were made, to be reduced from the reference surface selected. After being corrected physical (generally modern tools to measure distances apply this correction automatically) distances measured to be applied, in order, the following discounts: Reducing the chord; Reduction of the reference ellipsoid surface; Reduction plan stereographic projection in 1970. This stage of preliminary processing geodetic observations and reduction in the chosen reference surface is considered performed by the user, for which the program will be introduced reduced to the reference surface observations.

**Key words:** Reducing the chord, compensation, projection system, topography

### INTRODUCTION

The 1970 stereographic projection is an azimuthal, perspective (using linear perspective laws) and determined (preserves angles) projection. The secant projection plan is being lowered by 3,502m as opposed to the tangent plane onto the equivalent sphere.

Almost the entire surface of Romania can be enframed in a circle with the radius of about 400 km. The centre of the circle is considered to be also the origin of the rectangular coordinate system XOY and it is situated on the north side of the town of Făgăraş, at the intersection of the 46° north latitude parallel and the 25° longitude meridian. This proves that the whole country is divided into four quadrants. The OX axis is orientated towards North, and the OY axis is directed towards East. In order to reduce the number of calculations, a false axis system is used whose origin point is translated, in the same plan, 500km towards South and West; this way all

the referential points in the false system will have only positive coordinates.

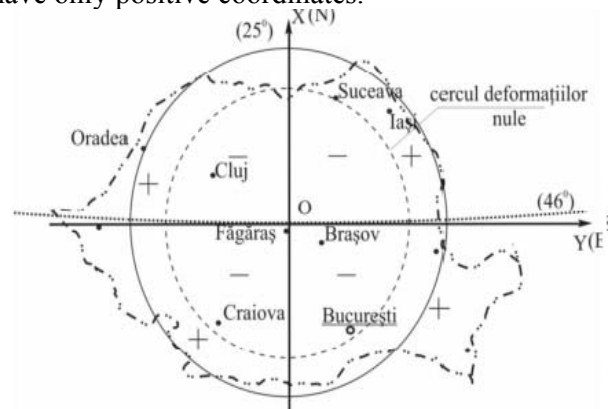


Figure 1 – The entire surface of Romania (Munteanu, 2003)

Reducing the projection plane directions is the operation of correcting the measured directions in the state geodesic network, through the application of angular corrections  $\delta$  called "corrections to reduce the chord". This operation is necessary because, in the plane of projection, flat images of GEODESIC triangles sides are not lines but are curved. To determine

the formula for the calculation of the corrections, we consider a spheric triangle, B1-B2-Q0 (B1, B2 are the extremities of a measured direction, and iar Q0 ( $\lambda_0, \varphi_0$ ) is the projection pole), on the sphere of medium RADIU R0 .

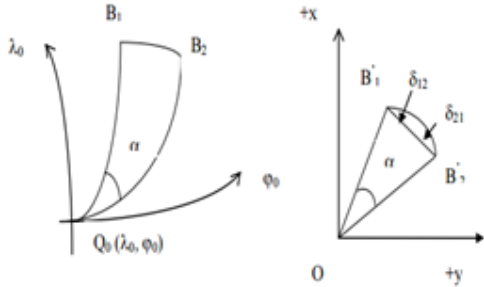


Figure 2 - The representation of the geodesic lines on the ellipsoid and on the projection plane (Palamariu, Padure, Ortelecan, 2002)

For the representation of spherical triangles in the plane, we consider the following properties of the stereographic projection: the projection is determined; the big circles passing through Q0 (verticals) are represented by line segments passing through the origin O; an arc will always be represent through an arc (the exceptions are the verticals).

The planar images of the tips of the spherical triangle are the points B1, B2 ' and ' O. The arcs of circle B1Q0 and B2Q0, belong to some verticals of the pole Q0, which are represented through the lines B1'O and B2 ' O, forming an angle  $\alpha$ , between them, equal to the one corresponding to the one on the sphere. The chord reduction refers to the deformation of the directions that were moved from the equivalent sphere on the plane of projection. All the directions from the sphere are projected as curved lines on the plane, with the exception of those which pass through the point opposite to the stereographic point S. These directions are projected as straight lines passing through the origin of the coordinate axes.

Any direction 1-2 from the sphere will be projected on the plan through a curved line, creating a spherical triangle with the directions O-1 and O-2 passing through the origin. Considering this, the only side of the triangle that is affected by the spherical excess is 1-2.

If the distance between 1 and 2 is sufficiently large (kilometre-order), we should take

intoaccount the size of the spherical excess, given by:

$$\varepsilon^{cc} = \rho^{cc} \frac{S}{R^2}$$

The size of the surface can be calculated using the formula:

$$S_1 = \frac{1}{2} \begin{vmatrix} x_1 & y_1 & 1 \\ x_2 & y_2 & 1 \\ 0 & 0 & 1 \end{vmatrix} = \frac{1}{2} \begin{vmatrix} x_1 & y_1 \\ x_2 & y_2 \end{vmatrix} = \frac{1}{2} (x_1 \times y_2 - x_2 \times y_1)$$

In these circumstances, the formula

$$\varepsilon^{cc} = \rho^{cc} \frac{S}{R^2} \text{ becomes :}$$

$$\varepsilon^{cc} = \frac{S}{2R^2} \rho^{cc} = \frac{\rho^{cc}}{4R^2} (x_1 y_2 - x_2 y_1)$$

Using the value in the previous formula, we can determine the azimuths from the plan, thus eliminating the effect of spherical excess. This helps us notice that, in the event of such determinations, the coordinates of the points 1 and 2 from the formula are the real ones, not the once affected by the translation of 500 km on the South and West direction.

## MATERIALS AND METHODS

For the calculation of the reduction at the chord corrections will take account the Figure 3.

The representation to be determined (to preserve angles in planes of projection)

Geodetic lines that pass through the pole projection (Q0) will be represented in the plane of projection by straight line segments passing through the origin of the axes.

Coastlines of great circles on the sphere that do not pass through the pole projection (Q0), will be represented by the arcs.

Based on these considerations, the projections in the plan projection directions will appear as shown in the Figure 4.

The representation is determined, so the sum of the angles of the figure of the plan shall be equal to the sum of the angles of the corresponding figure on the ellipsoid and results:

$$180^\circ + 2\delta = 180^\circ + \varepsilon$$

$$2\delta = \varepsilon$$

$$\delta = \frac{\varepsilon}{2}$$

(1)

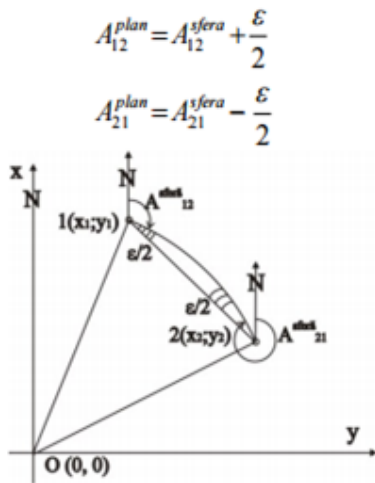


Figure 3 – Reducing the corrections at the chord

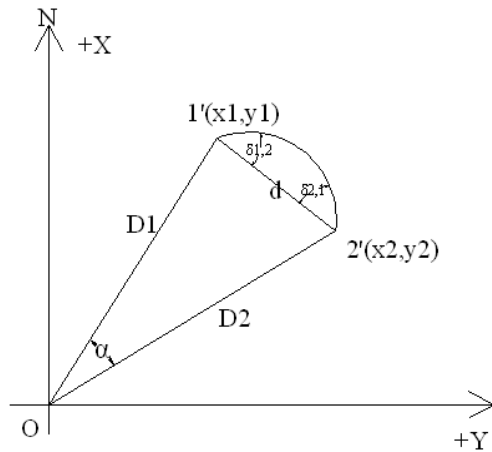


Figure 4 – Direction projected in the plan

In absolute value ( $\delta$ ), the correction shall be equal to half of the excess of a triangle formed by spherical  $\varepsilon$  from the target point and station pole  $Q_0$  of the projection. Calculating spherical excess is given by the relation :

$$\varepsilon^{cc} = \rho^{cc} \frac{S}{R^2} \quad (2)$$

Where:  $\varepsilon$  – spherical excess  
 $S$  – spherical triangle area  
 $R$  – the radius of the sphere  
 $\rho$  – the coefficient of transformation from radians in seconds.

The radius of the sphere is calculated according to the relationship :

$$R = \sqrt{MN} \quad (3)$$

where:  $M$  - the radius of the ellipse meridian  
 $N$  - the radius of curvature of the first vertical

$$M = \frac{a(1-e^2)}{W^3} \quad (5)$$

$$N = \frac{a}{W} \quad (6)$$

$a$  - large semimajor axis (Equatorial radius)

$e^2$  - first excentriciate

$$e^2 = \frac{a^2 - b^2}{a^2} \quad (7)$$

$b$  - small semimajor axis

$W$  - the auxiliary function

$$W = \sqrt{1 - e^2 \sin^2 B} \quad (8)$$

$B$  - latitude

Area of a triangle plane  $S_1$  can determine a determinant that contains the coordinates of the triangle and the peaks. The spherical triangle can assimilate with the triangle area plan.

$$S_1 = \frac{1}{2} \begin{vmatrix} x_1 & y_1 & 1 \\ x_2 & y_2 & 1 \\ 0 & 0 & 1 \end{vmatrix} = \frac{1}{2} \begin{vmatrix} x_1 & y_1 \\ x_2 & y_2 \end{vmatrix} = \frac{1}{2} (x_1 \times y_2 - x_2 \times y_1)$$

Replacing with the relationship (2) and (3) in relationship (1) is obtained:

$$\delta = \frac{\rho^{cc}}{4R^2} \times \begin{vmatrix} x_1 & y_1 & 1 \\ x_2 & y_2 & 1 \\ 0 & 0 & 1 \end{vmatrix} \quad (10)$$

## RESULTS AND DISCUSSIONS

The case study on the design of bearing in the directions of the Stereo 70 projection was done in three points of triangulation network relating to Cluj-Napoca. There were taken into study points like: Gradina Botanica, Chinteni și Calea Turzii. These are points of triangulation of the II, III and IV order.

Calculation of the corrections of the chord and the discount calculation global deformation response linear module is carried out with the coordinates of the points that have origins in the projection. In this case the coordinates will fall 1970 Stereo on the X and Y value of false origin 500,000 [m].

Table 1 - Stereo Coordonates

Stereo 1970 Coordonates		
Punct	X	Y
Gradina Botanica ( turn ) (803)	585444.580	392308.900
Chinteni (1102)	592195.620	391924.350
Calea Turzii (220)	582906.660	392258.000

Table 2 - Coordinates with origin in the projection pole

Coordinates with origin in the projection pole		
Punct	X	Y
Gradina Botanica ( turn ) (803)	85444.580	-107691.100
Chinteni (1102)	92195.620	-108075.650
Calea Turzii (220)	82906.660	-107742.000

According to the above relations are established the reduction at the chord corrections for the measured directions.

Table 3 - Corrections

Correction Name	Correction Value
$\delta_{803,1102}$	2.715103189
$\delta_{803,220}$	-1.086013276
$\delta_{220,1102}$	3.806277756
$\delta_{1102,220}$	-2.7151
$\delta_{220,803}$	1.086013
$\delta_{1102,803}$	-3.80628

On the basis of the area of the triangle plan are determineted the calculation of spherical excess:

$$\varepsilon = \frac{636620}{2 \times 6379,391^2} \times \begin{vmatrix} 85444.580 & -107691.100 & 1 \\ 92195.620 & -108075.650 & 1 \\ 82906.660 & -107742.000 & 1 \end{vmatrix} = -0.0103$$

The differences of these directional coefficients have been determined for reducing the angular adjustments in the plane of projection:

Table 4 – Amount of correction

Angular correction	The amount of the correction
$\delta_{803,220} - \delta_{803,1102}$	-3.801116465
$\delta_{1102,220} - \delta_{1102,803}$	1.091174568
$\delta_{220,1102} - \delta_{220,803}$	2.72026448
[ ]	0.0103

From this table, it appears that the amount of angular corrections from a network of triangulation triangle is equal to the inverse of the spherical excess value.

The sign for the reduction at the chord corrections shall be determined according to the direction of travel from the curve of the geodesic lines to the chord. When the meaning is directly clockwise the correction will get positive and negative otherwise.

The establishment of the sign must be done with great care because a wrong choice of the sign inserts a double error correction for the wrong set.

## CONCLUSIONS

The calculation of the corrections to reduce chord must precede the offset angles in triangulation networks, considering the fact that by applying these patches eliminate spherical excess. Patch size reduction from the chord is influenced by the length of the visa, the distance from the pole and the orientation of the projection of the visa.

The direction of the approaching visa guidance from the station point to the center point of projection, the correction value of chord discount shrinks .

Corrections discount values to string become meaningful and must be applied for second-order triangulation networks III, II, I.

## REFERENCES

- Moldoveanu, C., Geodezie, Editura Matrix Rom, București, 2004
- Ortelecan, M., Geodezie, Editura AcademicPres, Cluj-Napoca, 2006
- Munteanu, Gh., Constantin, Cartografie matematică, Editura Matrix Rom, București, 2003
- Palamariu, M., Pădure, I., Ortelecan, M., Cartografie și cartometrie, Editura Aeternitas, Alba-Iulia, 2002

## ESTABLISHING THE SPHERICAL EXCESS FOR THE GEODETIC NETWORKS OF THE THIRD ORDER

Răzvan Alex CIORBĂ, Radu Alexandru CREȚU, Mircea Emil NAP, Andreea Carmen ZAGOR

Scientific Coordinators: Prof. PhD Eng. Mircea ORTELECAN, Lecturer PhD Eng. Tudor SĂLĂGEAN

University of Agricultural Sciences and Veterinary Medicine of Cluj-Napoca, Calea Mănăștur 3-5, 400372, Cluj-Napoca, Romania | Tel: +40-264-596.384 | Fax: +40-264-593.792  
Email: raducretzu@yahoo.com

Corresponding author email: raducretzu@yahoo.com

### Abstract

*The object of our study is the spherical excess and the national geodetic network for the city of Cluj-Napoca. As a proof of the earth's rotundity, many place great reliance upon what is called the "spherical excess," which has been observed on making trigonometric observations on a large scale. The angles taken between any three points on the surface of the earth by the theodolite are, strictly speaking, spherical angles, and their sum must exceed 180 degrees; and the lines bounding them are not the chords as they should be, but the tangents to the earth. This excess is inappreciable in common cases, but in the larger triangles it becomes necessary to allow for it, and to diminish each of the angles of the observed triangle by one-third of the spherical excess. In other words, the spherical excess is represented by the difference between the sum of the angles of a spherical triangle and the sum of the angles of a plane triangle. The national geodetic network and the triangulation network represent the fixed points which form the base of all leveling procedures. Considering the distance between the points and the measurements accuracy, the points that form the geodetic network are classified in five categories: first order: the points are situated between 20-60 km, average 30 km, second order: the tips of the triangles are intercalated in the points of first order at distances between 10-20 km, average 15km, third order: the points are situated inside of the triangles of the second order at distances between 5-10 km, average 7 km, fourth order: the points are situated inside of the triangles of the third order at the average distance of 3 km, fifth order: the points are situated inside of the triangles of the fourth order at the average distance of 1.5 km. In our project we are using the points of the third order to determine the spherical excess in the city of Cluj-Napoca.*

**Key words:** spherical excess, spherical triangle, triangulation network, area, correction.

### INTRODUCTION

Distance and azimuthal observations made on the topographic surface between the points of the triangulation network are projected on the reference surface (ellipsoid or sphere of average radius). Thus, the lines which join the points of the triangulation network appear as curves, determining on the reference surface spherical triangles (Munteanu, 2003; Ortelecan and Sălăgean, 2014).

According to spherical trigonometry, a spherical triangle is defined as a figure formed on the surface of a sphere by three great circular arcs (section of a sphere that contains a diameter of the sphere) intersecting pairwise in three vertices. The spherical triangle is the

spherical analog of the planar triangle, and is sometimes called an Euler triangle (Figure 1).

As opposed to the geometric condition in a plane triangle, according to which the sum of its angles is 200 degrees, in a spherical triangle the sum of the angles, unaffected by measurement errors, will be equal to 200 degrees plus the spherical excess (Dima, 2005; Ortelecan, 2006).

In other words, the spherical excess is the amount by which the sum of the three angles of a spherical triangle exceeds two right angles.

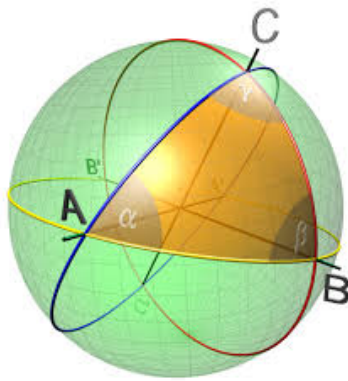


Figure 1. Spherical triangle

## MATERIALS AND METHODS

In order to calculate the spherical excess, we used the triangulation network for the city of Cluj-Napoca and processed the information using a CAD software and Microsoft Excel.

As method, we applied the reduction of the directions to the plane of the Stereographical 1970 Projection. This calculus operation is applied to the azimuthal directions measured in the geodetic triangulation network.

In principle, every direction that is reduced to the reference surface measured between two points will receive a correction  $\delta$ , whose value depends on the length of the sight, orientation and the distance towards the centre of the axis system xOy (Figure 2).

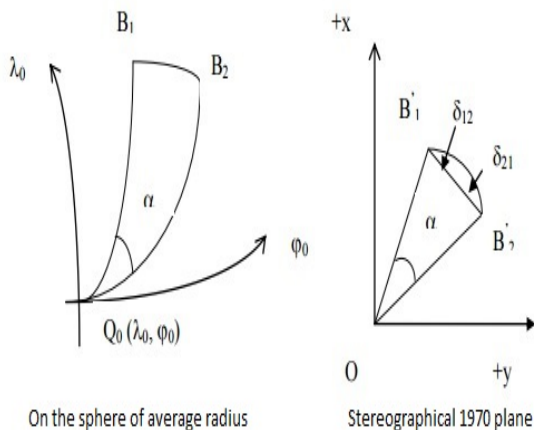


Figure 2. Reduction of the directions to the plane

## RESULTS AND DISCUSSIONS

The general formula for calculating the spherical excess is:

$$\varepsilon = \rho * \frac{S}{R^2}$$

where: S – spherical triangle area;

R – spherical radius.

Other formulas used in this study:

$$S_1 = \frac{1}{2} * \begin{vmatrix} x_1 & y_1 & 1 \\ x_2 & y_2 & 1 \\ 0 & 0 & 1 \end{vmatrix}$$

$$\delta = \frac{\varepsilon}{2}$$

$$\delta_{b-a} = -\delta_{a-b}$$

We picked three points from the triangulation network from our city to exemplify the calculus of the spherical excess regarding the third order points (Figure 3).

Table 1 - The point coordinates

Point number	x	y
40	592373.84	389535.84
42	590814.83	398767.73
47	586465.38	388398.37

Since the correction has small values (seconds or tens of seconds), it is enough to know the S area, with approximation, to calculate it.

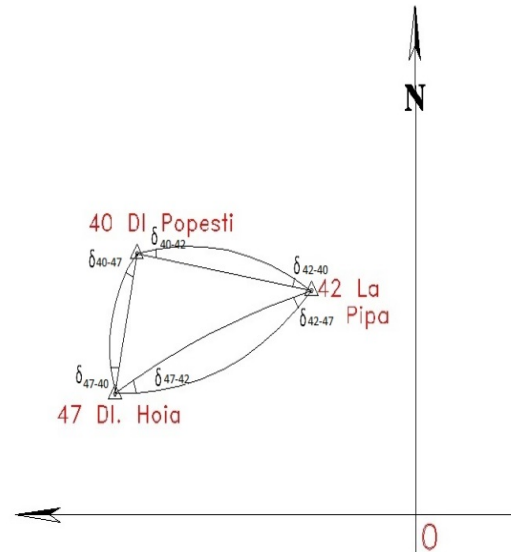


Figure 3 - The points taken into study

So, the spherical triangle area can be replaced with the area of the plane triangle, which we calculate using a determinant that has as elements the coordinates of the tips of the triangle and unity:

$$S_1 = \frac{1}{2} \begin{vmatrix} 592373.84 & 389535.84 & 1 \\ 590814.83 & 398767.73 & 1 \\ 586465.38 & 388398.37 & 1 \end{vmatrix}$$

To calculate the spherical excess, we used the general formula:

$$\varepsilon = 636619.7724 * \frac{28137789.78}{40691087304688.6} = 0.44056525$$

To eliminate the spherical excess, we used the reduction of the directions to the plane of the Stereographical 1970 Projection to calculate the  $\delta$  correction for reduction to the projection plane.

For finding  $\delta_{47-40}$  in  $\Delta 47-40-0$

$$S = \frac{1}{2} * \begin{vmatrix} 586465.38 & 388398.37 & 1 \\ 592373.84 & 389535.84 & 1 \\ 0 & 0 & 1 \end{vmatrix}$$

$$S = 813874728.7$$

$$\varepsilon = 636619.7724 * \frac{813874728.7}{40691087304688.6} = 12.7332243$$

$$\delta_{47-40} = \frac{12.7332243}{2} = 6.366612185$$

For finding  $\delta_{40-42}$  in  $\Delta 40-42-0$

$$S = \frac{1}{2} * \begin{vmatrix} 592373.84 & 389535.84 & 1 \\ 590814.83 & 398767.73 & 1 \\ 0 & 0 & 1 \end{vmatrix}$$

$$S = 3038010200$$

$$\varepsilon = 636619.7724 * \frac{3038010200}{40691087304688.6} = 47.5302453$$

$$\delta_{40-42} = \frac{47.5302453}{2} = 23.7651227$$

For finding  $\delta_{47-42}$  in  $\Delta 47-42-0$

$$S = \frac{1}{2} * \begin{vmatrix} 586465.38 & 388398.37 & 1 \\ 590814.83 & 398767.73 & 1 \\ 0 & 0 & 1 \end{vmatrix}$$

$$S = 2195975681$$

$$\varepsilon = 636619.7724 * \frac{2195975681}{40691087304688.6} = 34.3564557$$

$$\delta_{47-42} = \frac{34.3564557}{2} = 17.1782278$$

Checking rule:

In every triangle which belongs to the geodetic network from the plane of a projection, the sum of the correction for reduction to the projection plane of the three angles of the triangle, should be equal with initial  $-\varepsilon$  spherical excess.

$$-\varepsilon = (\delta_{47-42} - \delta_{47-40}) + (\delta_{40-47} - \delta_{40-42}) + (\delta_{42-40} - \delta_{42-47}) = -0.44056525$$

In our research, we found a particular case in which the correction and the spherical excess is almost null .

Using our data, we found out the following results through the method :

Table 2 - Point coordinates

Point number	x	y
213	588914.72	389913.78
238	583061.97	397113.41
0	500000	500000

$$S = \frac{1}{2} * \begin{vmatrix} 588914.72 & 389913.78 & 1 \\ 583061.97 & 397113.41 & 1 \\ 500000 & 500000 & 1 \end{vmatrix}$$

$$S = 2077019.28$$

$$\varepsilon = 636619.7724 * \frac{2077019.28}{40691087304688.6} = 0.03249536$$

## CONCLUSION

The tolerance with which the checking rule must be satisfied depends on the triangulation order: 0.03'' for the third order triangulation.

As we found out on the direction 213-238-0, the spherical excess is almost null, this happens when the station point, sight point and the origin of the axis are collinear.

## ACKNOWLEDGEMENTS

This research work was carried out with the support of Prof. PhD. Eng. Mircea Ortelecan, Lecturer PhD. Eng. Tudor Sălăgean from the University of Agricultural Sciences and Veterinary Medicine.

## REFERENCES

- Dima N., 2005, Geodezie, Editura Universitat, Petroșani
- Munteanu C., 2003, Cartografiematematică, Editura Matrix Rom, București
- Ortelecan M., Sălăgean T., 2014, Geodezie lucrări practice, Editura Risoprint, Cluj-Napoca
- Ortelecan M., 2006, Geodezie, Editura Academic Pres, Cluj-Napoca

## CADASTRE IN EUROPE

**Alexandra-Maria DAMIAN, Andreea-Maria STANCU**

**Scientific Coordinators: Prof. PhD. Eng. Raluca MANEA  
Assist. Eng. Vlad PAUNESCU**

University of Agronomic Sciences and Veterinary Medicine of Bucharest,  
59 Marasti Blvd, District 1, 011464, Bucharest, Romania

Corresponding author email: alexandram\_damian@yahoo.com

### **Abstract**

*In this presentation we try to make a parallel in terms of systematic and sporadic land registration for three European countries. The countries that we have chosen are England, the Netherlands and Romania. We will discuss about a short history of cadastre, important laws governing land registration, the types of cadastre, the institutions responsible for cadastre in each country and the benefits of land registration.*

**Keywords:** cadastre, law, parallel, type, benefits

### **INTRODUCTION**

A cadastre commonly includes details of the ownership, the tenure, the precise location (some include GPS coordinates), the dimensions (and area), the cultivations if rural, and the value of individual parcels of land. Cadastres are used by many nations around the world, some in conjunction with other records, such as a title register. The cadastre is a fundamental source of data in disputes and lawsuits between landowners. Cadastral surveys document the boundaries of land ownership, by the production of documents, diagrams, sketches, plans (plats in USA), charts, and maps. They were originally used to ensure reliable facts for land valuation and taxation. An example from early England is the Domesday Book in 1086. Napoleon established a comprehensive cadastral system for France that is regarded as the forerunner of most modern versions. Compulsory land registration has existed in England only since 1926, though voluntary land registration started in 1862 and London has had compulsory registration since 1899. There has been a land register for Middlesex (the county next to London) since 1708. 1714. Initially compulsory registration only applied to specified geographical areas but since 1990 it has covered the whole country. Compulsory registration came about following major legal

reforms in 1925. Until 1925 many owners of real estate possessed a tenure called copyhold rather than freehold. Under legislation passed in 1925, copyholds were converted into freeholds and this necessitated the creation of a national register of ownership

In 1810 the introduction of a fiscal cadastre became actual after the earlier mentioned annexation of the Kingdom of the Netherlands by France. The French legislation came into power. Some years before, in 1808, Napoleon Bonaparte, who needed money to finance his activities, decided to establish a system of land taxation, based on an accurate inventory of land use and land ownership, with precise land survey of land parcels: a fiscal cadastre. In 1811 it was decided that also in the occupied Netherlands such a system of land taxation should be introduced. As a consequence, in 1812 the work started to survey the land, and to list users and owners of the land parcels.

The introduction of cadastre and land registry in Romania differ from province to province since the XIX century:

- In Transylvania, Banat and a part of Bucovina was adopted Austro-Hungarian system since 1794 and continue as „Cadastre Concretual” ( it refers at delimitation, description and representation of

limits localities, hydrographic networks and communication routes.

- in Wallachia and Moldavia since 1831, respectively 1832 engineers prepared by Gh.Asachi and Gh.Lazar try to introduce the cadastre.

-in the rest of the country, the cadastre is introduced after the first mondial war.

## **MATERIALS AND METHODS**

In order to characterize the cadastre the following indicators were used: types of cadastre in England, the Netherlands and Romania, legal requirement for registration of land ownership (compulsory or optional), the institutions responsible for cadastre in each country and the land register.

## **RESULTS AND DISCUSSIONS**

### **England**

The responsibility for registering applications relating to land rights including ownership, mortgages, burdens and easements rests on the Land Registry, which is a public Agency of the Ministry for Constitutional Affairs (the Ministry of Justice). The Head of the Land Registry is directly accountable to the Minister. He has extensive judicial powers and he and his staff will determine the great majority of all issues and disputes relating to land rights. The interests registered are guaranteed by the State and those whose rights are registered can be indemnified if they suffer loss through an error or omission on the register. Citizens are free to appeal to the High Court if they wish to challenge the decision of the Registry.

The Land Registry is responsible for keeping and updating the land register, which is open to public inspection. A certificate of registration is issued to each registered owner, or to the lender where the owner has taken a mortgage to buy the property. Each certificate and register incorporates an official plan, prepared by the Registry's staff, which includes the extent of the registered property and any registered rights or burdens. This official plan is based on the largest available scale of the national topographic map published by the Comparative Analysis on the

Cadastral Systems in the European Union 6 Ordonance Survey (the National Survey and Mapping Agency). When an owner seeks to sell or otherwise deal with the land, he uses a copy of his registered title as a proof of his or her ownership or other rights.

The aims of the Land Registry are:

- to maintain and develop a stable and effective land registration system throughout England and Wales as the cornerstone for the creation and free movement of interests in land;
- on behalf of the Crown to guarantee title to registered estates and interests in land for the whole of England and Wales;
- to provide ready access to and guaranteed land information as enabling confident dealings in property and security of title to achieve progressively improving performance targets set by the Lord Chancellor (the Minister of Justice) so that high quality services are delivered promptly and at lower cost to users.

The work of the Registry can be divided into two main areas:

- transactions which create, change or cancel entries on the register. The land register, which is wholly open to public inspection, is constantly updated by the registration of sales of property, associated mortgages and discharges of mortgages. Other registrations relate to the creation of new rights or a mortgage or discharge not associated with a purchase;
- searches and information enquiries. The majority of searches and enquiries are made by those contemplating buying or otherwise dealing with land or lending money on land. These are the essential enquiries made by an intending buyer or lender to ensure that there are no impediments, risks, or unknown burdens affecting the land. Under the English system the issue of an official certificate of search also gives the applicant 'priority' for 30 working days ahead of any other transaction that may arise. This system of protection is greatly valued by purchasers and lenders. A significant number of enquiries will also be made by those who wish to find out ownership and other information about the legal interests in a property. These enquiries could be from tenants, neighbours,

family members, creditors, law enforcement agencies, local municipalities and other official bodies.

The Land Registry has a Head Office in London and 24 regional offices throughout England and Wales. Each of these regional offices serves a defined geographical area comprising a number of municipalities. The Computer Centre is in Plymouth. In each Regional Office the Land Registrar is responsible for maintaining the land register for the region. Under the provisions of the Land Registrations Act the Land Registry must be a lawyer. He or she has extensive judicial powers under the law to grant title and to resolve disputes. Each Regional Registry is managed by an Area Manager who is responsible for finance, personnel, production, and meeting operational and financial Comparative Analysis on the Cadastral Systems in the European Union 22 targets. On average each office serves areas with a population of 2 million and employs in the region of 320 staff.

It is estimated that there are 23 million separate parcels of land of which nearly 20 million are registered. The majority of unregistered properties are government or municipal properties which have not been subject of any sale since compulsory registration provisions became law.

The Agencies responsible for land administration (cadastral) functions in England are:

Table 1.Type of registration system: title registration

	<b>England and Wales</b>
<b>National Mapping</b>	Ordnance Survey
<b>Land Registration</b>	Her Majesty's Land Registry
<b>Land Valuation</b>	Valuation Office
<b>Land Use</b>	Environment, and Agricultural Departments and County and Local authorities

## **The Netherlands**

In the Netherlands there exists one single land registry and cadastre. It comprises all lands, and all territorial waters, whoever is the owner. The main concept of the system of land registry and cadastre is the recording of the relationship between men and land, through a formal right. The State owns land, of course, however from a point of view of the civil code the State is an owner like anybody else. Also the rules for transfer etc. apply to the State, except for paying land taxes. There does not exist something as 'state lands'.

In the Netherlands a system of licensed private surveyors mandated to do the cadastral survey, does not exist. Land registration and cadastral mapping are tasks at national level, assigned by mandate (Civil Code and Cadastre Act) to the Cadastre, Land Registry and Mapping Agency. The Agency comprises a head office and 15 regional offices. In these offices the registers are kept, the boundaries surveyed, maps maintained and information disseminated. Since the merger with the Topographical Service of the Ministry of Defence, now called 'Topographical Service Kadaster', also their offices in Emmen are part of the organisation. However the private sector plays a role in the sense of being contracted to do specific jobs under the supervision and responsibility of the Agency. At date various levels of surveyors have their own association. Senior staff members of the Agency (surveyors, land registrars, managers etc.) are normally member of the Association for Cadastre, which is mainly a labour union type of association.

The land registers and cadastre serve a multipurpose aim. First of all the Civil Code prescribes 4 requirements for a legal transfer of rights 'in rem', namely right of disposal of the seller, agreement between buyer and seller, obligatory title, and recording in the public registers hold by the Agency.

The main concept of the system of land registry and cadastre is the recording of the relationship between men and land, through a formal right. The recording of the relationship men-right-land is based on the recording of notarial deeds. Public registers are registers in

which notarial deeds are recorded as they come in. They are comparable with the land registers kept by the courts in other countries. The public registers are kept in analogue format: books with paper deeds, copied to microfiche. Both cadastral registers and cadastral maps are 100 % in digital format.

Type of registration system: deeds registration.

### **Romania**

Definition of General Cadastre described with Law no. 247/2005 is: "general cadastre is the unitary and compulsory system of technical, economic and legal buildings all across the country; By building means one or more adjacent parcels, with or without construction belonging to the same owner, The means the area of land plot with the same category of use, out of the general cadastre system is meant for the entry in the realty advertising."

Today cadastre is an information system for all land and real estate, regardless of their destination and the owner. It consists of the general cadastre and special cadastres, called today and domain specific information systems. Thenationally efforts made by introducing general cadastre, program that is running today. Looking to the future introduction is a necessity and will depend on European policies or other state cadastre trend. Since 2004 established The National Agency for Cadastre and Land Registration (ANCPI), a public institution, which has as a priority the development and improvement of an effective registration system throughout the country, according to European standards. The goal for this institution, in the future, is to develop a complex computerized database, unitary, but also accessible and easy to maintain in the field of cadastre and real estate publicity. The agency has the authority, at the county level, of 42 cadastre and land registry offices (OCPI), local of 132 cadastre and land registry offices (BCPI) and the National Centre for Geodesy, Cartography, Photogrammetry and Remote Sensing (CNGCFT).

ANCPI developed a centralized application for managing real estate in Romania called "eTerra", which provides spatial data standardization at national level in terms of

land and buildings, creating a uniform and consistent database [2].

The data obtained and provided from ANCPI are important since this is used by the local government, in the real estate and the national and international business. By developing the "eTerra" application, data will be accessible online through the geoportal. The geoportal will be developed by ANCPI based on ESRI technology [2].

Licensed private surveyors can perform works in cadastre, geodesy and cartography in Romania, with a certificate of authorization issued by ANCPI. It is issued on the basis of an examination organized by ANCPI.

The main conditions that applicants must fulfill are specialized studies and experience in performing specific work field. To complete the work the authorized surveyors are contacted and paid by the owners, based on a tax free negotiations. Most specific, they perform measurements and technical work necessary to register : the ownership of a property unregistered in the Land Registry, peel off a building , adding two or more buildings with common borders , modification of the property , modification of the real estate. The works performed are subject to approval by ANCPI through OCPI, according to the Regulation on the approval, verification and acceptance of specialized works in cadastre , geodesy , topography and cartography. In case of registration in the Land Registry of juridical acts and deeds, authorized persons drawn cadastral documentation which are approved by the regional offices subordinate to ANCPI.

Type of registration system: deeds registration

### **CONCLUSIONS**

In this paper work we try to illustrate that The Netherlands, Romania and England have a very different system of cadastre. As we seen, it is not correct to say that the UK does not have a cadastre. Rather what it has are two types of cadastre that fulfil very specific functions. What the UK does not have is a general cadastre. These two types of cadastre are those for agricultural land and for real estate taxes. They have been created to enable

the government to fulfil specific functions. On the other hand, Romania has general cadastre and also special cadastre.

Another difference that we can see is that in The Netherlands a system of licensed private surveyors mandated to do the cadastral survey does not exist, which is not valid for Romania. Here are private surveyors licensed by ANCPI or OCPI.

As a resemblance, we can see that in these three countries the land registration is kept by a Head Office, which has in subordination Regional and Teritorial Offices, each one of them responsible for a specific area.

In conclusion, except the differences, cadastre benefits are the same in all three countries: security of real estate transactions, provide information about property(mortgage,

property rights), informations about the owner.

## **ACKNOWLEDGEMENTS**

This paper work was carried out with the support of Prof. PhD. Eng. Raluca MANEA and Assist. Eng. Vlad PAUNESCU.

## **REFERENCES**

- Research On Developing 3D Cadastre In Romania ,  
Laszlo Beata, Ana Ciotlaus  
[www.ancpi.ro](http://www.ancpi.ro)  
[www.cadastraltemplate.org](http://www.cadastraltemplate.org)  
<http://www.oicrf.org/>  
John Manthorpe – Comparative study-UK  
[www.fig.net/](http://www.fig.net/)  
<http://www.eurocadastre.org/>

## EVOLUTION OF HIGH SCHOOL EDUCATION IN IALOMITA COUNTY

Andrei Georgian DRAGHICI, Ioana VATRA

Scientific Coordinator: Assoc. Prof. PhD Mihai DORU

University of Agronomic Sciences and Veterinary Medicine of Bucharest, 59 Mărăști Blvd, District 1, 011464, Bucharest, Romania

Corresponding author: email: ady\_yo38@yahoo.com

### Abstract

The paper aims to present the evolution of higher education during the period between 2004-2014 in County Ialomita, including the towns of Slobozia, Urziceni, Fetesti, Tandarei, Cazanesti and Armasesti. It is based on the statistical data provided by the Ministry of Education and Research. During the analyses period, the percent of graduation of the baccalaureate exams has continuously decreased, so that in the year 2004 83,92% of the students had promoted the baccalaureate exams, while in 2014 only 57,06% did.

**Key words:** evolution, high school, graduation, baccalaureate

### INTRODUCTION

The baccalaureate exam is one of the most important exams in a student's life, representing the milestone from the pupil's life to the student's life. Nevertheless, the studies have shown a slight lack of interest from the pupils' part regarding the passing of this exam.

As a result of the research, the year 2004 is represented by the highest percentage of graduation (83.92%) while the year 2014 is represented by the lowest one (57.06%).

### MATERIALS AND METHODS

Story maps use geography as a means of organizing and presenting information. They tell the story of a place, event, issue, trend, or pattern in a geographic context. They combine interactive maps with other rich content-text, photos, video, and audio-within user experiences that are basic and intuitive.

For the most part, story maps are designed for general, non-technical audiences.

Many story maps are aimed at everyone, that is, anyone with access to the Internet and a

curiosity about the world. However, story maps can also serve highly specialized audiences.

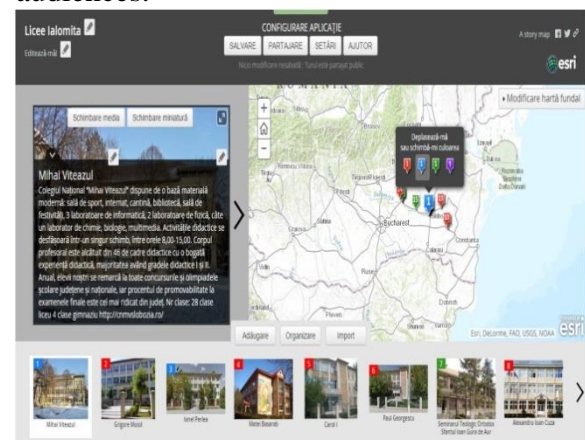


Figure 1

They can summarize issues for managers and decision makers. They can help departments or teams within organizations to communicate with their colleagues.

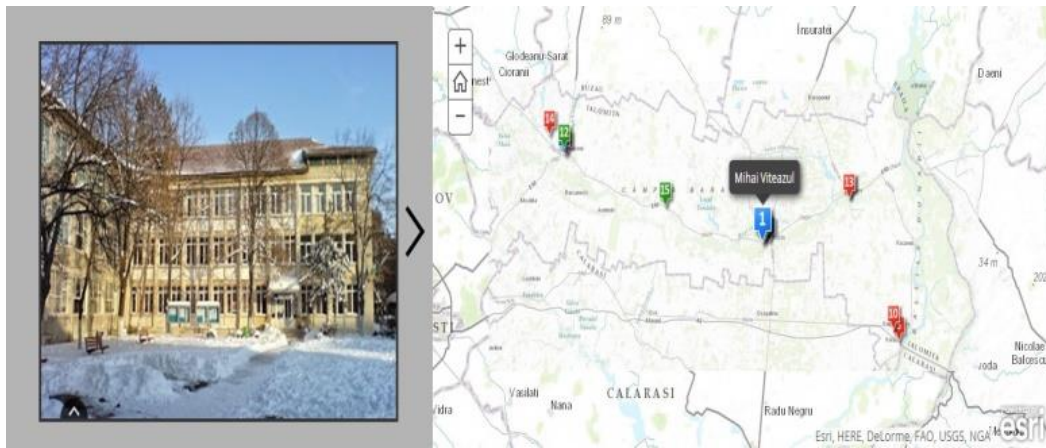


Figure 2

Although story maps can incorporate analytical tasks, they are not intended to do the heavy lifting of geographic information systems. They use the tools of GIS, and often present the results of spatial analysis, but don't require their users to have any special knowledge or skills in GIS. Story maps use interactive web maps created with ArcGIS Online, Esri's cloud-based mapping and GIS

system. ArcGIS web maps let you combine your own data, including spreadsheets and GIS data, with authoritative content and thematic maps from Esri and the GIS community, on top of our beautiful base maps. The web maps support visualization, queries, analytics, and pop-ups for map features with rich content including photos and graphs.

ID	Name	Address	City	Zipcode	description	thumb_URL	pic_url	School_Type	Lat	Long
1	Mihai Viteazul	Bulevardul U Slobozia		920022	<a href="http://cnmv.https://lh3.gichttps://lh3.goc">http://cnmv.https://lh3.gichttps://lh3.goc</a>			Colegiu National	44.56455	27.35444
2	Grigore Moisil	Strada Teilor Urziceni		925300	<a href="http://www.https://lh3.gichttps://lh3.goc">http://www.https://lh3.gichttps://lh3.goc</a>			Colegiu National	44.71182	26.64813
3	Ionel Perlea	Strada Mihai Slobozia		920093	<a href="http://www.https://lh5.gichttps://lh5.goc">http://www.https://lh5.gichttps://lh5.goc</a>			Liceu de Arte	44.5642	27.37661
4	Matei Basarab	Bulevardul M Slobozia		920031	<a href="http://www.https://lh6.gichttps://lh6.goc">http://www.https://lh6.gichttps://lh6.goc</a>			Liceu Pedagogic	44.56342	27.35409
5	Carol I	Strada C?i?ra Fete?ti		925150	<a href="http://ltcaro.https://lh5.gichttps://lh5.goc">http://ltcaro.https://lh5.gichttps://lh5.goc</a>			Liceu Teoretic	44.39079	27.84106
6	Paul Georgescu	Strada ?tefan ??nd?rei		925200	<a href="http://scoli.https://lh5.gichttps://lh5.goc">http://scoli.https://lh5.gichttps://lh5.goc</a>			Liceu Teoretic	44.63822	27.6637
7	Seminarul Teologic O	Strada Alexar Slobozia		920025	<a href="http://www.https://lh6.gichttps://lh6.goc">http://www.https://lh6.gichttps://lh6.goc</a>			Liceu Teoretic	44.56366	27.35914
8	Alexandru Ioan Cuza	Strada Lacul Slobozia		920024	<a href="http://www.https://lh6.gichttps://lh6.goc">http://www.https://lh6.gichttps://lh6.goc</a>			Liceu Tehnologic	44.57023	27.35836
9	Sffnta Ecaterina	Strada Pandi Urziceni		925300	<a href="http://www.https://lh6.gichttps://lh6.goc">http://www.https://lh6.gichttps://lh6.goc</a>			Liceu Tehnologic	44.71527	26.6406
10	Liceul Tehnologic de I	Strada Sirene Fete?ti		925150	<a href="http://gsiaf.https://lh6.gichttps://lh6.goc">http://gsiaf.https://lh6.gichttps://lh6.goc</a>			Liceu Tehnologic	44.41132	27.82019
11	Mihai Eminescu	Strada Lacul Slobozia		920024	<a href="http://www.https://lh6.gichttps://lh6.goc">http://www.https://lh6.gichttps://lh6.goc</a>			Liceu Tehnologic	44.56875	27.36107
12	Liceul Tehnologic?Ur	Strada Buz?u Urziceni		925300	<a href="https://www.https://lh6.gichttps://lh6.goc">https://www.https://lh6.gichttps://lh6.goc</a>			Liceu Tehnologic	44.72432	26.63873
13	Liceul Tehnologic???	Strada Fete? ?nd?rei		925200	<a href="http://www.https://lh3.gichttps://lh3.goc">http://www.https://lh3.gichttps://lh3.goc</a>			Liceu Tehnologic	44.6387	27.66218
14	Iordache Zossima	Arm?e?i		927030	<a href="http://www.https://lh6.gichttps://lh6.goc">http://www.https://lh6.gichttps://lh6.goc</a>			Liceu Tehnologic	44.74694	26.58609
15	Liceul Tehnologic C?	Strada G?rii C?z?ne?ti		927065	<a href="http://www.https://lh3.gichttps://lh3.goc">http://www.https://lh3.gichttps://lh3.goc</a>			Liceu Tehnologic	44.62522	27.0024

Figure 3

## RESULTS AND DISCUSSIONS

The graduation of the baccalaureate exam has continuously decreased from 83.92% in 2004 to 57.05% in 2014 and it has mostly been caused by the measures taken to fight fraud in

the organization and unfolding of the baccalaureate exam, stated the Minister of Education, Daniel Funeriu, for Mediafax. Above 55% of high school graduates in Ialomita who enrolled in the baccalaureate

exam in summer succeeded in passing the exam of maturity.

The percentage is lower than the one in the last years but the representatives of the School Inspectorate state that most of those who have failed the exam are from previous generations and that 60% of the candidates from the current series succeeded in passing the exam of maturity.

The College “MihaiViteazul” is on the first place with a percentage of 92.99%, The Theological Seminar “St. IoanGura de Aur” is on the second place with 88.89% (but with 100% from the current series) and the Art High School “IonelPerlea” is on the third place with 85.10%.

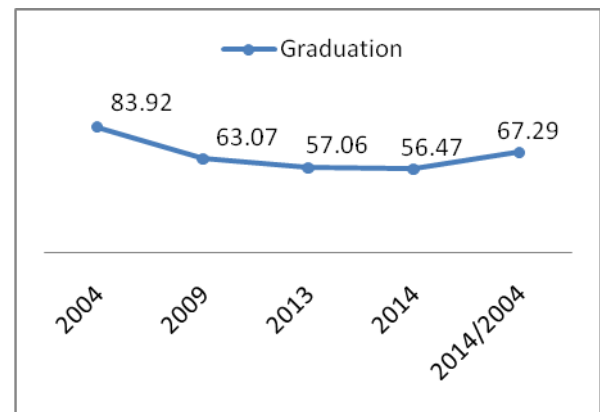


Figure 4. Evolution of graduation

At the opposite end there are the high schools from Grivita, Cazanesti, Mihail Kogalniceanu and Technologic Urziceni, where none of the candidates passed the exam.

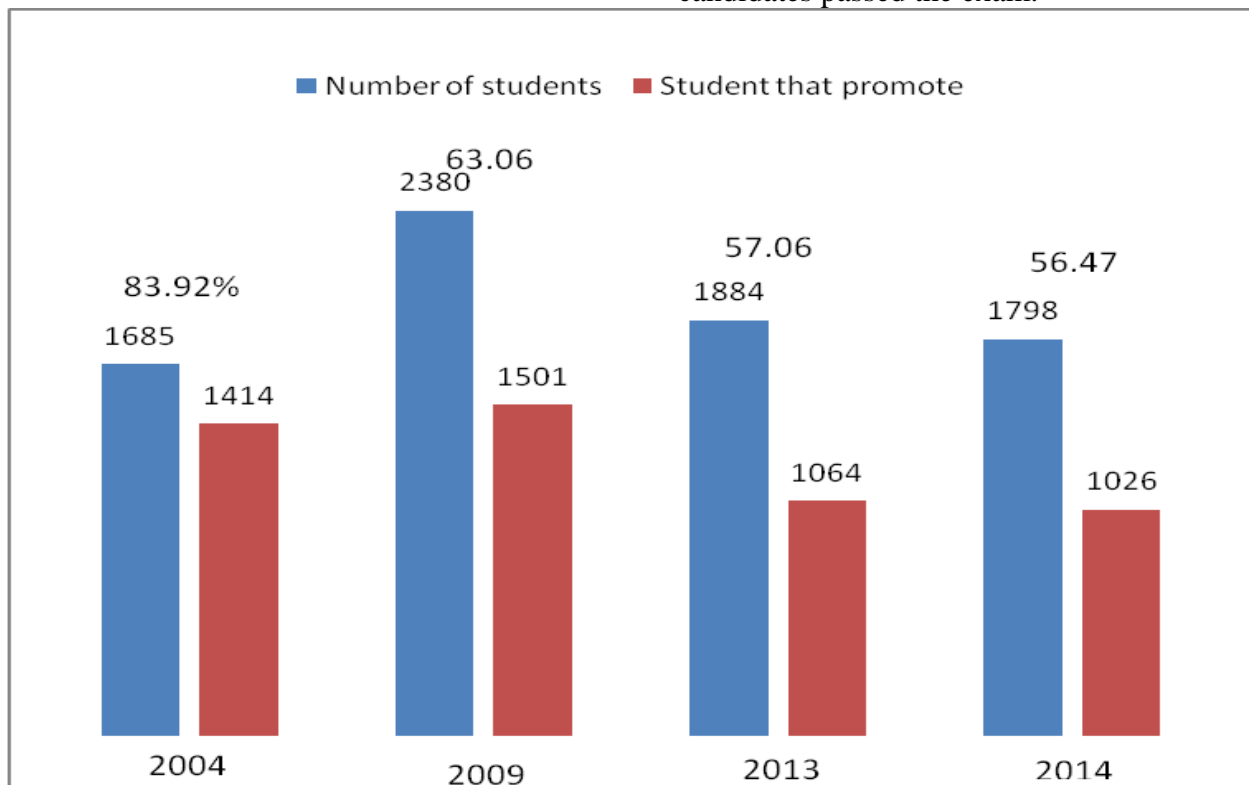


Figure 5. Statistic data

## CONCLUSIONS

The results of the baccalaureate exam have decreased because of the lack of vigilance from the supervisors' part and of the new regulations regarding the introduction and usage of the surveillance cameras but especially because of the students' lack of interest. The increased difficulty has also been an impediment in the graduation of the exam.

## REFERENCES

[www.arcgis.com](http://www.arcgis.com)  
[Bacalaureat.edu.ro](http://Bacalaureat.edu.ro)  
<http://www.isjialomita.ro/>  
<http://cnmvslobozia.ro/>  
<http://www.ltgm.ro/>  
<http://www.licped.ro/>  
<http://scoli.didactic.ro/liceul-teoretic-paul-georgescu-tandarei>  
<http://www.sfec.ro/>  
<http://www.grupscolartandarei.ro>

## ESTIMATING DEFORMATIONS OF GIURGIU-RUSSE BRIDGE SUPERSTRUCTURE USING ANALYTICAL PHOTOGRAMMETRY

Alina DUMITRU, Andra Maria DINOIU

Scientific Coordinator: Assoc. Prof. PhD. Eng. Gabriel POPESCU

University of Agronomic Sciences and Veterinary Medicine of Bucharest, 59 Mărăști Blvd, District 1, 011464, Bucharest, Romania, Phone: +4021.318.25.64, Fax: + 4021.318.25.67

Corresponding author email: alinadumitru1510@yahoo.com

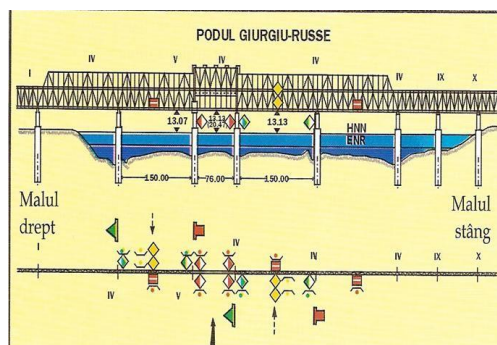
### Abstract

The main objective of the project is estimating deformations of Giurgiu-Russe bridge superstructure using analytical photogrammetry. The results of the observations help us to establish what is the deformations state of the bridge, and what kind of subsides can appear over the years. There are two methods for measurement of the subsides through photogrammetry: main time base and main real space base. Measurements were realized using a terrestrial photogrammetric camera UMK 10/1318 and digital processing was achieved using the relationships of the parallax differences in every superstructure pursuit mark.

**Key words:** bridge, Danube, deformations, photogrammetry.

### INTRODUCTION

The Friendship Bridge Giurgiu Russe is a steel bridge which connects Romanian south shore and Bulgarian north shore. The bridge was built with the aid of the Soviet Union (URSS). Also, the Soviets named “Friendship Bridge”, but after communist regimes fell (in the both countries), the bridge got the functional name “Danube Bridge”.



Picture 1. Giurgiu Russe bridge

The bridge is located 1 km downstream of Giurgiu and 4 km downstream of Ruse and it crosses the Danube at 489 kilometers from its shedding mouths. The construction began in 1952 and it was opened two years and a half later, in June 1954, designed by V. Andreev and N. Rudomazin. The bridge is 2.8 km long, and was the first bridge over the Danube (between

Romania and Bulgaria), it has two decks: a railway and a two-lane motorway. The central part is mobile and can be lifted for some types of boats.



Picture 2. Giurgiu Russe bridge

Photogrammetry can register objects and phenomena in a given time period and find a very good grounding in resolving the various problems in the field of scientific and engineering research. Exact reproduction of the objects photographed, new possibilities for automatic printing and using electronic computers offers certain advantages of photogrammetry for solving many technical cases from all sectors of the economy. Currently, in the world there is a wide range of highly technical methods for measurement of three-dimensional deformations, starting with

classical and terrestrial photogrammetry reaching interferometric chips.

In a three-dimensional image photogrammetry metric of an object can be obtained from two two-dimensional photos following the mathematical relationships of Photogrammetry. There are two principle methods of measurement of deformations using photogrammetry, namely:  
 the principle of the time (presented by Ed Dauphin and k. Torlegard)  
 the principle and actual space base (presented by John Adler).

## MATERIALS AND METHODS

In this paper we present the photogrammetric principle and the results obtained from the monitoring of traffic under deformations obtained from monitoring under the traffic bridge over Danube superstructure deformations from Giurgiu-Russe using real space base principle.

Photogrammetry observations have been performed with Chamber 10/1318 UMK on ORWO WP18, WP20 boards. For coverage of every openings of stereoscopic bridge have been marked on the ground 10 shooting stations (mid-firm upstream and 5 downstream of the bridge) and have picked up 16 adapters (pair) stereoscopic independent (8 for uploading static and 8 dynamic for uploading). In total for the studied area were made 40 normal shooting stations and were 64 ORWO boards.

On bridge's metal deck on the railway and road between 12 and 16 cells at the intersection of the diagonals and pillars outside with upper and lower of the beam were marked and the rivets encoded and scarce fuel were marked dotogrammetrics landmark. Shooting was executed simultaneously in the base heads for tracing deformations of the bridge under traffic and periodically to track the phenomenon of consolidation. Each stage of deformation is recorded progressively researched deck per couple stereoscopic independently.

The system used allows the operation of ON LINE and OFF LINE, program modules written in language Basic and Pascal (Turbo version) working under the MS-DOS operating system.

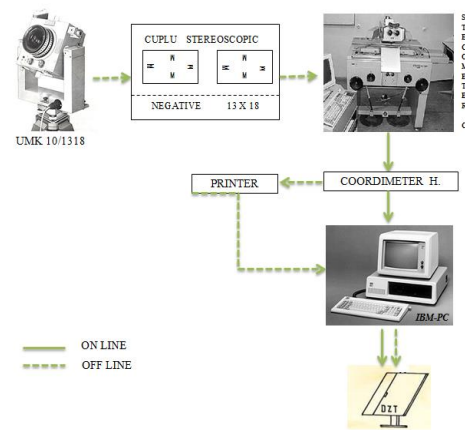


Figure 1. Operating system

## RESULTS AND DISCUSSIONS

Determine the behavior of the bridge during numeric was done by measuring the numerical Stecometru C image coordinates ( $x_D'$ ,  $x_S'$ ,  $px_S$ ,  $z'S'$ ,  $pz_S$ ) for static and load condition ( $x_D'$ ,  $px_D$ ,  $z'd$ ,  $pz_D$ ) for loading dynamic status.

Variation deformations in  $D_{xi}$ ,  $D_{yi}$ ,  $D_{zi}$  may be expressed simply by measuring the horizontal and vertical parallax on stereomodel successive requests. Because these can differ from Parallax couple to another just because of the change of the form of the deck's bridge subjected to loads, they are called parallax and deformation.

The value of three-dimensional deformations were obtained with the following relationships (1):

$$DX_i = b * \left( \frac{X'_D}{PX_D} - \frac{X'_S}{PX_S} \right)$$

$$DY_i = b * f * \left( \frac{PX_S - PX_D}{PX_S * PX_D} \right)$$

$$DZ_i = b * \left( \frac{Z'_D}{PX_D} - \frac{Z'_S}{PX_S} \right)$$

Where:

$$Z'_D = Z'D' + PZD;$$

$$Z'_S = Z'S' + PZS;$$

Relationships (1) shall be valid only for the normal case of shooting because they are deduced from the relationships (2):

$$\left( \frac{X'}{PX} \right)$$

$$X_i = b * \quad ;$$

$$\left(\frac{f}{pX}\right)$$

$$Y_i = b * ;$$

$$Z_i = b * \left(\frac{Z'}{pX}\right)$$

Similar can be found for cases diverted obtaining other formulas for  $D_{xi}$ ,  $D_{yi}$ ,  $D_{zi}$  but error's ellipsoids studied points are higher than in normal shooting cases.

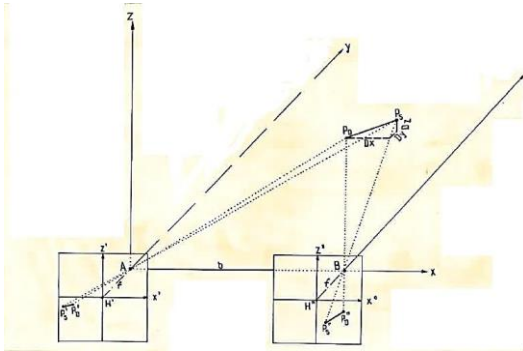


Figure 2. Coordinate systems

Accuracy of determining deformations of the deck's bridge through this method depends on the measurement errors of image coordinates from stecometru or from other stereocomparator precision guidance inner errors (main point position to the point of fotograma and middle focal length) obtained from the calibration of digital photogrammetric camera and precision measurement of the shooting.

Through the differentiation of (1) the precision of the method presented:

$$m_{DY} = \pm \sqrt{2} * \frac{Y^2}{b * f} * m_{PX}$$

Because the accuracy of the analysis and the  $D_{yi}$   $D_{xi}$  average twice as great result:

$$m_{DX} = m_{DZ} = m_{DY} / 2$$

The total average error occurred in a car chase between two successive phases:

$$M_D = \pm \sqrt{m_{DX}^2 + m_{DY}^2 + m_{DZ}^2}$$

Estimation of deformations the superstructure of bridges using analytical photogrammetry

In view of ensuring a very high accuracy in the determination that can occur at both the infrastructure and the superstructure of the bridge, was imposed as a necessity to use analytical photogrammetry and State of the art electronic computing.

Photogrammetric field observations were made with Zeiss Photheo 1318\19 and 10\1318

UMK camera, photographing the ORWO T01 and plates WP18.

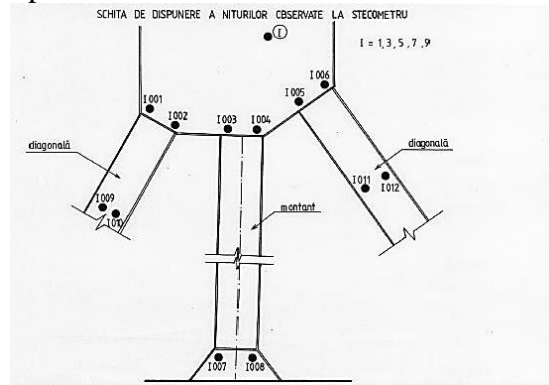


Figure 3

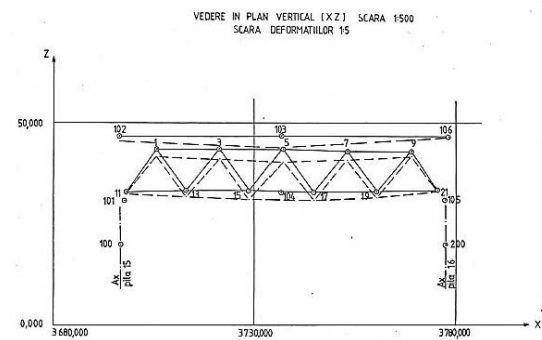


Figure 4

If we want to the superstructure's surveying of the bridge, the base and shooting distance must be choose while abiding by the rule of Gruber:

$$m_b = c * \sqrt{m_k}$$

where:

„mb” represents the scale denominator photogrammetric

„mk” represents the scale denominator that we want to get the plane

„c” is a constant and can take the following values:

$$C=150 \text{ for } 1:mk \geq 1:500$$

$$C=185 \text{ for } 1:mk \leq 1:100$$

In the relation  $1/mb=f/Y$  follows the shooting distance  $Y=f*mb$

The suport geodesic microtriangulation established of concrete depth pilasters outside the zone of influence; there were 10 shooting stations, 5 bridge upstream and 5 downstream from the bridge, which were determined in the local projection coordinates of the bridge, using precision apparatus, "WILD T3", electrooptic

tachometric "EOT 2000" and the level of compensation, the "Ni 007".

On the deck of the bridge between the metallic fuel cell no. 15 and 16 were at the intersection of the diagonals of the pillars with top flange of the beam and the bottom flange were marked with white paint rivets (bolts) that were subject to the comments fotogrammetrics. Also have scored fotogrammetric's landmark on bridge infrastructure, respectively at the base and crest cells No. 15 and 16.

They considered two different ways for the implementation of the phenomenon, the first is a less precise method that takes into account all the determinations of locating errors and the second procedure is strictly photogrammetric, the observations obtained with a high degree of confidence.

Determination of the reaction of the bridge in operation through the first process was done by measuring the numerical, Stecometer, C' and display on, Coorimeter, H' image coordinates in  $x', px', z', pz'$ . for rest and dynamic loading condition and the calculation of spatial coordinates spațiale  $XiF, YiF, ZiF$  socket of all characteristic points and landmark on the superstructure and infrastructure of Giurgiu-Russe bridge.

For photogrammetric coordinates were used the following relationships:

$$XiF = b \frac{x_i}{px_i};$$

$$YiF = b \frac{y_i}{py_i};$$

$$ZiF = b \frac{z_i}{pz_i};$$

where:  $Z'i = z_i' + pz_i$

The transition from model coordinate system to the geodetic coordinates has been done with the help of roto-translation, using the relations:

$$XiG = A0 + A1XiF + A2YiF + A3ZiF$$

$$YiG = B0 + B1XiF + B2YiF + B3ZiF$$

$$ZiG = C0 + C1XiF + C2YiF + C3ZiF$$

For more accurate assessment of the deformations which appear on the three axes of the coordinate-addressed a method which takes into account only the error of determining the focal distance ' f ' obtained from calibration Chamber, the error of determining the base "b" shooting and scoring errors at Stecometer.

The variation  $\Delta Xi, \Delta Yi, \Delta Zi$  may be expressed by measuring parallaxes' s on rest stereomodel

and successive requests stereomodelul. Deformations value has been obtained with the following relations:

$$\Delta X = b \left( \frac{x_s}{px_s} - \frac{x_R}{px_R} \right);$$

$$\Delta Y = b \frac{f}{px_R \cdot px_s} \left( \frac{px_R - px_s}{px_R \cdot px_s} \right);$$

$$\Delta Z = b \left( \frac{z_s}{pz_s} - \frac{z_R}{pz_R} \right)$$

Where:

$$Zs' = z_s' + pz_s ;$$

$$ZR' = z_R' + pz_R ;$$

$$R = S;$$

$$S = D$$

Accuracy of determining the spatial coordinates depends on the measurement errors of  $x', z'$ , and parallax  $px, pz$ , inner guidance elements (main point position to the point of photogram and middle focal length) obtained from the calibration of digital photogrammetric camera and measuring of the shooting.

Because we want the influence of measurement errors be minimal, the foundations have been measured on the ground with the accuracy of 1/100 000.

Since the measurements were made at stecometer C with a mean quadratic error of 0,002 mm, accuracy of spatial coordinates for obtaining photogrammetric obtained by differentiation of relations 1 is as follows:

$$m_y = \frac{Y}{bf} mp = \pm 4,4 mm ;$$

$$m_x = \frac{Y}{f} mx' = \pm 0,7 mm ;$$

$$m_z = \frac{Y}{f} mz' = \pm 1,0 mm$$

where:

$$mx' = 0,002 mm$$

$$mz' = 0,002\sqrt{2} mm$$

$$mpx = 0,002 mm$$

Total error obtained for calculating coordinates is:

$$M_m = \pm \sqrt{m_x^2 + m_y^2 + m_z^2} = \pm 4,6 mm$$

Finally the geodetic coordinates will be affected also by locating error, which in the case of the present work is  $\pm 0,050 m$ . Not satisfied of the accuracy of methods we resorted to the second detailed photogrammetric method.

Through the differentiation of relations (3) we obtained formulas for calculating the reliability for the second method:

$$m\Delta y = \pm \sqrt{2 \frac{y^2}{b^2} mp} = \pm \sqrt{2} \frac{(70.000)^2}{11294 \cdot 195,07} 0,002mm = \pm 0,13mm$$

Since x and z movements accuracy is on average twice as high (Ben Adler) yields:

$$m\Delta x = m\Delta z = 2m\Delta y = \pm 0,26mm$$

The overall average error detrminare of deformațiilor is:

$$Md = \pm \sqrt{m_{\Delta x}^2 + m_{\Delta y}^2 + m_{\Delta z}^2} = \pm 0,4mm$$

Table 1

Bridge superstructure fully loaded dynamic									
F=195.07mm		B=11.294m		Couple B03-B02					
Point number	Image coordinate				Model coordinate			Observations	
	x''	z''	Px	Pz	X <sub>f</sub>	Z <sub>f</sub>	Z <sub>f</sub>		
100	100.000	200.000	500.000	500.000	2.2588	4.4062	13.8116	„A” landmark at No.13 cell	
101	103.001	229.610	499.537	500.028	2.3286	4.4101	16.4957	„G1” landmark at No.13 cell	
102	98.728	275.632	499.610	499.981	2.2318	4.4097	17.3323	„G3” landmark	
103	214.048	275.708	499.703	500.898	4.8378	4.4053	17.3323	„G2” landmark	
104	212.241	234.937	499.236	500.914	4.8012	4.4128	16.6466	„G1” landmark	
1	124.368	263.034	498.933	500.210	2.8133	4.4133	17.3216		
3	168.808	263.088	498.978	500.349	3.8208	4.4133	17.3296		
5	213.343	263.144	499.030	500.004	4.8284	4.4148	17.3371		
11	103.249	233.371	499.172	500.043	2.3361	4.4133	16.6391		
13	143.538	236.442	499.184	500.373	3.2932	4.4134	16.6704		
15	190.032	236.487	499.266	500.724	4.2993	4.4312	16.6786		

Table 2

Bridge superstructure fully loaded dynamic									
F=195.07mm		B=11.294m		Couple A02-B02					
Point number	Image coordinate				Model coordinate			Observations	
	x''	z''	Px	Pz	X <sub>f</sub>	Z <sub>f</sub>	Z <sub>f</sub>		
103	199.322	240.170	500.701	500.537	4.3346	4.4823	17.0198	„G3” landmark	
104	200.000	200.000	500.000	500.000	4.6020	4.4883	16.1070	„G4” landmark	
105	314.930	196.134	501.093	499.238	7.2306	4.4787	15.9659	„G3” landmark	
106	319.020	243.217	501.748	498.767	7.3149	4.4729	17.0134	„G6” landmark	
200	317.034	164.983	501.868	499.303	7.2678	4.4718	13.2330	„B” landmark at No.16 cell	
1163	311.725	194.805	501.613	499.276	7.1311	4.4741	15.9194	Landmark on No.16 cell	
3	201.226	229.771	500.037	500.374	4.6313	4.4882	16.7994		
7	246.283	230.294	500.821	499.224	5.6377	4.4812	16.7723		
9	291.274	230.496	500.826	499.231	6.6912	4.4812	16.7633		
15	177.832	201.338	499.299	500.187	4.0976	4.4948	16.1652		
17	222.336	200.869	500.318	499.838	5.1152	4.4930	16.1070		
19	267.234	201.980	500.944	499.323	6.1373	4.4801	16.1112		
21	309.616	202.331	500.626	499.228	7.1153	4.4829	16.1277		

Table 3

F=195.07mm B=11.294m											
Couple B05-B02 and A01-B01											
Point number	Image coordinates (under load)				Image coordinates (rest)				Deformations		
	X''s	Px <sub>s</sub>	Z''s	Pz <sub>s</sub>	X''r	Px <sub>r</sub>	Z''r	Pz <sub>r</sub>	ΔX (mm)	ΔY (mm)	ΔZ (mm)
100	100.000	500.000	200.000	500.000	100.000	500.000	200.000	500.000	0.0	0.0	0.0
101	103.173	499.723	229.603	500.021	103.001	499.537	229.610	500.028	0.0	-1.4	-3.9
102	99.232	500.073	275.633	500.003	98.728	499.610	275.632	499.991	0.0	-4.1	-13.6
103	214.333	500.168	275.638	500.134	214.048	499.703	275.708	500.898	0.0	-4.1	-34.6
104	212.434	499.464	234.922	500.147	212.241	499.236	234.937	500.914	0.0	-1.8	-23.0
1	124.307	499.372	264.988	500.030	124.368	498.933	263.034	500.210	0.0	-3.7	-18.9
3	169.230	499.399	263.040	500.104	168.808	498.973	263.088	500.349	0.0	-3.7	-23.7
5	213.780	499.449	263.100	500.143	213.343	499.030	263.144	500.304	0.0	-3.7	-32.7
11	103.478	499.381	233.371	500.021	103.249	499.172	233.371	500.043	0.0	-1.8	-7.7
13	143.797	499.418	236.417	500.071	143.538	499.184	236.442	500.373	0.0	-2.1	-13.2
15	190.261	499.443	236.442	500.127	190.032	499.206	236.487	500.724	0.0	-2.1	-22.4

Table 4

F=195.07mm B=11.294m

Point number	Image coordinates (under load)				Image coordinates (rest)				Deformations		
	X''s	Px <sub>s</sub>	Z''s	Pz <sub>s</sub>	X''r	Px <sub>r</sub>	Z''r	Pz <sub>r</sub>	ΔX (mm)	ΔY (mm)	ΔZ (mm)
200	300.000	500.000	200.000	500.000	300.000	500.000	200.000	500.000	0.0	0.0	0.0
103	182.490	498.936	275.028	501.206	182.427	499.403	276.090	500.014	0.0	-4.2	-19.7
104	182.969	498.172	234.861	500.661	182.929	498.633	235.351	500.014	0.0	-4.2	-19.3
105	297.893	499.279	231.172	499.727	297.845	499.231	230.903	500.000	0.0	-0.4	-1.7
106	301.985	500.000	278.234	499.232	301.918	499.090	277.472	500.014	0.0	-0.1	-0.4
(rest)											
5	184.189	498.638	263.520	500.035	184.259	498.242	263.080	501.047	0.0	-3.7	-27.9
7	229.178	498.663	263.543	500.020	229.260	499.044	266.686	500.395	0.0	-3.4	-21.6
9	274.166	498.666	263.197	500.020	274.239	499.038	263.475	499.765	0.0	-3.3	-12.6
15	160.786	498.634	236.903	500.001	160.796	497.453	233.193	500.882	0.0	-10.8	-24.8
17	203.460	498.634	236.137	500.001	203.484	498.689	234.777	500.468	0.0	-0.3	-21.3
19	250.133	498.643	236.930	500.020	250.106	499.109	236.931	500.098	0.0	-4.2	-14.7
21	292.532	498.682	237.286	500.020	292.573	498.783	237.376	499.737	0.0	-0.9	-3.3

Table 5

Point number	Image coordinates (under load)				Image coordinates (rest)				Deformations		
	X''s	Px <sub>s</sub>	Z''s	Pz <sub>s</sub>	X''r	Px <sub>r</sub>	Z''r	Pz <sub>r</sub>	ΔX (mm)	ΔY (mm)	ΔZ (mm)
100	100.000	500.000	200.000	500.000	100.000	500.000	200.000	500.000	0.0	0.0	0.0
1001	119.211	499.418	261.744	500.003	119.172	499.574	261.803	499.574	0.0	-1.3	-13.7
1002	120.308	499.418	260.995	500.003	120.280	499.574	261.060	499.574	0.0	-1.3	-13.6
1003	122.797	499.402	260.959	500.017	122.280	499.574	261.030	499.572	0.0	-1.5	-14.3
1004	123.182	499.402	260.954	500.017	122.785	499.574	261.030	499.572	0.0	-1.5	-14.2
1005	125.555	499.427	261.208	500.017	123.165	499.560	261.271	499.572	0.0	-1.2	-13.2
1006	126.645	499.422	261.969	500.017	125.515	499.570	262.053	499.563	0.0	-0.8	-13.5
1007	122.812	499.422	234.780	500.017	126.626	499.529	234.857	499.563	0.0	-0.9	-12.1
1008	123.210	499.434	234.773	500.011	122.803	499.529	234.857	499.561	0.0	-0.8	-11.4
1009	111.641	499.414	249.760	500.011	123.195	499.545	249.602	499.582	0.0	-1.1	-13.1
1010	112.006	499.414	249.512	500.011	111.619	499.545	249.564	499.592	0.0	-1.1	-12.9
1011	134.041	499.414	249.495	500.011	111.986	499.232	249.589	499.953	0.0	-1.3	-13.3
1012	134.397	499.414	249.728	500.011	134.032	499.565	249.035	499.553	0.0	-1.3	-13.0
3001	164.011	499.460	262.053	500.000	134.395	499.599	262.234	499.533	0.0	-1.2	-21.3
3002	165.129	499.460	261.265	500.000	163.970	499.599	261.454	499.086	0.0	-1.2	-21.1
3003	167.467	499.460	261.237	500.037	165.083	499.599	261.440	499.086	0.0	-1.2	-21.8
3004	167.858	499.460	261.213	500.037	167.438	499.611	261.422	499.077	0.0	-1.3	-21.8
3005	169.580	499.460	262.183	500.037	169.558	499.611	262.394	499.077	0.0	-1.3	-22.1
3006	170.696	499.468	262.940	500.031	170.661	499.611	263.151	499.077	0.0	-1.3	-24.7
3007	167.524	499.458	234.792	500.037	167.512	499.535	235.002	499.078	0.0	-0.9	-19.4
3008	169.905	499.458	234.787	500.037	167.903	499.549	235.002	499.078	0.0	-0.8	-19.8

## CONCLUSIONS

Photogrammetry is one of the most accurate methods for determining that a construction slump may suffer. In the example shown, the amount of bridge compaction is micrometric so the bridge superstructure has not undergone major changes.

## REFERENCES

- Popescu G., 2014. Note de curs "Monitorizarea deformării construcțiilor"  
 Popescu G., 2014. Note de curs "Fotogrametrie analitică"

## **TECTONIC PLATES: STUDY OF MOVEMENT AND DEFORMATION - AREA VRANCIOAIA**

**Mihnea Mircea MITRACHE, Georgiana Maria MOTOI, Oana PIELEȘTEANU**

**Scientific Coordinators: Prof. PhD Eng. Cornel PĂUNESCU, Lect. PhD Eng. Gheorghe IOSIF**

Faculty of Agriculture and Horticulture, Str. Libertății, No. 19, Craiova, Romania  
Phone: +40 251 418 475, Email: contact@agrocraiova.ro

Corresponding author e-mail: mihnea@yahoo.com

### **Abstract**

*In this paper we approach the study of tectonic plates, their classification according to their size and phenomena that occur due to movement of tectonic plates. In the content, there is also presented how they formed faults and the classification according to their geometry and genetic. We follow Vrancea's fault behavior through displacements and deformations that occur over time. This study is conducted by placing the parts in strategic objectives, monitoring benchmarks in time through leveling method of geometric means of order 0.*

**Keywords:** plate tectonic, displacements, deformations, Vrancea area.

### **INTRODUCTION**

The globe is divided into continental and oceanic regions, so we can say that the earth's crust has a different structure and development of geological importance.

Tectonic plates: The tectonic plate is a very large piece of crust, the total area of tectonic plates forming the Earth's surface. Earth's crust is divided by several tectonic plates and is divided into three subdivisions:

- Main (macroplates)
- Secondary (mezoplates)
- Tertiary (microplates)

Today it is known that there are seven macroplates:

- North American plate
- South American plate
- Antarctic plate
- Eurasia plate
- African plate
- Indian-Australian plate
- Pacific plate

Geological or tectonic structures are forms of reservoir rocks. Tectonic structures are formed after bending, cracks and other movements on deformations.

The movement is the changing of the spatial position of a point on the surface of land subjected to applications. (I. A. Kosîghin,

1962)

Deformation is the changing of the shape of an object by increasing or decreasing between characteristic points of the pursued object. Crust deformations present various sizes and shapes, they can be very small and very difficult to distinguish, but they also can reach spectacular dimensions. Deformations can be discontinuous, characterized by the fracture plans (disjunctive) and continuous deformation that make up the crease field. Between these two categories there is a continuous transition. (I. A. Kosîghin, 1962)

Tectonic movements. We distinguish four types of tectonic movements (V.V. Belousov – 1948):

Oscillatory movements - are the vertical movements of the earth's crust caused by its lifting and sinking because the crust rises in a place and immerse in another.

Crease movements - are the plastic deformation of the earth's crust, followed by the thinning strata in creases.

Breaking movements - is the formation of fractures or cracks in the earth's crust.

The movements of magma – represent the molten mass which is moving through the earth's crust.

The exogenous factors participate in an important way in the formation of the aspect of

the structure, the morphology and the construction material. Common and continuous interaction of the exogenous and endogenous factors lead to the formation of geological structure which is conditioned by the internal movements and by the internal development of earth, the endogenous factors occupying a leading role. (I. A. Kosîghin, 1962)

Factors influencing crust movements:

After the last ice age, there were changes in the amount of land that have been totally issued and suddenly by the pressure caused by the weight of ice, modifying the steady state of the earth's crust and mantle. Restoring equilibrium state is carried out slowly, with a speed that depends on the viscosity of the magma and hence vertical movements of the earth's crust. (Mircea Rebrisoreanu, 2003)

Plate Tectonics justify the crust's macromovements. The lithosphere consists of several moving plates that float on the asthenosphere. The direction and size of the tectonic plates are different resulting the following phenomena:

Formation of new crust portions it resulting from the divergent movement of the tectonic plates, thus the magma breaks through the asthenosphere to the surface.

The disappearance of portions of the earth's crust is due to mutual converging movements of the tectonic plates, so one of the plates gets into the other.

Shallow Earthquakes are caused by mutual sliding plates, by the shape of some frictions, and they generate the moving of continents and macromodifications in the structure of gravitational field and shape of the geoid.

The action of volcanoes generates displacements and deformations of local character.

Due to natural and anthropogenic factors changes in the upper crust appear and also generates displacements and deformations of local character.

Atmospheric factors are considered secondary factors that generate displacement and deformation of the crust.

Shifts and deformations in the crust along the coasts are due to tide seas.

The factor which is the root of an earth fissure is the earth tide, this it is characterized by raising and lowering the earth's crust under the

action of the Sun and Moon. (Mircea Rebrisoreanu, 2003)

Faults: The common rupture plan of two tectonic compartments after which occurs their displacement, placing them one against the other, constitutes a fault. Faults usually occur in portions under high tension and general layers. (Mircea Rebrisoreanu, 2003)

Geometry of a fault:

Fault plan (P) - is the surface on which the two compartments formed by rock fracture move (Fig. 1);

Direction of the fault (af) - is the line resulting from the intersection of the fault plan with a horizontal plan (Figure 1);

fault direction orientation ( $\delta$ ) - is the angle between the direction of the fault and the geographical meridian (Figure 1);

fault inclination ( $\beta$ ) - is the dihedral angle formed between the fault plan and a horizontal plan (Figure 1);

Jump fault (step or leap) (ab) - is the movement of two points on the two compartments adjacent initially measured on the fault plan (Figure 2).

There are several types of jumps:

- Jump on tilt (ae; SI) - is total jump component is measured on tilt and represents the size of compartments displacement measured along the line of greatest slope of the fault plan;

- Vertical jump (ad; Sv) - is the vertical component of the total jump ;

- Horizontal jump (eb = ac) - is the horizontal component of the jumping on tilt, reflected in the amount of movement in the horizontal plan;

- Stratigraphic jump (Ss) - is the proper movement range of the lithological formations deposit (equal to the stratigraphic thickness of the deposits formed in the "tectonic gap"). (Mircea Rebrisoreanu, 2003).

*Classification of the faults is done by geometric and genetic elements:*

By the angle of the tilt of the fault plan to a horizontal plan:

- inclined faults (fault plan makes with the horizontal plan an angle different from  $0^\circ$  and  $90^\circ$ );

- vertical faults (fault plan makes with the horizontal plan an angle of  $90^\circ$ ).

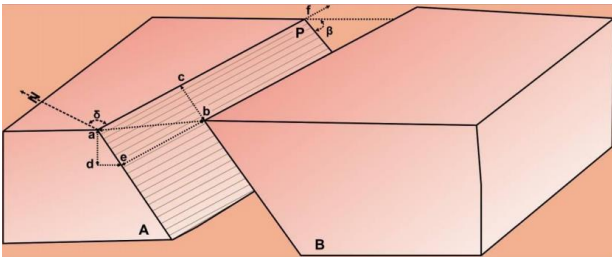


Figure 1. The movement of tectonic compartments in the plane of the fault (block diagram)

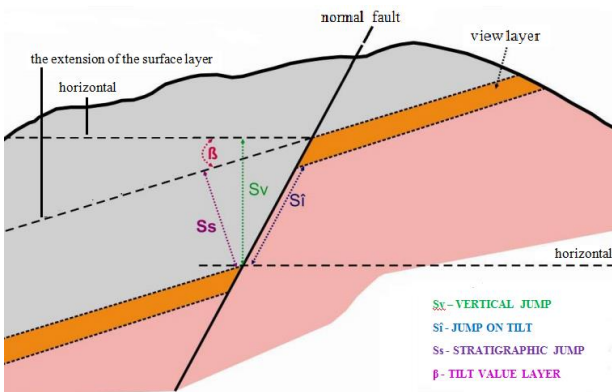


Figure 2. Jump fault (vertical section)

By direction of the movement of the compartment on fault plan:

In the case of inclined faults with vertical jump:  
 - normal faults – the compartment above the fault plan moves downward, gravitational (arising under distension);

- reverse faults - compartments are displaced on fault plan "antigravity" (arising in compressional regime).

In the case of the detachment faults (with horizontal jump):

Transcurrent fault - compartments are moved only horizontally:

- dexter fault - tectonic compartment opposite the observer is shifted to the right;

- senestre fault - tectonic compartment opposite the observer is shifted to the left.

Transforming faults - are horizontally displaced fractures affecting oceanic rifts and usually have a path perpendicular to the rift.

Transforming faults develop in the direction parallel to the Euler networks, as opposed to rifts having a parallel route with their meridians.

By the report of the fault plan tilt and rock layers:

- Comply fault - the fault plan inclined in the same direction as that of the layers without the inclination to have, necessarily, the same value;

- otherwise faults (irregular) - inclined fault plan backward the strata tilt.

After the report of the fault direction and the direction of layers: directional, horizontal and oblique.

After pairing mode of faults in the system of faults (= conjugate faults) - terms derived from cartographic allure: the relay faults, parallel faults, concentric faults, radial faults, etc.

In the case of the faults is observed the thickness increase in submerged compartments and its decrease in high compartments. These variations are of sudden character, in jumps and a more quiet on the wings; they represent an important clue, to be fastened to study faults accurately, because they enable to assess their training period and duration of their formation.

Displacements on faults. There is a close link between folds and faults resulting from the study of various kinds of anticline crease affected by faults. Subduction-related anticline folds develop on their flanks with large tilt exactly where layers were subjected to a high voltage. The amplitude of the faults related to folds in the lower horizons is higher, and in the upper is smaller, so it is established that faulting and folding are just different forms of unique tectonic movements.

The mechanical properties of the rock, depth of the deformation, the deformation speed, etc. presents an important role in the smaller or larger development of faults.

Creases and cover rocks can develop due to lateral movement in basis, and in this case, faulting preceded the folding. Faults on which plan's occurs displacement while increasing wrinkles are syngeneic to the process of folding.

Romania is on three continental tectonic plates whose meeting point is Vrancea area: East European plate, Intra-Alpine subplate and Moesian subplate (Fig. 3). Each of these continental tectonic plates are directly influenced by movements or pressures that confronts plate part.

Strong earthquakes in Romania occur at depths of 60-200 km, they occur at the junction of three tectonic continental plates, they are called subcrustal earthquakes, they have very high energy and are felt over large areas. Shear are produced, determined by the compression, this means that continental plates are pushed

together and one cedes at a certain depth. Breaking is determined by pressure from big land plate movements and by the influences which they have on micro-plates or subplates in Romania. In most cases, earthquakes are tectonic earthquakes, which are the result of sustained movement of lithospheric blocks along newly formed or existing faults in advance. (Liviu Constantinescu, Dumitru Enescu, 1985).

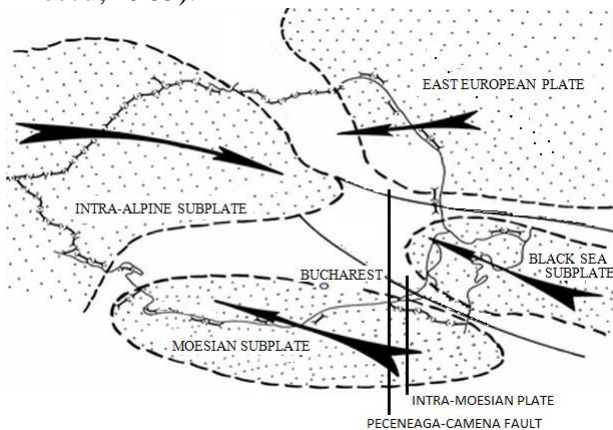


Figure 3. The meeting point of three continental plates (Vrancea)

Romania is tested also by earthquakes at a depth of 5-40 km, which are called between crustal earthquakes and they occur in areas of fault rupture (Mountains Fagaras, Timisoara area, system faults Carei - Oradea fault St. George on the edge of the North Dobrogea etc.). Research in this area has led so far to achieve fault plan solutions for about 100 earthquakes in Vrancea. Most Vrancea intermediate earthquakes are produced by sliding tilt, this being the reverse faulting, earthquakes ie compression. Only in a few cases it is normal faulting earthquakes or transcurent faulting. It was concluded that most of Vrancea earthquakes, especially in the strong ones, null vector direction is parallel to the direction of the Carpathian arc and direction of axis of crease- system. (Liviu Constantinescu, Dumitru Enescu, 1985)

## MATERIALS AND METHODS

In the measurements it was used the reference system the Black Sea 1975. As a method it was present the geometric leveling method by means of order 0, with accuracy of  $\pm 1 \text{ mm}\sqrt{L}$  measured in km and a maximum length of 30 m

portee, and as camera measurements, the NI 007 Zeiss, which belongs to the group of instruments compensating, with pendulum, high precision, together with the following accessories:

- a set of small groom with invar tape series: 50324, 50323;
- two sets of large groom with invar tape series: 26 707, 26 708 and 49 636, 54 686;
- Six leveling bolt weighing about 5 kg each.

Best verification of the equipment used was getting very close level differences between back and forth using the same section:

- the same level and the same set of surveyor's pole;
- same level and different sets of surveyor's pole;
- different levels and the same set of surveyor's pole;
- different levels and different sets of surveyor's pole.

Leveling repeatedly show that any point on the Earth's surface is moving or lifting or diving. Thus it is concluded that vertical tectonic movements on the surface have a general and continuous character. It follows that it is not possible an exact calculation of the influence of measurement errors on the elevation difference which is obtained by comparing the two leveling.

Geometric leveling is known as direct leveling (level difference is obtained from the difference in the readings on the surveyor's pole). It is widely used because of its very good accuracy. It is made with leveling tools called levels. Their axis of sight can be brought into a horizontal position. (Manea Raluca, 2010)

Geometric leveling middle. Leveling goal is to determine the difference in level between two points A and B. On each of the two points there is placed one surveyor's pole in perfect vertical position. Division 0 of the surveyor's pole is at the bottom. Halfway between points A and B are placed leveling tool. (Cornel Păunescu, Ileana Spiroiu, Marian Popescu, Vlad Păunescu).

We consider the meaning of A to B, surveyor's pole located at A is called back surveyor's pole and the surveyor's pole placed in point B the surveyor's pole located in or before. Based on this, we calculate the difference of level that can be positive or negative. The horizontal plan

of the telescope described vial when two surveyor's pole will intersect at a certain height. This horizontal plan is viewed by cross-hair of the level. On perform two readings with the horizontal cross-hair, one on the back surveyor's pole, one on the surveyor's pole located in or before. The reading on the back surveyor's pole is marked with a, and the reading on the surveyor's pole located in or before with b. Considering  $P_0$  as zero datum plan, from point A goes a parallel to this plan. Also, the horizontal plan described by the telescope device is parallel to this plan. (Cornel Păunescu, Ileana Spiroiu, Marian Popescu, Vlad Păunescu).

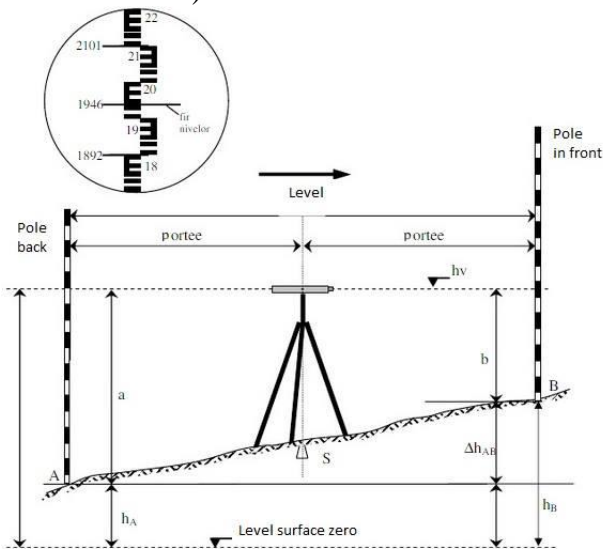


Figure 4. The principle of geometric leveling middle

From Figure 4 it can be seen:

$$\Delta h_{AB} = h_B - h_A \quad (1)$$

Where:

- $\Delta h_{AB}$  level difference between points A and B;
- $h_B$  altitude of the plane  $P_0$  to point B;
- $h_A$  altitude point A to  $P_0$  plan.

Also in Fig. 4:

$$\Delta h_{AB} = a - b \quad (2)$$

A and b are direct readings so it can be calculated the level difference. Knowing the elevation of one of the points, for example, A point, it can determine the share of the other point B of equation (1):

$$h_B = h_A - \Delta h_{AB} \quad (3)$$

Knowing the elevation of point A and having read the surveyor's pole back, we can calculate the altitude of the plan of sight  $h_v$  or height  $i_v$ .

plan. The altitude of the plan of sight (described by the telescope horizontally level) is the vertical distance between the plan and the plan of sight  $P_0$ .

$$i_v = h_A + a \quad (4)$$

Altitude point B resulting from altitude plan targeting:

$$h_B = i_v - b \quad (5)$$

The altitude plan of sight is used when it is desired to determine a large number of points around the level quoted. (Cornel Păunescu, Ileana Spiroiu, Marian Popescu, Vlad Păunescu).

## RESULTS AND DISCUSSION

The section between km.40 + 200 to km.59 + 000 DN 2 D was measured return fully, moreover sections were measured between R 70 and R 72 rappers.

It was intended that tolerance  $T = 1.5 \text{ mm}[\text{km}]$  round-trip between measurements is not exceeded. However, the steep sections due to readings taken at the ends groom to overcome this tolerance. The execution was carried out measurements in both directions so that the interval between the two measurements is minimized. Measurements return on the same section were not always performed by the same operator with the same set of surveyor's pole, or the same device. From this resulted the number of different stations back and forth between these sections. However, the respective sections, level differences between outbound and were within the tolerance. For the measurements was used the coincidence method pointing on the two graduated scales. It is obtained for each direction of measurement two level values difference level between the surveyor's poles placed behind and in front of the camera.

Benchmarks embodying moving points are called work parts and the stable ones - support parts. The total working parts and support parts with which it is followed the evolution of rock movement, is an observation station of displacement. The advantage is that they are stable in the long term and ensure continuously over time.

The landmarks are located both in the study area and they support changes horizontally and vertically but also in areas outside area

considered stable and representing the geodetic reference.

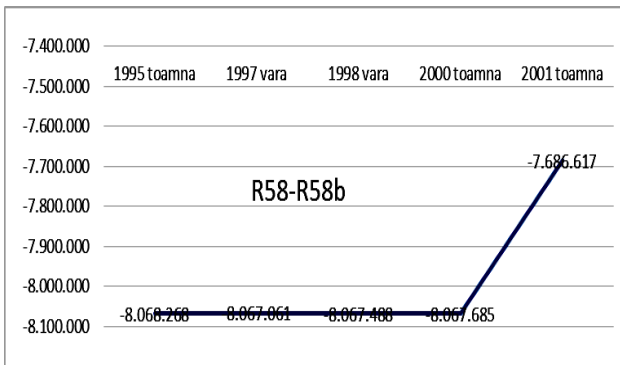


Figure 5. Landmarks behavior R58-R58b (1995 autumn – 2001 autumn)

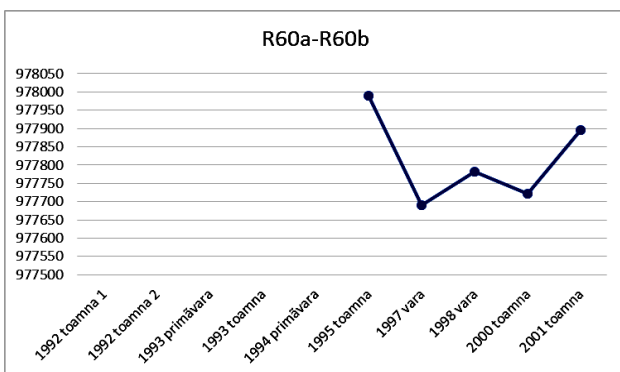


Figure 6. Landmarks behavior R60a-R60b (1995 autumn – 2001 autumn)

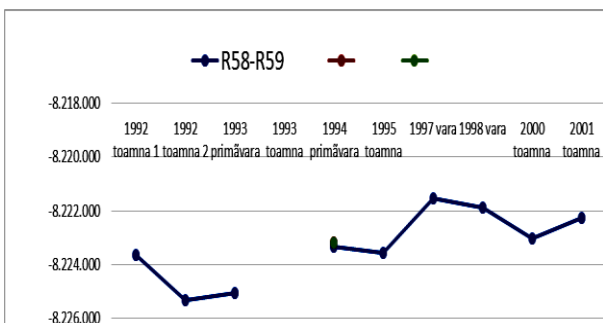


Figure 7. Landmarks behavior R58-R59 (1992 autumn – 2001 autumn)

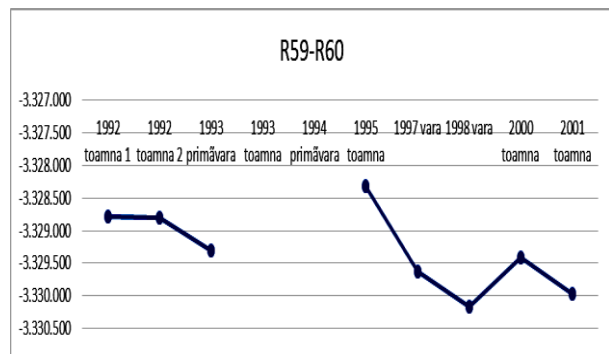


Figure 8. Landmarks behavior R59-R60 (1992 autumn – 2001 autumn)

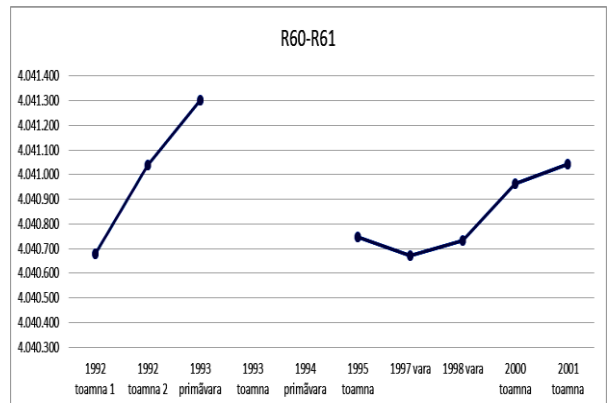


Figure 9. Landmarks behavior R60-R61 (1992 autumn – 2001 autumn)

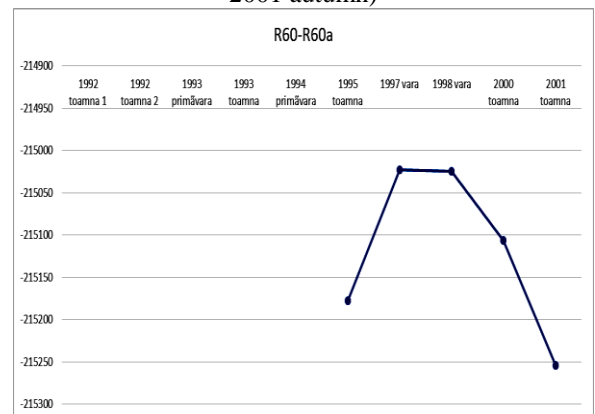


Figure 10 Landmarks behavior R60-R60a

Table 1. SUMMARY TABLE for leveling measurements performed in Vrancea

Landmarks	1992 autumn 1	1992 autumn 2	1993 spring	1993 autumn	1994 spring	1995 autumn	1997 summer	1998 summer	2000 autumn	2001 autumn
R58-R58b						-80.68	-80.67	-80.67	-80.68	-76.87
R58b-R58e						3.82	3.82	3.82	3.81	
R58e-R59						-5.37	-5.37	-5.37	-5.37	-5.36
<b>R58-R59</b>	-82.24	-82.25	-82.25		-82.23338 -82.23173 -82.23173	-82.24	-82.22	-82.22	-82.23	-82.22
R59-R59b						-36.21	-36.22	-36.23	-36.22	-36.22
R59b-R59a						3.43	3.43	3.43	2.93	2.93
R59a-R60						-0.5	-0.5	-0.5		
<b>R59-R60</b>	-33.29	-33.29	-33.29			-33.28	-33.3	-33.3	-33.29	-33.3
R60-R60a						-2.15	-2.15	-2.15	-2.15	-2.15
R60a-R60b						9.78	9.78	9.78	9.78	9.78
R60b-R61						32.78	32.78	32.78	32.78	32.78
<b>R60-R61</b>	X= 40.40678	X= 40.41040	X= 40.41303			X= 40.40746	40.41	40.41	40.41	40.41
<b>R61-R62</b>	0.42	0.42	0.42				0.42	0.42	0.42	0.42
<b>R60-R62</b>	40.82	40.83	40.83			40.83	40.82	40.83		
R62-R62a going							14.64			
R62a-R63 going							5.74			
<b>R62-R63 going</b>	X= 20.38495	X= 20.38491	X= 20.38245				20.38		20.39	20.39
R63-R63a						3.78	3.78			
R63a-R64						-11.86	X= -11.86311			
R63a-R63b							1.52			
R63b-R64							-13.38			
<b>R63-R64</b>	-8.08	-8.08	-8.08			-8.08	-8.08	-8.08		
R70-R70a										
R70a-R71							13.06	13.06		
<b>R70-R71</b>						18.15				
R151-R152a							-39.74	-39.74		
R152a-R152b						-1.23	-1.23	-1.23		
R152b-R152c						-0.09	-0.08	-0.08		
R152c-R153						8.6	8.6	8.6		
<b>R151-R153</b>				X= -32.45428	X= -32.45826 X= -32.46069 X= -32.46162		-32.45	-32.45		
<b>R151-R152</b>				-37.34	-37.34460 -37.34703 -37.34796					
<b>R152-R153</b>				4.89	4.89	4.89				
R153-R153a							23.88			
R153a-R154							17.78			
<b>R153-R154</b>				41.67	41.67		41.66	41.67		
R154-R154a							8.98	8.98		
R154a-R155							-22.86	-22.86		
<b>R154-R155</b>			-13.87	-13.88			-13.88	-13.88		
R155-R155a						-1.09	-1.08	-1.08		
R155a-R155b						4.72	4.72	4.72		
R155b-R156						4.84	4.84	4.84		
<b>R155-R156</b>				8.47	8.47	8.47	8.47	8.47		
R157-R157a							90.31	90.3	90.3	
R157a-R161							3.43	3.43	3.44	
<b>R157-R161</b>				X= 93.74329	X= 93.74348		93.74	93.73	93.74	
<b>R161-R162</b>				-65.09	-65.08		-65.09	-65.09	-65.1	-65.09
R162-R157b						11.94	11.95	11.95	15.1	7.79
R157b-R162a						-4.14	-4.13	3.15		
R162a-R162b						7.29	7.28			7.3
R162b-R162c						-22.28	-22.29	-44.73	-22.29	-22.29
R162c-R163						-22.44	-22.44			34.88
R163-R162d							-17.29	-17.29		
<b>R162-R163</b>				-29.63	-29.64	-29.63	-29.62	-29.62		
R163-R163a							45.78	45.78		
R163a-R163b							11.54	11.54		
R163b-R164							16.61	16.61		
<b>R163-R164</b>				73.94	73.94		73.93	73.93		
R165-R165a							2.99	2.99		
R165a-R165b							-45.55	-45.55		
R165b-R166							-97.66	-97.66		
<b>R165-R166</b>				-140.23	-140.24		-140.23	-140.23		

X = value obtained by calculation and not by direct measurement.

R61 = Landmark built into the wall Hall Barsesti;

R62 = Landmark buried in the schoolyard Barsesti;

R72 = Landmark built into the church wall Tulnici.

## CONCLUSIONS

In this work we determined vertical movements in Vrancea fault zones, Vrancea County. We investigated the vertical displacements and changes before and after earthquakes 13/10/1992 and 23/10/1992 by: "Precision measuring line Focsani - Targu Secuiesc between R 47 and R 70 landmarks". We studied the behavior of Vrancea area over a period of nine years from 1992 to 2001.

In this study we found that this area is active and holds various displacements and deformations by differences in level results over time.

Looking at the real value of movements and deformations were still necessary to monitor the area in order to have a permanent control of

speed, direction and deformations in the study area.

## REFERENCES

- Cornel Păunescu, Ileana Spiroiu, Marian Popescu, Vlad Păunescu - COURSE OF GEODESY – TOPOGRAPHY, Publisher University of Bucharest, Chap 17, p. 71-72.
- Liviu Constantinescu, Dumitru Enescu - VRANCEA EARTHQUAKES IN SCIENCE AND TECHNOLOGY, Publisher Academy Socialist Republic of Romania, Bucharest 1985, Chap. 4, p. 47-57.
- I. A. Koşighin, GENERAL TECTONIC, Publisher Tehnica, 1962, Chap 3, p. 381-382, 399, 422.
- Manea Raluca, GENERAL TOPOGRAPHY – COURSE NOTES ID, Publisher USAMVB, 2010, Chap. 5, p. 56-57.
- Mircea Rebrisoreanu, STRUCTURAL GEOLOGY, Publisher Universitas, Petrosani, 2003, Chap. 5, p.173-192.
- <http://google.imagine.com>

## ROMANIA-THE LAND OF MYSTERY

**Teodora MOTOCESCU, Alexandru MIHALCEA, Dragos DRAGANESCU, Dan MOCANU**

**Scientific Coordinator: Assoc. Prof. PhD. Eng. Doru MIHAI**

University of Agronomic Sciences and Veterinary Medicine of Bucharest, Faculty of Land Reclamation and Environmental Engineering, 59 Mărăști Blvd, District 1, 011464, Bucharest, Romania

Corresponding author email: teodora.motocescu@yahoo.com

### **Abstract**

*In this paper we want to capture the unseen part of Romanian tourism. The haunted places that we are going to talk about, were less publicized and placed in tourist routes, they dating since 13th century. These places belong to the natural environment (forests, hills, ponds) and constructions (castles, monasteries, hotels etc). Due to less developed infrastructure, the Romanian tourism suffers, occupying a slacker place between tourist countries in Europe. Bran Castle is the most visited haunted place in Romania stepping his threshold in 2014 over 560.000 tourists, of which 60% are foreigners. At the opposite is Fire Tower from Bucharest; this museum having no part of so many visitors. However, through this presentations we wish to draw the attention to the willing persons who want to discover something new. In conclusion at this chapter, Romania can be considered a rival. The method by which we want to make known this tourist route is by a StoryMap from ArcGIS Online (www.arcgis.com). In this StoryMap you will find information about address, directions, photos and a short history.*

**Key words:** tourism, Romania, haunted places

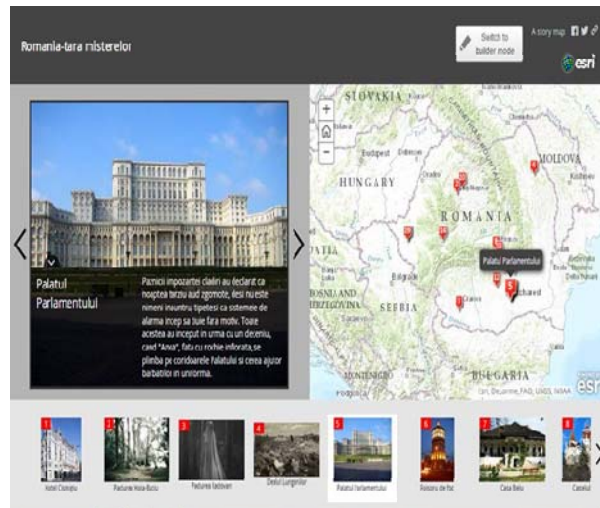
### **INTRODUCTION**

Tourism is an important factor for the development of the country and for people who like adventure. The tourist trail of haunted places in Romania we propose aims to inform and highlighting this places. Who can say that he does not like mysteries? And especially when it comes to places haunted by ghosts, mysterious appearances. Romania has numerous locations. Haunted places caught, always the imagination of all, because of the mystery surrounding them. Often, to attract tourists, castles are advertised as frightening places, with a dark history, from lost prisoners to enemies impaled and ghosts who walk freely in the corridors. Regarding tourism, in 2014 the number of foreigners is

estimated at 1.6 million, they spending in our country up to 755 million euros (0.6% PIB). In Tourism report of European Commission "Trends and Perspectives", in the second quarter of 2014 Romania ranks 10/23 countries in terms of increasing the number of tourist arrivals from Europe.

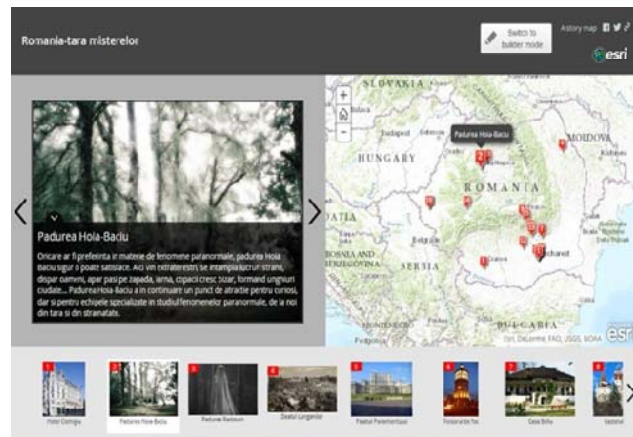
### **MATERIALS AND METHODS**

Story maps use geography as a means of organizing and presenting information. They tell the story of a place, event, issue, trend, or pattern in a geographic context. They combine interactive maps with other rich content - text, photos, video, and audio - within user experiences that are basic and intuitive.



For the most part, story maps are designed for general, non-technical audiences. Many story maps are aimed at everyone, that is, anyone with access to the Internet and a curiosity about the world. However, story maps can

also serve highly specialized audiences. They can summarize issues for managers and decision makers. They can help departments or teams within organizations to communicate with their colleagues.

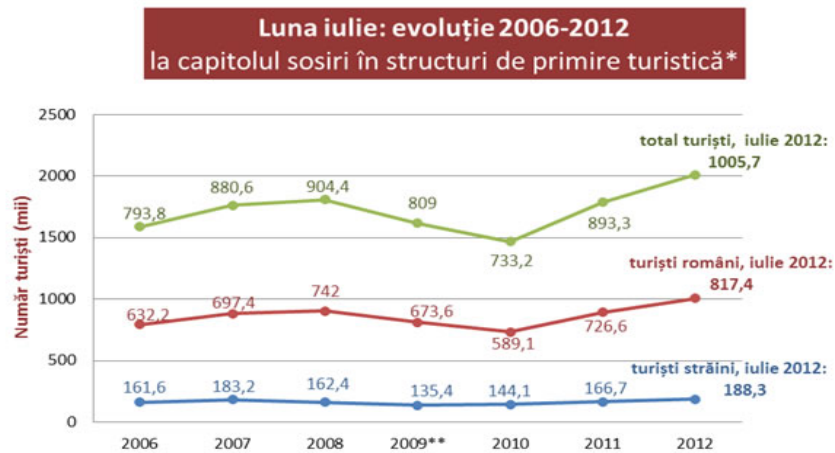


Although story maps can incorporate analytical tasks, they are not intended to do the heavy lifting of geographic information systems. They use the tools of GIS, and often present the results of spatial analysis, but don't require their users to have any special knowledge or skills in GIS. Story maps use interactive web maps created with ArcGIS Online, Esri's cloud-based mapping and GIS

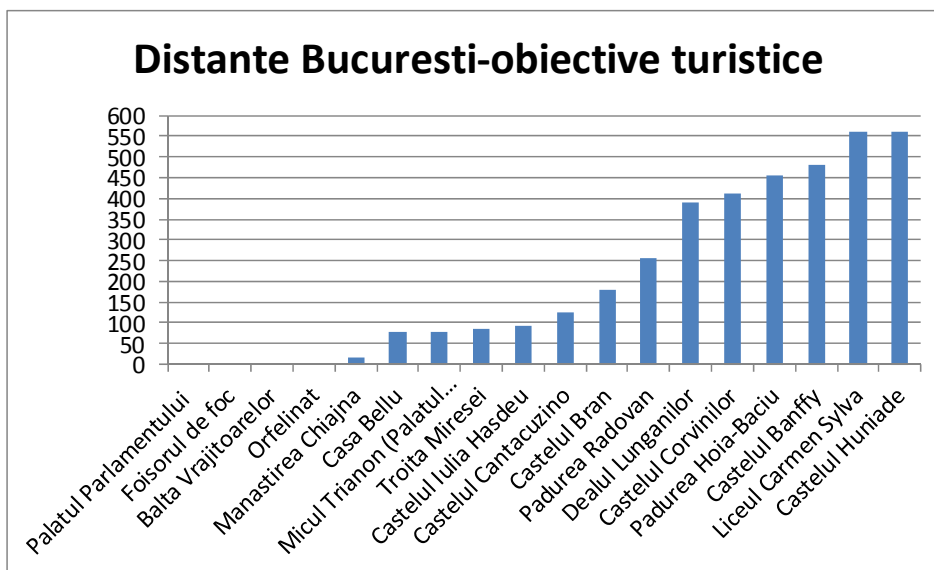
system. ArcGIS web maps let you combine your own data, including spreadsheets and GIS data, with authoritative content and thematic maps from Esri and the GIS community, on top of our beautiful basemaps. The web maps support visualization, queries, analytics, and pop-ups for map features with rich content including photos and graphs.

ID	Name	Address	Latitude	Longitude	Description	pic_url	Thumb_url
1	Hotel Csr Bd. Regiu	44.4351	26.09487	Dupa revch	http://www.lorbes.ro/wp-content/uploads/2012/12/50d193b4bc576-325x350.jpg		
2	Padurea H Cluj-Napo	46.7764	23.3203	Dicare ar	http://sto.http://storage.ons.monteractiv.ro/media/40/52/14006/463060/4/sacuu1.jpg		
3	Padurea R Judetul Di	44.1767	23.62831	Zeci de pe	http://ade.http://adevanul.ro/assets/adevanul.r/MImage/2013/02/13/731b1ef2354a78211834c15a/646x404.jpg		
4	Dealul Lur Comuna L	47.18501	27.1497	Dealul Lur	http://me.http://media.rtv.net/image/2013/01/v466/soldati_04397800.jpg		
5	Palatul Pa Str Izvor n	44.42606	26.09229	Pazin cu i	http://wn.http://www.lanatk.ro/wp-content/uploads/2014/11/26/29011_pa.atul-parlamentului-01.jpg		
6	Fosorul d Bd. Fasilor	44.48713	26.10504	Fosorul d	http://fac.http://www.sos.ro/ra-9/1ab34546116_Fosorul_d_e_fo-1.jpg		
7	Casa Belli Str. Oroda	45.00287	26.1348	Desi putri	http://wn.http://www.lundtiaclaeavictorie.ro/wp-content/uploads/2012/05/Belli_fundatiafoto.jpg		
8	Castelul B Str. Gener	45.51509	25.34713	Renumel	http://pei.http://pensiunea-scarisoara.ro/admin/uploads/images/castelul-bean.jpg		
9	Liviu Car.Bd. C. B. I.	45.75455	21.21605	agenatal	http://vwi.http://www.atismisul.ro/wp-content/themes/_stylebook/timesumb.php?rcuhttp://www.atismisul.ro/wp-content		
10	Castelul B Str. Princi	46.9504	23.81021	Faptel ca	http://img.http://img.5am.ro/images/slideshow/slice_250355_16187.jpg		
11	Munastre Calea Giul	44.47947	25.99799	Povestea	http://img.http://img.5am.ro/images/slideshow/slice_250355_16192.jpg		
12	Traita Mir Du 7, Can	44.70661	25.30064	in judetu	http://img.http://img.5am.ro/images/slideshow/slice_250355_16186.jpg		
13	Micul Tria Sat Florie	45.02645	25.29333	In 1907,	G http://fb.s http://fb.blog.spot.com/eqahia/99HUJ/77058/0VJ/AAAAAAAAAL8u/D7x3RAMzsw/1600/untitled-3737.jpg		
14	Castelul C Str. Castel	45.74847	22.88826	inclus, si	http://wn.http://www.monitorul.ro/documente/stories/2013/07/01/castelul%20covinilor.jpg		
15	Castelul C Str. Zamos	45.48190	25.54261	Realizat	http://wn.http://www.infoguideromania.com/files/castel-rantuzio-bustari-2.jpg		
16	Castelul f Bulevardu	45.13573	25.77255	Castelul "	http://ale.http://alexishoenix.org/images/romania/castel4488.jpg		
17	Baita Viaj Pudreua B	44.538	26.19955	Undeva in	http://ron.http://romanalapas.ro/wp-content/uploads/2013/09/baita-vrajitoarelor-romaniulapas.ro.jpg		
18	Orfelinat Strada Fra	44.43033	26.09993	istona ne	http://wn.http://www.si-de-si.ro/wp-content/uploads/2013/01/strada-francoza-din-Bururesti.jpg		
19	Castelul H Pata lunc	45.75315	21.22706	Prin anii	1 http://me.http://media.portal.ro/upload/image/Turism/Castelul-Hunade-din-Timisara.jpg		

## RESULTS AND DISCUSSIONS



(\*) analiză MDRT a datelor raportate de INS.  
(\*\*) sunt luate în calcul datele raportate în 2009



Bran Castle has made this year a total of over 490,000 visitors, according to estimates by Alexander Priscu Director's castle. He told MEDIAFAX that in the period from January to November, Bran Castle had a total of 477,004 tickets by paying; the estimate for December being 17,290 visitors. Parliament House was visited last year by 141,000 tourists, of which 80% were foreigners. Out of curiosity visits were received in 2011 more than 500,000 euros, according to Romania Libera. Tourists pay for a tour of the largest office buildings in the world large amounts of between 25 and 40 lei. According to information provided by the General Secretariat of the Chamber of Deputies, 2,276,322.12 lei institution earned from tourism last year, and most of the guests are Japanese, Americans, Spanish, Portuguese, Chinese and Israelis.

One of the architectural treasures of Romania, Bánffy Castle (Bontida) called once Transylvanian Versailles is bypassed by tourists. The foundation which manage the palace one day allowed free visit of the complex, but very few have shown interest Cluj offer. In three hours of opening the castle, only five people visited the former noble residence. Over 200,000 tourists visited Corvin Castle (Hunedoara) in the first nine months of 2014, 40% more than the same period in 2013, the castle museum director Constantin Sorin T inca, saying it would need investment of about 60 million. "The number

of visitors is growing at Corvin Castle, percentage, compared to last year, 40 percent more. The exact figures, in July-August, peak season, we had 107,000 tourists, and in August we recorded 3,200 tourists a day. Without October, there are 205,000, "said Tinca.

### CONCLUSIONS

Romania holds many haunted places waiting to be discovered so by the Romanian tourists and foreigners. Unlike last century they began to be much visited by tourists, especially foreign ones.

With the application that we realized we want to make known these places, to draw the attention of all fascinated people of mystery. Also we will provide the access routes to get there.

### REFERENCES

Geographic information system course-  
Conf.univ.dr.DoruMihai  
www.arcgis.com  
[http://ro.m.wikipedia.org/wiki/Lista\\_locurilor\\_presupuse\\_a\\_fi\\_bantuite\\_din\\_România](http://ro.m.wikipedia.org/wiki/Lista_locurilor_presupuse_a_fi_bantuite_din_România)  
<http://stirileprotv.ro/stiri/actualitate/povesti-cu-stafii-fata-moarta-in-putul-liftului-din-hotel-cismigiu-bantuie-inca-holurile.html>  
<http://realitatea.mobi/1294229>  
<https://www.youtube.com/watch?v=0SF0BKVnfeI&app=desktop>  
<http://m.unica.ro/articol/paranormal-locuri-bantuie-bucuresti-romania-vacanta-fantome-35787>

## COMPARATIVE ANALYSIS REGARDING THE ACCURACY DETERMINATION OF A POINT, USING THE LINEAR INTERSECTION METHOD AND MULTIPLE COMBINED INTERSECTIONS METHOD

Rares Catalin OROS, Diana-Ioana PLOSCARIU, Razvan Casian REBREAN, Vasile  
Beniamin TOLOMEIU

Scientific Coordinators: Prof. PhD Eng. Mircea ORTELECAN, Lect. PhD Eng. Tudor  
SALĂGEAN

University of Agricultural Sciences and Veterinary Medicine of Cluj-Napoca, Calea Mănăştur 3-5,  
400372, Cluj-Napoca, Romania | Tel: +40-264-596.384 | Fax: +40-264-593.792 Email:  
diana\_0410\_lavinia@yahoo.com

Corresponding author email: diana\_0410\_lavinia@yahoo.com

### Abstract

*This paper aims to present a comparative analysis regarding the accuracy determination of a point, using the linear intersection method and multiple combined intersections method. To determine the coordinates of the new points we always measure a much higher number of directions than we need. Those directions help to discover measurement errors, a better precision. Before definitive calculations of network points, there will be made some compensations with the purpose to determine each point one time with a higher probability of its coordinates value. Higher order triangulation networks are compensated by rigorous methods namely: indirect measurements method and conditioned measurements method. Whichever method of compensation applied, before compensation is introduced in the calculation direction measurements are being checked on the field, are reduced to the center of points and are also reduced in Gauss or Stereographic projection plan. By solving the triangulation networks aimed at inducing the plane coordinates of geodetic points, using known quantities of plane coordinates geodetic points and connecting lines between geodetic points.*

**Keywords:** point, intersection, error, precision, compensation, network

### INTRODUCTION

Preliminary processing of geodetic observations used in triangulation networks is to determine the elements needed to build functional-stochastic model of the actual processing and reduction of network observations considered on the same reference surface ellipsoid or projection plan). The problem of errors propagation in triangulation networks aims to highlight the influence of triangulation networks shape over the determination errors of length, orientation of directions in the network and coordinates of points (Ghițău, 1983; Ortelecan, 2006). Probable error propagation in a network triangulation can be determined only with a concomitant compensation, calculating the mean square error of any element compensated from the network, then there can be taken steps to improve network configuration by performing new measures

and a new compensation (Ghițău, 1997; Postelnicu and Coatu, 1980). For immediate practical purposes, the optimal configuration problem of network triangulation can be reduced to the possibility of establishing characteristic errors of a network formed by or combination of these (Moldoveanu chains of triangles, rectangles with two observed diagonals, polygons with a central point, 2002; Dima, 2005).

Whichever way of achieving the network triangulation, this requires the determination of an initial length using the older process development geodetic base either by direct measurement using electromagnetic devices. Geodetic bases measurements or of initial directions is a critical operation that must be very precise because when an closure error is detected in a triangulation series on a final direction, is necessary to ensure that this error is due to propagation angular errors and less to the errors of geodetic base measurements

(Ortelecan and Sălăgean, 2014).

## MATERIALS AND METHODS

Linear intersection method is to determine the coordinates of a new point P2 (XP2,YP2), knowing only the old point coordinates 309 (X309,Y309), 300 (X300, Y300), P1 (XP1, YP1), P3 (XP3, YP3), P4 (XP4, YP4) and measured distances between the new point and the old point.

To determine the coordinates of P2 (XP2,YP2) provisional coordinates are determined in the first stage XP2,YP2, using the coordinates of two points and measured distances from these to P2.

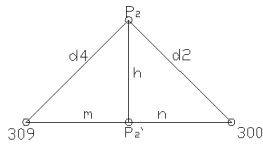


Figure 1. Linear Intersection

$$m = \frac{d_4^2 - d_2^2 + d_{309,300}^2}{2 * d_{309,300}} \quad n = \frac{d_2^2 - d_4^2 + d_{309,300}^2}{2 * d_{309,300}}$$

$$h = \sqrt{d_4^2 - m^2}$$

Using the theory of indirect measurements will determine, in the second stage the probable corrections:

$$x_{P2} = x_{309} + m * \cos \theta_{309,300} + h * \cos(\theta_{309,300} - 100)$$

$$y_{P2} = y_{309} + m * \sin \theta_{309,300} + h * \sin(\theta_{309,300} - 100)$$

Solving the system of correction equations:

$$-a_1 dx P2 - b_1 dy P2 + l_1 = v_1$$

$$-a_2 dx P2 - b_2 dy P2 + l_2 = v_2$$

$$-a_3 dx P2 - b_3 dy P2 + l_3 = v_3$$

$$-a_4 dx P2 - b_4 dy P2 + l_4 = v_4$$

$$-a_5 dx P2 - b_5 dy P2 + l_5 = v_5$$

For measured distances will write the errors equations and will obtain the following direction coefficients:

$$a_1 = \cos \theta_{P2-P3} \quad b_1 = \sin \theta_{P2-P3}$$

$$a_2 = \cos \theta_{P2-300} \quad b_2 = \sin \theta_{P2-300}$$

$$a_3 = \cos \theta_{P2-P1} \quad b_3 = \sin \theta_{P2-P1}$$

$$a_4 = \cos \theta_{P2-309}$$

$$b_4 = \sin \theta_{P2-P3}$$

$$a_5 = \cos \theta_{P2-P4}$$

$$b_5 = \sin \theta_{P2-P3}$$

Calculation of free terms:

$$l_1 = D_{P2-P3C} - DP2-P3M$$

$$l_2 = D_{p2-300 \text{ calc}} - D_{p2-300 \text{ mas}}$$

$$l_3 = D_{p2-p1 \text{ calc}} - D_{p2-p1 \text{ mas}}$$

$$l_4 = D_{p2-309 \text{ calc}} - D_{p2-309 \text{ mas}}$$

$$l_5 = D_{p2-p4 \text{ calc}} - D_{p2-p4 \text{ mas}}$$

To solve the normal equations system is required a solution condition: [pvv] → minimum, and the will be calculates the normal equations coefficients:

$$[paa] dx P2 + [pab] dy P2 + [pal] = 0$$

$$[pab] dx P2 + [pbb] dy P2 + [pbl] = 0$$

The matrix system of correction equations is:

$$AX = l = v$$

A=coefficients matrix

X=matrix of unknowns

L=free terms matrix

V=correction matrix of measured elements

The unknown of correction equations is calculated using the equation:

$$A = \begin{pmatrix} a_1 & b_1 \\ a_2 & b_2 \\ a_3 & b_3 \\ a_4 & b_4 \\ a_5 & b_5 \end{pmatrix} \quad X = \begin{pmatrix} dx P2 \\ dy P2 \end{pmatrix}$$

$$l = \begin{pmatrix} l_1 \\ l_2 \\ l_3 \\ l_4 \\ l_5 \end{pmatrix} \quad v = \begin{pmatrix} v_1 \\ v_2 \\ v_3 \\ v_4 \\ v_5 \end{pmatrix}$$

$$p = \begin{pmatrix} p_1 & 0 & 0 & 0 & 0 \\ 0 & p_2 & 0 & 0 & 0 \\ 0 & 0 & p_3 & 0 & 0 \\ 0 & 0 & 0 & p_4 & 0 \\ 0 & 0 & 0 & 0 & p_5 \end{pmatrix}$$

$$Q_{xy} = \begin{pmatrix} Q_{xx} & Q_{xy} \\ Q_{xy} & Q_{yy} \end{pmatrix}$$

Provisional coordinates calculation:

$$(\Delta XP2)= XP2+\Delta XP2$$

$$(\Delta YP2)= YP2+\Delta YP2$$

To calculate the accuracy the following equations will be used:

$$m_0 = \pm \sqrt{\frac{[vv]}{n-k}}$$

$$m_{\Delta x_0} = \pm m_0 \sqrt{Q_{11}}; m_{\Delta y_0} = \pm m_0 \sqrt{Q_{22}};$$

n = the number of correction equations from the initial equation system(unsimplified);

k = the number of unknowns from the same equation system;

Q11, Q22 = wheighting coefficients established by the shown method in the theory of indirect measurements.

Multiple combined intersection is the most appropriate method, wich will be aplied whenever is possible. In this process, the stationary points will be both in the old and the new points, resulting mutual visas between points (Manualul inginerului geodez vol.II, 1973).

Multiple combined intersection

Provisional coordinates calculation will be determine from 309, 300, P1, P3, and P4, through forward intersection using the equations:

$$\begin{aligned} \text{Station P1} \quad & -dz P1 + l1 = v1 \\ & -dz P1 + a2dxp2 + b2dyp2 + l2 = v2 \\ & -dz P1 + l3 = v3 \\ & -dz P1 + l4 = v4 \\ & -dz P1 + l5 = v5 \end{aligned}$$

$$\begin{aligned} \text{Station 300} \quad & - dz 300 + a5dxP2 + b5dyP2 + l5 = v5 \\ & -dz 300 + l6 = v6 \\ & -dz 300 + l7 = v7 \\ & -dz 300 + l8 = v8 \\ & -dz 300 + l9 = v9 \end{aligned}$$

$$\begin{aligned} \text{Station P4} \quad & - dz P4 + l10 = v10 \\ & -dz P4 + l11 = v11 \\ & -dz P4 + a12dxP2 + b12dyP2 + l12 = v12 \\ & -dz P4 + l13 = v13 \\ & -dz P4 + l13 = v13 \end{aligned}$$

The system contains 15 equations with 5 principal unknowns (dx,dy,dzP1,300,P4) and 13 corrections (v1,...,v13).

Applying equivalence rules of Schreiber will obtain a system of:

$$\begin{aligned} a2d xp2 + b2d yp2 + l2 = v2 \quad & p=1 \\ & p=-1 \end{aligned}$$

$$a5dxP2 + b5dyP2 + l5 = v5 \quad p=1$$

$$a12dxP2 + b12dyP2 + l12 = v12 \quad p=-1$$

$$a12dxP2 + b12dyP2 + l12 = v12 \quad p=1$$

$$a12dxP2 + b12dyP2 + l12 = v12 \quad p=-1$$

System solving will be in the condition of minimum [pvv] → minimum and thus the normal system of equations is represented as:

$$[paa]dxP2 + [pab]dyP2 + [pal] = 0$$

$$[pab]dxP2 + [pbb]dyP2 + [pbl] = 0$$

Calculation of normal equations coefficients: Solving the normal equation system is achieved by Gauss-Dolittle method.

The most probable of coordinates of P2 :

$$(\Delta XP2)= XP2+\Delta XP2$$

$$(\Delta YP2)= YP2+\Delta YP2$$

Average error of observations :

$$m_0 = \pm \sqrt{\frac{[vv]}{n-k}}$$

Average error of probable values :

$$m_{\Delta x_0} = \pm m_0 \sqrt{Q_{11}}; m_{\Delta y_0} = \pm m_0 \sqrt{Q_{22}};$$

Writing matrix equation system of corrections has different accuracies and is represented by:

$$A * X = l = v$$

Calculation of ellipse errors:

$$a = m_0 \sqrt{\lambda_1}$$

$$b = m_0 \sqrt{\lambda_2}$$

$$m_0 = \pm \sqrt{\frac{[vv]}{n-k}}$$

$$\lambda_1 = \frac{Q_{xx} + Q_{yy}}{2} + \frac{1}{2} \sqrt{(Q_{xx} - Q_{yy})^2 + 4Q_{xy}^2}$$

$$\lambda_2 = \frac{Q_{xx} + Q_{yy}}{2} - \frac{1}{2} \sqrt{(Q_{xx} - Q_{yy})^2 + 4Q_{xy}^2}$$

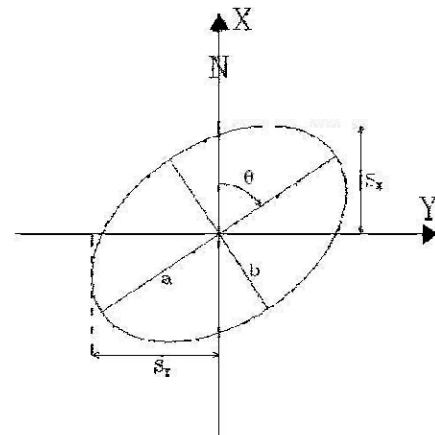


Figure 2. Ellipse errors

## RESULTS AND DISCUSSIONS

Indirect measurements theory applied to solve geodetic problems imposes to verify the calculation during their calculations and different stages.

These checks are performed by specified controls in the process of correction equations system and solving this system.

The final control of solving geodetic network consists in checking related directions orientation of geodetic points.

The value of orientation for any directions can be obtained using probable coordinates of the point determined.

This method is applied for the points of II, III and IV order and has the advantage that is much economical and easier.

It is almost the same as the method used in triangulations, with the specification of that the field measurements are done faster, no matter the visibility (day-night)

In this case there are needed error equations after the provisional coordinates are established.

Provisional coordinates are established in the same way as solving trilaterations, by conditioning measurements theory, and error equations will have the shape as in the case of distance measurements.

For the indirect measurement method the problem to find probable correction system through mathematical conditions of the network that express the related direct measurement and the data that will be calculated.

Every mathematical condition will be under the form of correction equation. The number of correction equation it is equal with the total number of effectuated measurements. Every geodetic observation has an equation and this represents a real advantage for compensation of networks.

For compensation of triangulation network through indirect observations method the unknown data for equation will be chosen from separate coordinates from station.

As a case study we performed measurements inside our campus, University of Veterinary Medicine Cluj-Napoca (Figure 3)



Figure 3

To determine the new point P2, we used the total station TCR805 (Figure 4).



Figure 4. Leica TCR 805

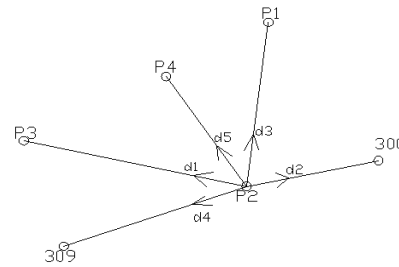


Figure 5. Linear intersection

### Known coordinates

Den. Pct	x	y	z
309	585570.98	390938.3	356.123
300	585590.473	391005.6	356.85
P1	585621.914	390982	355.117
P3	585594.967	390929.7	355.566
P4	585609.607	390960.1	355.308

### Provisional coordinates calculation:

m	41.345
n	28.730
m+n	70.076
h	2.130

cosω	0.998675469
ω	3.276983186
θ 309,300	78.77742215

$A_t^*P^*L=$	-0.7885977
	0.39970342

$XP_2$	585584.5271
$YP_2$	390977.3711

	0.002920
	0.006398
V=	0.000789
	-0.004600
	-0.001484

Result of correction equations system:

a	b
0.213996	0.9768344
0.206388	0.9784702
0.992367	0.1233174
0.327223	0.9449471
0.824001	0.5665886

Calculation of standard deviation:

$S_0=$	0.004348477
$S_{dx}=$	0.001426434
$S_{dy}=$	0.001097492

$l_1$	-0.044707
$l_2$	0.000000
$l_3$	-0.081423
$l_4$	0.000000
$l_5$	-0.081736

Multiple combined intersection

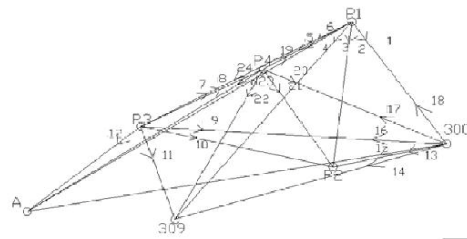


Figure 6. Multiple combined intersection

Results of normal equation system:

	5	0	0	0	0
	0	5	0	0	0
P=	0	0	5	0	0
	0	0	0	5	0
	0	0	0	0	5
$A_t^*P=$	1.06998224	1.031939645	4.9618364	1.636115888	4.120004119
	-4.8841722	4.892351231	0.6165872	4.724735421	-2.832943003

Known data:

Nr. Punct	X	Y
P1	585621,914	390982,017
300	585590,473	391005,560
P4	585609,607	390960,126
P3	585594,969	390929,716
309	585570,98	390938,25

Results for matrix of correction equation system:

Calculation of normal equation system:

	0.213996448	-0.9768344
	0.206387929	0.9784702
A=	0.992367274	0.1233174
	0.327223178	0.9449471
	0.824000824	-0.5665886

	1	0	0	0	0	0	0
	0	-1	0	0	0	0	0
P=	0	0	1	0	0	0	0
	0	0	0	-1	0	0	0
	0	0	0	0	0	0	0
	0	0	0	0	-1	0	0
	0	0	0	0	0	1	0
	0	0	0	0	0	0	1

$(A_t^*P^*A)=$		-
	9.29617815	0.211896696
	-0.2118967	15.70382185

$A_t^*P^*A=$	16472	-6231
	-6231	3230,7

$(A_t^*P^*A)^{-1}=$	0.10760418	0.001451938
	0.00145194	0.063698358

Results of normal equation system through Gauss-Dolittle method:

	a]	b]	l]	s]	Control
	64528,879751	8935,011022	630687,563238	557223,672465	
	-1	-0,138465305	9,773725589	8,635260284	8,635260284
<b>dx P2=</b>	<b>9,514420777</b>	50662,374025	179887,187871	120289,802824	
		-1237,189027	87328,34586	77156,14581	
		49425,184998	-92558,842008	-43133,657010	
		-1	1,872706031	0,872706031	0,872706031
<b>dy P2=</b>	<b>1,872706</b>				

Weight coefficients:

Q 11	Q22
0,000224447	0,001144346

Calculation of standar deviation:

<b>mo=</b>	<b>593,3662293</b>
<b>S<sub>dxP2</sub>=</b>	<b>2,364908701</b>
<b>S<sub>dyP2</sub>=</b>	<b>2,669000613</b>

Normal equation system also can be solved through matricial method:

	57,83208975	-35,1239585
	23,60985177	-14,339296
	82,13777778	-12,5054968
	33,53260736	-5,1053477
<b>A=</b>	59,56804764	-9,96999837
	24,31855362	-4,07023479
	78,27410904	-48,8611414
	31,9552712	-19,9474775

	-155,955297
	5,68434E-10
	-185,855618
	-6,662E-10
<b>L=</b>	-158,952754
	0
	-347,076853
	9,9476E-10

<b>(A<sup>T</sup>*P*A)<sup>-1</sup>=</b>	0,0002	0,000432866
	0,0004	0,001144346

<b>(A<sup>T</sup>*P*A)<sup>-1</sup>*A<sup>T</sup>*P*I)=</b>	<b>2,269479312</b>
	<b>-3,777680</b>

If is used the Gauss method or matricial method the results will be the same.

a	b	l
21,05772253	-167,7505486	71,8592278
8,596779222	-68,48387467	0
-127,6046434	-27,91818652	623,4552676
-52,09437753	-11,39755192	-1,42109E-10
215,9892425	-45,29436696	-1818,685343
88,17723902	-18,49134788	-1,7053E-09
-118,5619252	-172,6950997	1348,059234
-48,4027033	-70,50247924	9,9476E-10

Gauss		Matricial	
<b>dx P2=</b>	<b>2,269</b>	<b>dx P2=</b>	<b>2,269</b>
<b>dy P2=</b>	<b>-3,778</b>	<b>dy P2=</b>	<b>-3,778</b>

## CONCLUSIONS

Once with the appearance of electro-optic and radio telemeters, trilateration method was developed as a solving method of geodetic network and in the case of adding new points in geodetic network, the linear intersection method will be used. The necessary time elapsed on field in the case of linear intersections is shorter than the time elapsed on multiple combined intersections, and the cost of project will be reduced.

## REFERENCES

- Ghitau D., Geodezie si gravimetrie geodezica, Ed. Did. si Ped., Bucuresti, 1983
- Moldoveanu C., Geodezie, Ed. Matrix Rom, Bucuresti, 2002
- Ghițău D. et al., Teoria figurii pamantului, Editura Tehnică, Bucuresti, 1997
- Postelnicu Viorica and Coatu Silvia, Mica enciclopedie matematica, Editura Tehnică, Bucuresti, 1980
- Ortelecan Mircea, Geodezie, Editura AcademicPres, Cluj-Napoca, 2006,
- Dima Nicolae, Geodezie, Editura Univeritas, Petrosani, 2005
- \*\*\*Manualul inginerului geodez, vol II, Editura Tehnică, București, 1973
- Ortelecan M., Salagean T., Geodezie lucrari practice, Ed. Risoprint, Cluj-Napoca, 2014

## ASPECTS REGARDING THE PROJECTION OF TOPOGRAPHIC ELEMENTS FROM THE TOPOGRAPHIC SURFACE ON THE REFERENCE SURFACE

Grațîela PASCAL, Ioana Georgiana TEPUȘ, Anamaria Cătălina SALE, Raluca Elena TĂUTU

Scientific Coordinators: Prof. PhD Eng. Mircea ORTELECAN, Lecturer PhD. Eng. Tudor SĂLĂGEAN

University of Agricultural Sciences and Veterinary Medicine of Cluj-Napoca, Calea Mănăștur 3-5, 400372, Cluj-Napoca, Romania | Tel: +40-264-596.384 | Fax: +40-264-593.792

Corresponding author email: georgianatepus@yahoo.com

### Abstract:

*Projection of topographic elements from the topographic surface on the reference surface is a very important operation necessary because the field observations are reported at the geoid vertical by the position of the plumb line, while the calculus are performed on ellipsoid after the instrumental observation were projected on the reference ellipsoid after the normal direction to the ellipsoid. For the correction calculus of reduction on ellipsoid of geodetic observation is necessary the preliminary determination of the „N” geoid undulation and the deviation components of vertical line. There are several methods in which we can bring geodetic points of the topographic surface to the reference surface. Some of the methods are: the design method, the development method, the Pizzetti method, the Bruns-Helmert method.*

**Key words:** azimuth, corrections, ellipsoidal surface, topographic surface.

### INTRODUCTION

Ellipsoidal geodesy is that part from geodesy which is dealing with the study of ellipsoid rotation surface, reference, physics surface of Earth, and also is dealing with rigorous determination of shapes and dimensions to mathematical curve surface of the Earth (Dima, 2005).

All the geodetic measurements which are performed on the physics topographic surface of the Earth (which is considered of being the contact surface between land and atmosphere or land and water) must be reduced to geoid surface (Ortelecan, 2006).

When geodetic current measurements (trilaterations, triangulations, polygonometry), the geoid can be approximated with an rotation ellipsoid, flattened at the poles, having the big semi-axis (equatorial) approximately 6380 km. Also, for geodetic works of small precision, the geoid surface

will be approximated too with the surface of a medium radius sphere equal to 6370 km.

Through ellipsoidal geodesy methods is determined precisely the coordinates of a punctual network from the Earth surface, basic points of first order with the help of which we can determine then the points of second, third and fourth order necessary for obtaining the graphic representations on large surfaces (Ghițău, 1997).

### MATERIALS AND METHODS

Before being used in calculus, the geodetic observations reduce on ellipsoidal reference surface. This operation is necessary because the field observations are reported to geoid vertical, given by the position of plumb line, while the calculus are performing on ellipsoid after the instrumental observations were projected on the reference ellipsoid by the normal direction to the ellipsoid.

For the reducing calculation of geodetic observations on ellipsoid is necessary the

preliminary determination of the 'N' geoid undulations and of deviation vertical components  $\xi, \eta$ . Bringing the geodetic support network, existing on physics Earth surface, on the ellipsoidal reference surface can be achieved through many methods like : the design method and the development method (Postelnicu and Coatu, 1980).

In the development method the measured elements on physics surface of the Earth are reduced to the geoid surface (to the sea level), which will be subjected to a compensation depending on the geometry triangulation network. This method introduces systematic calculation errors, which get bigger as get further of the fundamental point and as outcome it can be used only for areas relatively small, for which it can be admitted that the reference ellipsoid folds perfectly over the geoid surface.

The designed method consists on bringing the measured elements (angles, directions, lengths) on the reference ellipsoid surface through the application of some corrections. In this method are known two versions : Pizzetti and Bruns-Helmert. The Pizzetti method has no applicability because of the fact that the vertical curvatures are unknown. The Bruns-Helmert consist of the projection of the "P" point from the physics surface of the Earth in 'P' point after the normal direction to the ellipsoid. The differences which are obtained through the use of both methods are insignificant (Manualul inginerului geodez vol.II, 1973).

Further, will be treated only the angular observations on which will be applied the following corrections: The correction for reducing to the geodetic line and the correction due to the height of the sighted point.

a) The correction for reducing to the geodetic line (figure 1) is applied to make the transition from the direct normal section, through which is represented the observation

line on the ellipsoid surface, to the geodetic line. Considering the 'AB' observation line on the Earth surface is represented on ellipsoid through the 'AB' normal section, which has the 'Am' azimuth, obtained from measurements. The geodetic line being 'Ac' azimuth, it requires to correct the direct normal section azimuth with a 'C1' correction (named the correction for reducing to the geodetic line):

$$C_1 = Am - Ac \Rightarrow Ac = Am - C_1$$

The expression of the angular value of the 'C1' correction has the following formula:

$$C_1 = \frac{e^2 \cdot s^2}{12 \cdot R_m^2} \cdot \rho'' \cdot \cos^2 \varphi_m \cdot \sin 2Am \quad \text{In}$$

which:

$e^2$ = the first excentricity

$s$ = the distance between A and B in kilometers

$R_m$ = the medium radius for the medium latitude  $\varphi_m$

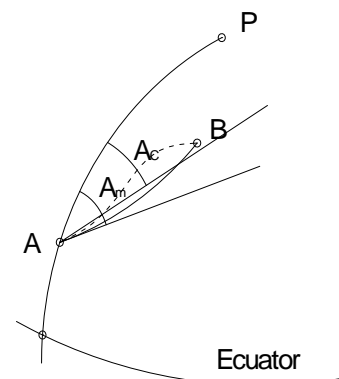


Figure 1- Reduction correction of the geodesic line

b) The correction due to the height of the sighted point (figure 2) is used because the points situated on the topographic surface have different heights, the observation lines are not included by the same level surface. Considering that 'A' is situated right on the ellipsoid surface (zero level surface) and 'B', the point to which the observation is made, will be on a certain level surface and it will have an 'H' height towards 'A'. The

representation of 'B' on ellipsoid surface is made according to the normal direction to the ellipsoid which is passing through this point in 'B1'.

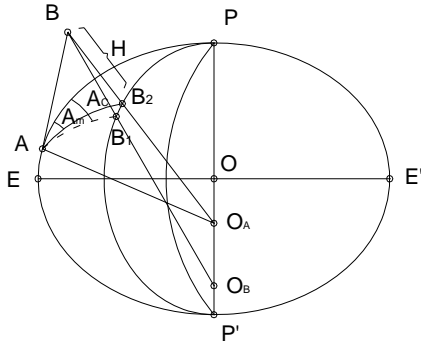


Figure 2 - The correction due to the height of the sighted point

Measuring the direction of the 'AB' azimuth will be obtained the angle which is made by the normal direction section 'AB2' with the meridian 'A' point.

So having measured the 'Am' angle must be determined 'Ac' through the application of an 'C2' correction named the correction due to the height of the sighted point.

$$Ac = Am + C_2$$

$$C_2 = \frac{e^2 \cdot H}{2M_2} \cdot \rho^2 \cos^2 \varphi_2 \cdot \sin 2Am$$

In which:

H- the height of the sighted point

M2- the small curvature radius in 'B' with latitude  $\varphi_2$

The correction due to the height of the sighted point is taken into consideration only if  $H \geq 20m$ .

c)The sides measured by electronic devices such as total stations (figure 3) are also processed preliminary through the application of physics corrections. The 'D' distance resulting after this operation is situated to the level of the two points between the measurement was made. So, it is necessary the knowledge of ellipsoidal heights 'H1' and 'H2' and therefore the geoid undulations in these points (figure 4).



Figure 3. Total station

In the bellow figure is applied the generalized Pitagora equation resulting:

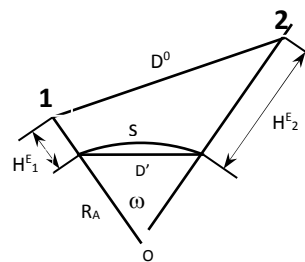


Figure 4. Reducing distances to reference surface

Developing the relation and introducing the notations:

$$(D^0)^2 = (R_A + H_1^E)^2 + (R_A + H_2^E)^2 - 2(R_A + H_1^E)(R_A + H_2^E) \cos \omega$$

$$\cos \omega = 1 - 2 \sin^2 \frac{\omega}{2}; \quad D' = 2R_A \sin \frac{\omega}{2}; \quad \Delta H_{12}^E = H_2^E - H_1^E$$

Is obtained:

$$(D^0)^2 = R_A^2 + 2R_A H_1^E + (H_1^E)^2 + R_A^2 + 2R_A H_2^E + (H_2^E)^2 - 2(R_A + H_1^E)(R_A + H_2^E) + 4R_A^2 \left(1 + \frac{H_1^E}{R_A}\right) \left(R_A + \frac{H_2^E}{R_A}\right) \sin^2 \frac{\omega}{2} =$$

$$= (H_1^E)^2 - 2H_1^E H_2^E + (H_2^E)^2 + \left(1 + \frac{H_1^E}{R_A}\right) \left(R_A + \frac{H_2^E}{R_A}\right) (D^0)^2 =$$

$$= (\Delta H_{12}^E)^2 + \left(1 + \frac{H_1^E}{R_A}\right) \left(R_A + \frac{H_2^E}{R_A}\right) (D^0)^2$$

$$D' = \sqrt{\frac{(D_0)^2 - (\Delta H_{12}^E)^2}{\left(1 + \frac{H_1^E}{R_A}\right) \left(1 + \frac{H_2^E}{R_A}\right)}}$$

The length of the 's' arc which represents the length of the measured side reduced on the ellipsoidal surface is obtained with the following formula:

$$s = R_A \omega = 2R_A \frac{\omega}{2} = 2R_A \operatorname{arc} \sin \frac{D'}{2R_A}$$

## RESULTS AND DISCUSSIONS

We picked three points from the triangulation network from our city to exemplify the calculus of the correction for reducing to the geodetic line, the correction due to the height of the sighted point and the reducing of the measured sides by the electronic devices.

We know:

Point	x	y	z
DL.Borzas	586099.15	399284.5	464.51
DL. Melic	586811.57	400084.26	401.14
DL. Criseni	585419.13	400957.18	478.19

The calculus steps are:

1. The transformation of degrees, minutes and seconds in radians
2. The calculus of the ellipsoidal reference parameters

3. The calculus of the distance

$$D1 = 10.7105477 \text{ km}$$

$$D2 = 16.4343496 \text{ km}$$

$$D3 = 18.0562609 \text{ km}$$

4. The calculus of azimuth

$$A = \theta + \gamma \Rightarrow A1 = 0.79734878694$$

$$A2 = 2.36543219489$$

$$A3 = 5.15365918203$$

5. The calculus of medium radius:

$$R_m = \sqrt{M \cdot N} \Rightarrow R_{m1} = 6335338.65$$

$$R_{m2} = 6237026.775$$

$$R_{m3} = 6206286.737$$

$$M = \frac{a(1-e^2)}{W^2}$$

$$N = \frac{a}{W}$$

$$W = \sqrt{1 - e^2 \sin^2 B}$$

6. The calculus of the radius after an azimuth:

$$R_a = \frac{M \cdot N}{N \cos^2 A + W \sin^2 A} \Rightarrow$$

$$R_{a1} = 6335345.289$$

$$R_{a2} = 6229984.436$$

$$R_{a3} = 6343470.093$$

7. The calculus of corrections:

$$C_1 = \frac{e^2 \cdot s^2}{12 \cdot R_m^2} \cdot \rho'' \cdot \cos^2 \varphi_m \cdot \sin 2Am$$

$$C11 = 0.000000407$$

$$C1 = -0.000001303$$

$$C31 = -0.01323112$$

$$C12 = 32.58069$$

$$C22 = -45.934$$

$$C32 = -26.0681$$

8. The calculus of the length of the chord

$$D' = \sqrt{\frac{(D_0)^2 - (\Delta H_{12}^E)^2}{\left(1 + \frac{H_1^E}{R_A}\right) \left(1 + \frac{H_2^E}{R_A}\right)}}$$

$$D1' = 1069.105$$

$$D2' = 1641.513$$

$$D3' = 1805.44$$

9. The calculus of the measured length side, reduced on the ellipsoidal surface

$$s = 2 * R_a * \arcsin \frac{D'}{2 * R_a} \Rightarrow$$

$$s1 = 1069.105$$

$$s2 = 1641.513$$

$$s3 = 1805.44$$

## CONCLUSIONS

Analyzing the calculus performed above we came to the following conclusions: due to the fact that the distances among the three points (Dealul Borzaș, Dealul Melic și Dealul Crișeni) which are included between ten and eighteen kilometers, the correction for reducing to the geodetic line may not be taken into consideration because the corrections resulted after the application of calculus do not fit into the given criteria, since these are too small.

Also, because of the fact that the altitude of the three points are bigger than 20 meters we applied the correction due to the height of the sighted point. It can be observed significant differences among the

corrections, so we can say that the observation lines are included by the different level surfaces.

Furthermore, through the reducing of the measured sides performed with electronic devices we can notice that it is not necessary the knowledge of the vertical deviations among the points because the obtained results for the chord length ( $D'$ ) and also for the arc length ( $s$ ) are equal.

In conclusion, the projection of topographic elements from the topographic surface on the reference surface require a laborious calculation, therefore the final results are more accurate, so closer to the reality.

## REFERENCES

- Ghițău D. et al., Teoria figurii pamantului, Editura Tehnică, București, 1997
- Postelnicu Viorica and Coatu Silvia, Mica enciclopedie matematica, Editura Tehnică, București, 1980
- Ortelecan Mircea, Geodezie, Editura AcademicPres, Cluj-Napoca, 2006,
- Dima Nicolae, Geodezie, Editura Univeritas, Petrosani, 2005
- \*\*\*Manualul inginerului geodez, vol II, Editura Tehnică, București, 1973

## **FACTORS THAT AFFECT THE PRECISION OF POINT COORDINATES TAKEN WITH GPS EQUIPMENT IN MOUNTAIN AREA OF BRAȘOV COUNTY**

**Claudia PRĂJANU**

**Scientific Coordinator: Lect. PhD. Eng. Cornel Cristian TEREȘNEU**

Transilvania University of Brașov, Faculty of Silviculture and Forest Engineering, 1, Șirul  
Beetoven, 500123, Brașov, Romania, Phone: +40 268 41 86 00 Fax: +40 268 47 57 05

Corresponding author email: prajanu.claudia@yahoo.com

### **Abstract**

*The paper aims to identify and analyse factors that affect the precision of determination in the horizontal plane of points, located within a larger forest area in Brasov county. For this purpose 2704 points were measured using a GPS equipment. The precision of such measurements is affected by a series of factors like the forest canopy and the terrain orography. The coordinates of the points were obtained using the semi-kinematic method, Stop&Go with post-processing, which has an average precision, acceptable in this field. The points were then grouped according to the following criteria: localization, forest formation, orography, exhibition (S-N, E-V), forest consistency (<0.7, 0.7-0.8, 0.9-1.0), tree age (21-40 years, 41-60 years, 61-80 years, 81-100 years, >100 years). The points have been processed using software AutoCAD Map 3D and specific modules of ArcGIS. Data have been processed using a statistical program, Statistica 8.0. The distributions were analysed using several statistical indicators (maximum, minimum, mean, standard error of mean, mode, frequency of mode, standard deviation, coefficient of variation). Accuracies obtained were analyzed both for each category as well as for combinations of 2, 3 and 4 factors. After analysing all the results obtained, it can be expressed the idea that, on the whole, the accuracy of determining the point coordinates in forest lands is relatively good and that there are rare cases where exaggerated values are obtained.*

**Key words:** GPS, precision of measurements, statistical analysis, GIS

### **INTRODUCTION**

Once the property law had been adopted problems regarding the division of surface appeared. Given the great number of land owners it was necessary to establish and measure forest areas within the properties (Tereșneu et al, 2011). In this purpose the use of total station in mountain areas is not indicated and the use of photogrammetric methods is too expensive (Boș, 2011). The use of the GPS system is more suited for this situation, but the downside for this approach is that there exists, in these circumstances, a series of factors which affect the precision of measuring. Aside of the delays in the ionosphere and troposphere, of the ephemerides, the difference between the satellite and the receiver watch (Păunescu et al, 2012), the number of visible satellites (Wang et al., 2014), the precision can be affected by the forest canopy (Ordonez Galan et al, 2013, Weilin et al, 2000, Zhang et al,

2014), the terrain orography (Tereșneu, 2011, Tereșneu et al., 2011), the composition (Ordonez Galan et al, 2011, Yosimura and Hasigawa, 2003) and the age of the forest. The paper aims to identify and analyse factors that affect the precision of determination in the horizontal plane of points, located within a larger forest area in Brasov County.

### **MATERIALS AND METHODS**

The research was conducted in a forest area in Brasov County using two dual-frequency GPS receivers (a Trimble ProXT type and a Trimble ProXH type), the cadastral plans, 1:5.000 scale, orthophotoplans from 2005 and land descriptions. The coordinates of 2704 points were obtained using the direct measuring method. The points were grouped according to the following criteria: localization, forest formation, orography, exhibition (S-N, E-V), forest consistency (<0.7, 0.7-0.8, 0.9-1.0), tree age (21-40 years, 41-60 years, 61-80 years,

81-100 years, >100 years). The data from the GPS receivers were processed using Trimble GPS Pathfinder Office and then were imported in AutoCAD Map 3D, where the topography was created and the errors were corrected using the ArcInfo and ArcCatalog modules. The GIS project was concluded

using the ArcMap module. The statistical analysis was realized using the Statistica 8.0 program (Tereşneu, 2007, Tereşneu et al, 2014).

## RESULTS AND DISCUSSIONS

Table 1. Statistic description of observed distribution by location of points

Location of points	Min	Max	Mean	Standard error of mean	Mode	Frequency of Mode	Standard deviation	Coefficient of variation
Forest	0.100	15.400	1.022	0.028	0.600	133	1.007	98.580
Border	0.200	8.200	0.990	0.024	0.500	116	0.762	76.971
Forest Roads	0.100	6.000	0.556	0.041	0.300	60	0.573	103.145
Open wood	0.300	7.000	1.273	0.139	0.600	9	1.141	89.604
Alpine barren zone	0.100	0.500	0.128	0.005	0.100	82	0.056	43.832

Table 2. Mean, quartiles and percentiles depending on location of points

Location of points	Median	Quartile		Percentile			
		Lower	Upper	90.00	95.00	99.00	99.50
Forest	0.800	0.600	1.150	1.700	2.300	6.400	6.900
Border	0.800	0.500	1.200	1.800	2.300	3.900	5.400
Forest Roads	0.400	0.300	0.600	0.900	1.400	3.300	6.000
Open wood	0.800	0.600	1.600	2.400	3.400	7.000	7.000
Alpine barren zone	0.100	0.100	0.100	0.200	0.200	0.200	0.500

The tables presented above show a series of statistical indicators calculated for each category of point locations from the first column. Looking at the values from the eighth column we can state that the standard deviation is achieved for the points located in the forest area and the lowest for the alpine barren zone. The other locations have a standard deviation within the two limits.

The horizontal precision with the highest frequency is 0.1m for the alpine barren zone, 0.3m for forest roads, 0.5m for points located on borders and 0.6m for open woods and forests. We can see that the highest precision is obtained for the alpine barren zone.

By looking at the mean values for the horizontal precision we can state that the location with the highest precision on average is the alpine zone, followed by the forest roads. We can see that for the mean for the border, open wood and the forest area exceeds the value 1.000. Because of the high values of the coefficient of variation we can't use the mean to describe the experimental distributions. Even lower values for the

coefficient of variation are obtained for the points situated in the alpine zone (43.8%).

The tables presented above show a series of statistical indicators calculated for each category of point locations from the first column. Looking at the values from the eighth column we can state that the standard deviation is achieved for the points located in the forest area and the lowest for the alpine barren zone. The other locations have a standard deviation within the two limits.

The horizontal precision with the highest frequency is 0.1m for the alpine barren zone, 0.3m for forest roads, 0.5m for points located on borders and 0.6m for open woods and forests. We can see that the highest precision is obtained for the alpine barren zone.

By looking at the mean values for the horizontal precision we can state that the location with the highest precision on average is the alpine zone, followed by the forest roads. We can see that for the mean for the border, open wood and the forest area exceeds the value 1.000. Because of the high values of the coefficient of variation we can't use the mean to describe the experimental

distributions. Even lower values for the coefficient of variation are obtained for the points situated in the alpine zone (43.8%).

The tables presented above show a series of statistical indicators calculated for each category of point locations from the first column. Looking at the values from the eighth column we can state that the standard deviation is achieved for the points located in the forest area and the lowest for the alpine barren zone. The other locations have a standard deviation within the two limits.

The horizontal precision with the highest frequency is 0.1m for the alpine barren zone, 0.3m for forest roads, 0.5m for points located on borders and 0.6m for open woods and forests. We can see that the highest precision is obtained for the alpine barren zone.

By looking at the mean values for the horizontal precision we can state that the location with the highest precision on average is the alpine zone, followed by the forest roads. We can see that for the mean for the border, open wood and the forest area exceeds the value 1.000. Because of the high values of the coefficient of variation we can't use the mean to describe the experimental distributions. Even lower values for the coefficient of variation are obtained for the points situated in the alpine zone (43.8%).

Other statistical indicators like the median, the quartile, the percentile and the analysis of the cumulative relative frequency distribution are more suitable for describing the experimental distributions.

The graph from figure 1 represents the cumulative relative frequency distribution in the case of the points located in the alpine barren zone. The median has a value close to the arithmetic mean only in the case of the alpine zone, but the difference between the

two indicators reaches approximately 0.5 m in the case of open woods. 50% of observed values have a horizontal precision under 0.4 m when the point is located on forest roads and under 0.8 m when the point is located in forest areas, open woods or on the border. 75 % of observed values have a horizontal precision under 0.1 m for the points located in the alpine zone. 10% of observed values have a horizontal precision over 0.9 m when the point is located in forest areas, open woods or on the border.

Because the problem of horizontal precision has a major importance in the forestry sector we will treat the points measured in the forest zone separately. For this purpose the points were grouped according to the following criteria: localization, forest formation, orography, exhibition (S-N, E-V), forest consistency (<0.7, 0.7-0.8, 0.9-1.0), tree age (21-40 years, 41-60 years, 61-80 years, 81-100 years, >100 years). The relative frequency distributions for each criterion are shown in figure 2.

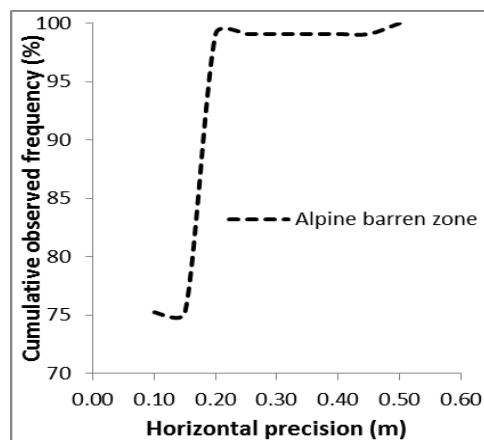
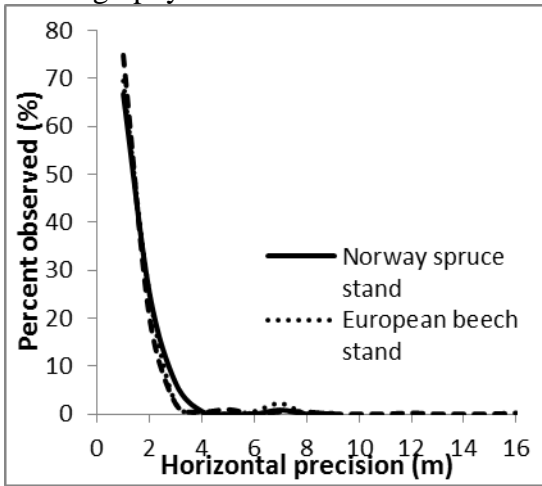
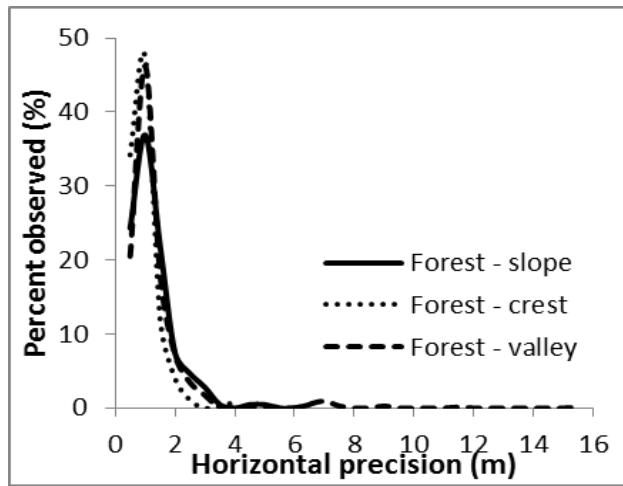


Figure 1. Distribution of cumulative relative frequency distribution by horizontal precision

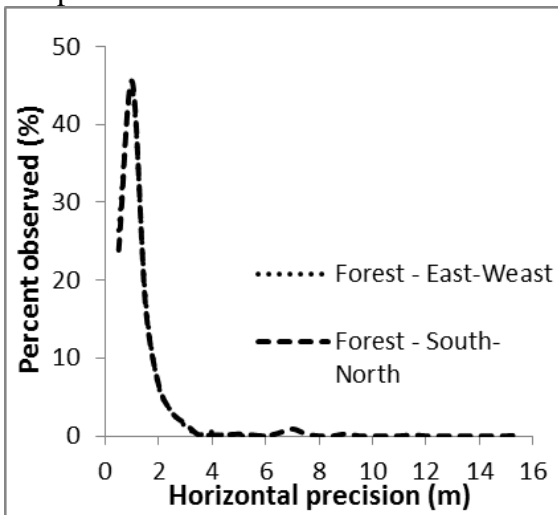
a – orography



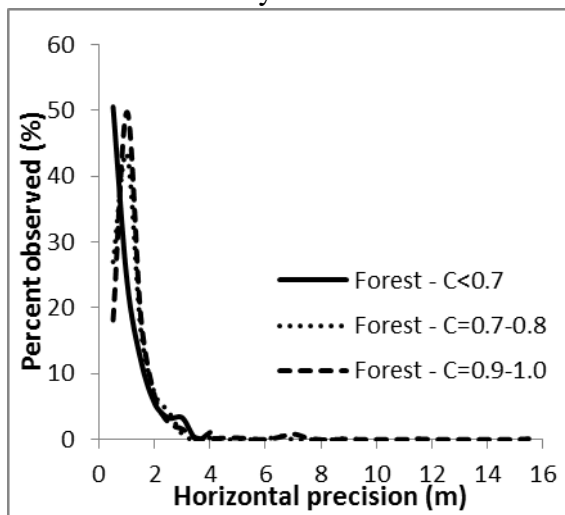
b – exhibition



c - species



d – consistency



e – age

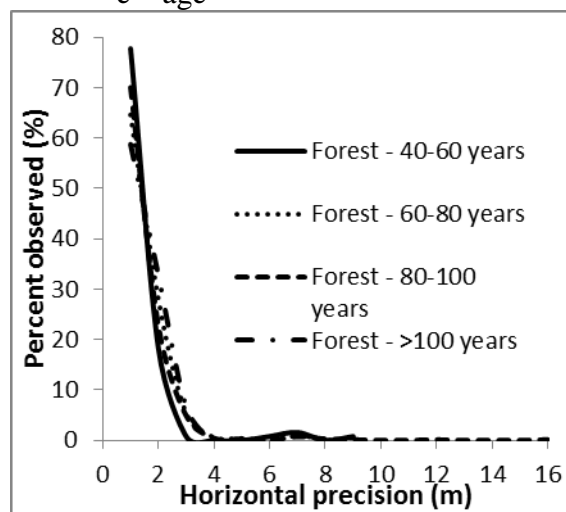


Figure 2. Relative frequency distribution observed for the points in the forest

Table 3. Points located in forest, grouped after five criteria

Number	Criterion	Category
1	Orography	Forest slope
2		Forest-crest
3		Forest-valley
4	Exhibition	Forest E-W
5		Forest S-N
6	Species	Norway spruce
7		European beech
8		Mixed
9	Consistency	C<0.7
10		C=0.7-0.8
11		C=0.9-1.0
12	Age	21-40 years
13		41-60 years
14		61-80 years
15		81-100 years
16		>100 years

Table 4. Statistic descriptive of observed distribution in forest by studied criteria

Nr. crt.	Categories of forests	Min	Max	Mean	Standard error of mean	Mode	Frequency of mode	Standard deviation	Coefficient of variation
1	Forest slope	0.300	6.200	1.077	0.052	0.400	27	0.767	71.246
2	Forest-crest	0.100	3.900	0.774	0.027	0.600	60	0.513	66.313
3	Forest-valley	0.100	15.400	1.129	0.044	0.700	77	1.211	107.285
4	Forest E-W	0.100	6.400	0.922	0.028	0.600	57	0.661	71.696
5	Forest S-N	0.200	15.400	1.091	0.043	0.600	76	1.190	109.057
6	Norway spruce	0.100	8.800	1.044	0.031	0.600	75	0.828	79.358
7	European beech	0.100	8.700	1.046	0.087	0.600	20	1.165	111.380
8	Mixed	0.200	15.400	0.998	0.059	0.400	48	1.213	121.571
9	C<0.7	0.100	3.600	0.818	0.077	0.500	18	0.734	89.725
10	C=0.7-0.8	0.100	8.800	0.973	0.041	1.000	39	0.784	80.585
11	C=0.9-1.0	0.200	15.400	1.102	0.039	0.600	95	1.127	102.268
12	41-60 years	0.100	8.700	0.936	0.105	0.400	19	1.174	125.474
13	61-80 years	0.200	6.900	1.094	0.036	multiple	59	0.802	73.272
14	81-100 years	0.100	15.400	1.034	0.044	0.500	67	1.136	109.826
15	>100 years	0.500	8.800	1.221	0.073	1.000	23	0.944	77.345

The results indicate a low variation of the horizontal precision for the points situated on the ridge, a mild one for the points located on the slope, and a large variation for points in a valley. At the same time, it is observed that the horizontal precision varies less for a terrain that has a favourable exposure in respect to the satellite's movement (E-W) than for a terrain which doesn't have a favourable exposure (S-N). In the case of a mixed forest the variation of the precision is higher than for the Norway spruce and European beech forests, which have the same interval of variation. The differences in

consistency have led to a maximum of 3.6 m for forests with consistency less than 0.7, a maximum of 8.8m for forests with consistency between 0.7 and 0.8 and 15.4m forests with consistency greater than 0.9. The arithmetic mean suggests a better horizontal precision for the points situated on the ridge (0.77m) than for the points located on the slope or in a valley, the last two having close values (1.07m and 1.12m). In the case of a forest area the average horizontal precision is inversely proportional with the consistency of the forest. For the forests with consistency under 0.7 the value of the average precision is

0.81m and it gets lower as the consistency rises.

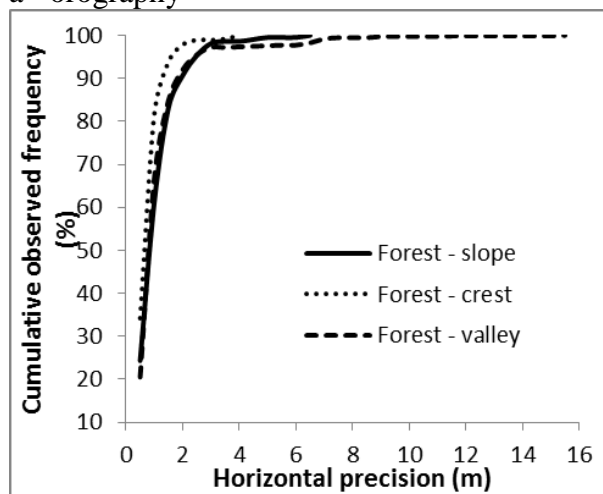
The age of the forest is also a factor which influences the precision. We can see that the mean horizontal precision is directly proportional (in value) with the age. An average precision of 0.93m was obtained for a 41-60 years old forest and a greater value of 1.22m for a 100 years old one.

For most cases, the standard deviation is higher than the arithmetic mean and the coefficient of variation is higher than 100% for European beech forests, mixed forests, forests that are located in a valley and for a 100 years old forest.

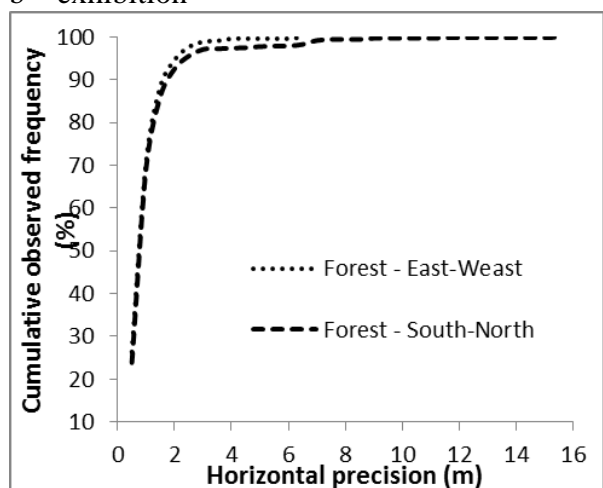
If we analyse the mode values in relation with each criterion we observe the following:

In case of orography the most frequent modal value is 0.7m for a forest located in a valley, 0.6m for a forest on a crest and 0.4m for a forest on a slope.

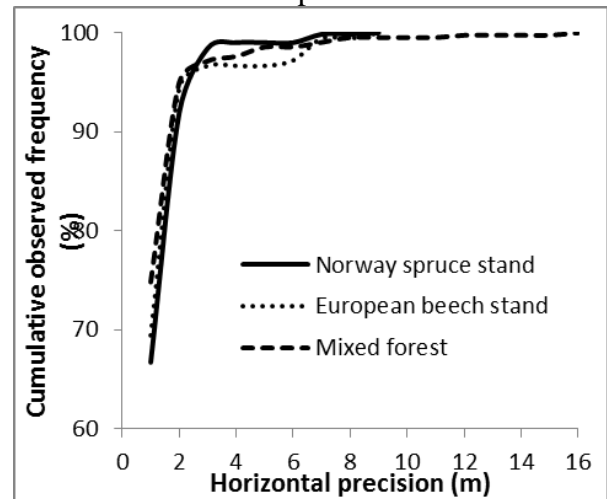
a - orography



b - exhibition



c - species



d - consistency

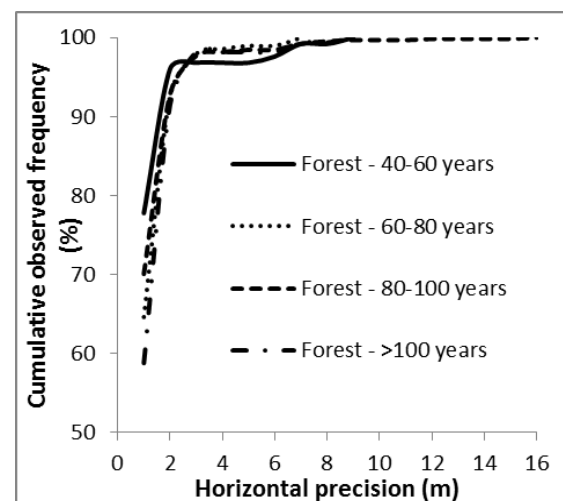
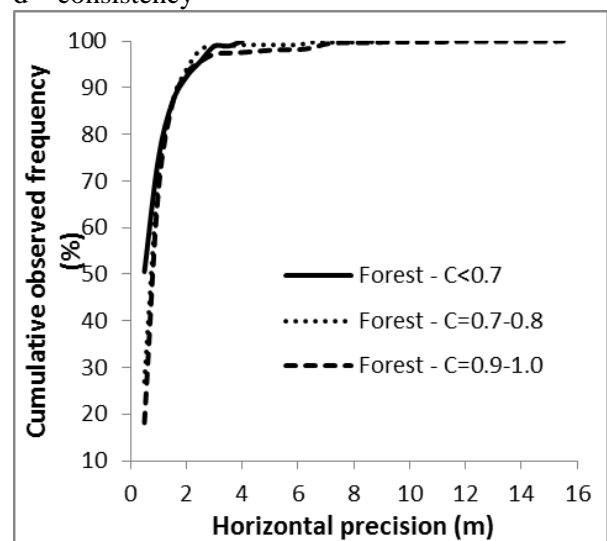


Figure 3. Cumulative relative frequency distribution observed for the points in the forest

In case of exposure the modal value is 0.6m for both cases analysed, but with a higher frequency in the case of S-N exposure (76).

In case of vegetation the modal value is 0.4m for mixed forests, 0.6 for both Norway spruce and European beech forests

In case of consistency the modal value is 0.5m for a consistency less than 0.7, 1.0m for a consistency between 0.7 and 0.8 and 0.6m for a consistency greater than 0.9

In case of age the modal value is 0.4m for the third class of age, 0.5m for the fifth class of age and 1.0m for a forest older than 100 years. To these results we add the analysis of

the cumulative relative frequency distribution from figure 3.

Figure 3 reveals that a better horizontal precision in the case of a forest located on a ridge than in the case of a forest located on a valley or a slope (Fig. 3a). We can see that the exposition of the terrain does not affect the precision because of the overlapping of the curves in figure 3.b. For the rest three criteria we can add that better precision is obtained for a mixed forest (Fig 3.c), for a consistency less than 0.7 (Fig 3.d) and for a 41-60 years old forest.

Table 5. Median, quartile and percentile by the categories

Nr. crt.	Categories of forests	Median	Quartile		Percentile			
			Lower	Upper	90.00	95.00	99.00	99.50
1	Forest slope	0.900	0.600	1.300	1.900	2.500	4.100	4.900
2	Forest-crest	0.600	0.500	1.000	1.300	1.600	3.500	3.800
3	Forest-valley	0.900	0.600	1.200	1.900	2.500	6.800	8.700
4	Forest E-W	0.800	0.500	1.100	1.700	2.200	3.100	3.800
5	Forest S-N	0.800	0.600	1.200	1.800	2.400	6.800	8.700
6	Norway spruce	0.900	0.600	1.200	1.800	2.300	3.900	6.600
7	European beech	0.800	0.500	1.100	1.650	2.100	6.600	8.700
8	Mixed	0.800	0.500	1.100	1.600	2.000	6.800	7.100
9	C<0.7	0.500	0.400	1.100	1.800	2.500	3.600	3.600
10	C=0.7-0.8	0.800	0.500	1.200	1.700	2.200	3.900	6.300
11	C=0.9-1.0	0.900	0.600	1.200	1.800	2.300	6.700	7.100
12	41-60 years	0.600	0.400	1.000	1.500	1.900	6.600	8.700
13	61-80 years	0.900	0.700	1.200	1.800	2.300	6.400	6.600
14	81-100 years	0.800	0.500	1.200	1.800	2.500	6.700	7.100
15	>100 years	1.000	0.800	1.400	1.900	2.300	6.300	8.800

According to the median 50% of the values have a horizontal precision under 0.6m for points on a ridge, under 0.9m for points on a slope or in a valley, and under 0.8m for any exposure. The precision isn't strongly affected by the vegetation (0.8 for European beech and mixed forests and 0.9 for Norway spruce).

In the case of a forest with consistency under 0.7 half of the points have a precision less than 0.8m and less than 0.8-0.9m for a higher consistency. In the case of a 41-60 years old forest, 50% of points have a precision under 0.6m, and a precision between 0.8 and 1.0m for older forests.

According to the 90.00 percentile 10% of points have a precision less than 1.8m for

Norway spruce and less than 1.6m for European beech and mixed forests. In the case of a 41-60 years old forest, 10% of points have a precision less than 1.5m, and a precision under 1.8-1.9m for older forests. For 99% of the points the precision is less than 3-4m. The exposure only affects 1% of the points, the precision being less than 6-7m for a point situated in a valley, with N-S exposure in a forest for European beech or mixed forest, regardless of age. Only for 0.5% of the points the precision is less than 3.6-3.7m for a point situated on a ridge, with E-W exposure in a forest with consistency under 0.7. Precisions less than 8.0m were obtained only for 0.5% of

the points which are located in European beech, in a valley with N-S exposure.

If we take into account only two criteria we can establish the following conclusions.

The horizontal precision is not influenced by the species if the measurements are made in the vegetation season (Crainic, 2011).

The precision is strongly affected by the terrain orography, in the case of norway spruce. The best results are obtained for the points on a crest, where there is a better satellite signal. Poor results, however pleasing, are also obtained for points located on a slope. The most unfavourable situation is recorded in the valley (Tereşneu, 2011, Tereşneu et al., 2011).

Age does not affect the accuracy of determining the coordinates of points in the norway spruce. In the case of European beech is observed the same distribution of precision, the precision being higher on a crest and lower on a slope.

In the case of the European beech forest better accuracy has been established for points situated on sunny exposures, to the detriment of those located unfavourable exposure in respect to the satellite's movement (conclusion must be regarded with reserve until another experiments will confirm this).

After consolidating the results obtained from the point of view of three criteria of analysis, it is found several theories.

The best accuracy has been obtained in the case of norway spruce situated on a hillside, between 21 and 40 years old or between 81 and 100 years old and it is found that the terrain orography has a huge impact on the precision.

In the case of norway spruce situated on a hill the exposure does not affect the precision, but in the case of an European beech forest a better accuracy is obtained on sunny exposures, a sign that, during the season of vegetation, shaded exposures are unfavourable for obtaining the horizontal coordinates of points using GPS equipment.

Consistency has an influence on the studied parameter in the case of the norway spruce located in a valley, for which accuracy is much better if consistency values are smaller.

Finally, analysing the influence of four factors, we can get the following conclusions.

The best accuracy is recorded in the case of norway spruce located on a crest or hill, over the age of 60 years, regardless of consistency.

Good precision is obtained in the case of norway spruce situated on hill, included in 2nd and 5th class of age, regardless of consistency.

Acceptable results are obtained in the case of norway spruce situated on hill, contained in class 3 of age, whatever their consistency.

## CONCLUSIONS

The terrain orography has the most powerful and visible influence on the accuracy of determination in the horizontal plane of coordinates of points using GPS equipment type. A higher precision is obtained in the case of a forest located on a ridge than on a hillside. The forest situated in a valley has the worst precision. The influence of species is distinguished in combination with other factors, explained in following affirmations.

The sunny exposure favours the precision in the European beech forest, while in the norway spruce forest more favourable is a partially sunny exposure.

Forest consistency does not affect the precision of point's determination. This has approximately the same value regardless of the size of the consistency index.

Tree age does not have a visible influence on the accuracy, the values obtained being significantly closer, regardless of age class.

If we would make a ranking of the most favourable locations the first place would go to the alpine barren zone where there is no vegetation to block the signal and where we obtain the highest precision. The second place would go to the forest roads and the third to a Norway spruce forest located on a ridge or a slope, with over 60 years and with favourable exposure in respect to the satellite's movement.

As a result, the development of cadastral plans in such territories, using GNSS technology, is a viable and quick alternative, even if there are very large variations with regard to the level of accuracy, which has been influenced by various factors.

## ACKNOWLEDGEMENTS

The research work was carried out with the guidance and support of my scientific coordinator, Lecturer PhD. Eng. Cornel Cristian Teresneu.

## REFERENCES

- Boş N., 2011. Geomatica și realizarea bazei cartografice a fondului forestier din România. *Revista pădurilor* 6: 27-36.
- Crainic, Gh.C., 2011. Researches concerning the modernization of topo-geodetic works from the forestry sector. PhD thesis. Transilvania University of Brasov.
- Dogan, U., Uludag, M., Demir, D.O., 2014. Investigation of GPS positioning accuracy during the seasonal variation. *Measurement* 53: 91-100.
- Janez G., Adrados C., Joachim J., Gendner J.P., Pepin D., 2004. Performance of differential GPS collars in temperate mountain forest. *Comptes Rendus Biologies*, 327: 1143-1149.
- Ordonez Galan C., Rodriguez Perez J.R., Garcia Cortez S., Bernardo Sanchez A., 2013. Analysis of the influence of forestry environments on the accuracy of GPS measurements by means of recurrent neural networks. *Mathematical and Computer Modelling*, Volume 57, Issues 7-8, 2016-2023.
- Ordonez Galan C., Rodriguez Perez J.R., Martinez Tores J., Garcia Nieto P.J., 2011. Analysis of the influence of forestry environments on the accuracy of GPS measurements by using genetic algorithms. *Mathematical and Computer Modelling*, Volume 54, Issues 7-8, 1829-1834.
- Păunescu C., Dimitriu S.G., Mocanu V., 2012. Sistemul de determinare a poziției utilizând sateliți (GNSS). University of Bucharest Publishing House, Bucharest, 204p.
- Sawaguchi I., Nishida K., Shishiuchi M., Tatsukawa S., 2003. Positioning precision and sampling number of DGPS under forest canopies. *Journal of Forest Research* 8: 133-137.
- Sigrist P., Coppin P., Hermy M., 1999. Impact of forest canopy on quality and accuracy of GPS measurements. *International Journal of Remote Sensing*, volume 20, Issue 18: 3595-3610.
- Tachiki Y., Yosimura T., Hasegawa H., Mita T., Sakai T., Nakamura F., 2005. Effects of polyline simplification of dynamic GPS data under forest canopy on area and perimeter estimation. *Journal of Forest Research* 10: 419-427.
- Taczanowska K., Gonzales L.M., Garcia-Masso X., Muhar A., Brandenburg C., Toca-Herrera J.L., 2014. Evaluating the structure and use of hiking trails in recreational areas using a mixed GPS tracking and graph theory approach. In *Applied Geography*, Volume 55: 184-192.
- Tereșneu C.C., 2011. Some aspects of accuracy of determining the coordinates points in forestry. *Studia Universitatis "Vasile Goldiș" Arad, Seria Științe Inginerești și Agro-Turism*, vol. 6, Issue 2, p. 7-10.
- Tereșneu C.C., Vasilescu M.M., Hanganu H., Vlad-Drăghici H.G., Tamaș Șt., 2011: Analiză GIS privind implicațiile redeterminării poziției bornelor silvice. *GeoPreVi* 2011, *Geodezie prezent și viitor* 1: 355-364.
- Tereșneu C.C., Vorovencii I, Vasilescu M.M., 2014: Statistical study on the accuracy of determining points coordinates in mountain forests from Bran-Brasov, Romania. 14th SGEM Geoconference on Informatics, Geoinformatics and Remote Sensing, *Conference Proceedings*, Vol. 3: 893-900.
- Vorovencii, 2014: A change vector analysis technique for monitoring land cover changes in Copsa Mica, Romania, in the period 1985-2011. *Environmental Monitoring and Assessment* 186 (9): 5951-5968.
- Vorovencii, 2014: Detection on environmental changes due to windthrows using Landsat 7 ETM+ satellite images. *Environmental Engineering and Management Journal* 13 (3): 565-576.
- Wang H., Zhan X., Zhang Y., 2008. Geometric dilution of precision for GPS single-point positioning based on four satellites. *Journal of Systems Engineering and Electronics* 19(5): 1058-1063.
- Weilin L., Buo X., Yu L., 2000. Applications of RS, GPS and GIS to Forest Management in China. *Journal of Forestry Research*, 11: 69-71.
- Wing M.G., Frank, J., 2011. Vertical measurement accuracy and reliability of mapping-grade GPS receivers. *Computers and Electronics in Agriculture* 78(2), 188-194.
- Yosimura T., Hasegawa H., 2003. Comparing the precision and accuracy of GPS positioning in forested areas. *Journal of Forest Research* 8: 147-152.
- Zhang H., Zheng J., Dorr G., Zhou H., Ge Y., 2014. Testing of GPS Accuracy for Precision Forestry Applications. *Arabian Journal for Science and Engineering* 39(1): 237-245.

## STUDIES REGARDING THE DETERMINATION OF GEOMETRIC DIMENSIONS AND GEOMETRICAL DEVIATIONS COMPARING WITH THE PROJECTED ONES FOR FUEL TANKS

Codruța – Rozica SILVĂȘAN-PAȘCA, Simona – Lenuța MLEȘNIȚE

Scientific Coordinators: Prof. PhD Eng. Mircea ORTELECAN, Lecturer PhD Eng. Tudor SĂLĂGEAN

University of Agricultural Sciences and Veterinary Medicine of Cluj-Napoca, Calea Mănăștur 3-5, 400372, Cluj-Napoca, Romania | Tel: +40-264-596.384 | Fax: +40-264-593.792

Corresponding author email: codruta.silvasan@yahoo.ro

### Abstract

The study was realised having purpose to make the topographical measurements in view of determining the geometrical dimensions and the geometrical deviations of the tank for rating his technical condition. First of all we made the recognition of the placing area of the tank subjected to determinations and in the same time the visual inspection was made and were determined a number of 16 stationary points . For the field work were used full stations and GNSS receptors. The geometrical dimensions and the geometrical deviations of the bottom of the tank were determined by inside measurements from one stationary point . The measurements processing was made with specialized programs from my own equipment. The results of the measurements regarding the geometrical dimensions and the shape deviations of the tank have been submitted in specialised statements provided by the beneficiary.

**Key words:** fuel tank, geometrical dimensions, deviations, deformations, measurements.

### INTRODUCTION

The measuring of deformations means all measurements realised to establish a permanent or elastic deformation of objects, under the influence of internal and external forces. Such deformations, and the need to refer them, appear in various fields. Using the topo-geodetic measurement methods has particular importance (Coșarcă, 2011).

The displacement means changing the position of a point of the construction submitted to solicitations and deformation means changing the relative distance between the points of that construction (Ortelecan and Pop, 2005).

The movements may be linear (in the case of translational movement) or square (in the case of rotary movements) (Palamariu and Popa, 2009). In the category of linear movements and deformations are: - settlements, or downward vertical movement of construction foundations due to deformation of the foundation soil; - Bulging or lifting up which is the vertical movement of building foundations; - Arrows of some construction elements (beams, columns, slabs) subjected to vertical or horizontal loads causing bending thereof; - Biases due to uneven settlements without interference of geometrical constructions and their component elements, that can be expressed by linear or angular value; - Cracks and fissures, which are breaks in the plane or in separate parts of the structure, due to uneven subsidence and the occurrence of additional stresses; - Horizontal displacements, of some elements of the building or the construction as a whole, due mostly to horizontal forces (pushing the earth, pushing water, etc.), or change in the balance of the soil foundation construction (Pop and Ortelecan, 2005).



a) Deformation

b) Displacement

Figure 1. Deformation and displacement

## MATERIALS AND METHODS

Body of property that has the tank R4 (Figure 2) subject to topographic measurements in order to determine the geometric dimensions and geometrical deviations is owned by Rompetrol Warehouse Craiova , Dolj County.

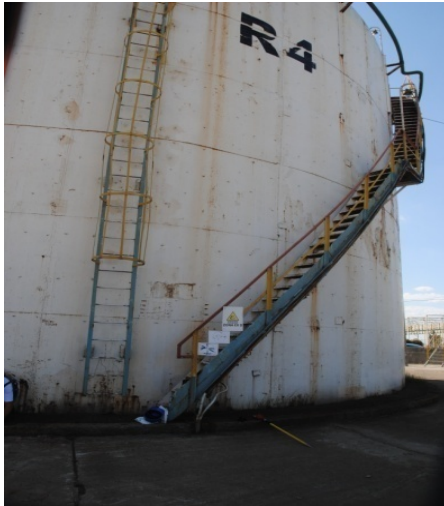


Figure 2 Fuel tank R4

During field reconnaissance it was identified the site of the 3150 m<sup>3</sup> R4 tank and station points were set so that they can perform in all necessary measurements to determine the geometric dimensions and geometrical deviations requested. For the measurements were determined following points:

- starting point and traverse closure, denoted by RPT2;
- point of orientation for the traverse, denoted by RPT1;
- traverse points, marked from R41 to R49 and R410 to R416.

The point RPT2 was established in the tank R4 and RPT1 point was established in the tank R1, both near the wall of the containment tank. R41-R49 and R410-R416

points were established in the 16 rays from the manhole shaft clockwise.

To realise the traverse measurements and sideshot for external details, it was used a total station Leica TCR 1205 (Figure 3), for sideshots representing details inside the tank, it was used a total station Leica TC 410 C, and for determining the coordinates of starting, closing and guidance of the traverse used ProMark2 Ashtech GNSS receivers type. Given the location of the tank R4, i.e. a retention tank with high walls allowing visibility only inside it was established as a method for determining the coordinates of the station points, closed traverse on the starting point.



Figure 3. Total station Leica TCR 1205

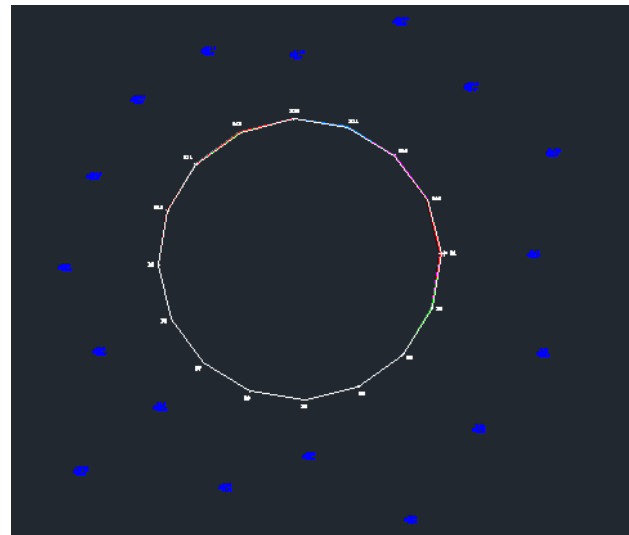


Figure 4 Related to the fuel stations

Outline of measuring the R4 tank - For realizing the measurements with sufficient

accuracy , there were used topographic measuring instruments (level and theodolite). The circumference of the reservoir was divided into 16 arcs of a circle (Figure 3), resulting in eight diameters. There were measured :

- The bottom of the tank for each of the 8 diameters ;
- Shell height and verticality deviation measured between core and mantle -cap combination for each of the 16 points on the circumference ;
- The diameter of each sleeve tank for the 8 diameters thereof;
- Local defects of the shell for the entire outer surface thereof .

### RESULTS AND DISCUSSIONS

Checking the bottom of the tank geometry R4 - According to Norm C 220 , for tanks made by rolling , local deformations of the bottom of the tanks must fall within  $\pm 30$  mm length of 3.00 m . As shown in the bottom profiles (Figure 5), based on made measurements, the measured deviations are above this level. Generally the bottom of the tank has a sinusoidal profile with a minimum in the center and maximum in the area near the mantle.

Compared to the virtual center line of the bottom there were measured large deviations in the following areas:

- Positive deviations between the D1 point and the center tank 40 mm and 43 mm

positive deviations between the center of the tank and the 43mm D9 point;

- Negative deviations in the D2 point near the sheath (35 mm) and positive deviations in the opposite diametral area D10 (45 mm);
- Positive deviations in the D3 point near the sheath (49 mm) and in the opposite diametral area D11 (35 mm);
- Positive deviations in the point D4, near the mantle (69 mm);
- Positive deviations in the D5 point near mantle (60 mm);
- Positive deviation in the D6 point near the sheath (61 mm);
- Positive deviation in the point D7 near the mantle (44 mm) and in the opposite diametral area, from the point D15 and the reservoir mantle (57 mm);
- Negative deviation in the D8 point near the sheath (28 mm) and positive drift in the opposite diametral area, from the point D16 and the reservoir mantle (75 mm).

The measurements confirm the results of visual inspection. Also, the measurements yielded relatively high rate differences between diametrically opposed points detailed in Table 1.

Verification of the geometry of the tank shell R4 - According to the Standards R4 tank C220 offset from verticality and the height difference between the top and bottom (Figure 6) must be less than  $\pm 60$  mm ( tanks manufactured by rolling with a volume of 2000 ... 5000 m<sup>3</sup> ) .

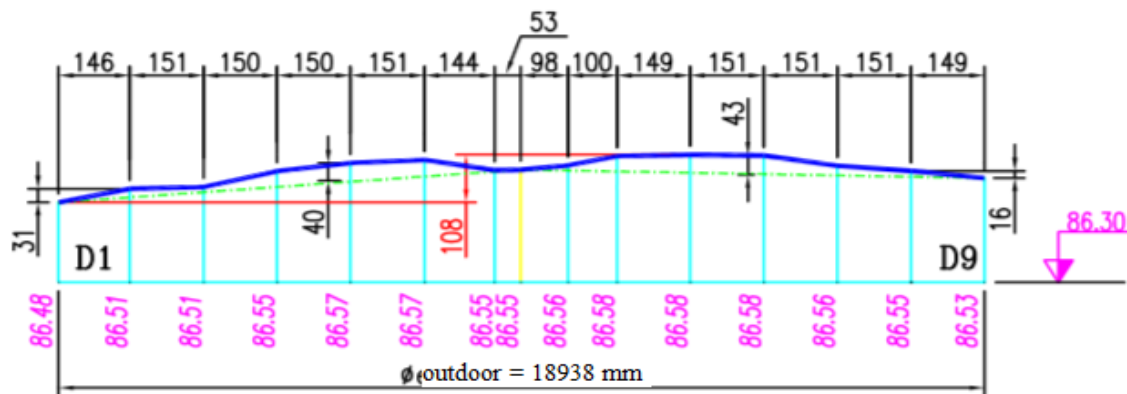


Figure 5. Example of Section of the Bottom (D1-D9 diameter)

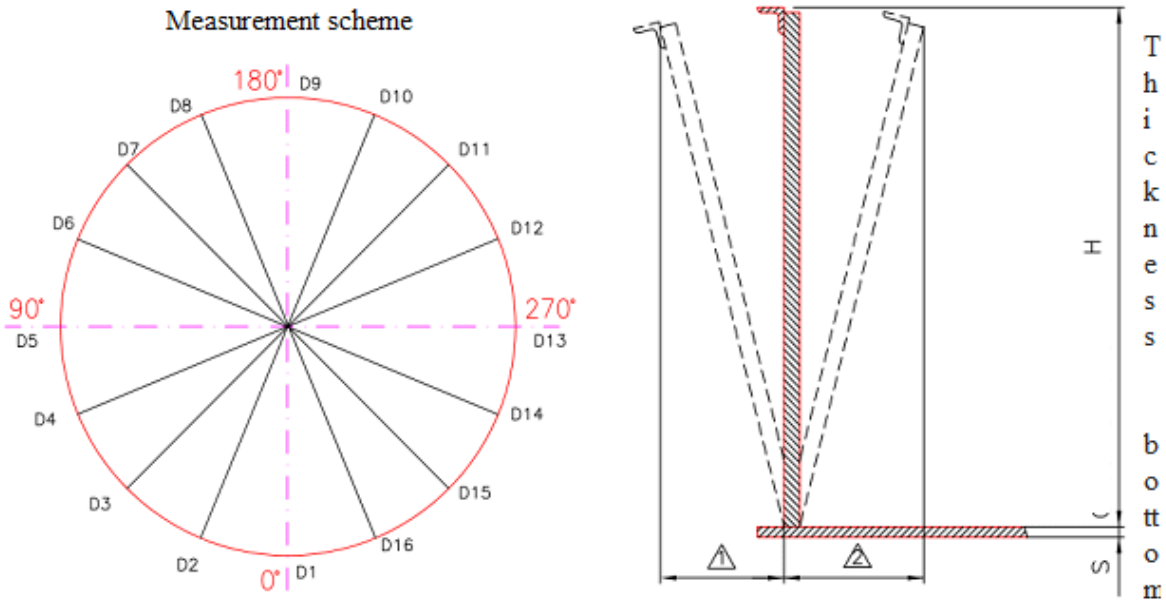


Figure 6. Offset from verticality and the height difference between the top and bottom

From the measurements sheet it is found that the deviation from verticality is in some measure points above the permissible limits according to Table 2.

Deviation from the shell height falls within acceptable limits. The deviation of the diameter of the cover, according to Norm C 220 must be within  $\pm 60$  mm. To determine the relative deviation was considered average diameter (arithmetic mean of the diameters measured for each sleeve (Figure 7).

Table 1 - Diameters

Nr. crt.	Diameter	Share	Difference (mm)
1.	D1 – D9	D1: 86.48; D9: 86.53	50
2.	D2 – D10	D2: 86.45; D10: 86.55	100
3.	D3 – D11	D3: 86.45; D11: 86.55	100
4.	D4 – D12	D4: 86.46; D12: 86.55	90
5.	D5 – D13	D5: 86.46; D13: 86.45	70
6.	D6 – D14	D6: 86.48; D14: 86.54	60
7.	D7 – D15	D7: 86.50; D15: 86.51	10
8.	D8 – D16	D8: 86.52; D16: 86.50	20

Table 2. Deviations

Nr. crt.	Measuring point	Deviation (mm)
1.	D1	-94
2.	D2	-72
3.	D10	+69
4.	D11	+97
5.	D12	186
6.	D16	-62

Sheet measurements shows that the diameter D8 - D16 of the sleeve V relative deviation exceeds allowable deviation. In addition, V2 ... V7 shells absolute deviation, calculated as the difference between the maximum diameter and the minimum diameter of the shell thereof, is greater than the permissible deviation. The largest absolute deviation is recorded for Virola V and lowest for Virola I. Based on data sheet thicknesses tank geometry, resulting average diameter of each sleeve jacket, in Table 3.

Analyzing the data in the table above, it appears that the maximum difference between the inner diameters is  $18974 - 18952 = 22$  mm. Concerning the local deformations (concavity, convexity), Norm C 220 requires it to be within the range  $\pm 12$  mm on length of 1.00 m. Sheet measurements shows that the tank has 17 local deformation zones (Figure 8) exceeding the allowable deviation. Most of them are in the area between the axes of  $90^\circ$  and  $180^\circ$ , on the entire height of the tank, which is the welding of the mounting on site, of the shell.

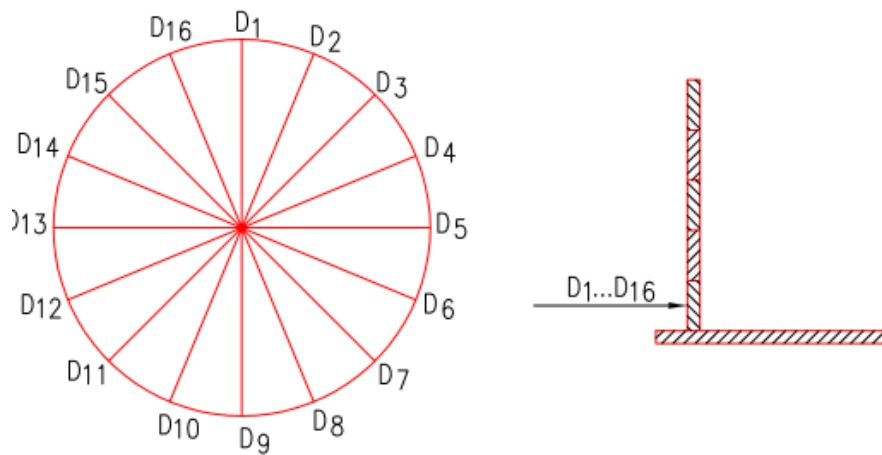
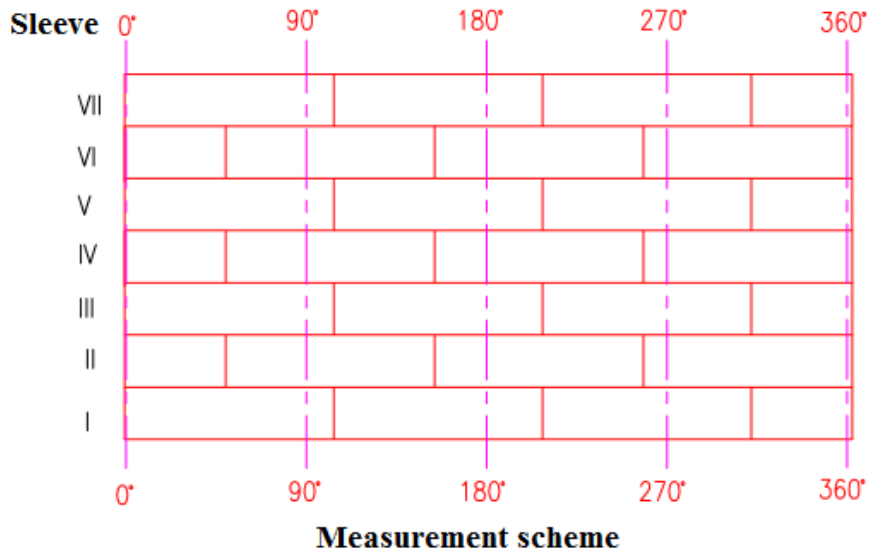


Figure 7. Diameter of the cover

1. A negative deviation: the distance between the perpendicular lower point of welding of the sheath to the cap and the horizontal plane of the container is in its interior. Positive deviation: the distance between the perpendicular lower point of welding of the shell with the cover of the container and the horizontal plane is situated outside it.

Verification of R4 tank compaction - No measurements were performed to establish the foundation subsidence but measurements analysis revealed a mean difference of level between the top and bottom of the tank and the foundation ring of about 6 cm. This value can be regarded as settling tank on the elastic bed of the foundation...Sheet measurements

shows that the bottom subsidence occurred in the points D1 ... D5 and between axes 0 and 90 of the tank. On the other hand, an attempt to seal the space between the shell and the foundation ring with asphalt mortar does not lead to the prevention of water infiltration below the bottom of the tank.

Moreover, this measure could exacerbate corrosion of the weld bottom corner and outer sheath because the water does not evaporate from the area after the cessation of the rain. During winter, the frozen water in the area of contact between asphalt mortar and combination bottom-shell also hastens corrosion.

Nr. crt.	Number sleeve	Average diameter outdoor (mm)	Average thickness of the sheet (mm)	Average diameter interior (mm)
1.	V1	18972,5	8,65	18955
2.	V2	18982	7,74	18966
3.	V3	18987	6,72	<b>18974</b>
4.	V4	18966	6,65	18953
5.	V5	18972	6,70	18959
6.	V6	18965	6,71	<b>18952</b>
7.	V7	18972	6,63	18959

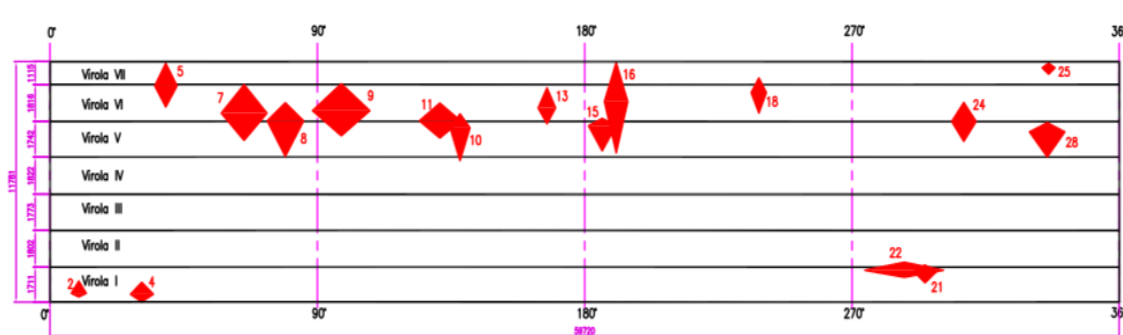


Figure 8 Local deformation zones

## CONCLUSIONS

The causes of deformations can be summarized into two groups: a) deformations that may occur due to the action of permanent or temporary factors: nature of the terrain, the static structure of the building, normal wear or responding to changing meteorological factors; b) deformations that may occur also because of mistakes in execution, the use of improper materials or due to external influences such as earthquakes, vibration, flooding or underground works.

Particular importance of displacements measurements is given to the fact that it can achieve both geometrical sizes actual control (displacements, size, flatness, roughness) and the fact that a number of other physical quantities can be determined by measuring the effect produced by this materialized effect by the movement of a point (pressure, force, level, temperature, etc.) which are usually characterized by small movements (linear and angular).

Following studies on reservoir R4 on determining the geometric dimensions and geometrical deviations is found that the largest deformations are between axes 0 and 90 of the tank. Measurement, processing, calculation and representation settlements, horizontal

displacements or inclinations of higher buildings can be done today with Topographic modern technologies, automated, which associated with the correct application of specific methods, gives the guarantee of a fair highlights of instability phenomena of the buildings.

Thus, based on studies and concrete results in various stages of research, we found that choosing the correct methods and appropriate technology, is sure a correct interpretation of the measured values and further processed on the basis of calculation algorithms based on the concepts of processing the observations of the theory of measurement errors.

## REFERENCES

- Constantin Coșarcă, Măsurători inginerești - Aplicații în domeniul construcțiilor (partea I), Editura Matrix Rom, București, 2011
- Pop Nicolae, Miercea Ortelecan, Topografie Inginerească, Editura Academic Pres, Cluj Napoca, 2005
- Marcel Palamariu, Alexandru Popa, Urmărirea comportării terenurilor și construcțiilor, Seria Didactică, Alba Iulia, 2009
- Ortelecan Miercea, Pop Nicolae, Metode topografice de urmărire a comportării construcțiilor și terenurilor înconjurătoare, Editura AcademicPres, Cluj Napoca, 2005
- <http://www.ct.upt.ro/users/SorinHerban/Mudc.pdf>

## EXTENSION OF THE WATER NETWORK IN THE TOWN HOLBAV TECHNICAL AND LEGAL ASPECTS

Raluca Veronica ȘERBAN

Scientific Coordinator: Lect. PhD. Eng. Cornel Cristian TEREȘNEU

Transilvania University of Brasov, Faculty of Silviculture and Forest Engineering, 1,  
ȘirulBeetoven, 500123, Brasov, Romania, Phone: +40268 418600 Fax: +40268 475705,  
Email: raluca.veronica.serban@gmail.com

Corresponding author email: raluca.veronica.serban@gmail.com

### Abstract

*In this work it is desirable to show legal and technical aspects of extension of the water network in the town Holbav, Brașov county. Having regard to geographical positioning and orographic for the locality, legal aspects of this work aimed at removing some land areas of forest fund. To perform the measurements necessary to project the extending the network of water use has been made of a total station SOKKIA and apparatus GNSS. Total station was used in carrying out the lift network, being a network supported on known points. GNSS equipment has been used in determining the points station using their positioning by process static and the procedure Real Time Kinematics (RTK). On this occasion shall be investigated and process accuracy Real Time Kinematics (RTK) for the forestry sector and the factors that influence the accuracy. In the work of extending the network of water in this town Holbav, Brașov county desired positioning of a new water basin at an altitude of upper front positioning existing basin, with a view to enlargement, as well as more advantageous uses of the network, and profitable in relation to the cost of use of the network. From a technical point of view, the network of lifting has been carried out between the existing and new pit they wanted to place it virtually. Whereas it is desirable to place a new water basin inside Holbav locality, in a wooded area, concerned into the forestry of this territorial administrative units will reach legal aspect. So for the area where it is desirable the location of water basin must be that this area will be taken permanently out of the forest, and for the surface where it will place new pipes must be temporarily out of forest fund (for the work of fitting and location). In conclusion, in order to achieve a work for the forestry sector must be attained both legal aspects of the job, but special attention should be paid to technical aspect from the point of view of the difficulty with which can also be done from the point of view of accuracy which is difficult to attain.*

**Key words:** RTK, topographic survey, compensation, forestry.

### INTRODUCTION

In the locality Holbav, Brașov county, it is intended to extend the water network, placing a new water basin at an altitude superior to existing water basin in that area. It is desired location basin of water in that area to facilitate distribution of water in the locality. Considering that the new location is a mountain area must make a documentation in order to obtain approval for permanent or temporary employment removal from the national forestry Fund lands. The entire documentation to be done, I will be focus in this work on raising the topographic surface required for removing definitive/temporary employment of national forest fund. In carrying out the topographic surface network I will use both GNSS equipment and methods, as well as total station

and classical methods traverse and lifting plan details.

### MATERIALS AND METHODS

In order to achieve raising the topographic surface required for removing definitive/temporary employment of national forest fund has been used in the determination GNSS equipment end-points and the points of station within traverses on the new location. GNSS equipment was used to determine details coordinates in the field.

To determine the end points of the traverse has been used static positioning.

Static measurements receivers are fixed in the time concerned measurements - also known as "sessions". The results shall be deducted from subsequent successive measurements carried

out by the receiver at specific time intervals pre-set called "era of measurement", as a rule common to all receivers involved in a working session. (Chițea& All, 2013)

For the positioning of the station traverse points in the new location and the detail of the existing water network was used purely cinematic method, i.e. the method to real-time kinematic (RTK).

Method Real Time Kinematic (RTK) is a method for the determination of the relationship between a point known to control and a point unknown carriers using measurements of the phase. A base station with known position transmit corrections toward the receiver or receivers mobile. Procedure provides a high accuracy in real-time, and the results obtained are not features processed. In the early days GPS, kinematic positioning and high were not frequently used for that the methods of resolution ambiguous were still ineffective. Later, when the resolution ambiguous, such as on-the-fly (OTF) have become available, Real time kinematic and other similar methods of positioning have become widely used. (Chițea& All, 2013)

All topographical lift to achieve has been used Total station and classical method of traverse supported on known points (point what have been previously determined with equipment and techniques GNSS). Using this method have been measured points of detail on the ground on section of new location. Total station and traverse method has been used only to the portion of the field where it is desirable to location of water basin, area that new location. Method traverse, apart from the fact that it constitutes a method of distinct thickening of the support network is a method of carrying out the topographic networks raise, but can be a lifting way detail. (Chițea& All, 2011)

Traverse is a broken polygonal line, where mutual position of the points is determined by measuring distances between the point of breaking and by measuring the angle at the point of breaking of polygon element. In each workstation traverse shall be measured horizontal angular directions, distances and Vertical angles. As a rule of measurement we can establish that first point in the measurement to be the point of traverse at rear (base station or

the point of previous guidance), and the second to be the point of traverse next. (Manea)

In a classic traverse to measure horizontal angles in all the old and new points, with a value of "0" on the horizontal circle always introduced on the previous point (back).. Horizontal angles during traverse shall be measured on the same side of traverse. (Chițea& All, 2011)

Vertical angles (tilt angles) using Total station are measured automatically, once with endorsing required point. It also distances are measured electronically. For the calculation of coordinates of points from both the traverse and the measurement of details (further measurement operation), will use horizontal angles, tilt angles and distances reduced on the horizon, to be obtained from the distance at an angle and the tilt angle (data measured in the field).

## RESULTS AND DISCUSSIONS

GNSS equipment using static method of measured points were end of lift network, these being measured and RTK method.

For the positioning of the station points, the end of the lift network, but also for other significant detail in the work was pure cinematic process use in real time. In the positioning of these points has been given special attention, therefore, to define more precisely the position of each point we achieved successive measurements. The final coordinates of points resulting in average.

In this respect I will analyse the accuracy of positioning of points depending on HRMS and VRMS, as average of all measurements to determine the coordinates of a point (Table 1), (Figure 1).

Table 1. Accuracy HRMS, VRMS of the points of station

No Point	1	2	3	4	5
HRMS Avg	0.0031	0.0032	0.0035	0.0054	0.0035
VRMS Avg	0.0054	0.0059	0.0082	0.0115	0.0064
No Point	6	7	8	9	10
HRMS Avg	0.0035	0.0040	0.0083	0.0034	0.0043
VRMS Avg	0.0062	0.0071	0.0107	0.0064	0.0071

HRMS represents tolerance defined by radius of a circle which contains 50% of individual measurements which are carried out, or less

than the radius circle inside which there is a probability of 50% to find out they, respectively position accuracy in the horizontal plane. (Carlson Software, 2007)

VRMS shall mean tolerance as defined by a sphere where a point can be found, with a probability of 50 %, respectively accuracy in the vertical plane. (Carlson Software, 2007)

HRMS and VRMS are expressed in meters. Both the table and the graph can be seen as positioning accuracy in both horizontal and vertical plane is very good. On the horizontal plane can be seen as most have accuracy for positioning of 3 mm. And in the vertical plane can be seen as an average for positioning is 7 mm.

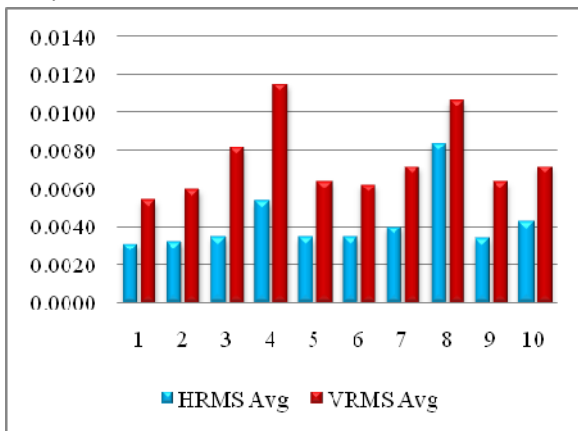


Figure 1. The positioning accuracy of the points of station



Figure 2. The overlaying of points collected with GPS on orthophotomap

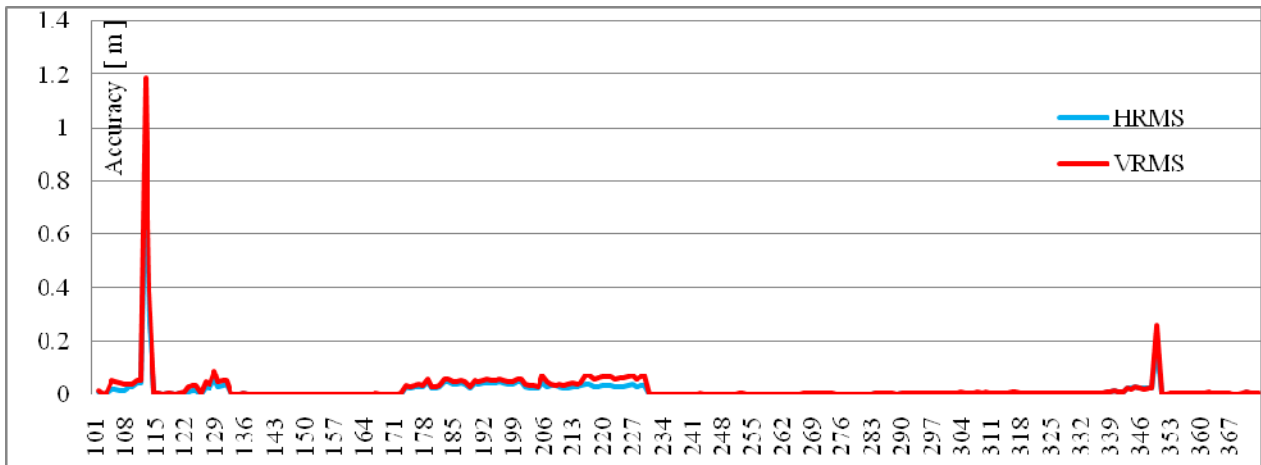


Figure 3. The positioning accuracy of the points of detail positioned by the method RTK

Here infer that points have been positioned with an accuracy particularly good taking into account the positioning method and the area in

which they were carried out measurements. Taking into account an measurements have been carried out in a wooded area position

accuracy may suffer. What can be observed for items 4 and 8 (points surrounded by trees), these points with lowest accuracy on both horizontal and vertical planes (Figure 2).

It also can be analysis and position accuracy of points of detail determined by method Real time kinematic. These points of detail means vicinal road Vârf la Cruce-Măgura (new road). For the positioning of these points were not given special attention as in the above analysis points. The coordinates of these points have been determined through a series of single measurements. But you can see easily how vegetation can influence the accuracy of positioning both in horizontal and in vertical plane (Figure 3, Figure 4).



Figure 4. Overlapping points of detail on orthophotomap

For measuring network has used a type of SOKKIA total station. It is mentioned as a measuring network connects with vicinal road Vârf la Cruce-Măgura (new road) whose points have been determined previously (Figure 5).

Measuring network was achieved in locally, starting with arbitrary coordinates 1000,1000,800 (first point of station), which coincides with point 4 point determined with the GNSS equipment and methods. The orientation measured on the point 2 of station, concerned point 3 positioned with the GPS.

In total traverse contains 15 points, of which 13 of them are station points, and 2 points are orientation points, point 2 and 15 of the traverse what coincides with points 3 and 10 respectively determined with GPS. Traverse closes on point 14 of station (respectively point 9 positioned with the GPS), to the orientation on the point 15 (Figure 6).



Figure 5. Points of detail taken over and RTK traverse

In the traverse have been measured and the details on the ground that the majority in cases means vicinal road Vârf la Cruce-Măgura (new road).

Download land license was done with Pro LINK software version 1.15 (Tereşneu, 2012), which automatically calculated from the coordinate traverse, depending on horizontal and vertical angles, distances and orientations measured in the field. Placing from arbitrary coordinates (1000, 1000, 800) for the first point of station, all measured points were positioned in a local reference system.

For the points in the traverse have coordinated in the reference system Stereographic 1970 we did coordinate transformation from common points 1, 2, 14, 15 (points stations in local system), and points 4, 3, 9, 10 (points determined with equipment GNSS, points determined in the system Stereograph 1970). This coordinate transformation was effected with TopoSys software version 4.2 (Tereşneu, 2012), using a spatial transformation using Helmert parameters

Subsequently the coordinate transformation operation have been compensated for station points within the measurement network. The classical compensation depending on the end points (orientation points), respectively known

points determined with particular attention in previous steps. After getting the coordinates of the station were compensated and corrected coordinates of detail points, measured in the traverse.

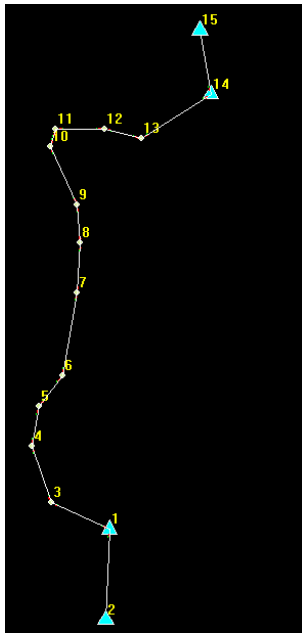


Figure 6. Traverse supported on end points

All of these operations means the appearance of technical work extending the network of water from the point of view of cadastre and land measurements. The measurements of the amount of land, processing and processing of the data collected necessary for carrying out the topographic surface lift required for removing definitive/temporary employment of national forest fund.

## LEGAL ASPECTS

Documentation to be compiled in order to obtain approval for permanent or temporary employment removal from the national forestry fund lands includes the following information:

The eject request final beneficiary and/or temporary employment land in the national forest fund, which was addressed to the territorial subunitatii specialty of central public authority responsible for forestry place land;  
 Memorial techno-justifying the need of removal definitive or temporary employment of forest land in national fund;  
 Plan for Employment in the area;

The detail Plan objective of a site;

A copy of the map that is materialized landscape planners target site;

Technical Data transmission-grubbing;

Pedologicalstudy for land offered as compensation, in the case of applications for permanent putting with offset;

Raising the topographic surface required for definitive removal/temporary employment of national forest fund;

Documents, in hard copy, by which proof of ownership of land required for definitive removal/temporary employment of national forest fund;

The land register references land which shall be made available in offset or the land register references for the entire property on which it holds the recipient;

The subject of a favourable opinion by the county forest division which provides management or the provision of services for forest land required;

County forest division confirmed that manage/forestry services, in the case of applications for temporary employment;

The Agreement of owner for forest lands in which to specify including that the land is not in dispute;

The Agreement of the environment or the point of view of the authority of the environment, as appropriate;

Copy of the document for the payment of the fee for permanent putting or guarantee for temporary use.

According to forestry Code (Law No 46/2008) this provides:

It may be permissible to reduce national forestry surface through removal final, for the achievement of the objectives of national interest, declared of public interest and in accordance with the provisions of the law.(Art. 36, para. (1))

On request, the applicant land on which are to be carried out objectives referred to in paragraph (1) can compensate for land area planted with an equivalent area and trustworthiness, in which case shall not be paid the equivalent of land national forest fund, but shall be paid in advance other obligations cash.(Art. 36, para. (2))

Compensation referred to in paragraph (2) shall be carried out in equivalent value, under the

conditions in which the surface of the site given compensation may not be less than the area land covered by forest removal from the fund. (Art. 36, para. (3))

Can be removed from national forest fund, only on condition that their compensation, without reducing forestry area and the anticipated payment of financial obligations, only those land necessary for the realization of or extending following categories of objectives:

a) exploitation necessary following mineral resources: coal, rocks useful, aggregated minerals, ores and mineral waters;

b) structures of receipt functions with tourism tourist accommodation, units of cult, objective social, sporting and medical, triplet of local interest, drinking water supplies, c) Homes or holiday houses, forest fund only in private property;

d) point installed in the forest before 1990, contained in the forest management plan in force on 1 January 1990, in the category "occupations and litigation" (Art. 37, para. (1)) Compensation referred to in paragraph (1) shall be carried out physically with a plot of land which has five times the value of the land which shall be removed permanently from the fund forestry, and surface of the site given as compensation may not be less than three times the surface of the site which is the subject of removal from the fund forestry. (Art. 37, para. (3))

Fields with which is carried out compensation referred to in paragraph (1) shall be the only outside national forest fund, but its adjacent suitable for woodlands. In a situation in which a minimum area of land which is carried out compensation is greater than 20 ha, it may not be adjacent forestry, but must be compact. Unable to achieve compensation of land situated in Alpine area and subalpina. (Art. 37, para. (4))

Land removed from the Fund and forest land received as compensation acquired legal status of the land on which they are intended to replace. (Art. 37, para. (8))

Temporary employment of forest land in the background is only permitted on a specified period of time, for the purpose of achieving the objectives of the kind referred to in Article 36 and in Article 37 (1) (a) and to ensure payment of financial obligations anticipated by the

recipient of approval of removal of forest fund for that objective. (Art. 39, para. (1))

In the case in which, for the achievement of the objectives referred to in Article 37 (1) (b) - (c), are necessary and other adjacent land for the organization of construction site, they will be temporarily occupied, for a maximum period of one year and in an amount equal to not more than 10 % of the area requested to be permanently forest fund. (Art. 39, para. (4))

Period in respect of which it is hereby approved temporary employment of land from the fund forestry includes the time needed for carrying out the works lands under conditions to be suitable for woodlands. (Art. 39, para (5))

Considering all these mentioned and the fact that the surface wants to permanently remove from the forestry is 357 square meters, the surface you need to impersonate, equivalent must not be of a smaller area of 1071 square feet. But this condition is fulfilled, as equivalent will yield a surface of 2000 square meters stripped down from the pasture 2292254 square meters, registered with the topography number 1513/1/ 1/1/ 1/1/ 4/1/ 1/1, and to the number of Land Register 100295, pasture within one and the same localities.

In terms of the surface to be removed temporarily from the national forestry Fund, this is represented by the future water pipe in length from 2195 meters.

For it will submit in advance the financial obligations for approval to remove the forest for that objective. In this sense, there will lodge the security, equivalent to the fee charged for definitive removal of land from the forest compensation fund, which shall be paid in advance of issue of approval and shall be deposited in the fund for the improvement of agriculture fund with destination forestry; the rent, which shall be paid in the case of owner, forestry private property of the natural and legal persons, i.e. the public property of territorial-administrative units; for owned forests of the state, 50% of the lease payment shall be deposited in the fund for the conservation and regeneration of forests and 50% shall be paid administrator; The equivalent loss of growth determined by mass exploitation woody before the age technical exploitability disused objectives; the value of the land concerned; expenses for re-installing



## 3 D MODELLING

**Daniela TRANA**

**Scientific Coordinator: Assoc. Prof. PhD. Levente Dimen**

” 1 Decembrie 1918 “ University of Alba-Iulia, 15-17, Unirii Street, 510009, Alba-Iulia, Romania,  
Phone: +40258.811.512, Fax: + 40258.812.630, Email: arad\_danielle@yahoo.com

Corresponding author email: arad\_danielle@yahoo.com

### **Abstract:**

*This project is about the improvement of traditional methods for surveying, documenting and WBE (Web-based Education) for Archaeological Sites and Cultural Landscapes & Heritage (CLH); especially by synergy effects gained by the combination of ICT low-cost techniques as innovative practices under digital Photogrammetry. I used the PhotoModeler Scanner, the Direct –Digital RECTifier, PhotoScan Pro (Agisoft) and the Calib softwares, in order to practice and manage to create the 3d model of a Egyptian Building façade, of a Monument, of the Pillar, Sarcophagus, Lion Statue and the Sphinx Sculpture .*

**Key words:** photogrammetry, 3d modeling, softwares

## **INTRODUCTION**

Photogrammetry is an estimative scientific method that aims at recovering the exact positions and motion pathways of designated reference points located on any moving object, on its components and in the immediately adjacent environment. Photogrammetry employs high-speed imaging and the accurate methods of remote sensing in order to detect, measure and record complex 2-D and 3-D motion fields. Photogrammetry belongs to measurement techniques, which aims to study and define precisely the shape, size and position in space of the objects, based on the measurements of one or more photos of the objects.

## **MATERIALS AND METHODS**

### **Notebook**

For all project calculations and operations, I used a laptop DELL model Inspiron 3521 (Figure 1).



Figure 1. Dell Inspiron 3521

### **Camera**

For the acquisition of the images for the photogrammetric analysis: NIKON COOLPIX S220 (Figure 2).



Figure 2. Nikon COOLPIX S220

### **Total Station**

For the measurements, I used a South NTS-350R Total Station (Figure 3).



Figure 3. South NTS-350R Total Station

### **Direct –Digital RECTifier**

Direct is a program which rectifies images. Rectifying is a transformation process used to project two-or-more images onto a common image plane. It corrects image distortion by transforming the image into a standard coordinate system.

### **Photo Modeler Scanner**

PhotoModeler Scanner provides the tools to

create accurate, high quality 3D models and measurements from photographs. The process is called photo-based 3D scanning. It provides results similar to a 3D laser scanner. This 3D scanning process produces a dense point cloud (Dense Surface Modeling, DSM) from photographs of textured surfaces of virtually any size.

PhotoModeler Scanner is a sophisticated tool to build accurate Dense Surface Models and get measurements from your photos. Use PhotoModeler Scanner to build:

Dense Surface Models where a large number of 3D points are needed.

Models that traditionally would require a 3D laser scanner

Scale-independent object modeling - model small objects or big scenes.

**PhotoScan Pro (Agisoft)**

Agisoft PhotoScan Pro allows generating high resolution georeferenced orthophotos and exceptionally detailed DEMs / textured polygonal models. The fully automated workflow enables a non-specialist to process thousands of aerial images on a desktop computer to produce professional class photogrammetric data. It also works with terrestrial photographs, enabling the use in archaeology and cultural heritage documentation.

**RESULTS AND DISCUSSIONS**

**1. Mosaic of the Egyptian Building Façade**

The Egyptian Building façade was made with Digital RECTifier. Photo-Modeler Scanner program was used in order to calibrate the camera and to create the 3D model of the War Memorial Monument and the Pillar. The creation of the 3D model of the Lion statue, the Sarcophagus and the Sphinx sculpture was made with Agisoft PhotoScan Professional.



Figure 4. Final version of the mosaic

**2. Camera calibration**

In order, to calibrate the camera, the first and very important step is to turn off the auto-

focus setting in the camera. Then two (2) pictures, one (1) landscape or zero(0) degrees and one (1) portrait or ninety (90) degrees, have to be taken from each angle and each side of the calibration grid. The calibration grid should fill up the photo window frame as much as possible and the coded targets must be clearly seen in the photo taken. The calibration would be more accurate if there are no irrelevant noises in the photo. Finally the photos can be added in the PhotoModeler Scanner program and follow the next steps in order to begin the procedure.

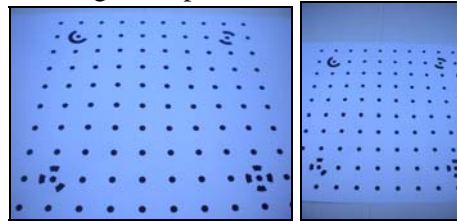


Figure 5. Landscape and portrait picture of the calibration grid

**3. War Memorial Monument**

I had to create a 3D-model of the monument by using PhotoModeler Scanner Program. I took pictures all around the monument. From all taken photos I chose six to use for the project.

After inserting the pictures in the program, the images needed to be orientated. To do this, I spotted and referenced at least six common and significant points at two pictures until all of the six pictures were orientated and the significant points were referenced with each other.



Figure 6. The finished 3D-model of the War Monument

**4. Pillar**

I also had to create a 3D-model of the pillar by using PhotoModeler Scanner Program. I took pictures all around the pillar. In the end, eleven photos were used for the process. The steps remain the same as for the Monument, such as spotting points and referencing them always on two pictures, getting surfaces and shaping them. The pillar represented a

challenge because of the special form, which is similar to a cylinder.

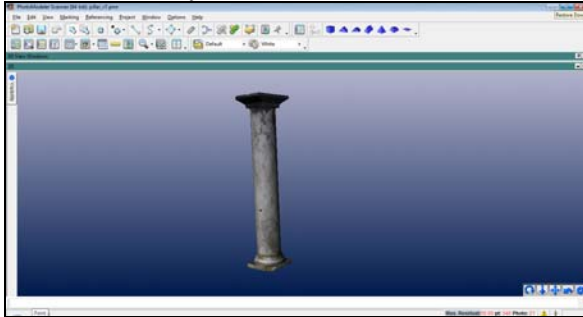


Figure 7. The finished pillar with “Quality textures” on the surfaces

## 5. Sarcophagus

## 6. Lion Statue

## 7. Sphinx Sculpture

For every project, Sarcophagus, the Lion Statue and the Sphinx Sculpture, I did in Photoscan, the steps remain the same:

- Add all photos ;
- Select “Workflow → Align Photos”;
- Select “Workflow → Build Dense Cloud”;
- Select “Workflow → Build Mesh”;
- Select “Workflow → Build Texture”;
- Add Scales;
- Delete outliers.

For the model of the sarcophagus, I used 19 images in total. I tried to take photographs from all sides around the object, as well as some pictures showing the inside between the two vertical stone plates.

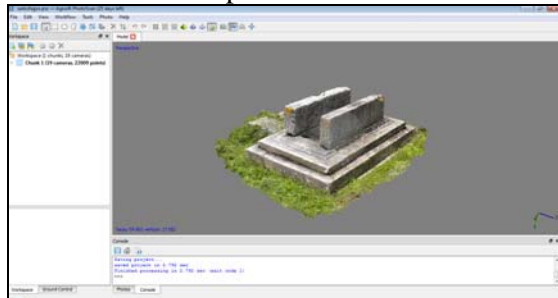


Figure 8. Finished 3D-model of Sarcophagus

The model of the lion statue in front of the Museum of Archeology was created by using 15 images from all around.

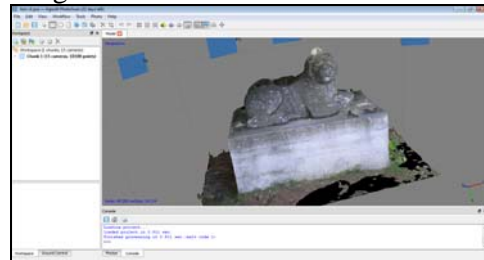


Figure 9. Finished 3D-model of the Lion Statue

Inside the Museum, I took several images of a sphinx sculpture in order to create a model. All in all, I used 23 of these images in the software.

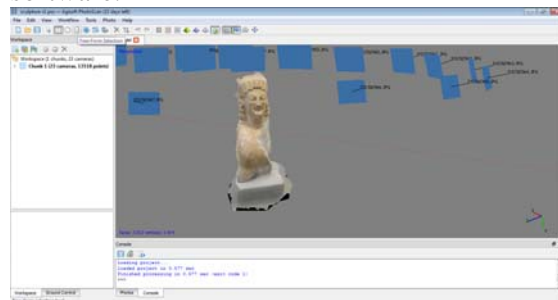


Figure 10. Finished 3D-model of the Sphinx Sculpture

Because of these programs, I was able to produce 3D-models with low-cost hardware (> 10 MP camera) that can easily be used. Despite the non-expensive equipment, the output and final product was quite satisfying and surprisingly nice looking. Obviously, the accuracy was not always very good especially regarding the pillar. This is caused by the amateur equipment.

## CONCLUSIONS

Among the benefits of 3Dmodels with PhotoModeler Scanner, I mention the followings:

- opportunity of real image acquisition with very realistic 3D models, that are applied in a large variety of fields;
- less time for field work, more time for data processing;
- minimizes the probability of unscanned zones due to shadowing effect of roughness elements and overhanging zones due to proximity to the target and the possibility of scanning from different angles and overlapping the scanning results;

providing high precision and complex data; using 3D technology, 3D models can be created; can be combined with other well established high precision surveying techniques; All in all, I definitely got deeper in topics of photogrammetry by applying programs to nice objects in reality.

## ACKNOWLEDGEMENTS

This work was supported by the Erasmus IP project financed by the European Union. I thank the Technological Institution of Kavala for their support, and the guidance and generous support in providing hardware and software licenses for training. I also wish to specifically thank the professional staff of the Technological Institute of Kavala during my stay, Mr. Athanasios STYLIADIS, Mr. Lazaros SECHIDIS, Dr. Tamás Jancsó, Mr. Vasilis TSIOKAS, Mr. Sorin HERBAN, Dr. Laszlo GERGELY, Dr. Beatrice VILCEANU, Mr. Levente DIMEN, for their valuable

participation, contributions, instructions and help – my work would not have been feasible without their gracious assistance. I also acknowledge the dedicated efforts of my team members.

## REFERENCES

- Maricel Palamariu, Levente Dimen, 2003, “Notions of terrestrial photogrammetry “, Didactica Publishing House, Alba-Iulia, p. 5  
<http://en.wikipedia.org/wiki/Photogrammetry>  
<http://www.nikonusa.com/en/Nikon-Products/Product-Archive/Compact-Digital-Cameras/COOLPIX-S220.html>  
<http://compreviews.about.com/od/budgetnote/fr/Dell-Inspiron-15-3521.html>  
<http://www.shambhaviimpex.com/total-station.html>  
<http://www.photomodeler.com/products/scanner/default.html>  
<http://www.agisoft.ru/products/photoscan/profession>  
<http://www.agisoft.ru/products/photoscan/professional/>  
Lessons about 3 D modelling, Greece



**SECTION 05**  
**FUNDAMENTAL SCIENCES**



## METHODS OF APPROXIMATING THE RIEMANN INTEGRALS AND APPLICATIONS

Ana ALEXANDRU

Scientific Coordinator: Assist. Cosmin NIȚU

University of Agronomic Sciences and Veterinary Medicine of Bucharest, 59 Mărăști Blvd, District 1, 011464, Bucharest, Romania, Phone: +4021.318.25.64, Fax: + 4021.318.25.67, Email: alexandru\_ana2000@yahoo.com

Corresponding author email: nicosro2001@yahoo.com

### Abstract

Often, in practice, one reaches to incalculable integrals, but which can be approximated by numerical methods. In fact, in terms of application, there is no need for the exact result, but for knowing its value with an accuracy no matter how good. In this paper we present two methods to approximate Riemann integrals: the method of rectangles and trapezoids method. After reviewing the theoretical results, we consider some applications, focusing on the precision of approximations.

**Key words:** Riemann integral, rectangle method, trapezoidal method, approximation, precision

### INTRODUCTION

Sometimes, in our practice work, we obtain integrals with incomputable primitives, called transcendental integrals. In some cases, these integrals can be calculated with more advanced techniques, such as complex analysis, but most of the times they can only be approximated by numerical methods. The most elementary methods are linked to Riemann sums: rectangles method, trapezoids method, Simpson's method, Hermite's method, Newton's method etc. In this article, we consider only first two methods. We begin by proving the formulas and then we apply them to several integrals, some of which have important applications.

### MATERIALS AND METHODS

We follow (Grigore, 1990), (Munteanu and Stanica, 2006) and (Rosca, 2000) for the proofs.

The rectangles method

In mathematics, especially in integral calculus, the rectangle method (also called the midpoint or mid-ordinate rule) computes an approximation to a definite integral, made by finding the area of a collection of rectangles

whose heights are determined by the values of the function. Specifically, the interval  $[a, b]$  on which the function has to be integrated is divided into  $n$  equal subintervals of length

$$h = \frac{b-a}{n}$$

The rectangles are then drawn so that either their left or right corners, or the middle of their top line lies on the graph of the function, with bases running along the  $Ox$ -axis.

This process is illustrated by the next figures: Figure 1, Figure 2, Figure 3. (see [http://www.maa.org/external\\_archive/joma/Vol\\_ume7/Aktumen/Rectangle.html](http://www.maa.org/external_archive/joma/Vol_ume7/Aktumen/Rectangle.html) and <http://www.mathcs.emory.edu/~cheung/Courses/170/Syllabus/07/rectangle-method.html>).

Inner Rectangles. For the lower sum, corresponding to inner rectangles, we use Leftbox approximation on the interval  $[-1, 0]$  and the Rightbox approximation on the interval  $[0, 1]$ .

Middle Rectangles. To obtain middle rectangles, we simply use Middlebox approximation on the entire interval  $[-1, 1]$ .

Outer Rectangles. For the upper sum, corresponding to outer rectangles, we use Rightbox approximation on the interval  $[-1, 0]$

and the Leftbox approximation on the interval  $[0, 1]$ .

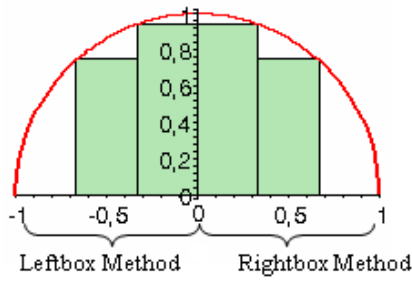


Figure 1. The inner rectangle approximation

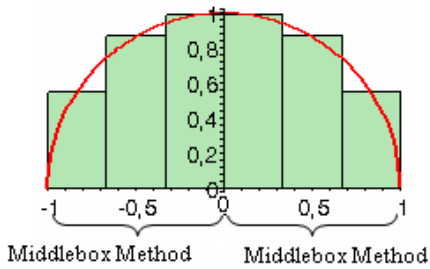


Figure 2. The middle rectangle approximation

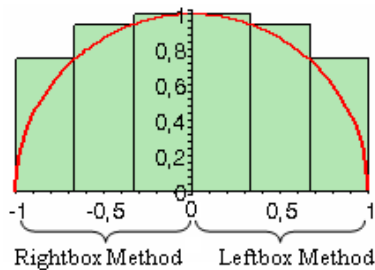


Figure 3. The outer rectangle approximation

The approximation to the integral is then calculated by adding up the areas (base multiplied by height) of the  $n$  rectangles, giving the formula:

$$\int_a^b f(x)dx = h \cdot \sum_{i=0}^{n-1} f(x_i)$$

$$h = \frac{b-a}{n}$$

where  $x_i = a + ih$ .

The formula for  $x_i$  above gives  $x_i$  for the Top-left corner approximation.

A graphic representation of the rectangle method we can follow in the next figures:

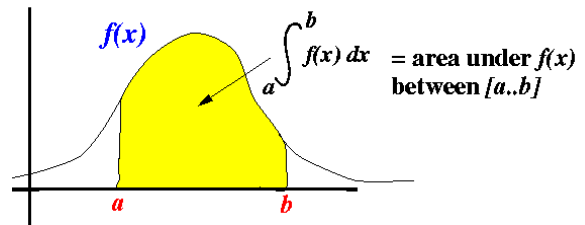


Figure 4. The domain of studying the area of one function

The next step for us is to divide the specified area (the coloured one) in subintervals (rectangles). The more rectangles we have, the better the approximation is. For this aspect, the rectangles are then drawn so that either their left or right corners, or the middle, of their top line lies on the graph of the function, with bases running along the  $Ox$ -axis:

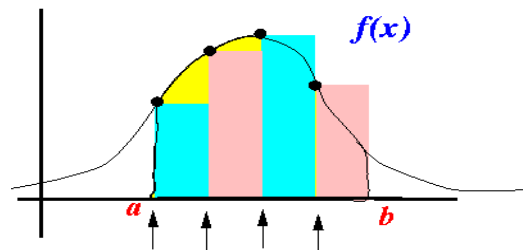


Figure 5. Rectangles as subintervals

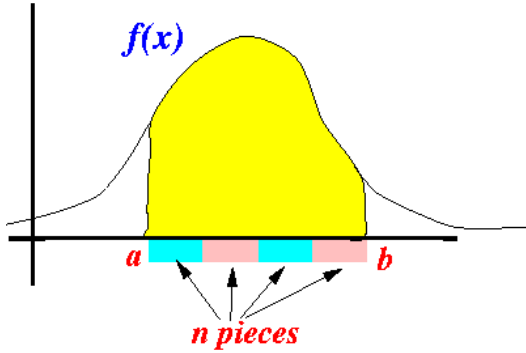


Figure 6. Dividing in subintervals

For computing the entire interval of studying, we should summarize all the subintervals we have got.

As n gets larger, this approximation gets more accurate.

In fact, this computation is the spirit of the definition of the Riemann integral and the limit of this approximation as  $n \rightarrow \infty$  is defined and equal to the integral of f on  $[a, b]$  if this Riemann integral is defined.

Note that this is true regardless of which  $i^*$  is used, however the midpoint approximation tends to be more accurate for finite n.

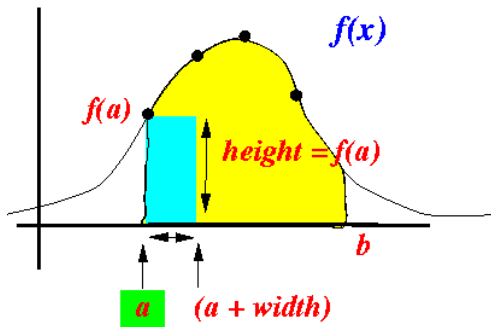


Figure 7. Computing the integral function

## Numeric quadrature

We are going to take  $[a, b] \subset \mathbb{R}$ ,  $x_1, x_2, \dots, x_n$  distinct points of  $[a, b]$  interval (a division) and  $f: [a, b] \rightarrow \mathbb{R}$ , a continuous function.

By a quadrature formula we mean an quality of the type :

$$S(f) = \sum_{i=1}^n c_i f(x_i), \text{ where } c_i \in \mathbb{R}, \forall i = \overline{1, n}.$$

By numerical integration we mean an approximation of the type:

$$\int_a^b f(x) dx \approx S(f)$$

For  $n \in \mathbb{N}^*$ ,  $h = (b-a)/n$ ,  $x_i = a + ih$ ,  $\forall i \in \overline{0, n-1}$ . If  $S_i(f)$  is a quadrature formula of

the function f on the  $[x_i, x_{i+1}]$  interval,  $\forall i \in \overline{0, n-1}$ , then it can be defined the summed quadrature formula:

$$S^{(n)}(f) = \sum_{i=0}^{n-1} S_i(f)$$

The rectangular quadrature formula:

The rectangular quadrature formula is:

$$S(f) = \int_a^b P\left(f, \frac{a+b}{2}, x\right) dx$$

Considering Newton's formula of representing polynomial interpolation, we get:

$$P\left(f, \frac{a+b}{2}, x\right) = f\left(\frac{a+b}{2}\right)$$

Then,

$$S(f) = \int_a^b f\left(\frac{a+b}{2}\right) dx = (b-a) f\left(\frac{a+b}{2}\right)$$

If  $f \in C^1([a, b])$ , from the formula of evaluation of the error, at the interpolation, we will have:

$$\left| f(x) - P\left(f, \frac{a+b}{2}, x\right) \right| \leq \left| x - \frac{a+b}{2} \right| \cdot \max_{x \in [a, b]} |f'(x)|$$

Then,

$$\left| \int_a^b f(x) dx - S(f) \right| = \left| \int_a^b \left( f(x) - P\left(f, \frac{a+b}{2}, x\right) \right) dx \right| \leq$$

$$\int_a^b \left| f(x) - P\left(f, \frac{a+b}{2}, x\right) \right| dx \leq$$

$$\leq \max_{x \in [a,b]} |f'(x)| \cdot \int_a^b \left| x - \frac{a+b}{2} \right| dx = \frac{(b-a)^2}{4} \cdot \max_{x \in [a,b]} |f'(x)|$$

Observation: If  $f$  is derivable in the point  $\left(\frac{a+b}{2}\right)$ , then the rectangular quadrature formula can be obtained by the formula:

$$S(f) = \int_a^b P\left(f, \frac{a+b}{2}, \frac{a+b}{2}, x\right) dx$$

In that case, if  $f \in C^1([a,b])$ , from the formula of evaluation of the error at the interpolation, we are going to have:

$$\left| f(x) - P\left(f, \frac{a+b}{2}, \frac{a+b}{2}, x\right) \right| \leq \frac{1}{2} \left| x - \frac{a+b}{2} \right|^2 \cdot \max_{x \in [a,b]} |f'(x)|, \quad \forall x \in [a,b].$$

Then:

$$\left| \int_a^b f(x) dx - S(f) \right| = \left| \int_a^b \left( f(x) - P\left(f, \frac{a+b}{2}, \frac{a+b}{2}, x\right) \right) dx \right| \leq \int_a^b \left| f(x) - P\left(f, \frac{a+b}{2}, \frac{a+b}{2}, x\right) \right| dx \leq \max_{x \in [a,b]} |f''(x)| \cdot \int_a^b \left( x - \frac{a+b}{2} \right)^2 dx = \frac{(b-a)^3}{24} \cdot \max_{x \in [a,b]} |f''(x)|$$

The summed quadrature formula of the rectangle is:

$$\begin{aligned} S_D^{(n)}(f) &= \sum_{i=0}^{n-1} (x_{i+1} - x_i) f\left(\frac{x_i + x_{i+1}}{2}\right) = \\ &= \frac{b-a}{n} \sum_{i=0}^{n-1} f\left(\frac{x_i + x_{i+1}}{2}\right) \\ &= h \sum_{i=0}^{n-1} f\left(\frac{x_i + x_{i+1}}{2}\right) \end{aligned}$$

And if  $f \in C^2([a,b])$  then we will have the error evaluation :

$$\left| \int_a^b f(x) dx - S_D^{(n)}(f) \right| \leq \sum_{i=0}^{n-1} \left| \int_{x_i}^{x_{i+1}} f(x) dx - S_i(f) \right| \leq \frac{(b-a)^3}{24n} \cdot \max_{x \in [a,b]} |f''(x)|$$

Where  $S_i(f)$  is rectangular quadrature formula applied to the  $f$  function on the  $[x_i, x_{i+1}]$  interval  $\forall i = \overline{0, n-1}$ .

The trapezoidal method

In numerical analysis, the trapezoidal rule (also known as the trapezoid rule or trapezium rule) is a technique for approximating the definite integral.

$$\int_a^b f(x) dx$$

The trapezoidal rule works by approximating the region under the graph of the function  $f(x)$  as a trapezoid and calculating its area. It follows that

$$\int_a^b f(x) dx \approx (b-a) \left[ \frac{f(a) + f(b)}{2} \right]$$

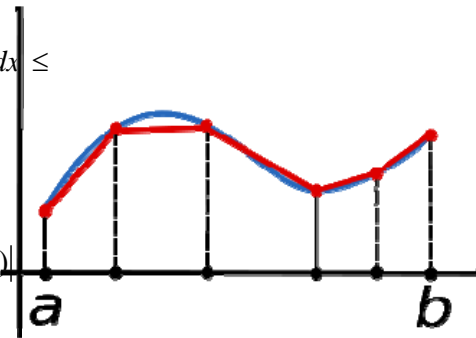


Figure 8. The trapezoidal rule

Applicability and alternatives

The trapezoidal rule is one of a family of formulas for numerical integration called Newton–Cotes formulas, of which the midpoint rule is similar to the trapezoid rule.

Moreover, the trapezoidal rule tends to become extremely accurate when periodic functions are integrated over their periods, which can be analyzed in various ways.

The quadrature trapezoidal formula is:

$$S(f) = \int_a^b P(f, a, b, x) dx$$

From Newton's formula of representing of polynomial interpolation we have the equality

$$\begin{aligned} P(a, b, f, x) &= f(a) + f(a, b)(x-a) = \\ &= f(a) + \frac{f(b) - f(a)}{b-a}(x-a). \end{aligned}$$

Then,

$$S(f) = \int_a^b \left( f(a) + \frac{f(b) - f(a)}{b-a}(x-a) \right) dx =$$

$$= (b-a)f(a) + \frac{f(b) - f(a)}{b-a} \cdot \frac{(b-a)^2}{2}$$

$$= \frac{b-a}{2} \cdot (f(a) + f(b))$$

If  $f \in C^2([a, b])$ , from error evaluation formula at the interpolation we have:

$$|f(x) - P(f, a, b, x)| \leq$$

$$\leq \frac{1}{2} |(x-a)(x-b)| \cdot \max_{x \in [a, b]} |f''(x)|, \quad \forall x \in [a, b]$$

Thus,

$$\left| \int_a^b f(x) dx - S(f) \right| =$$

$$= \left| \int_a^b (f(x) - P(f, a, b, x)) dx \right| \leq$$

$$\leq \int_a^b |f(x) - P(f, a, b, x)| dx \leq$$

$$\leq \frac{1}{2} \max_{x \in [a, b]} |f''(x)| \cdot \int_a^b (x-a)(b-x) dx =$$

$$= \frac{1}{2} \max_{x \in [a, b]} |f''(x)| \cdot \frac{(b-a)^3}{6} = \frac{(b-a)^3}{12} \cdot \max_{x \in [a, b]} |f''(x)|$$

The summed quadrature trapezoidal formula is:

$$S_T^{(n)}(f) = \frac{1}{2} \sum_{i=0}^{n-1} (x_{i+1} - x_i) (f(x_i) + f(x_{i+1})) =$$

$$= \frac{b-a}{2n} \sum_{i=0}^{n-1} (f(x_i) + f(x_{i+1}))$$

$$= h \sum_{i=0}^{n-1} \left( \frac{f(x_i) + f(x_{i+1}))}{2} \right)$$

For which, if  $f \in C^2([a, b])$ , we will have the error evaluation:

$$\left| \int_a^b f(x) dx - S_T^{(n)}(f) \right| \leq \sum_{i=0}^{n-1} \left| \int_{x_i}^{x_{i+1}} f(x) dx - S_i(f) \right| \leq$$

$$\leq \frac{(b-a)^3}{12n^2} \cdot \max_{x \in [a, b]} |f''(x)|$$

where  $S_i(f)$  is the trapezoidal quadrature formula of the  $f$  function applied on the  $[x_i, x_{i+1}]$  interval,  $\forall i \in \overline{0, n-1}$

## RESULTS AND DISCUSSIONS

1) Approximate the integral  $\int_0^1 x^3 dx$ . It is a very simple integral, whose primitive is calculable:

$$\int_0^1 x^3 dx = \frac{x^4}{4} \Big|_0^1 = \frac{1}{4} = 0,25$$

We will also approximate it with both methods. The calculations are done with QUATTRO PRO software. If we denote  $f(x) = x^3$ , then  $f'(x) = 3x^2$  and  $f''(x) = 6x$ ,  $x \in [0, 1]$

Approximation 1) By rectangles method

We denote  $M = \max_{x \in [0, 1]} |f'(x)| = 3$  and let  $\varepsilon$  be the error of approximation. In order to that  $\frac{(b-a)^2}{4n} \cdot M \leq \varepsilon$  it suffices that

$$n \geq \left\lceil \frac{(b-a)^2 \cdot M}{4\varepsilon} \right\rceil + 1$$

In our case, for  $\varepsilon = 10^{-2}$  we must take  $n \geq 76$ .

a=	0
b=	1
h=	0.013157
n=	76

$X_i$	$(X_i + X_{i+1})/2$	$f((X_i + X_{i+1})/2)$
0	0.006578947	2.847536083E-07
0.013157	0.006578947	2.847536083E-07
.....	.....	.....
0.98684210	0.993421052	0.9803927207865
1		

We obtained

$$S_D^{(76)} = 0.249978$$

Approximation 2) By trapezoids method

$$M = \max_{x \in [0,1]} |f''(x)| = 6$$

We denote  $\varepsilon$  be the error of approximation. In order that

$$\frac{(b-a)^3}{12n^2} \cdot M \leq \varepsilon$$

it suffices that

$$n \geq \left\lceil \sqrt{\frac{(b-a)^3 \cdot M}{12\varepsilon}} \right\rceil + 1$$

In our case, for  $\varepsilon = 10^{-2}$  we must take  $n \geq 8$ .

a=	0
b=	1
h=	0.125
n=	8

$X_i$	$f(X_i)$	$[f(X_i)+f(X_{i+1})]/2$
0	0	0.0009765625
0.125	0.001953125	0.0087890625
0.25	0.015625	0.0341796875
0.375	0.052734375	0.0888671875
0.5	0.125	0.1845703125
0.625	0.244140625	0.3330078125
0.75	0.421875	0.5458984375
0.875	0.669921875	0.8349609375
1	1	

We obtain

$$S_T^{(8)} = 0.25390625$$

Remark. The trapezoids method converges much faster than the rectangles method so we will do the rest of our applications only with the trapezoids method.

2) Approximate the integral  $\int_1^2 \frac{\ln(1+x)}{x} dx$ .

In this case, the primitive is in calculable (transcendental), so we can't compute the integral by elementary methods. We approximate it using the trapezoids method.

$$f : [1, 2] \rightarrow \mathbb{R}, f(x) = \frac{\ln(1+x)}{x}$$

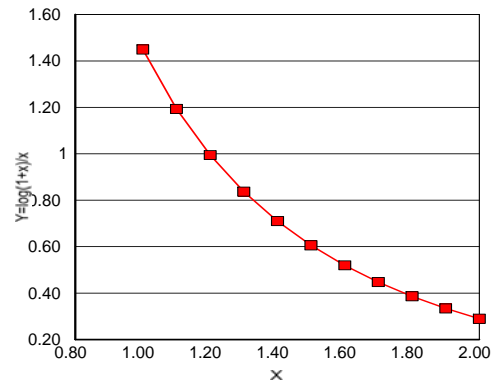
Let

We have

$$f''(x) = -\frac{1}{x^2} + \frac{1}{(x+1)^2} - \frac{1}{x(x+1)} + \frac{\ln(1+x)}{x}$$

In order to estimate the maximum value of  $|f''(x)|$  we trace the graph using the CHART command in QUATTRO

x	f''(x)
1	1.45
1.1	1.19
1.2	0.99
1.3	0.84
1.4	0.71
1.5	0.61
1.6	0.52
1.7	0.45
1.8	0.39
1.9	0.33
2	0.29



Using the OPTIMIZER command in QUATTRO, we find.

Thus, for  $\varepsilon = 10^{-5}$  we must take  $n \geq 110$ .

We obtain

$$\int_1^2 \frac{\ln(1+x)}{x} dx \approx S_T^{(110)} = 0.26678$$

3) Approximate the integral  $\int_{\frac{\pi}{3}}^{\frac{\pi}{2}} \frac{\sin x}{x} dx$ .

The primitive is transcendental.

Let

$$f : \left[ \frac{\pi}{3}, \frac{\pi}{2} \right] \rightarrow \square, f(x) = \frac{\sin x}{x}$$

We have

$$f''(x) = \frac{-x^3 \sin x - 2x^2 \cos x + 2x \sin x}{x^4}$$

We find

$$M = \max_{x \in [0,1]} |f''(x)| = 0.23$$

Thus, for  $\varepsilon = 10^{-5}$  we must take  $n \geq 15$ .

We obtain

$$\int_{\frac{\pi}{3}}^{\frac{\pi}{2}} \frac{\sin x}{x} dx \square S_T^{(15)} = 0.38529$$

4) Approximate the integral  $\int_0^1 e^{-x^2} dx$ .

The primitive is transcendental.

Let

$$f : [0,1] \rightarrow \square, f(x) = e^{-x^2}$$

We have

$$f''(x) = (-2 + 4x^2)e^{-x^2}$$

We find

$$M = \max_{x \in [0,1]} |f''(x)| = 2$$

Thus, for  $\varepsilon = 10^{-5}$  we must take  $n \geq 130$ .

We obtain

$$\int_0^1 e^{-x^2} dx \square S_T^{(130)} = 0.74682$$

Remark. (see

[http://en.wikipedia.org/wiki/Normal\\_distribution](http://en.wikipedia.org/wiki/Normal_distribution))

$$f(x) = \frac{1}{\sigma\sqrt{2\pi}} e^{-\frac{(x-\mu)^2}{2\sigma^2}}$$

In statistics  $f(x) = \frac{1}{\sigma\sqrt{2\pi}} e^{-\frac{(x-\mu)^2}{2\sigma^2}}$  is the density function of the normal distribution  $N(\mu, \sigma^2)$  (with the mean  $\mu$  and the standard deviation  $\sigma$ ). Many random variables or phenomena have a normal distribution, whose graph is also known as the bell of Gauss: the marks from a test, people's heights, people's IQ etc.

The probability to have values in  $[a, b]$  is

$$P(a \leq N(\mu, \sigma^2) \leq b) = \int_a^b \frac{1}{\sigma\sqrt{2\pi}} e^{-\frac{(x-\mu)^2}{2\sigma^2}} dx$$

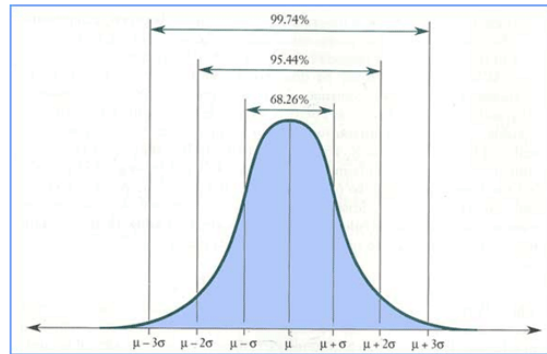


Figure 9. The Gaussian bell

An integral which can be approximated in the same manner as before.

5) Approximate the integral  $\int_0^{2\pi} \sqrt{1+3\sin^2 x} dx$ .

(an elliptic integral)

The primitive is transcendental.

Let

$$f : [0, 2\pi] \rightarrow \square, f(x) = \sqrt{1+k\sin^2 x}, k \geq 0$$

We have

$$f''(x) = \frac{4k^2 \cos^2 2x + (2k^2 + 4k) \cos 2x - 2k^2}{4 \left( \frac{2+k-k\cos 2x}{2} \right)^{\frac{3}{2}}}$$

We could have used QUATTRO for computing the maximum, but, using modul's properties, we found the general inequality

$$|f''(x)| \leq 2k^2 + k, x \in [0, 2\pi]$$

So, for  $k=3$

$$M = \max_{x \in [0, 2\pi]} |f''(x)| < 21$$

For  $\varepsilon = 10^{-5}$  we should have taken  $n \geq 3000$ , so, for the sake of simplicity, we took  $\varepsilon = 10^{-2}$ , for which it suffices to consider  $n \geq 209$ .

We obtain

$$\int_0^{2\pi} \sqrt{1+3\sin^2 x} dx \square S_T^{(209)} = 9.68844$$

Remark.

<http://en.wikipedia.org/wiki/Ellipse>.

(see

Using, for example, line integrals the circumference of an ellipse with the semi-axes  $a > b > 0$  is

$$\oint_E ds = b \int_0^{2\pi} \sqrt{1 + \left(\frac{a^2}{b^2} - 1\right) \sin^2 x} dx$$

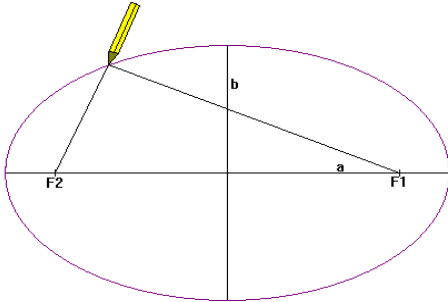


Figure 10. An ellipse

Unfortunately, this integral, called *elliptic*, is transcendental, so we can only approximate it.

Taking  $\frac{a^2}{b^2} - 1 = k \geq 0$ , we have to evaluate

$$\int_0^{2\pi} \sqrt{1 + k \sin^2 x} dx$$

In fact, we see that our last calculation represents an approximation for the circumference of the ellipse with  $a = 2$  and  $b = 1$ .

Our result is very close to Ramanujan's approximation:

$$C \approx \pi \left[ 3(a+b) - \sqrt{(3a+b)(a+3b)} \right] = 9.6884210$$

## CONCLUSIONS

We successfully managed to calculate (approximately) some important integrals, mainly with transcendental primitives. Rectangles formula is a little easier to apply, especially if we take the the extremities instead of the middle, but trapezoids formula is faster. Although, there exist even faster methods. Sometimes, in order to get a good approximation, we must take a big value for  $n$ , which makes the problem difficult in QUATTRO or EXCEL. In this cases, a programming language or routine would be better.

## REFERENCES

- Grigore G, 1990, *Lecții de analiză numerică*, Ed. Universității din București ;  
 Munteanu, I.P., Stanică D., 2006. *Analiză numerică. Exerciții și teme de laborator*, Ed. Universității din București ;  
 Roșca I, 2000, *Analiză numerică*, Ed. Universității din București;  
[http://en.wikipedia.org/wiki/Normal\\_distribution](http://en.wikipedia.org/wiki/Normal_distribution)  
[http://www.maa.org/external\\_archive/joma/Volume7/Aktumen/Rectangle.html](http://www.maa.org/external_archive/joma/Volume7/Aktumen/Rectangle.html)  
<http://www.mathcs.emory.edu/~cheung/Courses/170/Syllabus/07/rectangle-method.html>  
<http://en.wikipedia.org/wiki/Ellipse>

## ENERGETIC EFFICIENCY OF PUMPING STATION

Catalin BOTEA, Daniel Ionut CARAMIDARU

Scientific Coordinator: Lect. PhD. Eng. Dragos DRACEA

University of Agronomic Science and Veterinary Medicine, Faculty of Land Reclamation and Environmental Engineering, 59 Mărăști Blvd, District 1, 011464, Bucharest, Romania, Phone: +40213183076

Corresponding author email: botea.catalin@hotmail.com

### Abstract

The aim of this paper is to emphasize lower energy consumption in pump station that is equipped with variable speed pumps. This paper presents a comparison between different pump stations in terms specific energy consumption. We considered the following situations: adjusting the flow by valve and adjusting the flow by varying the speed. The study showed that pump station equipped with variable speed pumps are more efficient than the ones with fixed speed.

**Key words:** poms, energy consumption.

### INTRODUCTION

The fluid transport was a great challenge for human. Since old times people moved water wherever they needed; a great irrigation system was the Hanging Gardens of Babylon one of the 7th Wonders of the World, with great consumption of resources and energy.

### MATERIALS AND METHODS

The data used in this study (flow and height) were from Bragadiru irrigation pump station and the used pumps where both with fixed and variable speed, Grundfos HS 200-150-381/367 3\*400V, 60Hz, 5 equipments with 500m<sup>3</sup> flow rate per equipment and 65m pumping height (Figure 1). The data analysis was performed by Grundfos WebCAPS Software (see Grundfos WebCaps <http://net.grundfos.com/Appl/WebCAPS/custom?userid=GFRomania>).

### RESULTS AND DISCUSSIONS

First measurements were performed using equipment with fixed speed at flow rate 2500

m<sup>3</sup>/h, efficiency 83%, energy consumption 530 kW and 1780 rpm. The experiments showed that by reducing the flow rate from valve to a 2100 m<sup>3</sup>/h value, the efficiency, power and NPSH decreased and pumping height increased (Table 1, figures 2, 3, 4).

Table 1. Efficiency, power and NPSH values for different flow rates of fixed speed pumps

Q	H	P	$\eta$	NPSH
m <sup>3</sup> /h	m	kW	%	m
2500	65,4	530	83,8	3,52
2400	66	518	83,1	3,39
2300	66,6	507	82,3	3,31
2200	67,1	493	81,3	3,25
2100	67,6	480	80,2	3,21



Figure 1. Grundfos HS Pumps

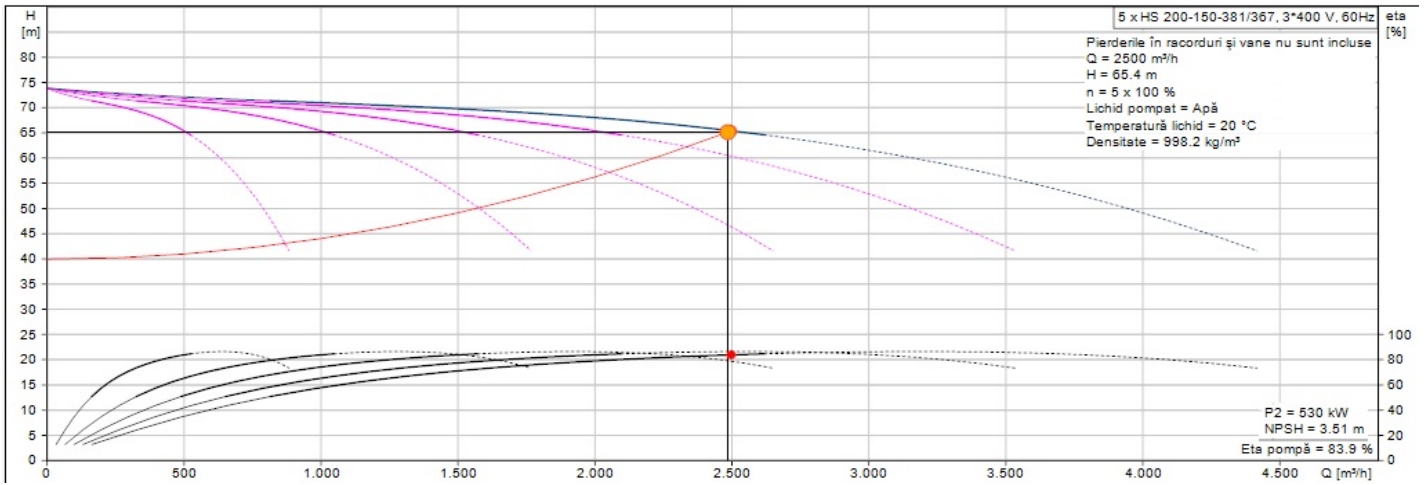


Figure 2. Operating point pumps whit fixed speed at 2500m<sup>3</sup>

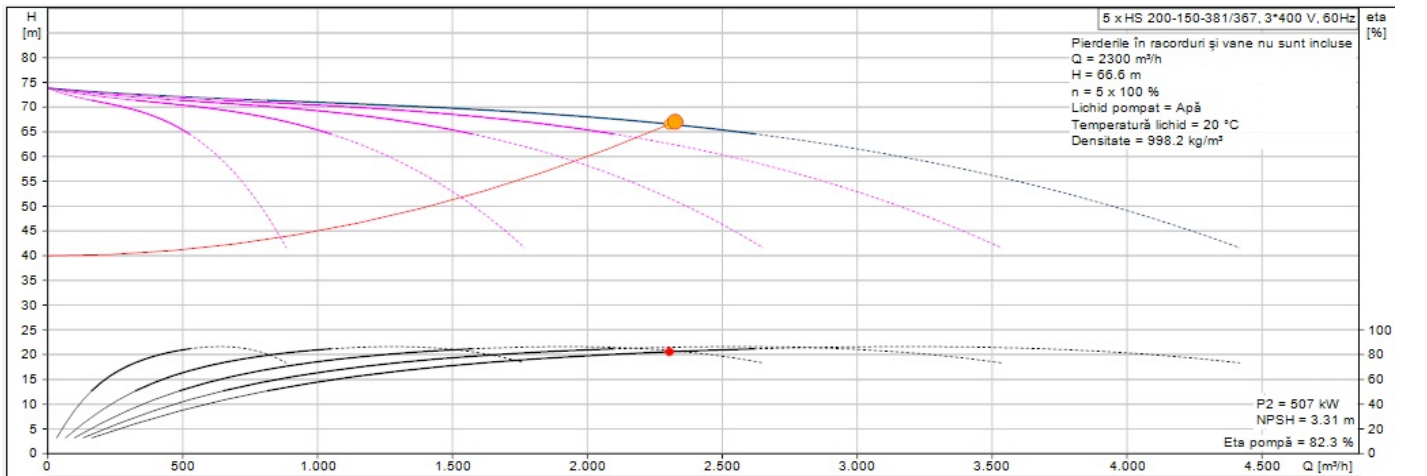


Figure 3. Operating point pumps whit fixed speed at 2300m<sup>3</sup>

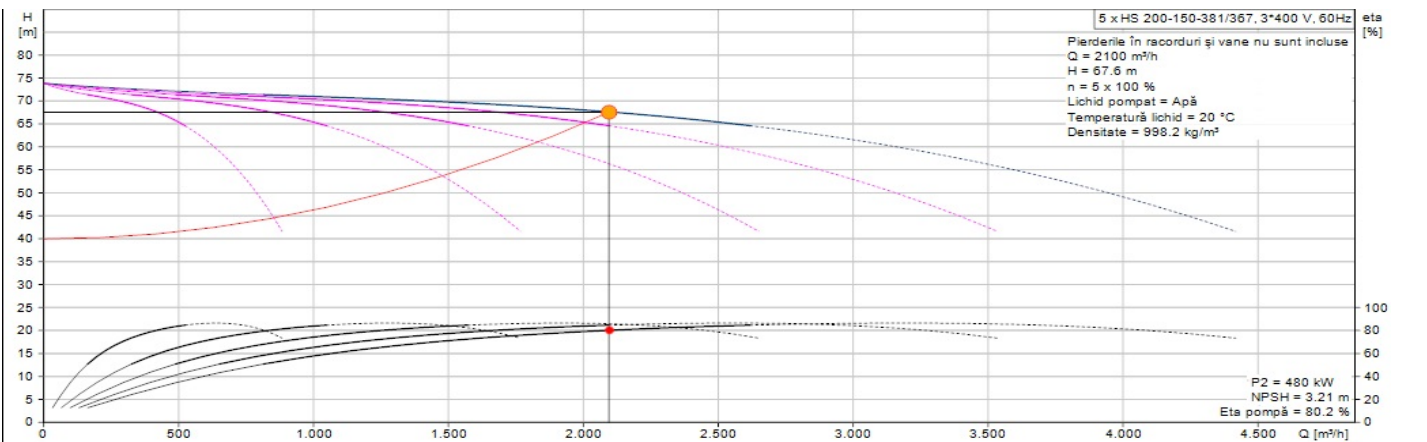


Figure 4. Operating point pumps whit fixed speed at 2100m<sup>3</sup>

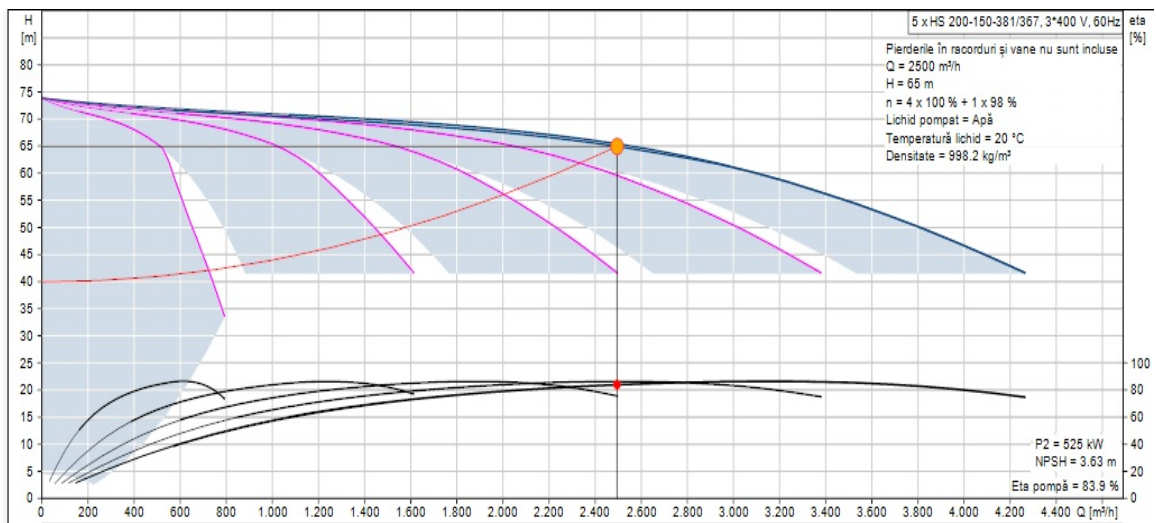


Figure 5. Operating point pumps whit mixed speed at 2500m<sup>3</sup>

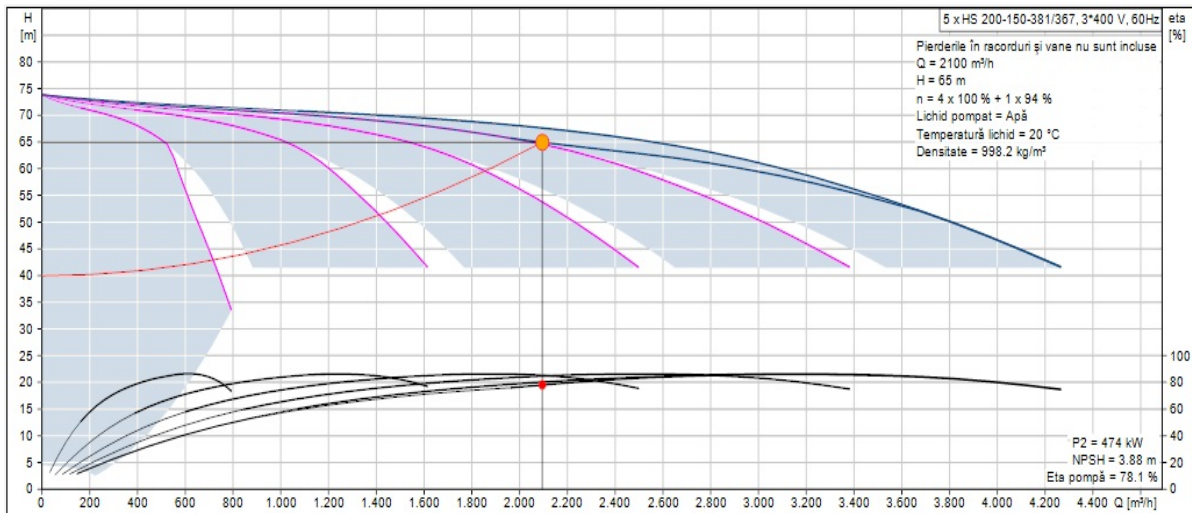


Figure 6. Operating point pumps whit mixed speed at 2300m<sup>3</sup>

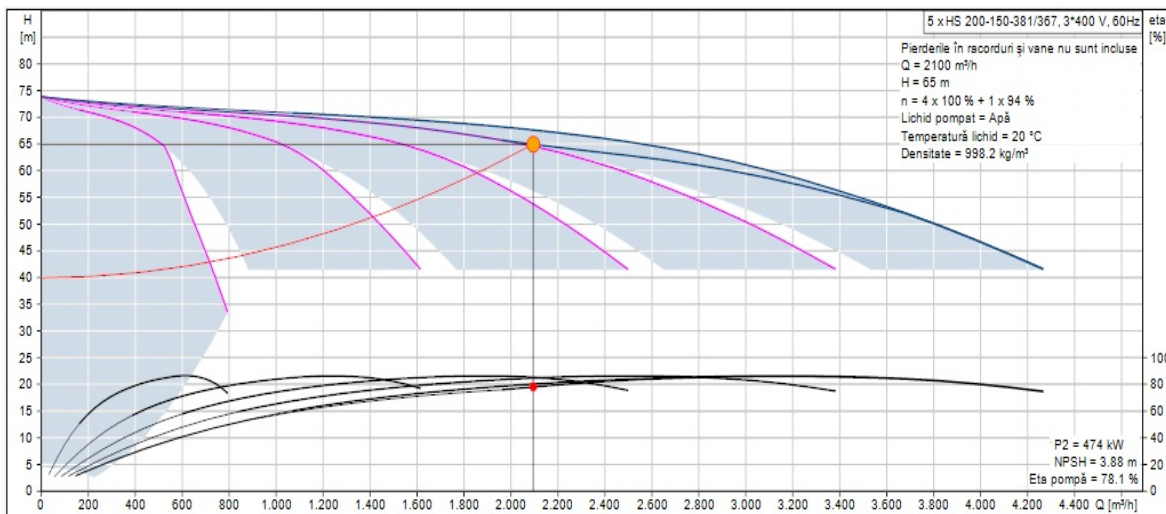


Figure 7. Operating point pumps whit mixed speed at 2100m<sup>3</sup>

The next experiment used mixed pump because the pumping height could not be kept at different flow rate without closing the valve.

If the pumping height is kept constant, there is no more stress and energy loss in the network (Burchiu et al., 2006). Table 2 and figures 5, 6, 7 show the operating point and energy consumption in mixed pump station.

Table 2. Data about second pump station at different flow rate

Q	H	P	$\eta$	NPSH	$N^{-1}$
m <sup>3</sup> /h	m	kW	%	m	%
2500	65	527	83.9	3.58	99
2400	65	511	83.1	3.58	97
2300	65	496	82	3.58	96
2200	65	482	80.4	3.66	95
2100	65	474	78.1	3.88	94

In the third experiment we used equipment with variable speed, keeping the flow rate and pumping height constant. The energy consumption is lower in this case, due to the variable speed pumps used.

Table 3. Data about third pump station at different flow rate

Q	H	P	$\eta$	NPSH	$N^{-1}$
m <sup>3</sup> /h	m	kW	%	m	%
2500	65	529	83.9	3.58	100
2400	65	512	83.1	3.58	99
2300	65	491	82	3.58	99
2200	65	475	80.4	3.66	98
2100	65	459	78.1	3.88	98

The study presented in this paper showed that pump station equipped with speed variation pumps are more efficient (figure 8). For example, at 2100 m<sup>3</sup> flow rate, the difference in energy consumption is 21 kW, which represents 4,4%. This value that appears to be

small, is in fact significant for irrigations, and means a major energy saving.

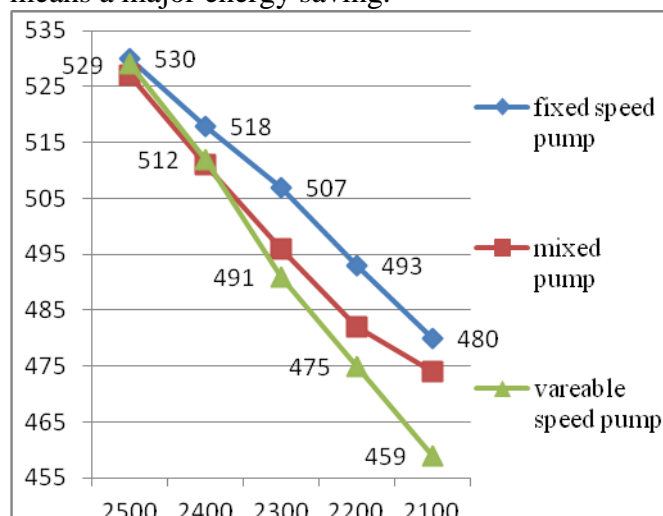


Figure 8. Consumed power function of flow rate for all three experiments considered

## CONCLUSIONS

Avoid restarting because it takes 700% more energy to start up the pump.

Using 100% of pump capacity the lifetime of the pump is that guaranteed by producer. Using under 100% of pump capacity we can extend the pump lifetime.

Avoid using the pump in rush hours because the electricity is expensive.

The ratio kW / m<sup>3</sup> between pumps is 0.21 for variable speed pumps and 0.22 for fixed speed pumps, which represents a major energy saving when speaking about great quantities.

## REFERENCES

- Grundfos WebCaps  
<http://net.grundfos.com/Appl/WebCAPS/custom?use rid=GFRomania>
- Victor Burchiu, Liviu Gherghiu, Alexandru Dudau, Ghidul utilizatorului de pompe, Atlas Press, 2006.